Springer Protocols

Terry J. McGenity
Kenneth N. Timmis
Balbina Nogales *Editors*

Hydrocarbon and Lipid Microbiology Protocols

Activities and Phenotypes

Springer

Springer Protocols Handbooks

More information about this series at http://www.springer.com/series/8623

Terry J. McGenity · Kenneth N. Timmis · Balbina Nogales
Editors

Hydrocarbon and Lipid Microbiology Protocols

Activities and Phenotypes

Springer

Editors
Terry J. McGenity
School of Biological Sciences
University of Essex
Colchester, Essex, UK

Kenneth N. Timmis
Institute of Microbiology
Technical University Braunschweig
Braunschweig, Germany

Balbina Nogales
Department of Biology
University of the Balearic Islands
and Mediterranean Institute for Advanced Studies (IMEDEA, UIB-CSIC)
Palma de Mallorca, Spain

ISSN 1949-2448 ISSN 1949-2456 (electronic)
Springer Protocols Handbooks
ISBN 978-3-662-49138-6 ISBN 978-3-662-49140-9 (eBook)
DOI 10.1007/978-3-662-49140-9

Library of Congress Control Number: 2016938230

Printed on acid-free paper

This Springer imprint is published by Springer Nature
The registered company is Springer-Verlag GmbH Berlin Heidelberg

Preface to Hydrocarbon and Lipid Microbiology Protocols[1]

All active cellular systems require water as the principal medium and solvent for their metabolic and ecophysiological activities. Hydrophobic compounds and structures, which tend to exclude water, although providing *inter alia* excellent sources of energy and a means of biological compartmentalization, present problems of cellular handling, poor bioavailability and, in some cases, toxicity. Microbes both synthesize and exploit a vast range of hydrophobic organics, which includes biogenic lipids, oils and volatile compounds, geochemically transformed organics of biological origin (i.e. petroleum and other fossil hydrocarbons) and manufactured industrial organics. The underlying interactions between microbes and hydrophobic compounds have major consequences not only for the lifestyles of the microbes involved but also for biogeochemistry, climate change, environmental pollution, human health and a range of biotechnological applications. The significance of this "greasy microbiology" is reflected in both the scale and breadth of research on the various aspects of the topic. Despite this, there was, as far as we know, no treatise available that covers the subject. In an attempt to capture the essence of greasy microbiology, the *Handbook of Hydrocarbon and Lipid Microbiology* (http://www.springer.com/life+sciences/microbiology/book/978-3-540-77584-3) was published by Springer in 2010 (Timmis 2010). This five-volume handbook is, we believe, unique and of considerable service to the community and its research endeavours, as evidenced by the large number of chapter downloads. Volume 5 of the handbook, unlike volumes 1–4 which summarize current knowledge on hydrocarbon microbiology, consists of a collection of experimental protocols and appendices pertinent to research on the topic.

A second edition of the handbook is now in preparation and a decision was taken to split off the methods section and publish it separately as part of the Springer Protocols program (http://www.springerprotocols.com/). The multi-volume work *Hydrocarbon and Lipid Microbiology Protocols*, while rooted in Volume 5 of the Handbook, has evolved significantly, in terms of range of topics, conceptual structure and protocol format. Research methods, as well as instrumentation and strategic approaches to problems and analyses, are evolving at an unprecedented pace, which can be bewildering for newcomers to the field and to experienced researchers desiring to take new approaches to problems. In attempting to be comprehensive – a one-stop source of protocols for research in greasy microbiology – the protocol volumes inevitably contain both subject-specific and more generic protocols, including sampling in the field, chemical analyses, detection of specific functional groups of microorganisms and community composition, isolation and cultivation of such organisms, biochemical analyses and activity measurements, ultrastructure and imaging methods, genetic and genomic analyses,

[1] Adapted in part from the Preface to *Handbook of Hydrocarbon and Lipid Microbiology*.

systems and synthetic biology tool usage, diverse applications, and the exploitation of bioinformatic, statistical and modelling tools. Thus, while the work is aimed at researchers working on the microbiology of hydrocarbons, lipids and other hydrophobic organics, much of it will be equally applicable to research in environmental microbiology and, indeed, microbiology in general. This, we believe, is a significant strength of these volumes.

We are extremely grateful to the members of our Scientific Advisory Board, who have made invaluable suggestions of topics and authors, as well as contributing protocols themselves, and to generous *ad hoc* advisors like Wei Huang, Manfred Auer and Lars Blank. We also express our appreciation of Jutta Lindenborn of Springer who steered this work with professionalism, patience and good humour.

Colchester, Essex, UK — Terry J. McGenity
Braunschweig, Germany — Kenneth N. Timmis
Palma de Mallorca, Spain — Balbina Nogales

Reference

Timmis KN (ed) (2010) Handbook of hydrocarbon and lipid microbiology. Springer, Berlin, Heidelberg

Contents

About the Editors

Terry J. McGenity is a Reader at the University of Essex, UK. His Ph.D., investigating the microbial ecology of ancient salt deposits (University of Leicester), was followed by postdoctoral positions at the Japan Marine Science and Technology Centre (JAMSTEC, Yokosuka) and the Postgraduate Research Institute for Sedimentology (University of Reading). His overarching research interest is to understand how microbial communities function and interact to influence major biogeochemical processes. He worked as a postdoc with Ken Timmis at the University of Essex, where he was inspired to investigate microbial interactions with hydrocarbons at multiple scales, from communities to cells, and as both a source of food and stress. He has broad interests in microbial ecology and diversity, particularly with respect to carbon cycling (especially the second most abundantly produced hydrocarbon in the atmosphere, isoprene), and is driven to better understand how microbes cope with, or flourish in hypersaline, desiccated and poly-extreme environments.

Kenneth N. Timmis read microbiology and obtained his Ph.D. at Bristol University, where he became fascinated with the topics of environmental microbiology and microbial pathogenesis, and their interface pathogen ecology. He undertook postdoctoral training at the Ruhr-University Bochum with Uli Winkler, Yale with Don Marvin, and Stanford with Stan Cohen, at the latter two institutions as a Fellow of the Helen Hay Whitney Foundation, where he acquired the tools and strategies of genetic approaches to investigate mechanisms and causal relationships underlying microbial activities. He was subsequently appointed Head of an Independent Research Group at the Max Planck Institute for Molecular Genetics in Berlin, then Professor of Biochemistry in the University of Geneva Faculty of Medicine. Thereafter, he became Director of the Division of Microbiology at the National Research Centre for Biotechnology (GBF)/now the Helmholtz Centre for Infection Research (HZI) and Professor of Microbiology at the Technical University Braunschweig. His group has worked for many years, *inter alia*, on the biodegradation of oil hydrocarbons, especially the genetics and regulation of toluene degradation, pioneered the genetic design and experimental evolution of novel catabolic activities, discovered the new group of marine hydrocarbonoclastic bacteria, and conducted early genome sequencing of bacteria that

became paradigms of microbes that degrade organic compounds (*Pseudomonas putida* and *Alcanivorax borkumensis*). He has had the privilege and pleasure of working with and learning from some of the most talented young scientists in environmental microbiology, a considerable number of which are contributing authors to this series, and in particular Balbina and Terry. He is Fellow of the Royal Society, Member of the EMBO, Recipient of the Erwin Schrödinger Prize, and Fellow of the American Academy of Microbiology and the European Academy of Microbiology. He founded the journals *Environmental Microbiology, Environmental Microbiology Reports* and *Microbial Biotechnology*. Kenneth Timmis is currently Emeritus Professor in the Institute of Microbiology at the Technical University of Braunschweig.

Balbina Nogales is a Lecturer at the University of the Balearic Islands, Spain. Her Ph.D. at the Autonomous University of Barcelona (Spain) investigated antagonistic relationships in anoxygenic sulphur photosynthetic bacteria. This was followed by postdoctoral positions in the research groups of Ken Timmis at the German National Biotechnology Institute (GBF, Braunschweig, Germany) and the University of Essex, where she joined Terry McGenity as postdoctoral scientist. During that time, she worked in different research projects on community diversity analysis of polluted environments. After moving to her current position, her research is focused on understanding microbial communities in chronically hydrocarbon-polluted marine environments, and elucidating the role in the degradation of hydrocarbons of certain groups of marine bacteria not recognized as typical degraders.

Introduction to Activities and Phenotypes

Florin Musat

Abstract

Crude oil and lipids greatly influence the structure and function of microbial communities, owing to merely physical effects such as hindering the diffusion of oxygen or light to communities trapped beneath oil layers, to toxicity of the highly soluble oil hydrocarbons, or to the utilization of hydrocarbons or lipids as growth substrates by microorganisms. This chapter brings together methods to investigate the effects of crude oil or lipids on the diversity and function of microbial communities. These can be principally grouped into protocols devoted to analyze the functional diversity of microbial communities in response to hydrocarbons or lipids, protocols aiming to resolve the specific interactions of microorganisms with hydrophobic phases, protocols to study the effects of hydrocarbons or lipids on bulk metabolic activities of microbial communities, and tools to identify specific genes involved in metabolic processes. Most of the protocols presented here can be applied directly on environmental samples, or on laboratory-scale micro/mesocosms, thereby allowing a direct comparison between pristine samples and samples contaminated experimentally with hydrocarbons.

Keywords Biosurfactants, Chemotactism, Crude oil, Functional diversity, Hydrophobic phases, Lipids, Methanogenesis, Respiration rates, Sulfate reduction, Transposon mutagenesis

Microbial communities are very complex assemblages, owing to the diversity of microbial species, with species richness estimated in the range of thousands per gram of soil, for example [1], to the interactions of microorganisms with each other and with the environment (e.g., attachment to sediment particles, formation of microcolonies or biofilms, or selection of functional types based on physical–chemical gradients). Consideration of crude oil or lipids as carbon and energy sources for microorganisms adds a new dimension to already very complex systems. Crude oils, for example, are very complex mixtures consisting, by moderate estimates, of tens of thousands of individual compounds. For that reason, contamination of a given environment with crude oil adds to the complexity of microbial communities' structure and function. Crude oils can interact and/or influence microbial communities in many ways. For example, oil spills in the open sea or at the surface of sediments lead to the formation of a viscous layer,

T.J. McGenity et al. (eds.), *Hydrocarbon and Lipid Microbiology Protocols*, Springer Protocols Handbooks, (2017) 1–6,
DOI 10.1007/8623_2015_145, © Springer-Verlag Berlin Heidelberg 2015, Published online: 18 November 2015

impending the diffusion of oxygen or light. This merely physical effect will greatly affect phototrophic and aerobic microorganisms trapped beneath the oil layers, leading to changes in respiration rates of the community as a whole, inhibition of photosynthesis, or even establishment of anoxic conditions in the case of very thick and dense oil layers. Crude oils have also a strong toxic effect on the meiofauna of marine sediments, for example, abolishing the ecological role of these organisms, which in turn will affect microbial communities. As an example, following massive oil spills in coastal environments, thick cyanobacterial layers developed on top of weathered oil slicks. One of the reasons for this development was the elimination by oil of invertebrates feeding on cyanobacteria, thereby allowing the latter to bloom. Elimination of the meiofauna by oil may have also other effects on the ecosystem as a whole, ultimately influencing the physiology and structure of microbial communities, such as abolishing the role of meiofauna in the aeration of sediments or providing hot spots of carbon and nitrogen from dead biomass. Crude oil hydrocarbons, notably the low-molecular-mass, highly soluble fraction, can also have a toxic effect on the microorganisms themselves. Nevertheless, probably one of the most remarkable features of microorganisms is their ability to utilize oil hydrocarbons as growth substrates. Biodegradation by microorganisms is essentially the main route of hydrocarbon removal from the environment, and relatively recent research has shown that in addition to the well-known aerobic degradation processes, anaerobic microorganisms can also grow with hydrocarbons as substrates under various electron acceptor conditions, such as sulfate-, metal-, or nitrate-reducing conditions, and even under methanogenic conditions.

This volume comprises protocols to analyze the functional diversity of microbial communities in response to hydrocarbons or lipids, the specific interactions of microorganisms with hydrophobic phases, the effects of hydrocarbons or lipids on the bulk metabolic activity of microbial communities (e.g., aerobic respiration, sulfate reduction, and methanogenesis rates), and the tools to identify specific genes involved in metabolic processes. Most of the protocols described here can be applied directly on environmental samples or on laboratory-scale micro-/mesocosms, thereby allowing a direct comparison between pristine samples and samples contaminated experimentally with hydrocarbons.

Microorganisms may show apparently contrasting responses to the presence of hydrocarbons or lipids. On the one hand, elevated concentrations of hydrophobic compounds, for example, of low-molecular-mass hydrocarbons which have relatively high water solubility, may constitute a solvent stress for microorganisms due to their tendency to accumulate in cellular membranes. As a response, microorganisms may alter the composition of the cellular membranes, one of the best-known examples being the conversion of

cis- to trans-unsaturated fatty acids, leading to a decrease in membrane fluidity. The cis–trans conversion is an enzymatic reaction, catalyzed by an isomerase which was found in several genera, including well-known hydrocarbon-degrading microorganisms. In this volume, protocols to determine the trans/cis ratio of unsaturated fatty acids are presented. These protocols can be applied in cultures, mesocosm experiments, or directly in the environment and provide a useful bioindicator to the extent of solvent stress response of individual microorganisms or the community as a whole. On the other hand, microorganisms can use hydrocarbons and lipids as growth substrates. In this case, growth is often limited by the hydrophobicity and in general poor water solubility of the would-be substrates, causing mass-transfer limitations. Obvious examples are high-molecular-mass hydrocarbons and lipids, such as long-chain alkanes and fatty acids. For example, *n*-hexadecane which is very often used as a model compound for the biodegradation of *n*-alkanes has a solubility in water of only 2.3×10^{-7} mmol L^{-1} [2]. To cope with these growth-limiting factors, microorganisms have developed various mechanisms to gain better access to hydrophobic substrates, including attachment to hydrophobic phases, a presently debated active uptake of hydrocarbons, production of biosurfactants, or chemotaxis toward hydrocarbons. In this section, protocols to measure the uptake/transport of hydrocarbons in microorganisms, the production of biosurfactants, and the chemotactic response of microorganisms toward hydrocarbons are presented. In addition, methods to assess the potential of microorganisms to interact with hydrocarbon layers are discussed.

A substantial section of this volume is dealing with physiological responses of microbial communities as a whole to the presence of hydrocarbons and lipids. Contamination of oxic environments, for example, by crude oil spills, could most likely result in changes of bulk respiration rates, either by reduction of oxygen consumption due to toxicity of oil components on the microorganisms or by stimulation of respiration due to enrichment of hydrocarbon degraders. The type and magnitude of the microbial community response depend on several factors, such as the chemical composition and the amount of spilled oil, the in situ temperature, the availability of other nutrients (e.g., nitrogen), or the preexposure of the microbial community itself to hydrocarbons, to name only a few. Measurement of bulk respiration rates could provide a useful tool to measure the overall activity of cells and to estimate, for example, if a microbial community is shifting toward hydrocarbon consumption. Here, two methods to measure respiration rates based on oxygen consumption are described. The methods are based on utilization of liquid cultures/samples and can thus be used with pure or enriched cultures, as well as with environmental water samples.

Contamination by crude oil of marine sediments (e.g., intertidal sediments) or soils may lead to rapid oxygen consumption and establishment of anoxic layers. In such layers, hydrocarbons and lipids can be used as substrates by anaerobic microorganisms such as sulfate reducers and methanogens. Since sulfate is relatively abundant in seawater, hydrocarbon degradation coupled to sulfate reduction is more frequent in marine environments, while methanogenesis is more common in terrestrial environments and in deeper marine sediments where other terminal electron acceptors have been depleted. During the past two decades, numerous sulfate-reducing bacteria (SRBs) have been enriched or isolated in pure culture that are able to degrade both aliphatic (*n*-alkanes of various chain lengths, cycloalkanes) and aromatic hydrocarbons. It has been also shown that sulfate-reducing bacteria can degrade hydrocarbons directly from crude oil. Molecular ecology studies have also revealed that phylogenetic lineages related to cultured hydrocarbon-degrading SRBs are abundant in hydrocarbon-impacted marine sediments, for example, natural gas or oil seeps. All these studies point out to an important role of SRB in degradation of hydrocarbons, and hence in the carbon and sulfur cycling, in anoxic environments. In this volume, protocols to measure the activity of sulfate-reducing bacteria in water injection systems are described. On a broader scale, the sulfate-reducing activity can be measured in the laboratory on any anoxic sample provided with crude oil or model hydrocarbons, as a diagnostic for the potential of SRBs to degrade hydrocarbons. The activity of sulfate-reducing microorganisms in oil field operations, e.g., water injection into reservoirs for secondary oil recovery, leads frequently to an increased sulfide content in the produced oil (souring). Souring can occur directly in the oil reservoir or in oil processing facilities and is a major concern for the oil industry. Understanding the activity (and the factors influencing it) of sulfate-reducing microorganisms is therefore essential to devise effective protocols for souring limitation in field operations. In this volume, protocols to study the souring potential in oil fields, as well as protocols to test the effectiveness of various souring control methods, are outlined. In anoxic environments where other electron acceptors (e.g., nitrate, Fe(III), sulfate) have been depleted, biodegradation of organic matter is carried out by methanogenic microorganisms. Relatively recently it has been shown that also hydrocarbons can be degraded by methanogenic microorganisms, a process which has been proposed to take place also in crude oil reservoirs. Protocols to measure methanogenesis on a laboratory scale, using cultures or slurry incubations, complete this section on evaluating the physiological capabilities of microbial communities in relation to hydrocarbons or lipids as substrates.

Crude oil is composed mainly of hydrocarbons, and hence it has a high load of carbon and a very low content of other elements

such as sulfur, nitrogen, and phosphorus [3]. Nitrogen in particular is a strongly growth-limiting element in many environments, and crude oil contamination will further misbalance the ratio of carbon to nitrogen. As a consequence, high concentrations of hydrocarbons or lipids may lead to a stimulation of N_2-fixing microorganisms. In this volume, methods to measure the impact of hydrocarbons on rates of N_2 fixation with bulk environmental samples or laboratory microcosms are described. In addition, protocols to measure N_2 fixation by individual cells, based on fluorescence in situ hybridization and nanoSIMS-based chemical imaging, are being presented.

In order to understand the role of individual species in the metabolism of hydrocarbons and lipids, one needs to assess the phenotypical (functional) diversity of a microbial community. In this volume, cultivation-based microtiter plates (microarrays) for the identification of microbial isolates and the functional fingerprinting of microbial communities are detailed. Although it is only emerging in the field of hydrocarbon and lipid microbiology, this approach has a great potential to screen large numbers of isolates under selective growth conditions. The protocol discusses the advantages of the phenotyping microarrays (e.g., the high throughput with respect to both number of isolates and number of substrates that can be tested), as well as the inherent limitations of the approach, mostly derived from the use of reduced dyes as indicators of cellular activity, or selection induced by the cultivation conditions. Finally, this volume addresses protocols to determine the role of specific, essential genes in catabolic pathways. Exemplified with identification of genes involved in the synthesis of poly(3-hydroxybutyrate), the disruption of single genes by transposon mutagenesis can be envisioned to be applicable to identify genes involved in the metabolism of hydrocarbons or lipids. This method is based on the use of one of the best-known transposons, Tn5, and the generation and analysis of Tn5-induced mutants in a target strain.

Overall, the protocols of the present volume allow to analyze the functions of microbial communities in relation to hydrocarbons and lipids at several levels, ranging from overall responses of microorganisms to hydrophobic phases and bulk activity measurements, to the functional diversity of microbial isolates and the role of specific genes in metabolic processes. The protocols have also a high range of applications, from environmental samples, laboratory incubations with sediments, or water samples to enriched or pure cultures, and their application may ensure a comprehensive understanding of the impact of hydrophobic mixtures on the functional (physiological) potential of microbial assemblages.

References

1. Curtis TP, Sloan WT, Scannell JW (2002) Estimating prokaryotic diversity and its limits. Proc Natl Acad Sci U S A 99:10494–10499
2. Eastcott L, Shiu WY, Mackay D (1988) Environmentally relevant physical-chemical properties of hydrocarbons: a review of data and development of simple correlations. Oil Chem Pollut 4:191–216
3. Tissot BP, Welte DH (1984) Petroleum formation and occurrence, 2nd edn. Springer, Berlin

Protocols for the Measurement of Bacterial Chemotaxis to Hydrocarbons

Jayna L. Ditty and Rebecca E. Parales

Abstract

Bacterial chemotaxis is the process by which bacteria sense and respond to environmental stimuli. While the mechanism for chemotaxis has been extensively studied in enteric bacteria, studies in soil bacteria that are attracted to aromatic acids and aromatic hydrocarbons in addition to sugars and amino acids are lacking. Here we describe detailed protocols for the quantitative and qualitative assessment of chemotaxis responses to analyze responses to hydrocarbon and aromatic acid attractants to identify the specific receptors involved.

Keywords: Aromatic hydrocarbons, Attractant, Chemotaxis, Energy taxis, Methyl-accepting chemotaxis protein

1 Introduction

The ability of bacteria to sense chemical gradients in their environment, and move toward the source of an attractant or away from the source of a repellant, is known as bacterial chemotaxis. Chemotaxis has been studied for over 60 years, primarily in the enteric *Escherichia coli* and *Salmonella* model systems. The bacterial chemotaxis system is based on a modified two-component signal transduction system that recognizes extracellular chemicals and relays that information intracellularly to effect a change in flagellar rotation, ultimately resulting in directed cellular movement (reviewed in [1–4]). Briefly, cytoplasmic membrane receptors called methyl-accepting chemotaxis proteins (MCPs) detect the presence of chemoattractant (or repellant) gradients through ligand-binding sites and transmit the binding signal to a soluble two-component relay system (CheA and CheY), which interacts with the flagellar machinery to modify flagellar rotation (Fig. 1). The resulting changes in the direction of flagellar rotation modulate swimming behavior and ultimately the movement toward attractants or away from repellants. In addition to their role in the detection of chemoeffector molecules, the MCPs are involved in adaptation, a

T.J. McGenity et al. (eds.), *Hydrocarbon and Lipid Microbiology Protocols*, Springer Protocols Handbooks, (2017) 7–42,
DOI 10.1007/8623_2015_112, Published online: 08 July 2015

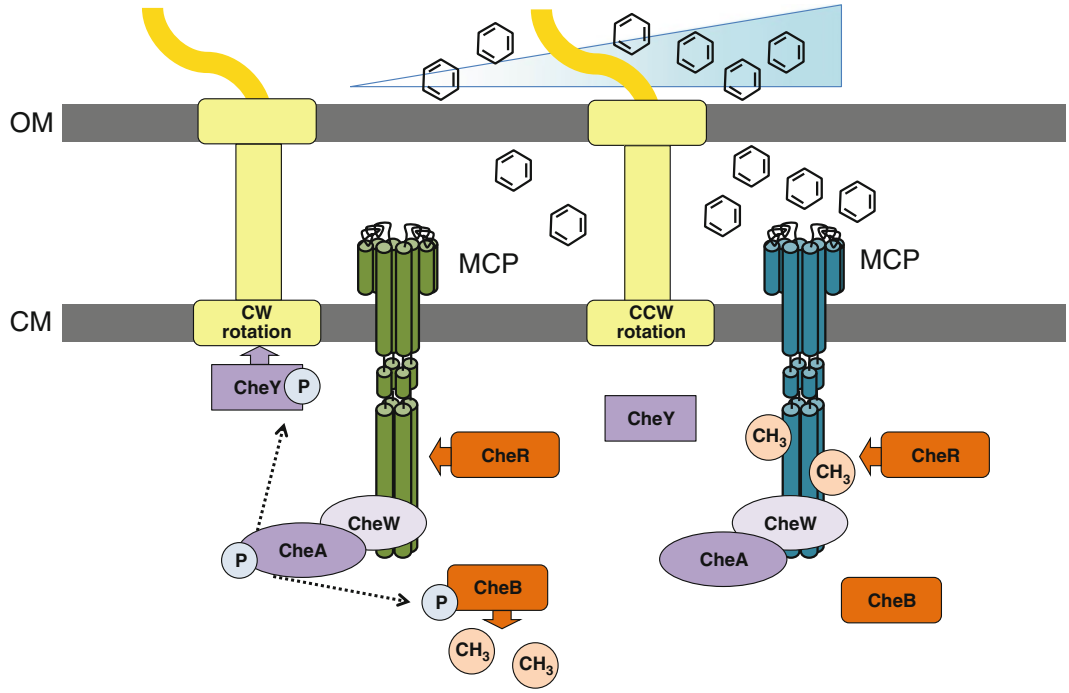

Fig. 1 General mechanism for chemotaxis in bacteria [1–4]. In the absence of attractant (*left*), CheA kinase, which is bound to cytoplasmic membrane chemoreceptors called methyl-accepting chemotaxis proteins (MCPs), actively autophosphorylates. CheA is a member of the two-component CheA-P/CheY-P signal transduction system, which directs clockwise (CW) rotation of the flagellar motor and causes frequent cellular "tumbles" or changes of direction. In the presence of chemoattractant (*right*), MCPs bind effector molecules through a ligand-binding domain located in the periplasm, and the signal is transmitted across the cytoplasmic membrane, causing a decrease in CheA kinase activity. Under these conditions, most of the CheY is unphosphorylated and no longer elicits tumbles, causing the cell to swim for a longer period up the gradient of attractant. A system for adaptation to increasing concentrations of attractant involves methylation of specific glutamate residues on the cytoplasmic side of the MCP by CheR (methyltransferase). In the absence of attractant, methylation by CheR is balanced by methyl group removal by CheB-P, a methylesterase that is active when phosphorylated by CheA-P. In the presence of attractant, CheB is unphosphorylated, and the increased methylation of the MCPs results in a conformational change that increases CheA activity

primitive "memory" mechanism mediated by methylation of specific amino acid residues on the cytoplasmic portion of the MCP that allow bacteria to sense, adapt, and respond to higher concentrations of chemoeffector molecules ranging over five orders of magnitude ([5], Fig. 1).

While many of the components that make up the bacterial chemotaxis system are conserved, the types and numbers of chemoeffectors detected by different bacteria vary widely [6, 7]. For example, *E. coli* has four known MCPs that primarily detect sugars and amino acids and one MCP-like energy taxis receptor (Aer), while soil bacteria such as the pseudomonads, which are known for their broad catabolic abilities, have significantly more chemoreceptor proteins. Based on genomic sequence analyses, *Pseudomonas*

aeruginosa PAO1 (an opportunistic pathogen) has 26 MCP-like genes [8], and *P. putida* F1 (a model strain for bioremediation [9]) has 27 MCP-like genes [10]. Various studies have shown that these and other soil bacteria respond to a wide variety of attractants, including aromatic acids and hydrocarbons [11–21]. The ability of bacteria to sense and respond to aromatic compounds and other pollutants has been linked to enhanced biodegradation of these types of compounds [22–26]. As such, there is significant interest in assessing the chemotactic responses of bacteria to aromatic acids and hydrocarbons.

The protocols for measuring chemotaxis have evolved over the years in response to different assessment needs. Some chemotaxis assays are quantitative, while others are qualitative. While more time-consuming and laborious, quantitative assays are particularly useful for comparing subtle differences in the responses of related strains; for example, partial defects in chemotactic responses often need to be quantified to determine if differences are significant. As a result, appropriate statistical analyses are also necessary. Qualitative assays are useful for the initial demonstration of a response to a chemical, for screening large numbers of chemicals, for determining if a response is inducible, and for screening the responses of large numbers of strains, such as in a search for a chemoreceptor mutant. Most qualitative assays provide a visual result that can be documented photographically using techniques that will be described here.

Oftentimes, the attractant under study also serves as a source of carbon and energy for the bacterial strain, and some of the chemotaxis assays described here require growth of the strain as part of the assay. In such assays, like the soft agar swim plate assay (see below), care must be taken to ensure that growth rates of strains being compared are similar. For example, if comparing the responses of a wild-type strain to a putative chemotaxis mutant, it is important to demonstrate that both strains have similar growth rates on the attractant before concluding that any observed differences are due to chemotaxis defects alone. In some cases, chemotactic responses are metabolism dependent, which can be due to the cell detecting an intermediate in the degradation of the test chemical or a response to the energy obtained when cells are growing on the test chemical. Therefore, assays must be carried out to differentiate between chemotaxis and energy taxis. In energy taxis, the most studied type of receptor (*E. coli* Aer and its orthologs) is a MCP-like protein with a characteristic topology that includes an N-terminal, cytosolic PAS domain followed by a pair of transmembrane regions linked by a short periplasmic loop [27–30]. This topology distinguishes aerotaxis/energy taxis receptors from prototypical chemoreceptors, which possess a periplasmic ligand-binding domain flanked by two transmembrane regions. The PAS domain of Aer detects the intracellular flux of oxidized and reduced

flavin adenine dinucleotide as a proxy for the cellular energy level, and cell behavior is modulated in response [27–30]. Analysis *aer* mutant strains and catabolic mutant strains can be used to differentiate between chemotaxis and energy taxis responses [31, 32].

Depending on the solubility, toxicity, and volatility of a particular attractant, some assays may be more or less useful, and the concentration of hydrocarbon used can be critical. Because of the toxicity of hydrocarbons, some chemicals may be attractants at low to intermediate concentrations and repellants at high concentrations (for an example, *see* Fig. 4b; [21]). As some assays can be used to monitor both positive and negative responses, it is important to test different chemoeffector concentrations and also use different types of assays to determine whether the chemical is being sensed as an attractant or repellant. In fact, it is always recommended that more than one type of assay be used to confirm any new response.

We cannot stress enough that the key to obtaining reliable and reproducible results from any chemotaxis assay is using cultures with a high percentage of motile cells. Use of poorly motile cultures will yield ambiguous data and a high level of frustration, and many of the **Notes** associated with the various chemotaxis assays described below give tips on how to best maintain motile cultures. Highly motile strains can be enriched by repeatedly passing cultures in soft agar plates (described in detail below). If possible, this enrichment for a motile population should be done before chemotaxis studies are initiated. Such cultures can be stored frozen and revived as needed as these cultures should retain a high number of motile cells once they are growing and actively metabolizing. It is highly recommended that this newly selected motile culture (and perhaps it should be given a new or modified strain name different from that of the original isolate) be used as the host strain for any future genetic manipulations (e.g., chemotaxis or metabolic mutants), so that all strains under study are isogenic, and no confounding mutations accumulate under selection in soft agar plates [33].

The chemotaxis protocols described here have simple equipment requirements and can be easily conducted in any microbiological laboratory. The overarching purpose of this chemotaxis protocol chapter is to outline protocols for either swim plate (Sect. 3.1), agar plug (Sect. 3.2), or capillary (Sect. 3.3)-based assays; describe the fundamental theory behind each type of assay and the advantages and limitations of each; and outline which type(s) of chemotaxis assay will best address your chemotaxis question. However, it should be noted that some chemotaxis techniques that require the use of specific equipment are not described in detail here. The following is a brief summary of these assays; please see the associated references for details. Computer-assisted motion analysis allows for the quantitative assessment of both motility and chemotaxis; however, this method requires computer software capable of tracking individual cells. The parameters of such software typically

must be optimized for each bacterial strain due to differences in cell size, shape, and swimming behavior. This assay monitors the swimming paths of individual cells in response to chemoattractants, and behavior is assessed quantitatively in terms of the average number of changes of swimming direction per second for a population of cells. For some bacteria, swimming speed changes (chemokinesis) in response to the attractant, and this can also be assessed using computer-assisted motion analysis [13, 34, 35]. Another version of a computer-assisted technique is the tethered cell assay, which requires specific anti-flagellin antibodies for the organism (or a close relative) under study. Cells are attached to a microscope slide by a single flagellum using the flagellin-specific antibody (multiply-flagellated cells must undergo a sheering process so that each cell on average retains a single flagellum). The direction of flagellar rotation changes in response to addition of a chemoeffector; these changes can be recorded and analyzed. Quantification can be carried out manually by analyzing videos of cells, but software capable of automated quantification makes the process much more efficient [36, 37]. Lastly, microfluidic assays require specially fabricated microfluidic chambers and computer software to analyze cell behavior. This type of assay can be used to test responses to competing gradients of attractants and/or repellants [38–41].

The specificities of MCP receptors for their cognate chemoeffectors have also been investigated via quantitative biochemical assays. For example, fluorescence resonance energy transfer (FRET) has been used to quantify the signal arising from a ligand-induced change in the binding of fluorescently labeled forms of CheY and CheZ. The FRET signal was shown to correlate linearly with chemotaxis [42]. In addition, isothermal titration calorimetry, which is used to detect changes in heat caused by molecular interactions, has been successfully used with purified MCP ligand-binding domains to quantify receptor/chemoeffector interactions [43, 44].

2 Materials

2.1 Swim Plate Assays

2.1.1 Qualitative Swim Plate Assay

1. Noble agar, 0.25 g in 50 ml distilled water (*see* **Note 1**)
2. Concentrated (2×) minimal salts broth (MSB [45]) with 0.1% Hutner's mineral base [46] in 50 ml distilled water (*see* **Note 2**)
3. Autoclave
4. 45°C water bath
5. Sterile stock carbon source
6. Three, 90 × 15 mm Petri dishes
7. Sterile toothpicks
8. Isolated bacterial colonies

9. 30°C incubator
10. Bucket of light (for backlighting) and digital camera (*see* **Note 3**)

2.1.2 Quantitative Swim Plate Assay

1. Overnight bacterial culture (3.0 ml) grown in Luria-Bertani medium [47] (*see* **Note 4**)
2. Noble agar, 0.5 g in 100 ml distilled water (*see* **Note 1**)
3. Concentrated (2×) minimal salts broth (MSB [45]) with 0.1% Hutner's mineral base [46] in 100 ml distilled water (*see* **Note 2**)
4. Autoclave
5. 45°C water bath
6. Sterile stock carbon source(s)
7. Three, 140 × 20 mm Petri dishes
8. Sterile 15 ml centrifuge tubes
9. Centrifuge
10. Sterile MSB medium
11. Sterile 150 × 13 mm glass test tubes
12. Spectrophotometer
13. P10 micropipette (and sterile tips)
14. 30°C incubator
15. Ruler, in mm
16. Bucket of light (for backlighting) and digital camera (*see* **Note 3**)

2.2 Agar/Agarose Plug-Based Assays

2.2.1 Agarose Plug Assay

1. Bacterial culture (10 ml) grown to mid-exponential growth phase (optical density at 600 nm between 0.3 and 0.7)
2. Sterile 150 × 13 mm glass test tubes
3. Spectrophotometer
4. Sterile stock carbon source(s)
5. 1.0 ml aliquots of 2% low-melting temperature agarose (NuSieve GTG Agarose, *see* **Note 5**) suspended in chemotaxis buffer (*see* **Note 6**)
6. Chemotaxis buffer (CB; 50 mM potassium phosphate buffer [pH 7.0], 0.05% glycerol,10 μM EDTA)
7. A few crystals of Coomassie blue
8. 65°C block heater
9. Razor blade
10. Plastic coverslips, 24 × 24 mm
11. Glass microscope slides, 26 × 75 mm

12. Glass coverslips, 24 × 24 mm
13. Phase-contrast microscope with ≥40× objective and 10× ocular objective
14. Sterile, 1.5 ml microfuge tubes
15. Microfuge
16. Sterile, aerated chemotaxis buffer (CB) (*see* **Note 6**)
17. P1000 and P20 micropipettes and sterile tips
18. Sterile stock solution 100 mM glycerol
19. Bucket of light (for backlighting) and digital camera (*see* **Note 3**)

2.2.2 Chemical-in-Plug Assay

1. Bacterial culture (10 ml) grown to mid-exponential growth phase (optical density at 600 nm between 0.3 and 0.7)
2. Sterile 13 × 150 mm glass test tubes
3. Spectrophotometer
4. 10 ml aliquots of sterile 4.0% Noble agar in 16 × 150 mm glass test tube
5. 10 ml aliquots of sterile 2× CB in 16 × 150 mm glass test tube
6. Sterile stock attractant source, 50× to 100× concentration
7. Sterile 90 × 15 mm Petri dish
8. 2.5 ml aliquots of 0.5% Noble agar in CB
9. 40°C block heater
10. Centrifuge
11. 33 × 10 mm Petri plates
12. Sterile P1000 micropipette tip
13. Sterile scissors (sterilize by dipping in ethanol and flaming)
14. Sterile glass rod (sterilize by dipping in ethanol and flaming)
15. Bucket of light (for backlighting) and digital camera (*see* **Note 3**)

2.2.3 Gradient Plate Assay

1. Overnight bacterial culture (5.0 ml) grown in Luria-Bertani medium [47] (*see* **Note 4**)
2. Sterile 13 × 150 mm glass test tubes
3. Sterile minimal salts broth (MSB [45]) with 0.1% Hutner's mineral base [46] in 50 ml distilled water (*see* **Note 2**)
4. Spectrophotometer
5. Noble agar, 0.25 g in 50 ml distilled water (*see* **Note 1**)
6. Concentrated (2×) minimal salts broth (MSB [45]) with 0.1% Hutner's mineral base [46] in 50 ml distilled water (*see* **Note 2**)
7. Autoclave
8. 45°C water bath

9. Sterile stock carbon source
10. Three, 90 × 15 mm Petri dishes
11. 10 ml aliquot of sterile 4.0% Noble agar in 16 × 150 mm glass test tube
12. 10 ml aliquot of sterile 2× CB in 16 × 150 mm glass test tube
13. Sterile stock attractant source, 50× to 100× concentration
14. Sterile 90 × 15 mm Petri dish
15. Sterile P1000 micropipette tips
16. Sterile scissors (sterilize by dipping in ethanol and flaming)
17. Sterile glass rod (sterilize by dipping in ethanol and flaming)
18. Sterile P10 micropipette tips and micropipettor
19. Bucket of light (for backlighting) and digital camera (*see* **Note 3**)

2.3 Capillary-Based Assays

2.3.1 Quantitative Capillary Assay

1. Bacterial culture (100.0 ml) grown to mid-exponential phase (optical density at 600 nm between 0.3 and 0.7)
2. Drummond Microcaps® 1-μl microcapillary tubes and bulb dispenser
3. Sterile glass scintillation vials
4. Sterile stock attractant
5. Two sterile forceps (sterilize by dipping in ethanol and flaming)
6. Bunsen burner and 95% ethanol
7. Sterile chemotaxis chambers: sterile 90 × 15 mm Petri dishes each containing a 25 × 75 mm glass microscope slide, a 22 × 22 mm glass coverslip, and a glass U-tube (*see* **Note 7**)
8. Sterile 13 × 150 mm glass test tubes
9. Sterile, aerated CB
10. Centrifuge
11. Phase-contrast microscope with ≥40× objective
12. Autoclavable squirt bottle containing sterile CB
13. Sterile 13 × 150 mm glass test tubes containing 1 ml CB for a tenfold dilution series
14. Luria-Bertani agar plates [47] or other general growth medium

2.3.2 High-Throughput Quantitative Capillary Assay

1. Bacterial culture (100.0 ml) grown to mid-exponential phase (optical density at 600 nm between 0.3 and 0.7)
2. Melted 3.0% general-purpose agar (about 100 ml)
3. At least 4 sterile 96-well plates (one "microcapillary" plate, one "attractant array" plate, one "cell" plate, and a series of "dilution" plates) and one sterile 96-well plate lid (wash plate)

4. Sterile P200 tip tray spacer
5. Multichannel pipette
6. 96 sterile Drummond Microcaps® 1-μl microcapillary tubes, flame closed on one end (*see* **Note 8**)
7. Vacuum chamber
8. Sterile 13 × 150 mm glass test tubes
9. Sterile, aerated CB
10. Centrifuge
11. Phase-contrast microscope with ≥40× objective
12. Square 120 × 120 mm LB plates

2.3.3 Qualitative Capillary Assay

1. Bacterial culture (100.0 ml) grown to mid-exponential phase (optical density at 600 nm between 0.3 and 0.7)
2. Drummond Microcaps® 1-μl microcapillary tubes
3. 5.0 ml 2% agarose in sterile CB
4. Sterile glass scintillation vials
5. Sterile stock attractant
6. Forceps
7. Bunsen burner and 95% ethanol
8. Chemotaxis chambers: a 90 × 15 mm glass Petri dish containing a 25 × 75 mm glass microscope slide, a 22 × 22 mm glass coverslip, and a glass U-tube (*see* **Note 7**)
9. Sterile 13 × 150 mm glass test tubes
10. Sterile, aerated CB
11. Centrifuge
12. Phase-contrast microscope with 4× and ≥40× objective, 10× ocular objective, and capability for negative contrast pseudo dark-field or oblique dark-field settings (*see* **Note 9**) equipped with a digital camera

3 Methods

The methods described here are grouped based on the source of the attractant. For example, in all swim plate assays (*see* Sect. 3.1), metabolism of the attractant by the bacterial cells is required in order to generate the concentration gradient that is sensed by the bacteria. In plug assays (*see* Sect. 3.2), the attractant is diffusing from a semisolid plug made of agar or agarose, and metabolism of the attractant chemical is therefore not required. Finally, in capillary-based assays (*see* Sect. 3.3), the chemical is diffusing from a microcapillary, and again, metabolism of the chemical is not required.

3.1 Swim Plate Assays

3.1.1 Qualitative Swim Plate Assay

Soft agar swim plate assays were first developed by Julius Adler to study chemotaxis in *E. coli* [48]. The assay is based on the ability of bacteria to detect metabolizable carbon sources in their environment. Bacterial cells are stabbed with a toothpick into the center of a Petri dish containing soft agar through which bacterial cells can swim (*see* **Note 10**), and a low concentration of attractant such that movement of the cells is necessary for the acquisition of carbon and energy source. A chemotactic response is visualized as a sharp ring of growth that forms as the bacteria move outward from the original point of inoculation as they multiply in number and swim through the agar, following the gradient of attractant created as they metabolize the compound.

The qualitative swim plate assay is very easy to set up and execute, and the responses of multiple strains can be compared on the same plate (Fig. 2a). Swim plates can be used to enrich for generally non-chemotactic and/or nonmotile mutants by sequentially transferring cells that do not move out from the point of inoculation and are also useful for the enrichment of chemoreceptor mutants [15, 49, 50]. This can be done following chemical or transposon mutagenesis, or the process can be used to identify spontaneous mutants. Once several transfers have been carried out, one should streak for single colonies on an appropriate medium and test individual colonies for the desired phenotype. Conversely, swim plates are recommended for the enrichment of highly motile populations of bacteria (*see* **Note 11**). A rich medium can be used for these swim plates (*see* **Note 12**), whereas a minimal medium should be used for analyzing responses to specific carbon sources.

The disadvantage of this assay is that only compounds that are metabolized by the bacterium of interest can be used as attractants, as the assay requires that the cells create their own chemical concentration gradient by metabolizing the attractant present in the soft agar medium. As noted in the introduction, since the response of cells to the attractant involves both growth and chemotaxis, only cultures with similar growth rates on the attractant under study can be compared using this assay. In addition, attraction to volatile aromatic hydrocarbons can be difficult to assess via this assay due to the requirement for a gradient to be generated in the agar plate.

1. Prepare swim plates by autoclaving the 50 ml Noble agar solution and 50 ml 2× minimal salts broth (MSB; 40 mM phosphate, pH 7.3; 0.1% ammonium sulfate; 0.1% rather than 1% Hutner's mineral base [46, 50] in separate Erlenmeyer flasks (*see* **Note 13**). After sterilization, cool to 45°C in a water bath.
2. Add the stock carbon source to the MSB salts solution to the appropriate final concentration (0.5–2.0 mM; *see* **Note 14**). Add the MSB salts solution to the Noble agar solution and mix.

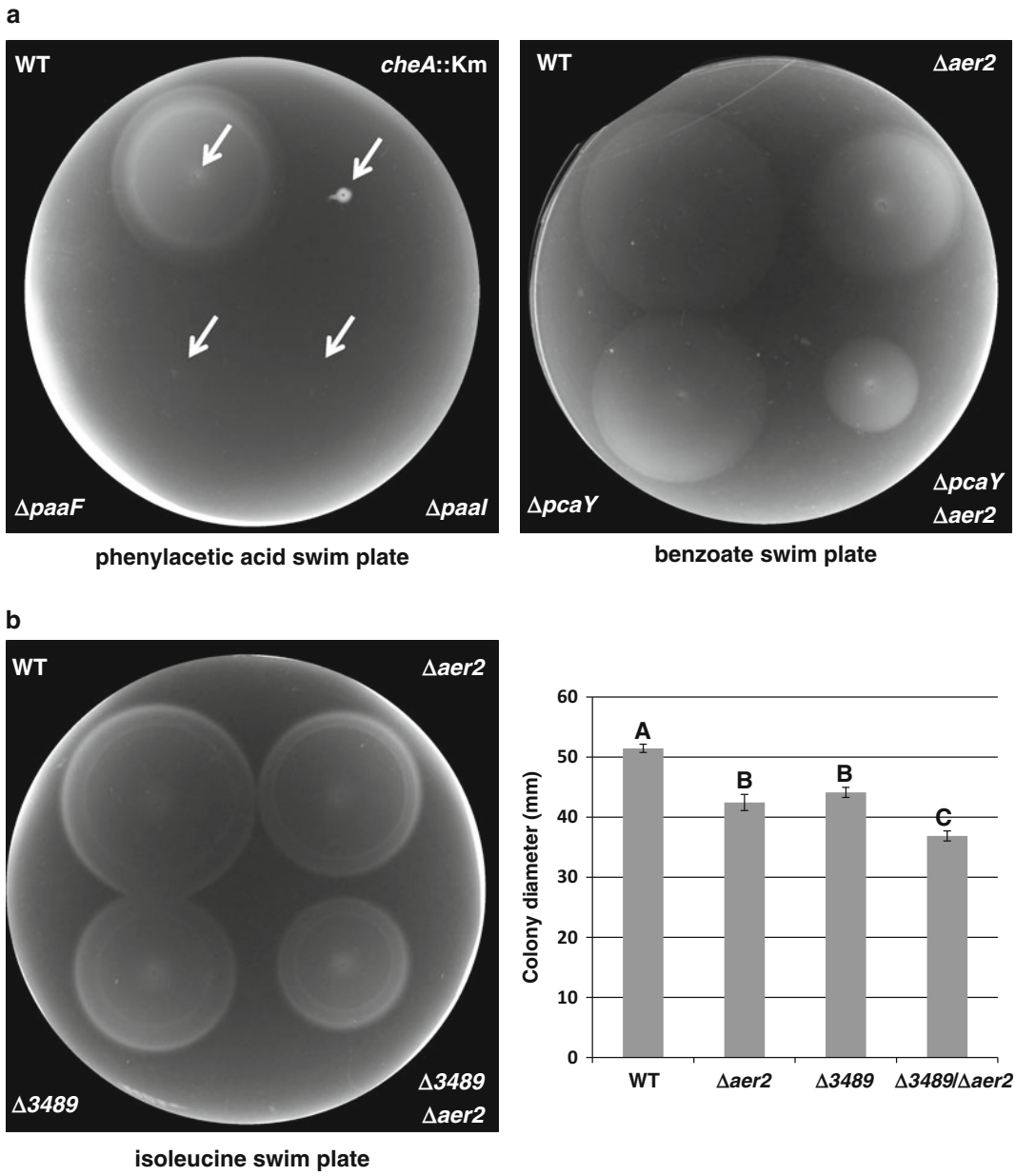

Fig. 2 Representative swim plate assay results. In these assays a chemotactic response is visualized as a sharp ring of growth that forms as the bacteria move outward from the original point of inoculation (center of the ring of growth, indicated by arrows) as they multiply in number and swim through the agar, following the gradient of attractant created as they metabolize the compound. (**a**) Qualitative swim plate assays. A representative image of *Pseudomonas putida* strains in soft agar (0.3%) containing 1 mM phenylacetic acid is shown (*left panel*). WT, wild-type strain *P. putida* F1; *cheA*::Km, a generally non-chemotactic strain with an insertionally inactivated *cheA* gene [31] can grow on the metabolizable carbon source but cannot respond; catabolic mutant derivatives of strain F1, Δ*paaF* and Δ*paaI* [31], are unable to grow on phenylacetic acid, and as metabolism of the test attractant is required for the analysis of chemotaxis by the swim plate method, the responses of these mutants cannot be evaluated with this assay. Qualitative swim plate assays comparing

3. Pour approximately 33 ml into individual 90 × 15 mm Petri dishes (*see* **Note 15**), and allow the plates to solidify at room temperature. The medium is only semisolid and plates must be handled very carefully and *never inverted* to avoid disturbing the agar.
4. Using a sterile toothpick, pick one colony and stab it into the agar at the center of the plate in a vertical motion. Alternatively, if comparing responses of multiple strains, stab a colony of each strain at equally spaced locations – typically up to four colonies can be compared on a single plate.
5. Place the swim plates in a 30°C incubator, *right side up* (*see* **Note 16**) and incubate until colonies form, typically 16 to 24 h (*see* **Note 17**).
6. After incubation, visually observe the swim plate for the presence or absence of a large, circular bacterial colony that migrated from the original point of inoculation (*see* **Note 18**).
7. Digitally record results from each trial for each condition by taking images with backlighting (*see* **Note 3**).

3.1.2 Quantitative Swim Plate Assay

Responses obtained in swim plate assays can also be quantified by carefully controlling the amount of cells inoculated and measuring either the final diameter of the growth ring or the rate of ring formation (Fig. 2b, left panel). Multiple replicate plates should be inoculated, diameters measured and averaged, and statistical analyses should be conducted (Fig. 2b, right panel) to demonstrate significant differences in attraction when assessing different strains [10]. In this assay the attractant is also the carbon and energy source, so the colony size results from a combination of both growth and chemotaxis. It is therefore important to inoculate equivalent numbers of cells and to confirm that the growth rates of any strains being compared are the same on the carbon source(s) under study before concluding that phenotypic differences are due specifically to chemotaxis defects. If growth rates with the compound differ in liquid medium, an additional chemotaxis assay that does not involve metabolism should be used [10]. When comparing multiple strains, the best results are obtained when the responses of various strains

Fig. 2 (continued) wild type and receptor mutants is shown (*right panel*). A soft agar plate containing 1 mM benzoate was inoculated with the wild-type *P. putida* F1 (WT), the energy taxis mutant Δ*aer2* [31], Δ*pcaY*, a mutant lacking the aromatic acid chemoreceptor [71], and the double mutant lacking both *pcaY* and *aer2*. The single Δ*pcaY* and Δ*aer2* mutants show a slightly reduced colony size on benzoate compared to wild type, whereas the double mutant shows a more significant defect. (**b**) Quantitative swim plate analyses. The colony diameters ($n \geq 3$) from quantitative isoleucine (1 mM) swim plates were measured (representative plate shown in the left panel). Means with the same letter are not significantly different ($p < 0.05$; one-way ANOVA, Tukey multiple comparison test)

are assessed on the same plate (*see* **Note 19**). Quantitative swim plate assays can be carried out in standard 90 × 15 mm Petri dishes, but colony size differences are often more obvious when large diameter Petri plates (140 × 20 mm) are used.

1. Inoculate cells in 3.0 ml of LB or other relevant medium and allow cultures to grow for 18 to 24 h prior to the experiment.
2. Prepare swim plates as described in **steps 1** to **3** in Sect. 3.1, except increase the total volume to 200 ml to pour three, 140 × 20 mm Petri plates.
3. Using sterile 15 ml centrifuge tubes, harvest cells from each overnight culture by centrifugation at 4,500 rpm for 5 min (*see* **Note 20**).
4. Remove the supernatant and add 5.0 ml of MSB medium and gently resuspend the cells by inversion (*see* **Note 21**).
5. Transfer 3.0 ml of each resuspended culture into sterile 13 × 150 mm glass test tubes and adjust the optical density at 600 nm to 0.40 ± 0.02 using sterile MSB medium (*see* **Note 22**).
6. Using a micropipette, remove a 2.0 μl aliquot of the resuspended cells from **step 5** and inoculate into the swim plates (*see* **Note 23**).
7. Place the swim plates in a 30°C incubator, right side up (*see* **Note 16**), and incubate for 16–24 h (*see* **Note 17**).
8. After incubation, visually observe the swim plate for the presence or absence of large, circular bacterial colonies that migrated from the original point of inoculation (*see* **Note 18**). Measure the diameter of the swim ring (in mm) from at least triplicate experiments.
9. Digitally record results from each trial for each condition by taking images with backlighting (*see* **Note 3**).

3.2 Agar/Agarose Plug-Based Assays

3.2.1 Agarose Plug Assay

Chemotaxis can be visualized qualitatively with the agarose plug assay [51]. This assay is useful for testing responses to volatile hydrocarbons, such as toluene, which are fairly soluble in aqueous medium [21]. In this assay, molten agarose containing the chemical to be tested is allowed to solidify between a microscope slide and a coverslip supported by two plastic strips (Fig. 3a). A suspension of motile cells is then introduced into the chamber surrounding the agarose plug. A response is indicated by the accumulation of a band of cells around the outside of the agarose plug, which may be immediately adjacent to the plug or somewhat further away (Fig. 3b). The location of the band of cells depends on the chemical concentration and whether it is being sensed as an attractant or a repellant. Responses can typically be seen within 5 min, and the assay does not involve growth on the compound. It does, however,

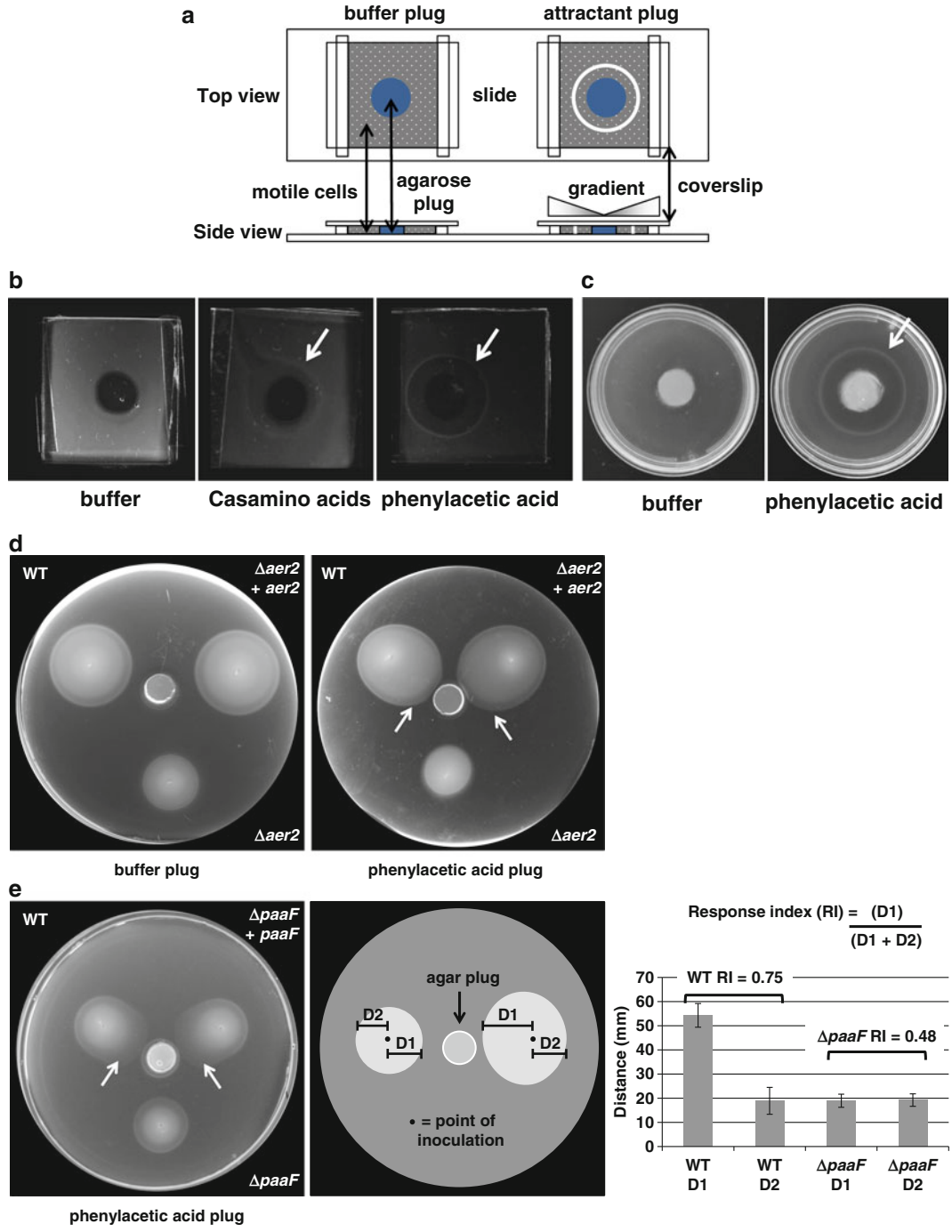

Fig. 3 Representative agar/agarose plug-based assays. (**a**) Graphical representation of an agarose plug assay. (**b**) Qualitative chemotactic response of *P. putida* F1 to 2% Casamino acids (*center panel*) and 5 mM phenylacetic acid (*right panel*), relative to an agarose plug containing buffer alone (*left panel*, negative control). The white arrows indicate a chemotactic response, which is visualized as a white ring of cells accumulating at the optimum attractant concentration that diffused away from the center plug. (**c**) Response

yield best results if the culture is very motile, so care should be taken when harvesting cells for the assay. Since repellants can elicit a response in the assay, an alternative assay should be carried out to definitively determine whether the hydrocarbon is being sensed as an attractant or a repellant.

The advantages of the qualitative agarose plug assay are that it is relatively quick and easy to set up, making it particularly useful for screening many isolates or mutant strains for responses or for screening responses to several different chemicals. This assay can be used to determine if a chemotactic response is inducible by pre-growing the cells in appropriate medium. In addition, the response is obvious to the naked eye, and it can be easily documented via digital imagery using backlighting [52] (*see* **Note 3**). A disadvantage is that some brands/batches of low-melting temperature agarose contain compounds that elicit chemotactic responses. It is therefore essential to set up control assays with plugs containing only buffer for every set of experiments.

1. Inoculate cells in an appropriate medium (10 ml) and grow the cells to mid-exponential growth phase to an optical density at 600 nm between 0.3 and 0.7 (*see* **Note 24**).
2. Prepare 10× stock solutions of control and test attractants and/or repellants (*see* **Note 25**). Set the stock solutions aside until use in the assay.
3. Melt 1.0 ml aliquots of 2% low-melting temperature agarose in a 65°C block heater. Add a few crystals of Coomassie blue and suspend (*see* **Note 26**). Keep the agarose molten until use in the assay.
4. Prepare the agarose plug chambers. Using a razor blade, score plastic coverslips into four equal strips and split. Set two plastic strips approximately 16 mm apart on a glass microscope slide. Place a glass coverslip on top of the two plastic strips for each chamber, making sure the edges of the glass coverslip will cover

Fig. 3 (continued) of *P. putida* F1 to 5 mM phenylacetic acid (*right panel*) as assessed by chemical-in-plug assays relative to a buffer control (*left panel*). The white arrow indicates a chemotactic response which is visualized as a white ring of cells accumulating at the optimum attractant concentration that diffused from the center plug. (**d**) Analysis of wild-type *P. putida* F1 (WT), the energy taxis mutant (Δ*aer2*), and the complemented mutant (Δ*aer2* + *aer2*) [31] to phenylacetic acid in gradient plug assays (*right panel*) compared to a buffer plug control (*left panel*). The white arrows indicate positive chemotaxis responses, which are visualized as oblong colonies growing toward the attractant-containing plug. Representative images from experiments conducted in triplicate are shown. (**e**) Quantitative analysis of gradient plate assays. Analysis of wild-type *P. putida* F1 (WT), the phenylacetic acid metabolic mutant (Δ*paaF*), and the complemented mutant (Δ*paaF* + *paaF*) to phenylacetic acid via gradient plug assays. One representative image ($n \geq 3$) is shown (*left panel*). Graphical representation showing the measurements taken for quantitative gradient plate assays (*center panel*). The D1 and D2 distances were averaged and used to calculate the response index (RI) for the wild-type *P. putida* F1 (WT) and Δ*paaF* catabolic mutant (*right panel*)

one-half of each plastic strip. Set the chambers aside until use in the assay.

5. Once the cells have reached exponential phase, check the culture for motility using a phase-contrast microscope (*see* **Note 27**).
6. Harvest cells in sterile 1.5 ml microfuge tubes. Harvest enough cell material to obtain 1.0 ml of cells with an optical density of 0.7 at 600 nm (*see* **Note 28**). To harvest the cell pellet, spin cells in a microcentrifuge for 3 min at 5,000 rpm (*see* **Note 20**).
7. Wash the cell pellet by removing the supernatant and gently resuspending the cells in 1.0 ml of sterile, aerated CB (*see* **Notes 6** and **21**) followed by centrifugation for 3 min at 5,000 rpm. Repeat this step to ensure that any residual carbon source or attractant has been removed from the cell suspension.
8. After the washes, gently resuspend the cell pellet in a final volume of 1.0 ml of aerated CB, and verify that the cell culture is motile via microscopy (*see* **Note 27**).
9. To prepare the agarose plug mixture, transfer 18 μl of the molten 2% low-melting temperature agarose into a sterile microfuge tube and add 2.0 μl of the 10× stock attractant or repellent solution and mix.
10. Remove the glass coverslip from the plug chamber. Quickly, aliquot 12 μl of the agarose plug mixture onto the glass microscope slide, centered between the two plastic strips. Wait approximately 30 s to allow the plug to cool slightly before covering with the glass coverslip. Allow the agarose to completely cool and solidify between the slide and coverslip for about 4 min before initiating the assay (*see* **Note 29**).
11. To initiate the agarose plug assay, flood the chamber with approximately 230 μl of the motile cell suspension and record the time. Make sure to completely fill the chamber with cells (*see* **Note 30**).
12. Allow the assays to incubate at room temperature (typically from 5 to 15 min, *see* **Note 31**) and then visually observe the area around the agarose plug for the presence or absence of a visible white ring of accumulated cells (*see* **Note 32**).
13. Digitally record results from each trial for each condition taking images with backlighting (*see* **Note 3**).
14. After the assay is complete, place the agarose plug chamber under the phase-contrast microscope to verify that the cells are still motile (*see* **Note 33**).

3.2.2 Chemical-in-Plug Assay

The chemical-in-plug assay was originally designed to detect and assess repellant responses in *E. coli* [53]. In these assays, a 2% Noble agar plug containing a repellant is placed on top of motile cells

suspended in 0.25% agar. A repellant response will result in the development of a clear area around the plug within approximately 30 min. Measurements of the distance from the plug to the ring have been used to generate concentration-response curves. Adaptations made to the original assay have allowed for the measurement of positive chemotaxis (Fig. 3c) in Petri dishes with an agar plug containing an attractant [31, 54]. Similar to the agarose plug assay, a positive chemotactic response is indicated by the formation of a dense ring of cells around or near the agar plug.

The advantages of the qualitative chemical-in-plug assay are similar to those of the agarose-plug assays. Responses do not require growth and can generally be seen within 30–60 min; therefore, the assay is useful for testing whether a response is inducible by pre-growing cultures under different conditions. In addition, since these assays are conducted using a suspension of motile bacteria in a Petri dish, it is possible to test multiple agarose plugs with different attractants in the same plate [54]. Finally, the cell responses are more stable because the cells are suspended in a low concentration of agar, making it easier to transport plates to a camera for documentation. It has been suggested that nonmotile and/or non-chemotactic mutant strains be used as negative controls for this assay, as false positive chemotactic responses have been observed using this method [55]. The protocol described here was designed to test one attractant in small-diameter (33 × 10 mm) Petri dishes [31].

1. Inoculate cells in 10 ml of an appropriate medium and grow the cells to mid-exponential growth phase to an optical density of 0.5 at 600 nm (*see* **Note 24**).
2. Prepare 2.0% agar plugs by first autoclaving 10 ml of 4.0% Noble agar in 16 × 150 mm glass test tubes. Keep the agar molten in a 40°C water bath. Add 10 ml of 2× CB for a final volume of 20 ml. Introduce the appropriate amount of attractant, repellent, or CB for the desired final concentration into a 90 × 15 mm Petri dish. Pour the 20 ml of 2% CB-Noble agar into the Petri dish (to an approximate depth of 5.0 mm) and swirl plate gently to mix the attractant with the agar (*see* **Note 34**).
3. Prepare the 2.5 ml aliquots of molten 0.5% Noble agar.
4. Once grown, collect a cell pellet from approximately 2.5 ml of the culture by centrifugation at 4,500 rpm for 5 min (*see* **Note 20**).
5. Decant the supernatant and gently resuspend cells by inversion with 2.5 ml 2× sterile, aerated CB (*see* **Notes 6** and **21**). Check for cell motility (*see* **Note 27**).

6. Mix the cell suspension by inversion with 2.5 ml of the molten 0.5% Noble agar, and pour the suspension into a 33 × 10 mm Petri plate.
7. Cut the tip off of a sterile P1000 micropipette tip. Using the uncut sterile end, excise a 2% agarose plug. Using a sterile glass rod, gently push the agar plug out of the micropipette tip and into the center of the Petri dish containing the cell suspension.
8. Allow the assays to incubate at room temperature for 30 min–1 h (*see* **Note 35**) and then visually observe the area around the agarose plug for the presence or absence of a visible white ring of accumulated cells.
9. Digitally record results from each trial for each condition taking images with backlighting (*see* **Note 3**).

3.2.3 Gradient Plate Assay

This assay combines aspects of the swim plate (*see* Sect. 3.1.1) and chemical-in-plug assay (*see* Sect. 3.2.2), allowing for the detection of responses to attractants that are not metabolized by the test organism [31, 56]. Although only compounds that serve as growth substrates can be tested as chemoattractants in the swim plate assay, this related gradient plate assay can be used to test chemotaxis to metabolizable or nonmetabolizable chemicals. The attractant is provided in an agar plug that is placed on the surface of a soft agar plate containing a medium with a carbon and energy source, preferably a weak or non-attractant for the bacteria. Cultures are inoculated approximately 2.0 cm from the attractant plug, and if the compound diffusing from the plug is sensed as an attractant, an oblong colony grows in the direction of the plug (Fig. 3d). A chemotactic response can typically be seen in 20–24 h depending on the strain, growth substrate, and attractant. Since nonmetabolizable substrates can be used, this assay can test responses of catabolic mutants as well as structural analogues of metabolizable compounds. Since the cells are growing during the assay, less care to maintain motile cultures is required. The response to the attractant can be quantified (Fig. 3e) by calculating a response index (RI), where the distance from the point of inoculation to the edge of the colony growth closest to the agar plug (D1) is divided by the sum of D1 and the distance from the point of inoculation to the edge of the colony growth farthest from the agar plug (D2). Calculated RI values greater than 0.52 and less than 0.48 were shown to correspond to attractant and repellent responses, respectively, while intermediate values represented nonresponses [56].

1. Inoculate cells in 5.0 ml of LB or other appropriate growth medium and place into the 30°C shaking incubator approximately 24 h prior to the experiment.
2. Prepare swim plates as described in **steps 1–3** in Sect. 3.1.1, but add sterile glycerol (or other appropriate carbon and energy source) to a final concentration of 1 mM.

3. Prepare agar plugs as described in **step 2** in Sect. 3.2.2.
4. Harvest a cell pellet from 3.0 ml of the overnight culture in sterile centrifuge tubes by centrifugation at 4,500 rpm for 5 min.
5. Remove the supernatant and add 5.0 ml MSB medium and resuspend the cells by inversion or pipetting.
6. Transfer 3.0 ml of the resuspended cells into a sterile 13 × 150 mm glass test tube and adjust the optical density to 0.5 at 600 nm using sterile MSB medium.
7. Cut the tip off of a sterile P1000 micropipette tip. Using the uncut sterile end, excise a 2% agarose plug. Using a sterile glass rod, gently push out the agar plug and place it onto the center of the Petri dish containing the solidified soft agar medium.
8. Inoculate the swim plates by pipetting 2.0 μl of the cell suspension from **step 7** 2.0 cm away from the center of the placed agar plug (*see* **Note 36**).
9. Incubate at 30°C for 20–24 h (*see* **Note 17**) and then visually observe the area around the point of inoculation and the agar plug. A positive response is indicated by an oblong colony migrating from the point of inoculation toward the agar plug.
10. Digitally record results from each trial for each condition taking images with backlighting (*see* **Note 3**).
11. For quantitative results, carry out at least three replicates and measure the radius of the colony toward and away from the plug for each strain. Calculate RI as shown in Fig. 3e (*see* **Note 37**).

3.3 Capillary Assays

3.3.1 Quantitative Capillary Assay

Chemotactic behavior can also be measured quantitatively by assessing the number of individual cells that respond to an attractant using the capillary assay [48, 57]. A microcapillary tube containing a solution of attractant is placed into a suspension of motile bacteria housed in a chemotaxis chamber (*see* **Note 38** and Fig. 4a). As the attractant diffuses from the mouth of the microcapillary tube into the surrounding medium, a concentration gradient of the attractant is formed. Chemotactic cells then respond to the concentration gradient by swimming up the gradient, and if the concentration is optimal inside, the cells will enter and accumulate in the microcapillary tube. This assay can also be used to assess repellant responses, as fewer cells accumulate in the microcapillary relative to the buffer controls (*see* Fig. 4b). A modified version of the capillary assay has also been used for the quantitative measurement of negative chemotaxis (*see* **Note 39**). After an incubation ranging from 30 to 60 min, the microcapillary tube is removed from the chemotaxis chamber, and the number of cells it contains is enumerated by serial dilution in sterile minimal medium followed by spreading on appropriate plates to determine colony-forming

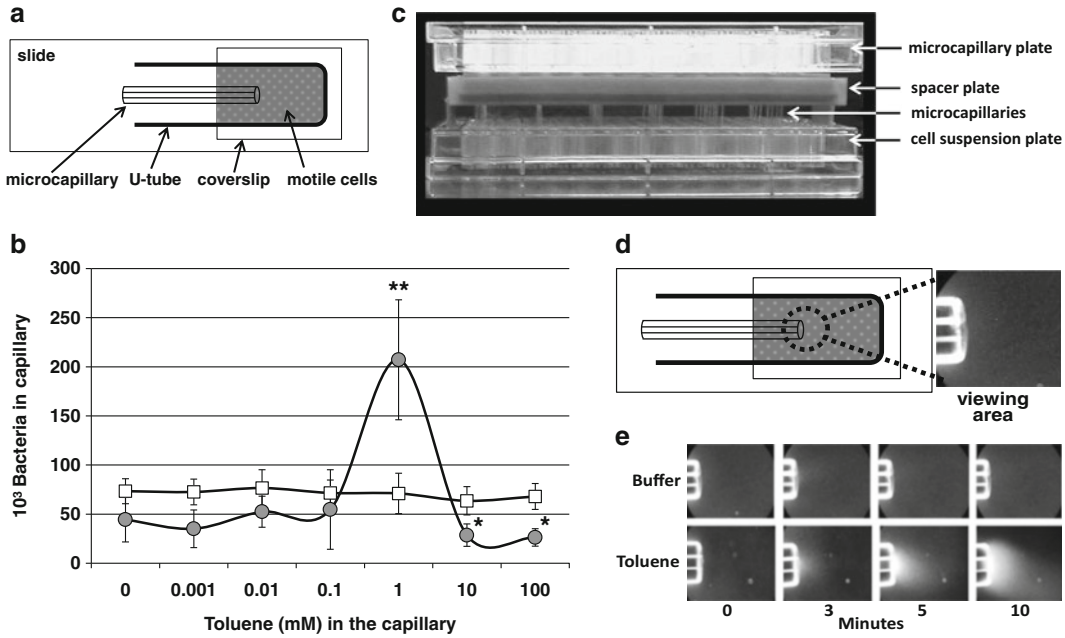

Fig. 4 Representative capillary-based assays. (**a**) Graphical representation of a quantitative capillary assay set up. (**b**) Quantitative chemotactic response of *P. putida* F1 to toluene shown in a concentration-response curve. Capillary assays were performed using 1 μl microcapillary tubes containing various concentrations of toluene suspended in chemotaxis buffer. The number of bacteria that migrated into each microcapillary was calculated by carrying out serial dilutions of the capillary contents. The resulting colonies were counted and used to calculate the number of bacteria present in the microcapillaries containing each concentration of toluene ($n \geq 15$), for both uninduced (grown in minimal medium containing pyruvate; *white squares*) and induced (grown in minimal medium containing pyruvate and toluene vapor; *gray circles*) cells. A significantly greater number of induced *P. putida* F1 cells were present in capillaries containing 1 mM toluene ($p < 0.05$, two-way ANOVA, Tukey multiple comparison test) compared to buffer alone and all other toluene concentrations tested, demonstrating an inducible response to this concentration (*double asterisk*). Significantly lower numbers of induced *P. putida* F1 accumulated in capillaries containing 10 and 100 mM toluene (both concentrations over the limit of solubility) compared to the uninduced cells ($p < 0.05$, *single asterisk*) and the buffer control, demonstrating an inducible repellant response to these high toluene concentrations. (**c**) Image of a high-throughput chemotaxis assay setup. (**d**) Graphic representation of a qualitative capillary assay setup. The main difference in qualitative assays is that the microcapillary is filled with attractant in a solid form, and the accumulation of cells responding to the attractant diffusing from the capillary are visualized by microscopy in the viewing area. (**e**) Response of induced *P. putida* F1 to a saturating concentration of toluene (*lower panels*) as assessed in qualitative capillary assays by dark-field microscopy relative to a buffer control (*top panels*). The white accumulation of cells at the tip of the microcapillary (viewing area) indicates a positive chemotactic response to toluene (saturated) over a 10 min time course

units (CFU)/ml to quantify the chemotactic response. A strong chemotactic response can even be visible to the naked eye as a white cloud of cells that accumulate around the mouth of the microcapillary tube. One can also use the capillary assay to qualitatively assess chemotaxis by direct observation (*see* Sect. 3.3.3).

Although the quantitative capillary assay is rather tedious and time-consuming, it provides a direct quantitative measurement of

the response of a population of bacterial cells to a gradient of attractant, which is what cells encounter in their natural environment. This assay can be used to determine the threshold concentration detected as well as the optimum concentration for the response by testing a range of attractant concentrations, which can be plotted in a concentration-response curve [15, 58]. In addition, when cells are grown under the appropriate conditions, this method can be used to determine if a response to a particular attractant is constitutive or inducible [15, 59–61]. Several biological and technical replicates should be carried out to obtain statistically significant results, and appropriate statistical analyses should be conducted to determine significant differences between concentration responses. Although the capillary assay is quite sensitive, the cells must be very motile to obtain reproducible results; therefore, checking the motility of washed cells is critical (*see* **Note 27**). In addition, if the cells lose motility over the course of the experiment, the results are not valid.

1. Inoculate cells in 100 ml of an appropriate medium and grow the cells to mid-exponential growth phase to a cell density between 0.3 and 0.7 at 600 nm (*see* **Note 24**).
2. Fill 1.0 μl microcapillary tubes with attractant or buffer as follows (*see* **Note 40**). Add 5.0 ml of sterile CB or attractant in CB to a sterile glass scintillation vial. Using sterile forceps, pick up a sterile 1.0 μl microcapillary tube and flame one end in a Bunsen burner until the end is melted closed and becomes red hot. Swipe the length of the microcapillary through the flame twice (*see* **Note 41**), and place the open end in the scintillation vial containing the attractant of interest. Repeat until you have enough filled capillaries for all planned test and control experiments plus a few extra just in case.
3. Set up the appropriate number of the chemotaxis chambers: a sterile glass U-tube sandwiched between a glass microscope slide and glass coverslip inside a sterile 90 × 15 mm glass Petri dish (*see* **Notes 7**, **38** and **42**).
4. Harvest cells from 10 ml of the bacterial culture in sterile centrifuge tubes by centrifugation at 4,500 rpm for 5 min (*see* **Note 20**).
5. Remove the supernatant and gently resuspend the cells in 5.0 ml sterile, aerated CB by inversion (*see* **Notes 6** and **21**).
6. Harvest the cells from **step 5** by centrifugation at 4,500 rpm for 5 min. Gently resuspend cells to an optical density of 0.1–0.15 at 600 nm in sterile, aerated CB. Check for cell motility (*see* **Note 27**).
7. Fill a chemotaxis chamber with the motile cell suspension.

8. Insert the capillary into the cell suspension (*see* **Notes 43** and **44**) and replace the lid of the Petri dish. Make note of the start time and incubate for 30 min at 30°C (or relevant temp/ time).
9. Repeat **steps 7–8** for each assay. Assays for each attractant and control should be conducted in triplicate.
10. After incubation, remove the microcapillary using sterile forceps and rinse excess cells from the outside of the capillary by rinsing with sterile CB.
11. Using an additional set of sterile forceps, break off the closed end of the microcapillary and expel the contents into the first tube of a tenfold serial dilution series (*see* **Note 45**). Place the chemotaxis chamber under the phase-contrast microscope to verify that the cells are still motile.
12. Complete the series of tenfold dilutions (*see* **Note 46**) and mix well. Plate aliquots onto duplicate LB plates and repeat for all dilutions.
13. Incubate at 30° for 24 h (or appropriate temperature/time). Count colonies from plates that have between 30 and 300 colonies, and calculate the response in CFUs/ml taking into account the dilution factor.

3.3.2 High-Throughput Quantitative Capillary Assay

One of the major drawbacks to the quantitative capillary assay is that it can be tedious and time consuming; however, the use of the high-throughput 96-well microtiter plate format capillary assay eliminates some of the time-consuming steps and also allows more replicates to be carried out simultaneously (Fig. 4c). This assay is based on the method developed by Bainer et al. [62] for *E. coli* and allows for multiple chemotaxis assays to be conducted at the same time [60]. Basically, microcapillaries that are sealed and suspended in a 96-well plate with 3% agar are filled with buffer or an attractant under vacuum. The plate with suspended microcapillaries is inserted into the wells of a second 96-well plate prefilled with a motile bacterial cell suspension with an empty sterile pipette tip tray inserted between the plates as a spacer. After incubation, the plate with the suspended microcapillaries is removed and the contents of each capillary are collected, diluted, and enumerated as CFUs by plate counts. This assay is designed for up to 96 simultaneous quantitative capillary assays to be conducted; the number of assays can be modified for your needs.

1. Inoculate cells in 100 ml of an appropriate medium and grow the cells to mid-exponential growth phase to an optical density between 0.3 and 0.7 at 600 nm (*see* **Note 24**).
2. Prepare the microcapillary plate by melting 100 ml of 3.0% agar and distribute 300 µl into each well of a 96-well plate using a multichannel pipettor (*see* **Note 47**). Allow agar to solidify.

3. Prepare the attractant array plate by distributing 100 μl of the attractant or CB into each well of a sterile 96-well plate (*see* **Note 40**).
4. Embed the flame-sealed end of the empty, sterilized and flame-sealed microcapillary tubes into each pad of agar in the microcapillary plate using sterile forceps (*see* **Note 48**).
5. Invert the microcapillary plate on top of the attractant array plate and completely submerge the microcapillaries in the solutions such that they are touching the bottom of the wells (*see* **Note 49**), forming a plate sandwich.
6. Fill the microcapillaries with solution by placing the plate sandwich in a vacuum chamber [63]. Pull a vacuum for 1 min (*see* **Note 50**).
7. Harvest 10 ml of the cells from **step 1** by centrifugation at 4,500 rpm for 5 min (*see* **Note 20**).
8. Gently wash and resuspend cells (*see* Sect. 3.2.1, **step 7**) to an optical density of 0.1–0.15 at 600 nm in sterile, aerated CB (*see* **Note 6**). Check for cell motility (*see* **Note 27**).
9. Prepare the cell plate by pipetting 300 μl of the washed cell suspension into each well of a 96-well plate (cell suspension plate). Invert a sterile P200 tip tray (spacer plate) on top of the cell suspension plate to serve as a spacer between the cells and the microcapillaries.
10. Remove the microcapillary plate from the plate sandwich and wash excess attractant solution from the outside of the microcapillaries by swirling the plate for 5 s in a sterile microtiter plate lid filled with sterile CB. Visually inspect the tips of the microcapillaries to ensure no air bubbles were inadvertently introduced (*see* **Note 44**).
11. Invert the microcapillary plate and submerge the microcapillaries through the spacer plate and into the cells of the cell suspension plate such that the tips of the microcapillaries are suspended in the middle of the cell suspensions.
12. Incubate at room (or other) temperature for 30–60 min depending on your strain and attractant. During this incubation period, prepare the first dilution plate by pipetting 200 μl of sterile CB into each well of a 96-well plate. For each subsequent tenfold dilution plate, dispense 180 μl of sterile CB into each well of a 96-well plate (*see* **Note 46**).
13. Remove the microcapillary plate and wash excess cells from the outside of the microcapillaries by swirling the plate for 5 s in a sterile microtiter plate lid filled with sterile CB.
14. Remove the microcapillaries from the agar pads using sterile forceps and place the tip end down into the respective wells of

the first dilution plate. Using an additional set of sterile forceps, break off the closed end of the microcapillary and expel the contents into the respective wells of the first dilution plate (*see* **Note 45**). Place a sample of the cells under the phase-contrast microscope to verify that the cells are still motile (*see* **Note 33**).

15. Complete the series of tenfold dilutions in the prepared 96-well plates (*see* **step 13**) using a multichannel pipettor and mix well. Using the multichannel pipettor, spot 10 µl aliquots onto duplicate square LB plates. Repeat for all dilutions (*see* **Note 46**).
16. Incubate at an appropriate temperature until the colonies are large enough to enumerate and calculate the response in CFUs/ml taking into account the dilution factor.

3.3.3 Qualitative Capillary Assay

In this modification of the quantitative capillary assay, cells accumulate (Fig. 4d, viewing area) at the mouth of a microcapillary containing an attractant in solid form, either as crystals of the chemical or suspended in agarose, to prevent cells from swimming into the capillary [10, 64, 65]. When viewed by dark-field (or pseudo dark field, *see* **Note 9**) microscopy, cells responding to the attractant diffusing from the capillary appear as a bright white cloud that accumulates over time (Fig. 4e, lower panel). Depending on the strain and attractant, responses can be observed in 1–30 min. This assay is useful for screening a range of potential attractants, different concentrations of attractants, the responses of different bacterial strains, or a series of mutant strains. It can also be used to determine if chemotactic responses are inducible by pre-growing cells under different conditions prior to setting up the assay. Another advantage to this method is that the response to a particular attractant or repellant can easily be followed through time if images are taken at multiple time points. The results of this qualitative assay have been quantified microscopically by counting the number of bacterial cells accumulating near the mouth of a capillary containing attractant [64]. The qualitative capillary assay has worked particularly well to test the ability of sparingly soluble compounds, such as naphthalene, to serve as chemoattractants [17].

1. Inoculate cells in 100 ml of an appropriate medium and grow the cells to mid-exponential growth phase to a cell density between 0.3 and 0.7 at 600 nm (*see* **Note 24**).
2. Fill 1.0 µl microcapillary tubes with attractant or buffer as follows (*see* **Note 40**). Melt 5.0 ml 2% agarose made in CB and place in a sterile glass scintillation vial. Add sterile attractant or buffer control to the molten agarose. While the solution is still molten, pick up a sterile 1.0 µl microcapillary tube using forceps, and flame one end in a Bunsen burner until the end is

melted closed and becomes red hot. Swipe the length of the microcapillary through the flame twice (*see* **Note 41**), and place the open end in the scintillation vial containing the attractant of interest. Allow the agarose to solidify.

3. Set up the appropriate number of chemotaxis chambers: a glass U-tube sandwiched between a glass microscope slide and glass coverslip inside a Petri dish (*see* **Note 38**).
4. Harvest cells from 10 ml of the bacterial culture in sterile centrifuge tubes by centrifugation at 4,500 rpm for 5 min (*see* **Note 20**).
5. Remove the supernatant and gently resuspend the cells in 5.0 ml aerated sterile CB by inversion (*see* **Notes 6** and **21**).
6. Harvest the cells from **step 5** by centrifugation at 4,500 rpm for 5 min. Resuspend cells to an optical density of 0.3 at 600 nm in sterile, aerated CB. Check for cell motility (*see* **Note 27**).
7. Fill a chemotaxis chamber with the motile cell suspension. Place the microscope slide under the 4× objective of a phase-contrast microscope equipped with a digital camera (*see* **Note 51**). Focus the image on the center of the cell suspension using a dark-field setting (*see* **Note 9**).
8. Remove one capillary tube from the solidified attractant and insert the capillary tube into the cell suspension (*see* **Notes 43** and **44**). Quickly, adjust the stage such that the tip of the microcapillary is in the center of the field of view and adjust the fine focus if necessary (*see* **Notes 52** and **53**).
9. If attempting to demonstrate a chemotactic response over time, obtain the first digital image as quickly as possible and record the time. Allow the cells to respond for up to 60 min and obtain the final digital image (*see* **Note 54**).
10. Verify under the phase-contrast microscope that the cells are still motile (*see* **Note 33**).

3.3.4 Competition Capillary Assay

One can determine whether the same or different chemoreceptors are used to detect two different attractants using a competition assay [58, 66]. The assay can be done either as a qualitative or quantitative assay. It is carried out by including a "competing" attractant, typically at its peak response concentration in both the cell suspension and in the capillary. The "test" attractant is present only in the capillary, and if both compounds are detected by the same chemoreceptor, the response to the test attractant will be reduced or eliminated. Results can be confirmed by switching the locations of the two attractants under study.

4 Notes

1. It is important to use a purified form of agar for chemotaxis assays, as contaminants in general-purpose agars can oftentimes be chemoattractants for various bacterial species. We have found Noble agar (Difco, Becton, Dickinson and Co, Franklin Lakes, NJ) to be the best choice of agars for chemotaxis applications.
2. A minimal medium should be chosen that suits the growth of your bacterial strain. We have found that lowering the concentration of base minerals in the medium aids in the chemotactic response.
3. The "bucket of light" is a quick and inexpensive apparatus that provides indirect illumination of swim agar plates, agarose plug assays, or chemical-in-plug assays via backlighting [52]. It is also helpful to acquire digital images as black and white or gray scale for best contrast.
4. A general-purpose growth medium that supports growth of the bacterial strain can be used for overnight cultures since the cells will be washed, diluted, and inoculated into the swim plate medium for growth.
5. The use of pure agarose is imperative, as we have found that many types of low-melting-temperature agarose contain contaminating compounds that are sensed by the bacteria as attractants. Because of this, negative controls lacking attractant in the plug are absolutely essential. We have also found that the agarose tends to degrade if solidified and remelted more than two times.
6. Chemotaxis buffer (CB) is typically a phosphate-based buffer that supports motility. The basic formulation of this buffer that is presented here has been used in studies with pseudomonads. In general, the CB should contain a chelating agent, such as EDTA, to remove traces of heavy metal ions that can inhibit motility [61]. However, the presence of magnesium ions seems potentially important in *E. coli* [67]. Therefore, the CB may need to be adjusted on a strain-specific basis. When used for resuspending obligate aerobes, the CB should be aerated by vigorous shaking to help cells maintain motility. In addition, an energy source such as glycerol can be added to prolong motility [17, 21]. For studies of chemotaxis toward phosphate, a phosphate-free HEPES-based buffer should be used [64].
7. Glass U-tubes can be easily made by flame sealing the ends of a 100-μl volume 5 cm glass capillary tube. Using two forceps placed at either end of the capillary tube, heat the center of the tube until it is bendable. Bring the two ends of the capillary

toward each other until a "U" shape has been formed, ensuring that the arms of the U-tube are parallel and in the same plane, such that they will lay flat on the surface of a microscope slide.

8. To save time, one can attach many capillaries in a line on sticky tape to flame seal the ends en masse. These can then be put in a glass scintillation vial and autoclaved.
9. When visualizing a qualitative response of cells to an attractant, it is often easier to image the cells using negative contrast pseudo dark-field or oblique dark-field settings on your phase-contrast microscope [68], such that bright white cell "clouds" can be seen and imaged on a black background. Pseudo dark-field images can be generated by setting the condenser to a different phase setting than what is appropriate for the chosen objective. The pseudo dark-field effect will allow for the visualization and imaging of white illuminated cells on a dark background.
10. Although soft agar plate assays are oftentimes referred to as "swarm plates" in the literature, a more appropriate name for these assays is "swim plate" assays. Swarming motility refers to movement across a solid surface with the use of flagella and/or pili, while swimming motility is the motile behavior of bacteria driven by flagella in a liquid or semisolid medium [69].
11. Bacterial populations with a higher percentage of motile cells can be obtained by transferring a culture from the outside of the ring of growth to the center of a fresh plate and repeating the process 2–3 times. After each transfer, the growing ring of cells should move more rapidly toward the edge of the plate. Once several transfers have been carried out, one should streak for single colonies from a sample obtained from the outer ring of the final swim plate. This culture should be stored as a frozen stock, and when revived it should retain a large percentage of motile cells. In some cases, particularly with some environmental isolates or laboratory strains that have been stored for many years, cultures have very few motile cells and will form a very asymmetric colony on the initial swim plate. This "bleb" of motile cells that escapes from the point of inoculation should be transferred to a fresh swim plate, and it may take more than three transfers to obtain a highly motile culture.
12. A general-purpose, complex growth medium that supports the robust growth of your bacterial strain is best used when selecting for motile variants. We have found the use of 0.1× LB medium to be an optimal concentration for the selection of motile pseudomonads in swim plates.
13. The protocol described here is for a total volume of 100 ml, which will generate approximately three swim plates. This protocol can be scaled up for larger numbers of swim plates as needed.

14. You may need to optimize the attractant concentration for your strain. We have found 1 mM to be a good starting concentration for aromatic acids. Volatile hydrocarbons should be added to the medium immediately before pouring plates, after the molten agar has cooled to 45 °C to minimize loss to volatilization.
15. It is important to pour thick swim plates to minimize desiccation. Swim plates should be used within a day or two of pouring the medium or they will dry out and become too solid for cell migration. Because of this issue and because of the fact that swim plates are difficult to store due to the low agar content, only pour the number of plates needed for the current experiment. If necessary, 2× soft agar and 2× minimal salts solutions can be made, autoclaved, and stored separately in airtight, microwavable containers until use.
16. It is important that you do not invert the plates for incubation. The agar solution is not solid enough to endure inverted growth conditions.
17. The growth time and temperature conditions will vary depending on the bacterial strain and the type and amount of carbon source. With slowly growing organisms or moderate thermophiles with optimum growth temperatures above 37°C, the plates should be incubated in a moist atmosphere to keep them from desiccating. This can be accomplished by placing the plates in a plastic container or ziplock plastic bag containing a damp paper towel.
18. Oftentimes, a cone-shaped double ring can be visualized in swim plates. The outermost ring near the bottom of the plate where cells may be more oxygen limited is formed due to energy taxis, in which the oxidation and reduction of FAD in response to metabolic changes in energy state directs swimming behavior [27, 28], while the inner ring represents the chemotactic response to the chemical attractant. We have found that conducting various chemotaxis assays in an *aer* mutant background is helpful in differentiating energy taxis vs. chemotaxis responses, especially because in some cases energy taxis can mask chemotaxis defects in the swim plate assay [31, 32, 70].
19. To allow for significant growth without interruption from neighboring colonies, we suggest that no more than three different strains should be assessed for chemotaxis in quantitative swim plate assays in regular 90 × 15 mm Petri dishes. The assay described here can be adapted for large diameter 140 × 20 mm Petri dishes that can contain 50 ml of swim plate medium. These plates can easily accommodate four strains.

20. When harvesting cells by centrifugation for chemotaxis assays that involve an immediate response (cultures are not growing during the assay), it is imperative to harvest cultures under gentle conditions to preserve the flagellar structure. Typically, bacterial flagella will remain intact during longer centrifugation times at slower speeds.
21. It is critical to gently resuspend cells from the pellet to preserve flagellar integrity. Gently inverting the centrifuge tube to distribute the cells back into solution accomplishes this. If necessary, cut a larger bore on a P1000 micropipette tip and resuspend by slow repeat pipetting to prevent shearing.
22. It is critical that the optical density of cells does not vary outside this range to ensure that equal numbers of cells are being used for each strain.
23. When inoculating the cells into the agar medium, dispense the cells midway into the agar to ensure the cells will be inducing swimming behavior. Do not allow the micropipette tip to penetrate through to the bottom of the plate. If given access to the solid surface of the bottom of the plate, swarming motility could potentially be induced [69].
24. We have found that this range in optical density yields highly motile cells. Different bacterial strains may be more or less motile at different stages of growth; therefore, this may need to be adjusted for your strain of interest.
25. CB alone should always be used as a negative control. This is extremely important because some bacteria are attracted to contaminants present in some batches of low-melting temperature agarose. If this is the case, a positive response can be interpreted only if the response to the plug containing attractant is obviously much stronger to the control plug. The response should also then be confirmed with an alternative assay. Positive controls should also be included to verify that the culture was motile and generally chemotactic. Typical positive control attractants include 2% (final concentration) Casamino acids or a simple attractant such as succinate at an appropriate concentration (e.g., 10 mM). Final concentrations for aromatic compounds will depend on their solubility and toxicity.
26. Coomassie blue is added to the agarose for contrast in photographic images so that the edge of the agarose plug can be easily discriminated from the surrounding cell suspension.
27. Only proceed with the assay if greater than 60% of the cells in the population appear to be motile under phase-contrast microscopy.

28. In our experience, this density is optimal for good contrast in photographic images. If the culture is too dense, it is difficult to visualize and document a white ring of cells because there is not enough contrast.
29. Allowing the agarose plug to completely cool and solidify is important so that it will not mix with or be diluted when the cell suspension is added to the chamber.
30. The average volume of the chamber space is 230 μl. To flood the chamber, place the tip of the suspension-filled 1,000 μl micropipette tip into the chamber space between the glass slide and touching the glass coverslip. As the micropipettor is carefully depressed, the cell solution will flood the chamber and surround the plug using surface tension. Gently pressing down on the coverslip while dispensing the suspension facilitates the process.
31. The incubation time may need to be adjusted depending on the bacterial strain. However, if an incubation time longer than 15 min is required to see a response, the cells may become limited for oxygen and may begin to respond to oxygen diffusing in at the open sides of the chamber.
32. Because the cells are inserted into the chamber from one direction and flood around the agarose plug, diffusing attractants from the agarose plug can be displaced in the directional currents generated by the insertion of cells, resulting in an oblong attractant plume to which the cells are attracted. Because of this, a comma-shaped ring of cells indicating a positive chemotactic response can often be seen (Fig. 3b).
33. Verification that the cells are still motile at this point in the assay should be carried out when negative results are obtained to confirm that the absence of a response was because the compound is not an attractant and not simply because the cells were sessile.
34. For aromatic compounds, we have found that a final concentration of 1.0–10 mM is optimum for a chemotactic response. It is useful to carry out some preliminary experiments to determine the optimum concentration.
35. If an incubation time longer than 60 min is required to see a response, it may be difficult to conclude that the response is to the attractant itself or could potentially be a response to a metabolic intermediate generated during the assay. Similarly, if checking whether or not a particular response is inducible, longer incubation times may result in induction of cultures that were not pre-grown in the presence of the attractant.
36. The optimum distance between the plug and the point of inoculation may need to be modified depending on the

solubility of the compound being tested. It is useful to carry out some preliminary assays varying distances (2–3.5 cm), and then use the best parameters to do the actual assays. Once the optimal spacing is determined, set up a cardboard template with the center (plug) and equidistant inoculation points marked for quick and reproducible inoculation.

37. Results from this method have been successfully quantified by measuring the distances from the site of inoculation to the colony edges closest and furthest from the attractant source and using those values to calculate a response index [56].
38. The chemotaxis chamber consists of a sterile U-shaped glass capillary tube (*see* **Note** 7) between a sterile glass microscope slide and a sterile glass coverslip, housed in a sterile Petri dish to maintain aseptic conditions. Batches of glass U-tubes, slides, and coverslips can be separately autoclaved, and chambers can be assembled as needed using flame-sterilized forceps.
39. For these assays, the test repellent is included in the bacterial suspension rather than the capillary, and the number of bacteria that enter the capillary to escape from the repellant is compared to a control lacking the repellant as a measure of chemorepulsion [53].
40. It is important to fill the microcapillaries just before the assay, especially for volatile compounds. Fresh stocks of volatile compounds should be used. With poorly soluble and/or volatile hydrocarbon attractants, it can be helpful to shake the compound solution until just before filling to keep the solution saturated.
41. Once sealed, heated, and submerged in the attractant or control solution, the attractant will be pulled into the capillary due to capillary action. Alternatively, capillaries can be filled under vacuum. Scintillation vials containing attractant solutions and sealed capillaries should be placed in a vacuum chamber as described in Sect. 3.3.2 [63].
42. Some researchers have had difficulty generating U-shaped tubes from glass capillaries to support the coverslip; as a result, the chamber set up has been modified with the use of two straight glass capillaries to overcome this issue [17].
43. Carefully roll and tap the microcapillary against the inside of the sterile Petri dish to remove residual attractant from the outside of the capillary.
44. Verify that an air bubble was not introduced at the tip of the microcapillary. The presence of an air bubble could keep the attractant from properly diffusing into the cell suspension. In addition, it could elicit an aerotaxis response.

45. A bulb dispenser that comes with the purchase of the microcapillaries can be used for expelling cells into the diluent. This step is typically the most difficult part of the capillary assay, as expulsion of the microcapillary contents can be tricky. Since such a small volume is being dispensed, it is helpful to place the tip of the microcapillary on the side of the glass test tube, so that surface tension will help draw the cell suspension from the microcapillary. An alternative way to address the expulsion problem is to break off the end (after rinsing the capillary) and place the microcapillary into a sterile microfuge tube and expel the contents via centrifugation.
46. The number of dilutions will need to be determined based on the bacterial strain and the strength of the response. To save time and agar plates, dilutions can be made in 96-well plates, and 10 μl aliquots can be spotted onto LB plates using a multichannel pipettor.
47. Sterile Texan™ (Excel Scientific, Victorville, CA) multi-well reagent reservoirs are helpful for the distribution of molten agar using a multichannel pipette. Once distributed, tap the 96-well plate to be sure no bubbles are present in the agar pads.
48. Be sure that the microcapillaries are submerged all the way to the bottom of each well so that they are securely embedded in the agar pad and the tips are at the same height. If you are conducting fewer than 96 assays, be sure to space the microcapillaries at equal distances (especially if you are only using a few rows), so that the assembled plate sandwich (**step 5**) will be balanced and well supported.
49. Tap the microcapillary plate to make sure all microcapillaries are touching the bottom of the attractant array plate. If the microcapillaries do not touch the bottom, they may not fill completely under vacuum.
50. You may need to test your vacuum settings and determine the amount of time needed to fill the capillaries. On average, each 1 μl capillary should take up 0.6 μl of solution. Be careful to release the vacuum slowly.
51. The optimum camera settings include black and white image, no flash, and the macro setting engaged.
52. It is helpful to set the microscope stage in the correct focus plane using a mock set up of the chemotaxis chamber with a microcapillary inserted before you begin the assays. Once you have focused on the tip of the microcapillary, you can easily remove and insert slides onto the set stage. Once the test microcapillary has been inserted, a quick fine focus adjustment should be all that is necessary before taking the first image.

53. You may also have to adjust the stage relative to the strength of your response. It is best to focus in the plane that corresponds to the middle of the capillary, such that the capillary itself is in focus and you can see the crisp edges lining the capillary.
54. Obtaining images of the chemotactic response at time zero and the end of the assay is sufficient. Typical assays should not take more than 30 min, and if an incubation time longer than 60 min is required to see a response, it may be difficult to differentiate if the response is to the attractant itself or could potentially be a response to a metabolic intermediate.

Acknowledgments

We thank Rita Luu, Jonathan Hughes, Benjamin Schneider, Janet Rollefson, and undergraduate students that participated in the BIOL464 Bioinformatics course at the University of St. Thomas for providing data and figures and Rita Luu for critically reading the manuscript. Chemotaxis studies were supported by a grant from the National Science Foundation to REP and JLD (MCB0919930). Any opinions, findings, and conclusions or recommendations expressed in this material are those of the authors and do not necessarily reflect the views of the National Science Foundation.

References

1. Armitage JP (1999) Bacterial tactic responses. Adv Microbial Phys 41:229–289
2. Bourret RB, Stock AM (2002) Molecular information processing: lessons from bacterial chemotaxis. J Biol Chem 277:9625–9628
3. Manson MD (1992) Bacterial motility and chemotaxis. Adv Microbial Phys 33:277–346
4. Manson MD, Armitage JP, Hoch JA, Macnab RM (1998) Bacterial locomotion and signal transduction. J Bacteriol 180:1009–1022
5. Bourret RB, Borkovich KA, Simon MI (1991) Signal transduction pathways involving protein phosphorylation in prokaryotes. Ann Rev Biochem 60:401–441
6. Armitage JP, Schmitt R (1997) Bacterial chemotaxis: *Rhodobacter sphaeroides* and *Sinorhizobium meliloti* – variations on a theme? Microbiology 143:3671–3682
7. Zhulin IB (2001) The superfamily of chemotaxis transducers: From physiology to genomics and back. Adv Microbial Physiol 45: 157–198
8. Parales RE, Ferrandez A, Harwood CS (2004) Chemotaxis in *Pseudomonads*. In: Ramos J-L (ed) *Pseudomonas* Volume I: Genomics, life style and molecular architecture. Kluwer Academic/Plenum, New York, pp 793–815
9. Gibson DT, Koch JR, Kallio RE (1968) Oxidative degradation of aromatic hydrocarbons by microorganisms I. Enzymatic formation of catechol from benzene. Biochemistry 7: 2653–2661
10. Parales RE, Luu RA, Chen GY et al (2013) *Pseudomonas putida* F1 has multiple chemoreceptors with overlapping specificity for organic acids. Microbiology 159:1086–1096
11. Gordillo F, Chávez FP, Jerez CA (2007) Motility and chemotaxis of *Pseudomonas* sp. B4 towards polychlorobiphenyls and chlorobenzoates. FEMS Microbiol Ecol 60:322–328
12. Grimm AC, Harwood CS (1997) Chemotaxis of *Pseudomonas* spp. to the polyaromatic hydrocarbon naphthalene. Appl Environ Microbiol 63:4111–4115
13. Harwood CS, Fosnaugh K, Dispensa M (1989) Flagellation of *Pseudomonas putida* and analysis of its motile behavior. J Bacteriol 171: 4063–4066

14. Harwood CS, Parales RE, Dispensa M (1990) Chemotaxis of *Pseudomonas putida* toward chlorinated benzoates. Appl Environ Microbiol 56:1501–1503
15. Harwood CS, Rivelli M, Ornston LN (1984) Aromatic acids are chemoattractants for *Pseudomonas putida*. J Bacteriol 160:622–628
16. Iwaki H, Muraki T, Ishihara S et al (2007) Characterization of a pseudomonad 2-nitrobenzoate nitroreductase and its catabolic pathway-associated 2-hydroxylaminobenzoate mutase and a chemoreceptor involved in 2-nitrobenzoate chemotaxis. J Bacteriol 189: 3502–3514
17. Lacal J, Muñoz-Martínez F, Reyes-Darías JA et al (2011) Bacterial chemotaxis towards aromatic hydrocarbons in *Pseudomonas*. Environ Microbiol 13:1733–1744
18. Neal AL, Ahmad S, Gordon-Weeks R, Ton J (2012) Benzoxazinoids in root exudates of maize attract *Pseudomonas putida* to the rhizosphere. PLoS One 7, e35498
19. Nogales J, Canales A, Jiménez-Barbero J et al (2011) Unravelling the gallic acid degradation pathway in bacteria: the *gal* cluster from *Pseudomonas putida*. Mol Microbiol 79:359–374
20. Parales RE (2004) Nitrobenzoates and aminobenzoates are chemoattractants for *Pseudomonas* strains. Appl Environ Microbiol 70:285–292
21. Parales RE, Ditty JL, Harwood CS (2000) Toluene-degrading bacteria are chemotactic to the environmental pollutants benzene, toluene, and trichloroethylene. Appl Environ Microbiol 66:4098–4104
22. Lacal J, Reyes-Darias JA, Garcia-Fontana C, Ramos JL, Krell T (2013) Tactic responses to pollutants and their potential to increase biodegradation efficiency. J Appl Microbiol 114: 923–933
23. Law AM, Aitken MD (2003) Bacterial chemotaxis to naphthalene desorbing from a non-aqueous liquid. Appl Environ Microbiol 69: 5968–5973
24. Long T, Ford RM (2009) Enhanced transverse migration of bacteria by chemotaxis in a porous T-sensor. Environ Sci Technol 43: 1546–1552
25. Marx RB, Aitken MD (2000) Bacterial chemotaxis enhances naphthalene degradation in a heterogeneous aqueous system. Environ Sci Technol 34:3379–3383
26. Paul D, Singh R, Jain RK (2006) Chemotaxis of *Ralstonia* sp. SJ98 towards *p*-nitrophenol in soil. Environ Microbiol 8:1797–1804
27. Alexandre G, Greer-Phillips S, Zhulin IB (2004) Ecological role of energy taxis in microorganisms. FEMS Microbiol Rev 28:113–126
28. Alexandre G, Zhulin IB (2001) More than one way to sense chemicals. J Bacteriol 183: 4681–4686
29. Taylor BL (2007) Aer on the inside looking out: paradigm for a PAS-HAMP role in sensing oxygen, redox and energy. Mol Microbiol 65: 1415–1424
30. Taylor BL, Watts KJ, Johnson MS (2007) Oxygen and redox sensing by two-component systems that regulate behavioral responses: behavioral assays and structural studies of *aer* using in vivo disulfide cross-linking. Methods Enzymol 422:190–232
31. Luu RA, Schneider BJ, Ho CC et al (2013) Taxis of *Pseudomonas putida* F1 toward phenylacetic acid is mediated by the energy taxis receptor Aer2. Appl Environ Microbiol 79: 2416–2423
32. Sarand I, Osterberg S, Holmqvist S et al (2008) Metabolism-dependent taxis towards (methyl)phenols is coupled through the most abundant of three polar localized Aer-like proteins of *Pseudomonas putida*. Environ Microbiol 10:1320–1334
33. Rabinovitch-Deere CA, Parales RE (2012) Three types of taxis used in the response of *Acidovorax* sp. strain JS42 to 2-nitrotoluene. Appl Environ Microbiol 78:2308–2315
34. Kojadinovic M, Sirinelli A, Wadhams GH, Armitage JP (2011) New motion analysis system for characterization of the chemosensory response kinetics of *Rhodobacter sphaeroides* under different growth conditions. Appl Environ Microbiol 77:4082–4088
35. Lopez de Victoria G, Zimmer-Faust RK, Lovell CR (1995) Computer-assisted video motion analysis: a powerful technique for investigating motility and chemotaxis. J Microbiol Methods 23:329–341
36. Kojadinovic M, Armitage JP, Tindall MJ, Wadhams GH (2013) Response kinetics in the complex chemotaxis signalling pathway of *Rhodobacter sphaeroides*. J R Soc Interface 10:20121001
37. Qian C, Wong CC, Swarup S, Chiam KH (2013) Bacterial tethering analysis reveals a "run-reverse-turn" mechanism for *Pseudomonas* species motility. Appl Environ Microbiol 79:4734–4743
38. Englert DL, Jayaraman A, Manson MD (2009) Microfluidic techniques for the analysis of bacterial chemotaxis. Methods Mol Biol 571:1–23
39. Englert DL, Manson MD, Jayaraman A (2009) Flow-based microfluidic device for quantifying bacterial chemotaxis in stable, competing gradients. Appl Environ Microbiol 75:4557–4564

40. Kalinin Y, Neumann S, Sourjik V, Wu M (2010) Responses of *Escherichia coli* bacteria to two opposing chemoattractant gradients depend on the chemoreceptor ratio. J Bacteriol 192:1796–1800
41. Rusconi R, Garren M, Stocker R (2014) Microfluidics expanding the frontiers of microbial ecology. Ann Rev Biophys 43:65–91
42. Sourjik V, Vaknin A, Shimizu TS, Berg HC (2007) In vivo measurement by FRET of pathway activity in bacterial chemotaxis. Methods Enzymol 423:365–391
43. Krell T, Lacal J, Garcia-Fontana C et al (2014) Characterization of molecular interactions using isothermal titration calorimetry. Methods Mol Biol 1149:193–203
44. Wu JG, Li JY, Li GY, Long DG, Weis RM (1996) The receptor binding site for the methyltransferase of bacterial chemotaxis is distinct from the sites of methylation. Biochemistry 35:4984–4993
45. Stanier RY, Palleroni NJ, Doudoroff M (1966) The aerobic pseudomonads: a taxonomic study. J Gen Microbiol 43:159–271
46. Gerhardt P, Murray RGE, Wood WA, Krieg NR (eds) (1994) Methods for general and molecular bacteriology. American Society for Microbiology, Washington, DC
47. Sambrook J, Fritch EF, Maniatis T (1989) Molecular cloning: a laboratory manual, 2nd edn. Cold Spring Harbor Laboratory, Cold Spring Harbor
48. Adler J (1966) Chemotaxis in bacteria. Science 153:708–716
49. Ditty JL, Grimm AC, Harwood CS (1998) Identification of a chemotaxis gene region from *Pseudomonas putida*. FEMS Microbiol Lett 159:267–273
50. Harwood CS, Nichols NN, Kim M-K, Ditty JL, Parales RE (1994) Identification of the *pcaRKF* gene cluster from *Pseudomonas putida*: Involvement in chemotaxis, biodegradation, and transport of 4-hydroxybenzoate. J Bacteriol 176: 6479–6488
51. Yu HS, Alam M (1997) An agarose-in-plug bridge method to study chemotaxis in the Archaeon *Halobacterium salinarum*. FEMS Microbiol Lett 156:265–269
52. Parkinson JS (2007) A "bucket of light" for viewing bacterial colonies in soft agar. Methods Enzymol 423:432–435
53. Tso W-W, Adler J (1974) Negative chemotaxis in *Escherichia coli*. J Bacteriol 118:560–576
54. Storch KF, Rudolph J, Oesterhelt D (1999) Car: a cytoplasmic sensor responsible for arginine chemotaxis in the archaeon *Halobacterium salinarum*. EMBO J 18:1146–1158
55. Li J, Go AC, Ward MJ, Ottemann KM (2010) The chemical-in-plug bacterial chemotaxis assay is prone to false positive responses. BMC Res Notes 3:77
56. Pham HT, Parkinson JS (2011) Phenol sensing by *Escherichia coli* chemoreceptors: a nonclassical mechanism. J Bacteriol 193:6597–6604
57. Adler J (1973) A method for measuring chemotaxis and use of the method to determine optimum conditions for chemotaxis by *Escherichia coli*. J Gen Microbiol 74:77–91
58. Mesibov R, Adler J (1972) Chemotaxis toward amino acids in *Escherichia coli*. J Bacteriol 112:315–326
59. Liu X, Parales RE (2009) Bacterial chemotaxis to atrazine and related *s*-triazines. Appl Environ Microbiol 75:5481–5488
60. Liu X, Wood PL, Parales JV, Parales RE (2009) Chemotaxis to pyrimidines and identification of a cytosine chemoreceptor in *Pseudomonas putida*. J Bacteriol 191:2909–2916
61. Moulton RC, Montie TC (1979) Chemotaxis by *Pseudomonas aeruginosa*. J Bacteriol 137: 274–280
62. Bainer R, Park H, Cluzel P (2003) A high-throughput capillary assay for bacterial chemotaxis. J Microbiol Methods 55: 315–319
63. Meyer G, Schneider-Merck T, Böhme S, Sand W (2002) A simple method for investigations on the chemotaxis of *Acidithiobacillus ferrooxidans* and *Desulfovibrio vulgaris*. Acta Biotechnol 22:391–399
64. Kato J, Ito A, Nikata T, Ohtake H (1992) Phosphate taxis in *Pseudomonas aeruginosa*. J Bacteriol 174:5149–5151
65. Nikata T, Sumida K, Kato J, Ohtake H (1992) Rapid method for analyzing bacteria behavioral responses to chemical stimuli. Appl Environ Microbiol 58:2250–2254
66. Liu X, Parales RE (2008) Chemotaxis of *Escherichia coli* to pyrimidines: a new role for the signal transducer Tap. J Bacteriol 190:972–979
67. Moench TT, Konetzka WA (1978) Chemotaxis in *Pseudomonas aeruginosa*. J Bacteriol 133: 427–429
68. Tkaczyk TS (2010) Field guide to microscopy. SPIE Field Guides. SPIE Press, Bellingham, pp 1–156

69. Kearns DB (2010) A field guide to bacterial swarming motility. Nat Rev Microbiol 8:634–644
70. Alvarez-Ortega C, Harwood CS (2007) Identification of a malate chemoreceptor in *Pseudomonas aeruginosa* by screening for chemotaxis defects in an energy taxis-deficient mutant. Appl Environ Microbiol 73: 7793–7795
71. Luu RA, Koostra C, Brunton V et al (2015) Integration of chemotaxis, transport, and catabolism in *Pseudomonas putida* and identification of the aromatic acid chemoreceptor PcaY. Mol Microbiol 96:134–147

Determining the Tendency of Microorganisms to Interact with Hydrocarbon Phases

Hauke Harms and Lukas Y. Wick

Abstract

Three procedures for the determination of the hydrophobicity of microorganisms and/or their tendency to physically interact with hydrocarbon phases are presented. These include the bacterial/microbial adhesion to hydrocarbon (BATH/MATH) test, hydrophobic interaction chromatography and contact angle measurements of filter-retained microbial cell layers.

Keywords: Bacteria/microbial adhesion to hydrocarbons (BATH/MATH), Contact angle measurement (CAM), Hydrophobic interaction chromatography (HIC)

1 Introduction

A common feature of hydrocarbons, oils and lipids is their poor tendency to dissolve in water. Instead, already small amounts of these compounds are likely to exceed the water solubility in a given environmental situation and to exist as a separate phase which forms a distinct, small (energy minimised when the compound is a liquid) interface with the adjacent water phase. Depending on the situation, the oil phase will float as a layer on top of surface water or groundwater or become dispersed as an oil-in-water emulsion. For microorganisms capable of degrading these compounds, this means that they either have to rely on the relatively small concentrations of water-dissolved compound or to interact directly with the nonaqueous phase. From the perspective of microbial nutrition, attachment to separate-phase substrates drastically shortens the paths of substrate diffusion through the water phase to the organisms or enables them to take up the substrate via nonaqueous-phase-based mechanisms.

T.J. McGenity et al. (eds.), *Hydrocarbon and Lipid Microbiology Protocols*, Springer Protocols Handbooks, (2017) 43–53,
DOI 10.1007/8623_2015_77, © Springer-Verlag Berlin Heidelberg 2015, Published online: 17 April 2015

1.1 Attachment to Hydrocarbons: Hydrophobic Interaction and Competing Forces

The tendency to attach to oil droplets or hydrocarbon crystals is very common among hydrocarbon-degrading microorganisms and appears to be a prerequisite for efficient biodegradation (see, e.g. [1]). However, a strong tendency to attach to oil might as well increase the bioavailability of toxic oil constituents to degrading microorganisms. Accordingly, interference with the attachment process, e.g. via the application of surface-active chemicals, may have quite contrasting effects [2]. Reduced oil degradation after surfactant-mediated detachment can be the consequences. On the contrary, surfactants may increase the attachment of hydrophilic bacteria by rendering them hydrophobic, which may result in increased biodegradation or toxicity as consequences of the enhanced bioavailability of the oil.

Many observations indicate that microbial attachment to hydrocarbons, oils and lipids represents an adaptation to the utilisation of these compounds. The strongest hints come from the finding that microorganisms may regulate their surface characteristics, depending on the need to interact with the separate phase. For instance, it has been observed that oil-degrading bacteria synthesise specific surface molecules that mediate the attachment and are capable of releasing them in order to detach from the hydrocarbon when the interaction is not needed anymore (*see* [3] for review). *Mycobacterium* spp. have been found to regulate the length (and thus the hydrophobicity) of mycolic acids in their cell envelopes depending on the hydrophobicity of their growth substrate [4].

While cell surface hydrophobicity is an important factor for the attachment to hydrocarbons, it is not the first one to become active when a microorganism approaches an interface. Besides the chemical complexity of a cell surface, the colloidal size of bacteria introduces further complication. The hydrophobic interaction, the expulsion of the cell surface components by strongly coherent water molecules, is acting only at a short distance corresponding to a few diameters of a water molecule. For the hydrophobic effect to become active, the microorganism has to come that close to the interface. The probability of such a close encounter, however, is controlled by longer-ranging colloidal forces accounted for in the classical DLVO theory of colloid stability [5]. The DLVO theory explains the interaction of colloidal particles with interfaces in terms of the interplay between van der Waals and electrostatic interactions. Applied to bacteria and environmental interfaces, the van der Waals interactions are typically attractive and thus counteract the electrostatic repulsion between typically negatively charged microorganisms and negatively charged environmental interfaces [6]. As the decay of both individual forces as a function of distance follows different laws, the DLVO theory allows for attractive energy minima at a distance of typically 5–10 nm from the interface [7]. This means that at least theoretically, microorganisms may attach without making direct contact with the interface, a situation that

should impede short-range hydrophobic interaction to take place. In reality, however, microbial surfaces are rough by virtue of their surface molecules, which in turn may find their way to the interface unless the balance between the long-ranging DLVO forces is highly unfavourable [7]. Whereas van der Waals interactions are entirely controlled by material properties of the two interacting partners, electrostatic interactions can be shielded by ions in the aqueous medium that separates the microorganisms and the interface, the extent of shielding being a direct function of the ionic strength. This leads to a situation where the hydrophobic effect may come into play between a given combination of hydrocarbon and microorganism under high salt conditions (e.g. in sea water), whereas the interaction is dominated by electrostatic repulsion in a low salt environment (e.g. in groundwater). Accordingly, the cell surface charge of bacteria has been inferred from their differential adhesion to hydrocarbons at low and high ionic strength [8].

From the foregoing, one can firstly conclude that electrostatic interaction is a force to be considered when attempting to predict microbial attachment to hydrocarbons. The latter may surprise when one considers that constituents of hydrophobic phases are unlikely to possess charges. The electrostatic charge of hydrocarbon droplets and its influence on bacterial attachment have, however, been recognised and accounted for [9]. It can at least partly be ascribed to the sorption of amphiphilic molecules to the hydrocarbon-water interface (e.g. fatty acids, anionic surfactants) and even be observed for hydrophobic polymers such as Teflon or polystyrene, which do not carry structural charges [10].

2 Materials

2.1 Protocol 1: Microbial/Bacterial Adhesion to Hydrocarbons

Bacterial suspension (OD_{578}: 0.4–0.6) in 0.01 M potassium phosphate buffer pH 7

Hexadecane

2.2 Protocol 2: Hydrophobic Interaction Chromatography of Bacteria: Column Filtration Experiments

PFA-Teflon (Teflon 350; DuPont) beads, 250–500 μm diameter

Glass columns of 10 cm length and 1 cm inner diameter with a glass frit at the bottom (Fig. 1)

Vacuum pump with tubing

Glass pipette (10 ml) with cut tip (2 mm opening)

Peristaltic pump with tubing

Bacterial suspension (OD_{280}: 0.6)

Phosphate-buffered salines of desired ionic strengths and pH

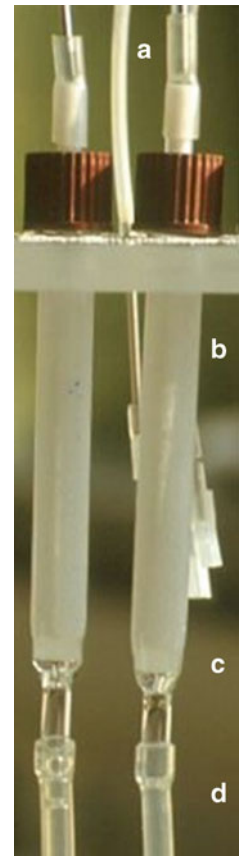

Fig. 1 Glass columns filled with PFA-Teflon beads for hydrophobic interaction chromatography of bacterial suspensions: *a* inflow tube, *b* glass column filled with PFA-Teflon, *c* glass frit to separate column bed from outflow, *d* outflow

2.3 Protocol 3: Contact Angle Measurements with Bacteria

Bacterial suspension (OD_{578}: 1–2) in 0.05 M phosphate-buffered saline pH 7

0.45 μm micropore cellulose acetate filters 2.5 cm diameter

Filtration set

Vacuum pump with tubing

Double-sided adhesive tape

Goniometer microscope

3 Methods to Study the Hydrophobicity of Microorganisms and the Interaction with Hydrocarbon Phases

Experimenters interested in hydrophobicity as a determinant of bacterial interaction can either directly address the interaction of interest or try to get an isolated view on the contribution of the

hydrophobic effect to the interaction. As an example, somebody interested in the attachment of certain bacteria to a specific type of diesel oil in groundwater may choose to perform an attachment experiment using the very combination of interaction partners and groundwater. A protocol for microbial (bacterial) attachment to hydrocarbons (MATH or BATH) is presented below (protocol 1). It relies on the partitioning of microbial suspensions between a hydrophobic phase, a water phase, and the interface between them. The outcome will be of use to predict the interaction in the groundwater aquifer of interest, but be of limited value for other situations such as the interaction of the same combination of bacteria and diesel in ocean water, which due to its high ionic strength shields electrostatic forces, not to mention the interaction of other combinations of bacteria and oils. A more isolated view on the hydrophobicity component and a higher degree of transferability will be obtained when the microbial attachment experiment is performed either at high ionic strength, at the pH at which the bacteria or the hydrocarbons are uncharged or, if these pH values are unknown, at a range of pH values (e.g. pH 2–7) that is likely include conditions at which electrostatic interactions are suppressed (variation of protocol 1).

An equivalent method for the direct investigation of the interaction with hydrophobic solids is a type of hydrophobic interaction chromatography in percolated columns which is adapted to whole bacteria (protocol 2; [10]). As in the MATH/BATH test, the choice of the composition of the mobile aqueous phase (pH, ionic strength) decides if the overall interaction is addressed or a more isolated view of effects of the organisms' hydrophobicity is gained. Pore geometries resulting from uniform, spherical collectors allow the calculation of collision rates, which through comparison with macroscopic filtration rates can be used to calculate collector efficiencies [11].

A more isolated view on the actual hydrophobicity of microorganisms is obtained when the interaction of water (or other liquids of known physicochemical characteristics) with microorganisms is addressed directly. This is typically done by contact angle measurements on closed layers of bacteria or fungi on micropore filters (protocol 3; [12, 13]). An advantage of contact angle measurements is that they generate data that can be used for interaction energy calculations. When results of contact angle measurements of bacteria are compared with results from the BATH test, the higher-resolution power of contact angle measurements becomes obvious. The BATH test appears to allow only a relatively rough qualitative distinction of hydrophilic, intermediate and hydrophobic organisms, depending on the tendencies to stay in the water, accumulate in the interface or enter the hydrophobic phase. Water contact angle measurement in contrast allows the continuous distribution of bacterial and fungal species over a scale ranging from about 20° (very hydrophilic) to more than 100° (very hydrophobic; [10, 13]).

3.1 Protocol 1: Microbial/Bacterial Adhesion to Hydrocarbons

The MATH/BATH test has been originally described by Rosenberg and co-workers in 1980 [14] and evaluates the *relative* hydrophobicity of microbial cells. As it is highly dependent on the variations in the experimental conditions (e.g. the ionic strength/pH of the aqueous phase, the hydrocarbon-type, the hydrocarbon to water volume ratios, the geometry of the test tubes or the mixing time [15]), there are many modifications described in literature. This protocol outlines a modification of the *kinetic* BATH test by Lichtenberg et al. [16].

Step 1: Preparation of Microbial Suspensions: Prepare bacterial cultures of known origin and growth history, as bacteria change their surface properties depending on growth phase, substrate utilised or environmental conditions. Harvest the cells by centrifugation, wash them at least twice in dilute potassium phosphate buffer (0.01 M, pH 7) and resuspend in a small volume of the same buffer.

Step 2: Microbial Adhesion to Hexadecane: Prepare cell suspensions of an optical density A_o (at 578 nm) of 0.4–0.6 (0.01 M potassium phosphate buffer; pH 7). Next, add 0.15 mL of hexadecane to 3 mL of the bacterial suspension, vortex the two-phase system for $t = 10$ s and then allow the two phases to settle for 10 min at room temperature. Measure after that A_t, i.e. the optical density in the water phase at time t. Vortexing, settling and OD measurement are repeated identically with the same sample until the total vortexing time has summed up to ≥ 60 s. Control experiments with suspension of identical optical density in the absence of hexadecane are recommended to account for potential changes in A_o during vortexing. As the BATH/MATH test strongly depends on pH and the ionic strength of the aqueous phase, strictly standardised conditions should be applied

Step 3: Data Analysis: Express the optical density ratios log (A_t/A_o)*100 and plot it as a function of the vortexing time (t). Linear least square fitting now yields the initial removal coefficient R_o (per time) as a measure of the adhesion of cells to hexadecane and hence offers their BATH/MATH-based hydrophobicity, i.e. with high R_o for hydrophobic cells. BATH/MATH-based hydrophobicity is normally derived from triplicate samples.

3.1.1 Time-Saving Alternative

For rapid screening of the partitioning of cells to hexadecane, vortex the above-described two-phase system for 1 min, allow the suspension to settle for 10 min at room temperature and measure the optical density A_t as described above. Express the BATH/MATH results as the proportion of the cells which have been excluded from the aqueous phase P (%), i.e. $P = 100 * (A_o - A_t)/A_o$. Note that this approach strongly depends on the hydrocarbon/water volume ratios and hence apply strictly standardised conditions.

3.2 Protocol 2: Hydrophobic Interaction Chromatography of Bacteria: Column Filtration Experiments

With this protocol, the interaction of bacteria with hydrophobic solid materials can be quantified. The protocol has been developed and tested with spheres of PFA-Teflon (a copolymer of perfluoroalkoxyheptafluoropropylene and polytetrafluoroethylene also referred to as Teflon 350; DuPont) of 250–500 μm average diameters, but can as well be conducted with other hydrophobic, spherical materials of similar, uniform size (*see* **Note 1**).

Step 1: Submersion of the Hydrophobic Polymer Granules: Place a layer of polymer granules of about 3 cm thickness into a serum bottle. Add a water volume bigger than the granule bed volume on top of the polymer. The extreme hydrophobicity of the polymer will keep the water from penetrating the porous bed. To make the water enter the pore space, exert for 3 min a negative pressure to the bottle by pressing a tubing (of equal diameter as the bottle neck) evacuated by a vacuum pump to the bottle opening. Upon relieving the negative pressure, part of the water will sink into the porous bed completely filling the pore space.

Step 2: Filling of Glass Columns with Submerged Polymer Granules: Place glass columns (Fig. 1) in a rack. At the lower end, the column should be delimited by a glass frit with pore size slightly smaller than the polymer granules. Connect the lower column outlets to plastic syringes filled with water and fill the columns from the bottom. Transfer the submerged polymer with a 10-mL glass pipette which has been cut to allow the polymer granules to enter. Avoid exposure of the beads to air. Fill all columns to the top while repeatedly agitating them to facilitate settling of the granules. Connect the top of the columns to tubing of a peristaltic pump and detach the syringes. Flush the columns with at least five pore volumes in continuous flow mode with the medium of choice for the filtration experiment. Adjust the flow velocity to a linear rate of 30 cm h^{-1}.

Step 3: Filtration Experiment: Replace the inflow solution by a bacterial suspension of an OD_{280} of 0.6 in the same medium at the same flow rate (*see* **Note 2**). Monitor the OD_{280} of the inflowing and outflowing suspension. Use the time-resolved effluent/influent data to establish a breakthrough curve (*see* Fig. 2).

Step 4: Data Interpretation: Use the model developed by Martin et al. [11] to calculate the collector efficiency from plateau effluent concentrations (*see* **Note 3**). Alternatively, infer actual collector efficiencies by comparison of plateau removal rates with those obtained under conditions resulting in collector efficiencies of 1, i.e. guaranteed adhesion of bacteria upon a single collision. These conditions can be obtained by complete suppression of electrostatic repulsion by either percolating cells suspended in phosphate-buffered saline of 1 M ionic strength or by varying the pH between 2 and 7 and choosing the resulting maximum removal for comparison (*see* **Note 4**).

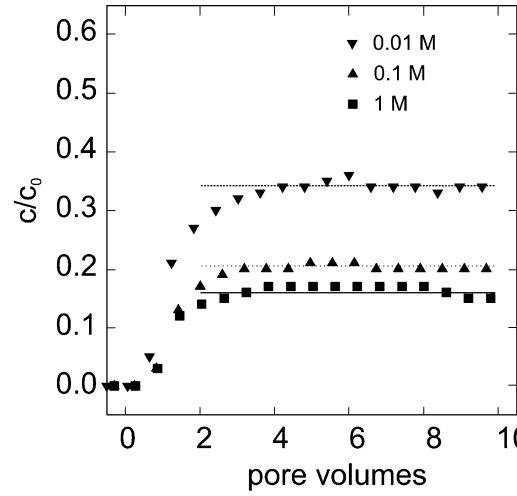

Fig. 2 Breakthrough curves obtained with *Pseudomonas putida* mt2 at various ionic strengths. Comparison of removal rates (difference between plateau height and 1) with those at 1 M were used to infer collector efficiencies at lower ionic strengths. In the present example, collector efficiencies of 0.94 (0.1 M) and 0.77 (0.01 M) were inferred from comparison with the assumed collector efficiency of 1 at an ionic strength of 1 M

3.3 Protocol 3: Contact Angle Measurements with Bacteria

Several experimental methods to measure surface contact angles exist, such as the static sessile drop, the dynamic sessile drop or the dynamic Wilhelmy method [17, 18]. Here we describe the commonly used *static sessile drop method*, which measures the angle formed between the liquid/solid and liquid/air interface after placement of a droplet of water on a bacterial lawn.

Step 1: Preparation of Microbial Lawns: Prepare bacterial cultures of known origin and growth history (*see* **Note 5**). Harvest the cells by centrifugation, wash them at least twice in dilute phosphate saline buffer (PBS) of an ionic strength of 0.05 M (per litre: 0.145 g KH_2PO_4, 0.595 g K_2HPO_4, 2.465 g NaCl) and resuspend them in a small volume of 0.05 M PBS to obtain an optical density at 578 nm of 1–2. Bacterial mats for measuring the contact angles are prepared by collecting the uniformly suspended cells on a 0.45 micropore membrane filters (20 mm diameter). The best way to reproducibly obtain homogeneous, continuous bacterial lawns is to slowly deposit ca. 50 layers of bacteria on the filter by applying negative pressure (i.e. by filtering a mixture of ca. 0.2 mL of cell suspension and 10 mL 0.05 M PBS) (*see* **Note 6**). Mount subsequently the wet membranes with double-sided adhesive tape to a microscopy slide (*see* Fig. 3) and dry them for about 2 h under standardised conditions (*see* **Note 7**).

Step 2: Contact Angle Analysis: Measure the cell hydrophobicity by a goniometer, if possible, with the help of an automated, real-time

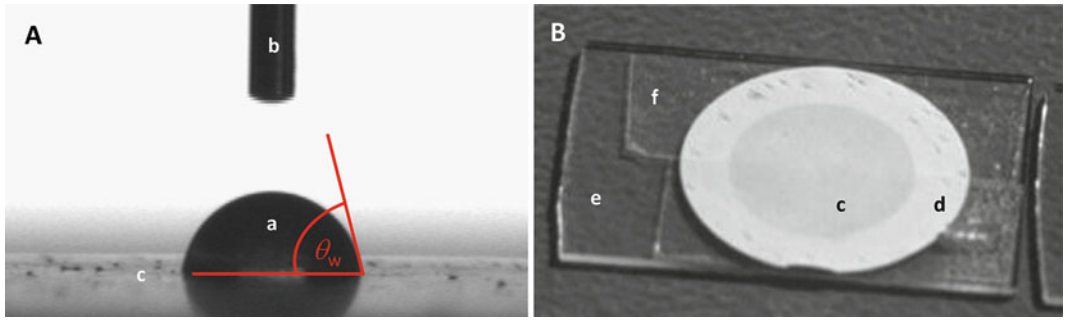

Fig. 3 (**A**) Video still of sessile water droplet (*a*) added by a needle (*b*) on a lawn of hydrophobic bacteria (*c*). (**B**) View of a bacterial lawn (*c*) collected on a micropore filter (*d*) fixed on a microscope slide (*e*) with a double-sided adhesive tape (*f*)

image analysis system (e.g. drop shape analysis system DSA 100; Krüss GmbH, Germany) to capture the contact angle of water θ_w (or any other pure liquid: θ_x) on the bacterial lawn. The basic requirements of a goniometer consist of a solid support system, a microsyringe for positioning the droplets on the bacterial lawns (Fig. 3) and a suitable measuring device to derive the contact angle from the droplets' measured height h and base width b according to $\theta = 2\ \tan^{-1}{*}(2\ h/b)$. In order to obtain statistically reliable data, place 3–5 droplets on each of triplicate filters (*see* **Note 8**).

Step 3: Data Interpretation: Microbial cells exhibiting water contact angles of $\theta_w < 20°$, $20° \leq \theta \leq 50°$ and $\theta_w > 50°$ are considered to be hydrophilic, intermediately hydrophilic and hydrophobic, respectively [10]. Contact angles are also used to obtain information on the free energies of surfaces. A more detailed description of the derivation and calculations of free energies is beyond the possibility of this protocol and is described elsewhere [19].

4 Notes

1. Due to lower static charge, less hydrophobic polystyrene is easier to handle.
2. UV detection at 280 nm is approximately six times more sensitive than at 600 nm, thus allowing filtration experiments with dilute suspensions.
3. An Excel file for convenient calculation of the collector efficiency can be obtained from the authors of this chapter.
4. Verify microscopically that the bacterial suspension does not aggregate.
5. Bacteria change their surface properties depending on growth phase, substrate utilised or environmental conditions.

6. Avoid rough and discontinuous bacterial mats as they lead to contact angle hysteresis.
7. Keep in mind that the water content of the sample can influence the contact angle values and that when studying unknown strains, analyses of water contact angles as a function of drying time are recommended.
8. Sometimes a strong time dependence of the contact angles after droplet placement (by preference with hydrophilic cells) is observed. It is hence important to standardise the interval (t) after which the measurement is taken. In literature, both extrapolation of the angle measured to $t = 0$ (more suitable for highly hydrophilic bacteria) and an establishment of a 'contact angle equilibrium' ($t = 5$–7 s) have been proposed.

References

1. Efroymson RA, Alexander M (1991) Biodegradation by an *Arthrobacter* species of hydrocarbon partitioned into an organic solvent. Appl Environ Microbiol 57:1441–1447
2. Owsianiak M, Szulc A, Chrzanowski L, Cyplik P, Bogacki M, Olejnik-Schmidt AK, Heipieper HJ (2009) Appl Microbiol Biotechnol 84: 545–553
3. Neu TR (1996) Significance of bacterial surface-active compounds in interaction of bacteria with interfaces. Microbiol Rev 60:151–166
4. Wick LY, Wattiau P, Harms H (2002) Influence of the growth substrate on the mycolic acid profiles of mycobacteria. Environ Microbiol 4:612–616
5. Rutter PR, Vincent B (1980) The adhesion of microorganisms to surfaces: physico-chemical aspects. In: Berkeley RCW, Lynch RM, Mellin J, Rutter PR, Vincent B (eds) Microbial adhesion to surfaces. E. Horwood, Chichester
6. Van Loosdrecht MCM, Lyklema J, Norde W, Zehnder AJB (1989) Bacterial adhesion: a physicochemical approach. Microb Ecol 17: 1–15
7. Jucker BA, Zehnder AJB, Harms H (1998) Quantification of polymer interactions in bacterial adhesion. Environ Sci Technol 32:2909–2915
8. Hamadi F, Latrache H, Zahir H, Bengourram J, Kouider N, Elghmari A, Habbari K (2011) Evaluation of the relative cell surface charge by using microbial adhesion to hydrocarbon. Microbiology 80:48–491
9. Busscher HJ, van de Beltgritter B, van der Mei HC (1995) Implications of microbial adhesion to hydrocarbons for evaluating cell-surface hydrophobicity. 1. Zeta potentials of hydrocarbon droplets. Colloids Surf B Biointerfaces 5:111–116
10. Rijnaarts HHM, Norde W, Bouwer EJ, Lyklema J, Zehnder AJB (1993) Bacterial adhesion under static and dynamic conditions. Appl Environ Microbiol 59:3255–3265
11. Martin RE, Bouwer EJ, Hanna LM (1992) Application of clean-bed filtration theory to bacterial deposition in porous media. Environ Sci Technol 26:1053–1058
12. Busscher HJ, Weerkamp AH, van der Mei HC, van Pelt AWJ, de Jong HP, Arends J (1984) Measurement of the surface free energy of bacterial cell surfaces and it relevance for adhesion. Appl Environ Microbiol 48:980–983
13. Smits THM, Wick LY, Harms H, Keel C (2003) Characterization of the surface hydrophobicity of filamentous fungi. Environ Microbiol 5:85–91
14. Rosenberg M, Gutnick D, Rosenberg E (1980) Adherence of bacteria to hydrocarbons – a simple method for measuring cell-surface hydrophobicity. FEMS Microbiol Lett 9:29–33
15. Rosenberg M (2006) Microbial adhesion to hydrocarbons: twenty-five years of doing MATH. FEMS Microbiol Lett 262:129–134
16. Lichtenberg D, Rosenberg M, Sharfman N, Ofek I (1985) A kinetic approach to bacterial adherence to hydrocarbon. J Microbiol Methods 4:141–146
17. Della Volpe C, Maniglio D, Sibini S, Morra M (2001) An experimental procedure to obtain the equilibrium contact angle from the Wilhelmy method. Oil Gas Sci Technol 56:9–22
18. Della Volpe C, Brugnara M, Maniglio D, Siboni S, Wangdu T (2006) About the

possibility of experimentally measuring an equilibrium contact angle and its theoretical and practical consequences. In: Mittal KL (ed) Contact angle, wettability and adhesion, vol 4. CRC, Boca Raton

19. Van der Mei HC, Rosenberg M, Busscher HJ (1991) Assessment of microbial cell surface hydrophobicity. In: Mozes N, Handley PS, Busscher HJ, Rouxhlet PG (eds) Microbial cell surface analysis. VCH, New York, pp 263–287

Protocol for the Measurement of Hydrocarbon Transport in Bacteria

Jayna L. Ditty, Nancy N. Nichols, and Rebecca E. Parales

Abstract

Due to the hydrophobicity, volatility, and relatively low aqueous solubility of aliphatic and aromatic hydrocarbons, transport of these chemicals by bacteria has not been extensively studied. These issues make transport assays difficult to carry out, and as a result, strong evidence for the active transport of hydrocarbons is lacking. Here we describe a detailed protocol for the measurement of hydrocarbon transport in bacteria and suggest key equipment and control experiments required to obtain convincing results.

Keywords: Aromatic hydrocarbons, Metabolic inhibitors, Radiolabeled substrates, Specific activity, Transport

1 Introduction

The mechanism of transport of aliphatic and aromatic hydrocarbons in bacteria is not well understood. Because hydrocarbons are innately hydrophobic, these molecules freely diffuse through cellular membranes, resulting in intracellular toxicity if not regulated (reviewed in [1]). Therefore, in order to grow on hydrocarbons, bacteria must take up sufficient amounts of these toxic chemicals to allow them to grow but must maintain intracellular concentrations below toxic levels [2–4]. It is not clear at this time if bacteria actively transport hydrocarbons or if they enter cells solely by diffusion.

In Gram-negative bacteria, the outer membrane is an effective permeability barrier for both hydrophilic and hydrophobic molecules due to the thick sugar layer supplied by lipopolysaccharide on the outer leaflet [5]. As such, some genes and proteins that allow for the passage of hydrocarbons across the Gram-negative outer membrane have been identified and characterized [6–13].

Mention of trade names or commercial products in this article is solely for the purpose of providing specific information and does not imply recommendation or endorsement by the US Department of Agriculture

T.J. McGenity et al. (eds.), *Hydrocarbon and Lipid Microbiology Protocols*, Springer Protocols Handbooks, (2017) 55–67,
DOI 10.1007/8623_2014_11, © Springer-Verlag Berlin Heidelberg 2014, Published online: 30 December 2014

However, there is little compelling evidence that suggests the need for active transport of hydrocarbons across the cytoplasmic membrane [14–17]. Due to the low polarity and lipophilic nature of aromatic hydrocarbons, these types of molecules freely pass through the cytoplasmic membrane [5]. Because of their low pK_as, aromatic acids are predominantly protonated at neutral pH, and these uncharged molecules can also freely permeate cell membranes. Aromatic acid and hydrocarbon concentration gradients can be established through diffusion and metabolism alone, which has led to the argument that active transport mechanisms may not be necessary for their uptake [18]. However, some transporter proteins and active transport mechanisms have been identified for aromatic acids [19–24]. On the other hand, genes encoding putative aromatic hydrocarbon transport proteins are generally not present in known hydrocarbon catabolic operons, and specific hydrocarbon transport mutants have not been isolated. In addition, there is conflicting evidence in the literature regarding active transport of hydrocarbons across the cell membrane [14–17]. Therefore, additional studies are needed to definitively determine whether active transport mechanisms are required for aromatic or aliphatic hydrocarbons.

One reason for the lack of data on hydrocarbon transport mechanisms is the technical difficulty of hydrocarbon transport experiments, due to the volatilization of hydrocarbons as well as their tendency to adsorb to glassware and plastic. Therefore, careful experimental procedures are required to accurately assess hydrocarbon uptake by cells. Results of assays with wild-type strains and mutants lacking the putative transport protein-encoding gene should be compared. For example, in *Pseudomonas putida*, the rate of transport of 4-hydroxybenzoate is reduced approximately 12-fold and transport of 3,4-dihydroxybenzoate (protocatechuate, 3,4-HBA) is reduced 18-fold in a *pcaK* mutant compared to wild type (Fig. 1a, b, and Table 1). PcaK is a permease specific for transport of 4-hydroxybenzoate and 3,4-dihydroxybenzoate [24]. Transport of benzoate, which is not a substrate for PcaK, is unaffected in the mutant strain (Fig. 1c).

Experiments attempting to demonstrate active transport of hydrocarbons should include strategies to distinguish between hydrocarbon transport versus the accumulation of intermediates resulting from metabolism of the substrate. This latter issue is particularly important for hydrocarbon substrates, which freely diffuse across cellular membranes. Assays with catabolic mutants unable to incorporate the hydrocarbon substrate into cell material and/or expression of the gene encoding the transport protein in a heterologous host lacking the hydrocarbon metabolic pathway can clearly distinguish hydrocarbon transport from metabolism (Fig. 1d). In addition, saturation due to active transport may be most obvious in strains that are not metabolizing the radiolabeled

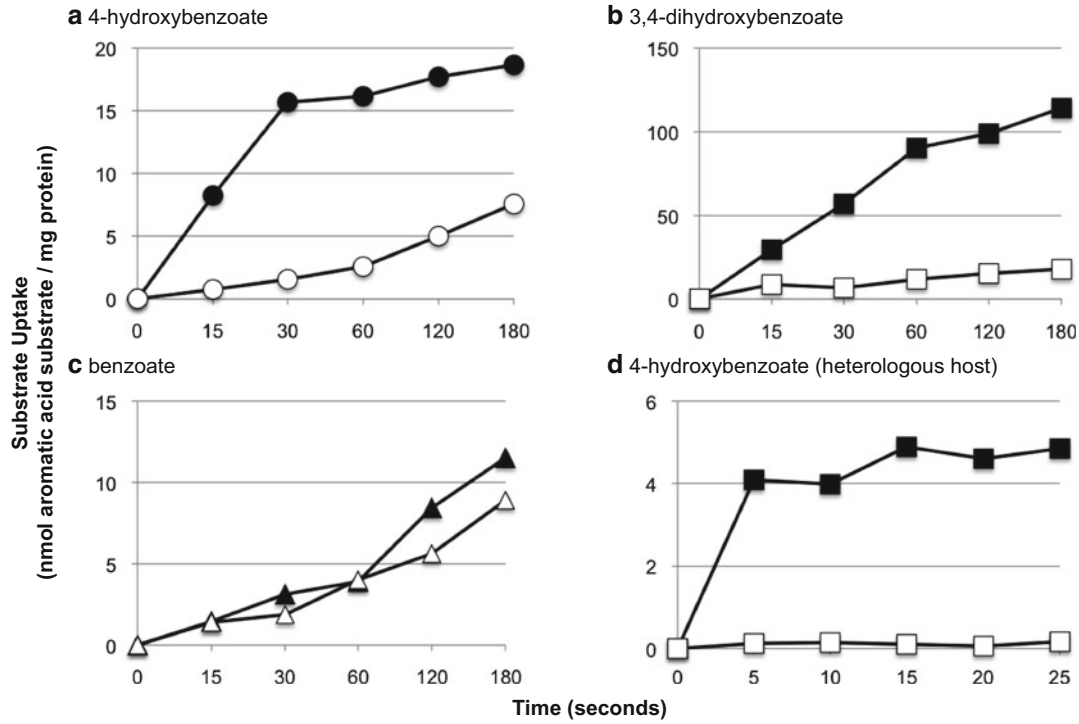

Fig. 1 Example of aromatic acid transport data using wild-type and mutant strains and a heterologous host. (**a**) Uptake of radiolabeled 4-hydroxybenzoate (*circles*), (**b**) 3,4-dihydroxybenzoate (*squares*), and (**c**) benzoate (*triangles*) by wild-type (*closed symbols*) and transport deficient *pcaK*$^{-}$ mutant (*open symbols*) *P. putida* strains. For these transport assays, cells were cultured under appropriate inducing conditions. Cells for assays of 4-hydroxybenzoate and 3,4-dihydroxybenzoate uptake were grown on 4-hydroxybenzoate, and cells for assay of benzoate uptake were grown on benzoate. The data shown are from a single representative assay carried out in duplicate. (**d**) Heterologous expression of the aromatic acid transporter PcaK in *E. coli* results in 4-hydroxybenzoate transport. When the PcaK protein is produced in a heterologous host incapable of metabolizing the substrate, transport saturates quickly (*closed squares*) relative to a vector control (*open squares*). Note that the *y*-axis values differ in panels *A*, *B*, *C*, and *D* and the *x*-axis is different in panel *D*. Data presented in *D* was adapted from Fig. 8 presented in [24] (Copyright © American Society for Microbiology, Journal of Bacteriology, volume 174, 1994, pp. 6479–6488)

substrate. Assays in the presence of specific metabolic inhibitors are also important to determine the type of energy source that is required for hydrocarbon accumulation [24].

The protocol described here is an updated compilation of published methods to measure aromatic acid and aromatic hydrocarbon uptake using radiolabeled substrates [2, 24–31]. While a few studies have reported the ability to assess transport of non-radiolabeled substrates [32–34], these assays have not yet been modified for the measurement of hydrocarbon uptake in bacterial systems and therefore are not described here. The general principle of the transport assay is to grow bacterial cultures under the appropriate conditions to ensure the transport system of interest is

Table 1
Rates of aromatic acid transport in wild-type and *pcaK*$^-$ mutant strains

	Specific activity[a]	
	Wild type[b]	*pcaK*$^-$
4-Hydroxybenzoate	31.3	2.47
3,4-Dihydroxybenzoate	89.2	4.95
Benzoate	3.76	2.79

The transport rates calculated here are based on the data presented in Fig. 1a–c, respectively. Rates were determined from the linear portion of each curve. Protein concentrations were calculated as outlined in Sect. 3.2
[a]nmol substrate/min/mg cellular protein
[b]Wild-type *P. putida* PRS2000 and the *pcaK*$^-$ mutant strain PCH722-Gm are described in [24]

induced. After harvesting the cells and removing any residual substrate from the growth medium, the cells are exposed to optimized levels of radioactive hydrocarbon substrate and samples are taken over time to measure accumulated substrate. Samples are filtered to remove unincorporated substrate and allow measurement of labeled substrate present inside cells. Transport results are presented as a specific activity rate relative to protein concentration.

2 Materials (*see* Note 1)

2.1 Preparation of the Transport Assay Cocktail

1. 1.0 M glucose
2. 1.0 M sodium succinate
3. 5.0 mM unlabeled hydrocarbon substrate (*see* **Note 2**)
4. 3.0 mM ^{14}C-labeled hydrocarbon substrate (*see* **Notes 2** and **3**)
5. 25 mM potassium phosphate buffer (KPB), pH 7: 1.53 ml 1.0 M K_2HPO_4 and 0.96 ml 1.0 M KH_2PO_4 in 100 ml distilled water total volume (*see* **Note 4**)
6. Acid-washed 13 mm disposable borosilicate glass test tubes (*see* **Note 5**)

2.2 Growth and Preparation of Cells

1. Aeration of cells: glass Pasteur pipette, tubing, and source of forced air
2. Cell suspension buffer: 25 mM KPB, pH 7
3. Bacterial cells: each bacterial strain grown to mid-exponential phase under appropriate growth conditions (*see* Sect. 3.2)
4. Protein precipitation: 25% trichloroacetic acid and 0.1 M NaOH
5. Protein assay reagents (e.g., Protein Bio-Rad Protein Assay Kit (Bio-Rad, Hercules, CA)).

2.3 Transport Assay

1. 0.2 μm pore size Whatman® polycarbonate membrane filters
2. Model 1225 Sampling Vacuum Manifold (Millipore, Billerica, MA)
3. Wash buffer: 25 mM KPB, pH 7
4. Digital minute/second timer
5. Scintillation vials, scintillation fluid, and scintillation counter

2.4 Determination of Energy Requirements

1. 30 mM sodium azide
2. 50 μM carbonyl cyanide *m*-chlorophenylhydrazone (CCCP)
3. 5 mM dinitrophenol (DNP)
4. 10 mM KCN

3 Methods

3.1 Preparation of the Transport Assay Cocktail

The key requirement for any transport assay cocktail is that it contains saturating amounts of substrate. While determining the saturating concentration of a volatile hydrocarbon can be difficult, it is necessary to ensure that saturating levels for each individual transporter/substrate pair are achieved before transport assays can be implemented; this ensures that cellular transport and the subsequent detection of intracellular substrate is not limited. In addition to the hydrocarbon substrate, the addition of easily metabolizable energy sources will ensure that the bacterial cells have sufficient energy to carry out active transport. Here, succinate and glucose are provided; however the energy source(s) should be chosen based on the metabolism of the microorganism of interest. Also, in the protocol described here, potassium phosphate buffer (KPB) pH 7 is used as the buffer for diluting and maintaining the cell suspension. If necessary, an alternative buffer that is more appropriate for the organism being studied should be substituted.

The transport cocktail should be mixed and used in a fume hood due to the volatility of the hydrocarbon substrate. In addition, the cocktail should be mixed immediately before each set of transport assays to reduce hydrocarbon adsorption to the glassware. We recommend the use of acid-washed borosilicate glass test tubes for both batch mixing and the dispersal of transport cocktail aliquots for individual assays, as hydrocarbons can stick to untreated glass and plastics (*see* **Note 5**). Investigators should also ensure that radioactive materials licensing and radioactive disposal contracts are current.

1. Combine the following for one transport assay:

   1.2 μl 1.0 M glucose (energy source)

   1.2 μl 1.0 M sodium succinate (energy source)

6.0 μl 5.0 mM unlabeled hydrocarbon substrate (*see* **Note 2**)

3.0 μl 3.0 mM ^{14}C-labeled hydrocarbon substrate

289 μl 25 mM KPB, pH 7

2. To make one large batch of transport cocktail, multiply the above values by the total number of planned assays, ensuring that enough replicates are available to determine statistical significance (typically in duplicate or triplicate). After mixing, 300 μl aliquots should be distributed into 13 mm acid-washed borosilicate glass test tubes for each transport assay to be conducted.

3.2 Growth and Preparation of Cells (see Note 6)

An important factor for the successful measurement of active transport is the use of cells that are harvested during the mid-exponential phase of growth, to ensure that the cells are metabolically active. Another important consideration is the specific growth requirements for different bacterial cultures. For example, it may be informative to grow bacterial cultures under both inducing and non-inducing conditions if transport of the substrate is regulated, so that the transport characteristics can be compared between the two growth conditions. It is also recommended that transport be tested in either a catabolic mutant incapable of growth on the transport substrate or expression of the transport gene in a heterologous host that is unable to metabolize the transport substrate. Results of assays in the absence of substrate metabolism allow for a clear differentiation between active accumulation of radiolabeled substrate due to transport and accumulation of radioactive intermediates resulting from metabolism of the transported substrate (Fig. 1d).

1. Grow cells in an appropriate growth medium (75–100 ml) under the optimal conditions for the organism under study (temperature, aeration, etc.). To determine if transport is inducible, cultures should be grown with and without potential inducing substrates. Cells should be harvested during mid-exponential phase.
2. Collect cells by centrifugation for 10 min at 5,000 × *g* at room temperature.
3. Wash the cells by resuspending the cell pellet in 50 ml of 25 mM KPB, pH 7.
4. Collect the cells by centrifugation. Resuspend the cell pellet in 25 mM KPB, pH 7, to a final cell density of 10^9 to 10^{10} cells/ml.
5. Aerate the cells by gently bubbling air through a Pasteur pipette until the start of the assay (*see* **Note 7**).
6. Remove 100 μl of the cell suspension for determining protein concentration. Precipitate the protein with 25 % trichloroacetic

acid (TCA) [35]. Resuspend the protein pellet in 100 µl 0.1 M NaOH, heat at 95°C for 10 min, and determine the protein-concentration using an appropriate method (*see* **Note 8**) [36, 37].

3.3 Transport Assay

Before starting transport assays, have the transport cocktail mixed and distributed (described in Sect. 3.1) and the cells harvested and aerated (described in Sect. 3.2). The transport assay is initiated by mixing cells with labeled substrate. Substrate uptake is halted at timed intervals by vacuum filtration followed by washing and vacuum filtration. Once cells and transport cocktail have been mixed, timed samples are immediately taken, on the order of seconds to minutes. The accumulation of intracellular radiolabeled substrate is then measured by scintillation counting of the cells retained on the filters.

1. Place 0.2-µM pore Whatman® polycarbonate membrane filters on the openings of a vacuum manifold (*see* **Note 9**). One filter is used for each time point of each assay. Place sealing stoppers on any openings not in use during the assay.
2. Assemble the vacuum manifold and turn on the vacuum. Leave the vacuum on for the duration of the assay.
3. Wash the filters by adding 2.0 ml of 25 mM KPB, pH 7, to each manifold opening. Wait until all the liquid is pulled through the filters.
4. Start the transport assay reaction by adding 300 µl of the cell suspension to 300 µl transport cocktail in the glass test tubes. Immediately, start a timer when the cells are added to the cocktail.
5. At timed intervals, transfer 100 µl of the transport assay mixture to a membrane filter on the vacuum manifold (*see* **Note 10**).
6. Immediately after the liquid has been pulled though the filter, wash the cells by adding 2.0 ml of 25 mM KPB, pH 7 (*see* **Notes 11** and **12**).
7. After all samples have been collected and washed, release the vacuum and place the filters in scintillation vials with an appropriate amount of scintillation fluid and determine DPM according to the instructions for your scintillation counter.
8. From the remaining unfiltered transport assay mix, remove two 20-µl samples and place each in a scintillation vial to obtain total counts of the radiolabeled hydrocarbon reaction mixture. In addition, determine the background DPM levels for two vials of scintillation fluid, without filters or reaction mix.

9. Before carrying out additional assays, check the level of liquid in the reservoirs of the vacuum manifold, and empty if necessary, discarding radioactive waste appropriately.

3.4 Determination of the Energy Requirement

Because active substrate transport requires energy, measuring uptake by starved cells can be used to determine if energy is required for transport. To determine whether energy in the form of either ATP or proton motive force is being used, metabolic inhibitors that deplete cellular ATP pools or dissipate the electrochemical gradient across the membrane can be used. Here we provide protocols for the use of sodium azide, which inhibits cytochrome oxidase; dinitrophenol (DNP) and carbonyl cyanide *m*-chlorophenylhydrazone (CCCP), which dissipate the proton gradient; and KCN, which eliminates electron transport. Many other inhibitors have been described [2, 24, 25, 28–31], and additional experiments to characterize the energy source are discussed elsewhere [29, 30].

1. Grow and wash cells as described in Sect. 3.2
2. Deplete cellular energy stores by resuspending cells in an equal volume of growth medium or buffer lacking an energy source. Incubate for 18 h under the same conditions used for growth (*see* **Note 13**).
3. Prepare two reaction mixtures as described in Sect. 3.1, but omit energy sources such as glucose or succinate from one mixture.
4. Carry out transport assays as described in Sect. 3.3 in duplicate, using reaction cocktails with and without added energy source. Compare the specific activities for the two conditions (calculate as described in Sect. 4.4) to determine if uptake occurred in the absence of energy source.
5. To assess the effect of metabolic inhibitors, treat starved cells as described in **Note 14**.
6. After inhibitor treatment, incubate cells with an energy source (10 mM glucose or succinate) for an additional 15 min. Perform transport assays to determine if cells exposed to an inhibitor can accumulate substrate.
7. Calculate specific activity of substrate uptake (*see* Sect. 3.5) and compare to results in the absence of inhibitors.

3.5 Calculations

The specific activity of the transporter can be calculated if cells accumulate hydrocarbons using a transport protein.

1. Subtract background counts from the counts obtained at each time point to obtain corrected disintegrations per minute (DPM) values.
2. Using the two 20-μl unfiltered samples, determine the amount of hydrocarbon substrate per DPM in the reaction. For

example, (65 μM hydrocarbon substrate/ml) (0.02 ml) = 1.3 nmol. The average of two 20-μl samples in this example gives approximately 20,000 DPM. Therefore, 1.3 nmol of hydrocarbon substrate/20,000 DPM = 6.5 x 10^{-5} nmol/DPM.

3. Determine the amount of substrate retained on each filter. Convert the DPM for each filtered assay sample to nmoles of hydrocarbon substrate accumulated by dividing the DPM for each filter by the value calculated in step 2. Plot the results versus time to determine the rate of uptake. If uptake is linear, the slope of the line can be used to determine the rate of uptake (Table 1). Convert the specific rate of uptake into nmoles accumulated per minute (*see* **Note 15**).
4. Correct for the amount of protein on each filter after determining the protein concentration in the saved 100 μl samples (Sect. 3.2, step 6).

   For example, (mg/ml protein calculated in Sect. 3.2, step 6) × (0.3 ml cells/0.6 ml total reaction volume) × (0.1 ml volume sample per filter) = total mg protein on each filter.
5. Determine the specific activity of uptake by dividing the nmoles of hydrocarbon uptake per minute (step 3) by the amount of protein present in the assay (step 4).

4 Notes

1. In the list of Materials (*see* Sect. 2), we provide the names of specific vendors for materials and a transport apparatus that have worked well in our experience.
2. The amounts used in this protocol generate a total saturating hydrocarbon substrate concentration of approximately 65 μM (50 μM unlabeled and 15 μM radiolabeled); however, saturating conditions may be different for each transport system. Saturating conditions should be experimentally determined on an individual basis. The total amount of added radioactive substrate should consist of 100,000 DPM per 100-μl reaction volume, and the unlabeled hydrocarbon substrate should then be added to supplement the total hydrocarbon concentration to ensure saturating levels. This method minimizes the amount of radioactivity used. The radiolabeled substrate of interest may not be commercially available and may be expensive or difficult to synthesize.
3. Solubility may be an issue with many hydrocarbon substrates. If this is the case, the hydrocarbon should be dissolved in an appropriate solvent [2] or surfactant [39], and the solvent or surfactant should be included in all control solutions.
4. The pH of the potassium phosphate buffer should be checked prior to use and adjusted to pH 7 if necessary.

5. Hydrocarbons are known to adsorb to glassware [40]. If adsorption is an issue with your substrate, the glassware should be treated with a chromic acid for 16 h followed by water rinse. The glassware should then be soaked for 16 h with nitric acid and again rinsed with water [2]. For easy and cost-effective removal of radioactive materials after each assay, disposable borosilicate glassware is recommended.
6. The experimental approach provided is appropriate for aerobic bacteria; adjustments will be necessary for assessing hydrocarbon transport in anaerobes.
7. Introducing air at a rate of approximately one air bubble per second keeps most bacterial cultures aerated without damaging or concentrating the cells over the course of the transport assays. In some cases, introducing an extended "aeration and starvation period" of 20–30 min may be helpful for the detection of radiolabeled substrate. This extended starvation period can help to deplete remaining intracellular substrate, thereby enhancing detection of the intracellular radiolabeled substrate.
8. Oftentimes, it is more convenient to store the cell samples and conduct protein assays at a later date. If this is the case, it is best to collect a cell pellet by centrifugation, remove the supernatant, and store the cell pellet at −20°C until use. When convenient, completely thaw the cell pellet and proceed with the TCA precipitation and subsequent protein assay.
9. Before the first assay, it is helpful to wet the openings of the vacuum manifold with approximately 0.5 ml of 25 mM KPB, pH 7, before placing the polycarbonate filters on the openings. This will help keep the filters in place while you assemble the vacuum manifold for the first time.
10. The appropriate time intervals between samples will need to be empirically determined for each transport system. A typical set of time intervals may be 5, 10, 15, 20, and 25 s or 15, 30, 60, 90, and 120 s. Depending upon how fast transport saturates, some initial time points may need to be taken faster than 5 s.
11. Due to the speed at which transport assays occur, it is often helpful to have two people conducting the assay. One person initiates the assay and removes samples at the timed intervals. The second person monitors the vacuum manifold openings and washes the cells when the liquid has been completely pulled through the filters. In a timed assay, it is important to wash each sample immediately after the supernatant has been pulled through the vacuum to eliminate any remaining substrate and prevent additional uptake.
12. Active transport of nonpolar substrates may be difficult to detect because the substrate can diffuse out of cells, especially during assays in which the cells are not actively metabolizing

the substrate and "trapping" it inside (such as in assays with a catabolic mutant). To minimize this possibility, collection of cell pellets by centrifugation through silicone oil may be preferred over filtration and aqueous washing of cells. Silicone oil terminates the reaction by stripping cells of the surrounding medium as the bacterial cells pass through the oil [24, 38].

13. Measure intracellular levels of ATP in cells concomitantly with transport assays to verify that energy stores have been depleted [29, 30, 41].
14. Approximate concentrations and exposure times for metabolic inhibitors: 30 mM sodium azide for 5–10 min, 10 mM potassium cyanide (KCN) for 5 min [2] 50 μM CCCP for 1 min, and 5.0 mm DNP for 1 min [24].
15. If the transport of hydrocarbon saturates quickly, the initial uptake rates should be calculated using time points that have not yet saturated. For example, the transport rates calculated for 4-hydroxybenzoate and 3,4-dihydroxybenzoate were determined from 0 to 60 s and the rate for benzoate was determined over 180 s, corresponding to the linear portion of each data set (Fig. 1a–c). In some cases, uptake may have already saturated by the first time point (Fig. 1d). In such cases, the experiment should be redesigned to take earlier time points. If it is not possible to take earlier time points, the initial rate may need to be estimated by extrapolating the values to zero.

References

1. Sikkema J, De Bont JAM, Poolman B (1995) Mechanisms of membrane toxicity of hydrocarbons. Microbiol Rev 59:201–222
2. Bugg T, Foght JM, Pickard MA, Gray MR (2000) Uptake and active efflux of polycyclic aromatic hydrocarbons by *Pseudomonas fluorescens* LP6a. Appl Environ Microbiol 66:5387–5392
3. Isken S, de Bont JA (1998) Bacteria tolerant to organic solvents. Extremophiles 2:229–238
4. Kieboom J, Dennis JJ, de Bont JA, Zylstra GJ (1998) Identification and molecular characterization of an efflux pump involved in *Pseudomonas putida* S12 solvent tolerance. J Biol Chem 273:85–91
5. van den Berg B (2010) Going forward laterally: transmembrane passage of hydrophobic molecules through protein channel walls. ChemBioChem 11:1339–1343
6. Belchik SM, Schaeffer SM, Hasenoehrl S, Xun L (2010) A beta-barrel outer membrane protein facilitates cellular uptake of polychlorophenols in *Cupriavidus necator*. Biodegradation 21:431–9
7. Hearn EM, Patel DR, van den Berg B (2008) Outer-membrane transport of aromatic hydrocarbons as a first step in biodegradation. Proc Natl Acad Sci U S A 105:8601–8606
8. Kahng H-Y, Byrne AM, Olsen RH, Kukor JJ (2000) Characterization and role of *tbuX* in utilization of toluene by *Ralstonia pickettii* PKO1. J Bacteriol 182:1232–1242
9. Kasai Y, Inoue J, Harayama S (2001) The TOL plasmid pWWO *xylN* gene product from *Pseudomonas putida* is involved in *m*-xylene uptake. J Bacteriol 183:6662–6666
10. Mooney A, O'Leary ND, Dobson AD (2006) Cloning and functional characterization of the

styE gene involved in styrene transport in *Pseudomonas putida* CA-3. Appl Environ Microbiol 72:1302–1309

11. Neher TM, Lueking DR (2009) *Pseudomonas fluorescens ompW*: plasmid localization and requirement for naphthalene uptake. Can J Microbiol 55:553–563
12. van Beilen JB, Panke S, Lucchini S, Franchini AG, Röthlisberger M, Witholt B (2001) Analysis of *Pseudomonas putida* alkane-degradation gene clusters and flanking insertion sequences: evolution and regulation of the *alk* genes. Microbiology 147:1621–1630
13. Wang Y, Rawlings M, Gibson DT, Labbé D, Bergeron H, Brousseau R, Lau PC (1995) Identification of a membrane protein and a truncated LysR-type regulator associated with the toluene degradation pathway in *Pseudomonas putida* F1. Mol Gen Genet 246:570–579
14. Calvillo YM, Alexander M (1996) Mechanism of microbial biphenyl sorbed to polyacrylic beads. Appl Microbiol Biotechnol 45:383–390
15. Feng Y, Park J-H, Voice TC, Boyd SA (2000) Bioavailability of soil-sorbed biphenyl to bacteria. Environ Sci Technol 10:1977–1984
16. Kim IS, Lee H, Trevors JT (2001) Effects of 2,2′,5,5′-tetrachlorobiphenyl and biphenyl on cell membranes of *Ralstonia eutropha* H850. FEMS Microbiol Lett 200:17–24
17. Master ER, McKinlay JJ, Stewart GR, Mohn WW (2005) Biphenyl uptake by psychrotolerant *Pseudomonas* sp. strain Cam-1 and mesophilic *Burkholderia* sp. strain LB400. Can J Microbiol 51:399–404
18. Harwood CS, Gibson J (1986) Uptake of benzoate by *Rhodopseudomonas palustris* grown anaerobically in light. J Bacteriol 165:504–509
19. Chae JC, Zylstra GJ (2006) 4-Chlorobenzoate uptake in *Comamonas* sp. strain DJ-12 is mediated by a tripartite ATP-independent periplasmic transporter. J Bacteriol 188:8407–8412
20. Collier LS, Nichols NN, Neidle EL (1997) *benK* encodes a hydrophobic permease-like protein involved in benzoate degradation by *Acinetobacter* sp. strain ADP1. J Bacteriol 179:5943–5946
21. D'Argenio DA, Segura A, Coco WM, Bunz PV, Ornston LN (1999) The physiological contribution of *Acinetobacter* PcaK, a transport system that acts upon protocatechuate, can be masked by overlapping specificity of VanK. J Bacteriol 181:3505–3515
22. Ledger T, Aceituno F, Gonzalez B (2009) 3-Chlorobenzoate is taken up by a chromosomally encoded transport system in *Cupriavidus necator* JMP134. Microbiology 155: 2757–2765
23. Leveau JH, Zehnder AJ, van der Meer JR (1998) The *tfdK* gene product facilitates uptake of 2,4-dichlorophenoxyacetate by *Ralstonia eutropha* JMP134(pJP4). J Bacteriol 180:2237–2243
24. Nichols NN, Harwood CS (1997) PcaK, a high-affinity permease for the aromatic compounds 4-hydroxybenzoate and protocatechuate from *Pseudomonas putida*. J Bacteriol 179:5056–5061
25. Ahmed S, Booth IR (1982) The use of valinomycin, nigericin and trichlorocarbanilide in control of the protonmotive force in *Escherichia coli* cells. Biochem J 212:105–112
26. Bateman JN, Speer B, Feduik L, Hartline RA (1986) Naphthalene association and uptake in *Pseudomonas putida*. J Bacteriol 166:155–161
27. Ditty JL, Nichols NN, Parales RE (2010) Measurement of hydrocarbon transport in bacteria. In: Timmis KN (ed) Handbook of hydrocarbon and lipid microbiology. Springer-Verlag, Heidelberg, pp 4214–4221
28. Heytler PG (1979) Uncouplers of oxidative phosphorylation. Method Enzymol 55:462–442
29. Joshi AK, Ahmed S, Ferro-Luzzi Ames G (1989) Energy coupling in bacterial periplasmic transport systems: studies in intact *Escherichia coli* cells. J Biol Chem 264:2126–2133
30. Kashket ER (1985) The proton motive force in bacteria: a critical assessment of methods. Ann Rev Microbiol 39:219–242
31. Linnett PE, Beechey RB (1979) Inhibitors of the ATP synthethase system. Methods Enzymol 55:472–518
32. Bermejo C, Haerizadeh F, Takanaga H, Chermak D, Frommer WB (2010) Dynamic analysis of cytosolic glucose and ATP levels in yeast using optical sensors. Biochem J 432:399–406
33. Fehr M, Lalonde S, Lager I, Wolff MW, Frommer WB (2003) In vivo imaging of the dynamics of glucose uptake in the cytosol of COS-7 cells by fluorescent nanosensors. J Biol Chem 278:19127–19133
34. Sedlak M, Ho NW (2004) Characterization of the effectiveness of hexose transporters for transporting xylose during glucose and xylose co-fermentation by a recombinant Saccharomyces yeast. Yeast 21:671–684
35. Ausubel FM, Brent R, Kingston RE et al (1993) Current protocols in molecular biology. Wiley, New York

36. Bradford MM (1976) A rapid and sensitive method for the quantitation of microgram quantities of protein utilizing the principle of protein-dye binding. Anal Biochem 72: 248–254
37. Lowry OH, Rosebrough NJ, Farr AL, Randall RJ (1951) Protein measurement with the Folin phenol reagent. J Biol Chem 193:265–275
38. Klingenberg M, Pfaff E (1977) Means of terminating reactions. Methods Enzymol 10:680–684
39. Volkering F, Breure AM, Rulkens WH (1998) Microbiological aspects of surfactant use for biological soil remediation. Biodegradation 8:401–417
40. Qian Y, Posch T, Schmidt TC (2011) Sorption of polycyclic aromatic hydrocarbons (PAHs) on glass surfaces. Chemosphere 82:859–865
41. Bagnara AS, Finch LR (1972) Quantitative extraction and estimation of intracellular nucleoside triphosphates of *Escherichia coli*. Anal Biochem 45:24–34

Respiration Rate Determined by Phosphorescence-Based Sensors

Michael Konopka

Abstract

Respiration rates can be a powerful diagnostic tool that provides insight into the metabolic activity of the cells. An optical-based method is well suited for making oxygen consumption measurements in microbial populations, whether on a model organism or environmental sample. This approach utilizes phosphorescent dyes since the lifetime of their excited state depends on the oxygen concentration. Two systems are described using closed sample chambers which can be constructed at minimal costs from off-the-shelf parts. The first system is designed around a glass cuvette utilizing an oil layer as an oxygen barrier. The second system is adapted to an existing microscope and uses a cavity well slide with a glass coverslip lid as the sample chamber. In both systems a photomultiplier tube or gated CCD camera is used for detecting the phosphorescent signal which, when calibrated, provides a reliable measurement of oxygen concentration over time.

Keywords: Environmental microbiology, Oxygen sensor, Phosphorescence lifetime, Respiration rate measurement

1 Introduction

Since cellular respiration changes in response to a wide number of stimuli, measuring respiration can play a fundamental role in understanding the metabolic state of microbial cells, whether they are model organisms, environmental isolates, or whole natural communities [1]. Respiration rates can be inferred by directly measuring the oxygen consumption (or uptake) by a cell sample over time. Dissolved oxygen concentrations can be measured by a variety of approaches [2, 3], although the most common method uses a Clark electrode because it fits the budget of most labs and requires a lower level of technical expertise to operate. However, the Clark electrode has a number of technical limitations which restrict its effectiveness. Not only does it suffer from signal drift and low sensitivity, but the electrode also consumes oxygen when performing measurements. Additionally, scaling the electrode down in size is difficult, so larger cultures or samples are required. Clark electrodes also require

T.J. McGenity et al. (eds.), *Hydrocarbon and Lipid Microbiology Protocols*, Springer Protocols Handbooks, (2017) 69–80,
DOI 10.1007/8623_2015_162, © Springer-Verlag Berlin Heidelberg 2015, Published online: 13 December 2015

frequent calibrations to ensure consistent, accurate respiration rate measurements.

Since sample chambers for Clark electrodes, and many other oxygen measurement systems, are open to the air, the rate that oxygen permeates into the sample must be determined as background for respiration rate calculations [4]. Electrodes measure oxygen at a single point or area in the sample chamber, so the diffusion of oxygen to the probe can also affect the calculation [5, 6]. A closed system with an oxygen sensor dispersed throughout the sample would minimize these concerns.

An optical probe of dissolved oxygen concentration is compatible with a closed system. Commonly used families of dyes for sensing oxygen in a sample include platinum porphyrins, palladium porphyrins, and ruthenium compounds, which all utilize phosphorescence to determine the oxygen concentration. Phosphorescence differs from fluorescence in terms of the timescale it takes for electrons to decay from the excited state to the ground state (Fig. 1). A fluorescent chromophore decays in picoseconds to nanoseconds, while it takes microseconds for the electrons from excited phosphorescent sensors to decay to the ground state. Part of the reason for the longer timescale is because they transition through an intermediate triplet state. While the electron is in the triplet state, oxygen competes with the photo decay of the electrons because it can accept a triplet-state electron and quench the photoluminescence. This is an inverse logarithmic relationship between oxygen concentration and phosphorescence lifetime, meaning that the higher the oxygen concentration, the faster the lifetime decay.

Phosphorescent sensors can be used to calculate the oxygen concentration using the Stern-Volmer equation:

$$I_0/I = \tau_0/\tau = 1 + K_Q\tau_0[O_2]$$

where I_0 and τ_0 are the intensity and phosphorescence lifetime, respectively, at 0% oxygen; I and τ are the intensity and phosphorescence lifetime, respectively, at the oxygen concentration $[O_2]$;

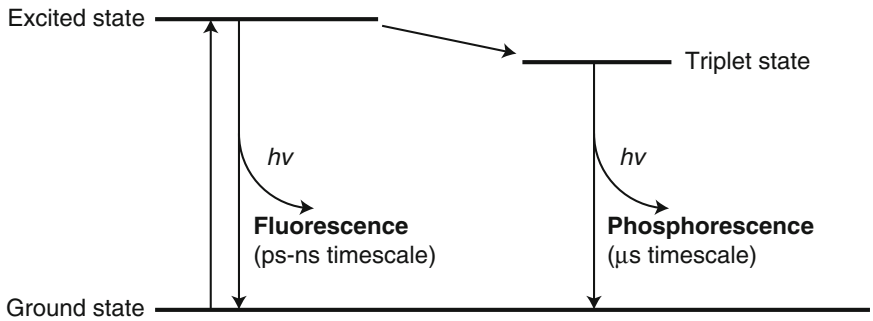

Fig. 1 Simplified representation of electron transitions between energy states for the excitation and emission during fluorescence and phosphorescence

and K_Q is the Stern-Volmer constant [3, 7]. While the intensity of phosphorescent sensors can be used to determine oxygen concentrations, measuring the phosphorescent lifetime has the advantages of being independent of dye concentration and photobleaching. Platinum meso-tetrakis(pentafluorophenyl)porphyrin is an excellent sensing dye because it has a linear response to oxygen concentration [8], although the dye must be imbedded in an oxygen-permeable material like polydimethylsiloxane (PDMS) or polystyrene beads [2, 3, 9]. There are also commercially available beads which are already embedded with a platinum porphyrin [10].

All that is needed to measure oxygen concentration by phosphorescence in a closed sample chamber is an excitation source and some method to measure the lifetime of the sensor. There are some commercially available systems for doing lifetime measurements, either in a cuvette or microplate reader, which could be adapted to doing high-throughput oxygen consumption measurements. However, unless one already has access to such systems, they may be cost prohibitive. In addition, plastic-based plates or containers have some limitations due to oxygen perfusion through those materials [4]. Below two systems are described which were first developed at the Microscale Life Sciences Center (MLSC) that can be constructed in the lab for less than $5,000. Both are similar in their design and instrumentation, although the implementation of the sample chamber differs. The first is a user-constructed benchtop system that uses a glass cuvette with a layer of oil to diffusional seal the sample chamber to oxygen. The second system adapts to an existing microscope by depositing the sensor at the bottom of a cavity well slide which is then viewed through an objective. Both are compatible with any aqueous-based cell sample, use a light-emitting diode as the excitation source, and can use a photomultiplier tube to collect signal. The microscope-based system is more versatile since it can also work with attached cells or use a gated charge-coupled device to image the sensor [11].

2 Materials

2.1 Oxygen Sensor

1. Platinum porphyrin-based sensor embedded in oxygen-permeable material (e.g., 40 nm FluoSpheres® carboxylate-modified microspheres – platinum luminescent, F-20886, Life Technologies, Grand Island NY)
2. Tabletop microcentrifuge (e.g., 5430, Eppendorf, Hamburg, Germany)
3. Ultrapure water

2.2 Device Input: LED to Sample

1. Light-emitting diode (LED) in appropriate range for chosen sensor. For commercially available beads referred to in Sect. 2.1, an LED in the range of 390–405 nm can be used (e.g., ThorLabs, Newton NJ).
2. Power supply.
3. Function generator.
4. Pulse delay generator (*see* **Note 1**).

2.3 Cuvette-Based Measurement

1. Photomultiplier tube (PMT)
2. Power supply (*see* **Note 2**)
3. Glass cuvette
4. Cuvette holder (e.g., CVH100, ThorLabs, Newton, NJ, or 13950, Newport, Irvine, CA)
5. Castor oil (Sigma-Aldrich, St. Louis, MO)
6. 600 nm long pass filter (e.g., AT600lp, Chroma, Bellows Falls, VT)
7. Oscilloscope (e.g., Tektronix, Beaverton, OR) or digital to analog (D/A) converter (National Instruments, Austin TX)
8. Preamplifier (optional, *see* **Note 3**)
9. Posts, clamps, and an optical breadboard (e.g., optional, Newport, Irvine CA)

2.4 Microscope-Based Measurement

1. PMT or gated charge-coupled device (CCD) camera (e.g., iStar ICCD, Andor, Belfast, Ireland)
2. Power supply (*see* **Note 2**)
3. Cavity well microscope slides (e.g., VWR, Radnor, PA, *see* **Note 4**)
4. Glass coverslip
5. Plasma cleaner (optional, *see* **Note 5**)
6. Ethanol (200 proof, meets USP specifications)
7. Sterile forceps or tweezers
8. Filter cube with dichroic mirror appropriate to LED and 600 nm long pass filter for the emission (e.g., T412lpxt and AT600lp, Chroma, Bellows Falls, VT) (*see* **Note 6**)
9. Oscilloscope (e.g. Tektronix, Beaverton, OR) or digital to analog (D/A) converter (National Instruments, Austin, TX)

2.5 Data Analysis

1. Computer
2. Data analysis software (e.g., MATLAB, MathWorks, Natick, MA)

3 Methods

The oxygen sensor, LED for excitation, and method for data analysis are all the same for both the glass cuvette and microscope-based methods.

3.1 Oxygen Sensor

The toxicity of potential oxygen sensors, including any compounds they may be in solution with, is an important consideration. Since commercially available beads are stored with an azide chemical to inhibit microbial growth, it must be removed from any stock solution prior to use for respiration measurements [3]. Pelleting by centrifugation and washing the beads are the simplest procedures (*see* **Note 7**).

1. Pellet the beads using a tabletop microcentrifuge (>6,300×*g* for 5 min). Remove the supernatant.
2. Wash and resuspend the beads with 2 mL ultrapure water.
3. To ensure that all preservative has been removed, pellet the beads again using a tabletop microcentrifuge (>6,300×*g* for 5 min). Remove the supernatant.
4. Concentrate the stock solution by a factor of 10 by resuspending in 0.2 mL ultrapure water.
5. Store washed bead solution at 4°C in the dark. The stock solution can be used for at least a year if kept dark to minimize photobleaching.

3.2 Device Input: LED to Sample

The LED requires both a power supply and method to pulse the light source.

1. Connect the power supply to the LED. Power supply settings will depend on the specific LED in the system.
2. Typically a square wave produced by a function generator at 5 Hz, 5 V peak-to-peak is sufficient to drive the light source. The function generator is connected to the LED through a pulse delay generator (*see* **Note 2**).

3.3 Cuvette-Based Measurement

3.3.1 Apparatus Construction

For best results, ambient light should be kept to a minimum when working with a benchtop system. Either working in a dark room or covering the entire system with a dark box would be sufficient. Using an optical breadboard with posts and clamps to fasten the components will improve the stability of the system. A simple schematic of the system is shown in Fig. 2.

1. The cuvette holder is positioned in front of the LED so that one face is perpendicular to the excitation source.
2. Align the 600 nm long pass filter next to the cuvette but at a 90° angle to the excitation source. Connect the PMT to the

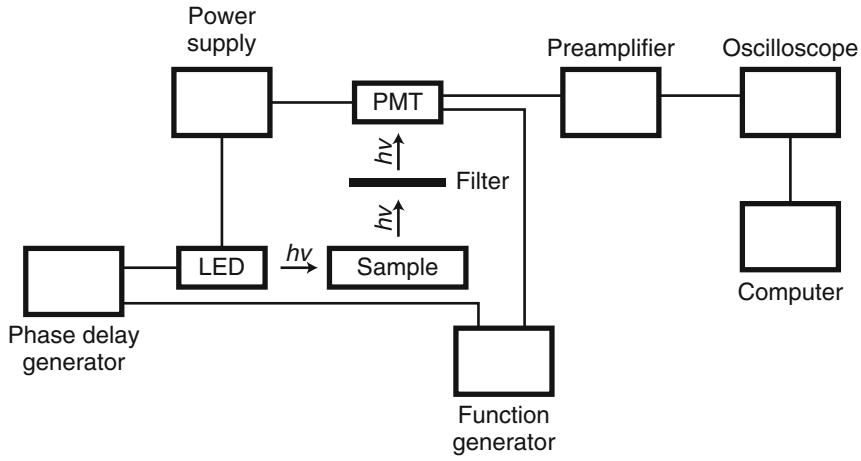

Fig. 2 Schematic for phosphorescence lifetime detection system using a PMT for detection. PMT can be replaced with gated CCD camera

power supply and position it just past the filter and pointing at the cuvette holder (*see* **Note 8**).

3. The PMT must be connected to a power supply and function generator to collect data. Depending on the sensor and PMT, the voltage required may vary. Try a starting voltage of 0.2–0.35 V until the system is optimized.
4. Connecting the PMT to a preamplifier may improve the signal-to-noise ratio of the system (optional, *see* **Note 3**).
5. The output from the PMT or preamplifier is routed to an oscilloscope, or through a D/A converter, which is then stored to a computer for data analysis.

3.3.2 Sensor Preparation

The sensor will be directly added from the stock solution of washed beads to the cell culture in the cuvette. The final concentration of bead/mL of culture required may depend on the sensitivity of the device, although 10–200× dilution from the stock bead solution should be sufficient [3].

3.3.3 Sample Measurement

1. Place 1–3 mL of cell culture (starting with an OD_{600} of 0.1 is recommended) in a sample glass cuvette (*see* **Note 9**).
2. Add prepared platinum porphyrin-based sensor (10–200× dilution from stock solution) directly to the cuvette and mix.
3. Add a layer of castor oil to the top of the liquid culture in the cuvette as an oxygen barrier (*see* **Note 10**).
4. Place the cuvette in the holder. Activate the LED pulses and begin recording the lifetime measurements.
5. Repeat the lifetime measurements until a respiration rate can be accurately measured, typically 5–30 min (*see* **Note 11**).

6. To relate respiration rate measurements to cell number or cell dry weight, collect an aliquot of the sample for further analysis (*see* **Note 12**).

3.3.4 System Calibration

The system must be calibrated with different concentrations of oxygen in order to extract the exact respiration rates from measurements [3]. While it may be possible to use only open air (21% O_2) and N_2-sparged air (0% O_2) in a two-point calibration curve, a 3–5 point calibration curve with premixed gas mixture is strongly recommended to improve accuracy.

1. Fill the glass cuvette with the same growth media or buffer as was used in the oxygen consumption measurements. Add prepared platinum porphyrin-based sensor at the same dilution and mix. Place the cuvette in the holder.
2. Place a needle or small tube attached to an N_2 gas line so that it is submerged below the surface of the media, and secure it in place with tape or other adhesive (*see* **Note 13**).
3. Turn on the gas and begin bubbling the media in the cuvette. Activate the LED pulses and begin recording the lifetime measurements.
4. Continue recording until the lifetime stabilizes at a constant value, which could take up to 30 min depending on the volume of media and flow rate of the gas. The stable value that is reached is the calibration value for 0% O_2 concentration (*see* **Note 14**).
5. Switch the needle or small tube to the next highest O_2 gas mixture. Repeat **steps 4** and **5** for all O_2 concentrations that are part of the calibration curve. The stable values that are reached in each case are the calibration values for the respective O_2 concentrations (*see* **Note 15**).

3.4 Microscope-Based Measurement

3.4.1 Apparatus Construction

The setup for a microscope-based measurement is very similar to that described in Sect. 3.3.1 for the glass cuvette-based system with most differences relating to having an existing microscope platform. Additionally, a gated CCD camera can be used instead of a PMT for the lifetime measurements. Since the setup for a PMT was described previously, this section will focus on parameters for the gated CCD camera with the understanding that the PMT could also be used on the microscope system by following section 3.3.1, **steps 3–5**.

1. Mount the LED on the back port of the microscope so it is in the excitation pathway.
2. Insert the filter cube and adjust the filter wheel so that the appropriate dichroic mirror and emission filter are in the optical path.

3. Mount the PMT or gated CCD to one of microscope camera (side or bottom) ports.
4. If using the gated CCD camera, connect it directly to the computer. This allows one to image the sensor spot, although it will be necessary to write some code using the camera's software development kit (*see* **Note 16**).
5. Connect the computer to the function generator associated with the LED so that starting the camera acquisition software will trigger the pulses to turn on the excitation light.

3.4.2 Sensor Preparation

Below one successful approach is described for adhering sensor beads to a glass slide, although there are also alternative approaches [2].

1. Thoroughly clean the cavity well slide. Rinse with ultrapure water. Blow dry with N_2 gas (*see* **Note 17**).
2. Plasma clean the cavity well slide for at least 1 min (optional, *see* **Note 5**).
3. Dip a sterile pipette tip (without the pipette itself) into the stock bead solution and then gently touch the middle of the cavity well with the pipette tip. Most of the bead solution will adhere to the glass surface. Allow the spot to dry.
4. Melt the beads by placing the slide on a hot plate at 170°C for 10 min [10].
5. Pick up the well slide with sterile forceps or tweezers. Rinse the slide by dipping it once in ethanol and then three times in ultrapure water.
6. Place well slide in a sterile container (e.g., petri dish) for storage at room temperature in the dark until needed for sample measurements.

3.4.3 Sample Measurement

1. Place an appropriate amount of sample to fill the cavity of a well slide already prepared with sensor (*see* **Note 9**).
2. Carefully place a glass coverslip over the well. Make sure to evacuate any excess sample and avoid introducing air bubbles to the sample well (*see* **Note 18**).
3. Place the well slide on a standard glass slide already on the microscope stage. Image the sensor dot using a 10× objective or any other objective with a suitably long working distance to image through both the glass slide and well slide. Either the PMT or CCD camera can be used as the detector.
4. Repeat lifetime measurements until a respiration rate can be accurately measured, typically 5–30 min (*see* **Note 11**).
5. To relate respiration rate measurements to cell number or cell dry weight, collect an aliquot of the sample for further analysis (*see* **Note 12**).

3.4.4 System Calibration

1. Place the well slide prepared with the sensor in a small petri dish or other transparent container which can be placed on the microscope stage (*see* **Note 19**).
2. Fill the petri dish with the same buffer or media used for the respiration rate measurements. Make sure that the sensor spot is covered with the liquid.
3. Place the petri dish containing the well slide on the microscope stage. Place a needle or small tube attached to an N_2 gas line so that it is submerged below the surface of the media and secure it in place by taping the tube to the microscope stage (*see* **Note 13**).
4. Turn on the gas and begin bubbling the media in the petri dish with the submerged well slide. Activate the LED pulses and begin recording the lifetime measurements.
5. Continue with the calibration as previously described for the cuvette system in **steps 3.3.4.4** and **3.3.4.5**.

3.5 Data Analysis

Measured lifetimes collected during the calibration with known oxygen concentrations are fit to the Stern-Volmer equation to determine the Stern-Volmer constant, K_Q (*see* **Note 20**).

$$\tau_0/\tau = 1 + K_Q \tau_0 [O_2]$$

Recorded data from the PMT will be an exponential decay such that

$$I = I_{t=0} e^{(-t/\tau)}$$

where t is time, τ is the lifetime, and $I_{t=0}$ is the initial intensity at time $t = 0$ s. The lifetimes can be determined by directly fitting to this equation with an analysis software package, although this may be computationally intensive. Since the Stern-Volmer equation is expressed relative to the lifetime at 0% O_2, τ_0, one can use the logarithm of the ratio of two points on (or two areas under) the decay curve (Fig. 3) as long as the same two points in time are used for all calibration and oxygen consumption measurements [3]. The area under the decay curve is the approach for measurements made using a gated CCD on the microscope-based system. The Stern-Volmer equation for fitting will take the alternative form of

$$\frac{\log(a_0/b_0)}{\log(a/b)} = 1 + \text{constant} \cdot [O_2]$$

where the subscripted terms denote the conditions at 0% O_2. After determining the fitting constant, the O_2 concentration can be determined for any measured lifetime. Fitting the O_2 concentration versus time gives the oxygen consumption rate for the sample.

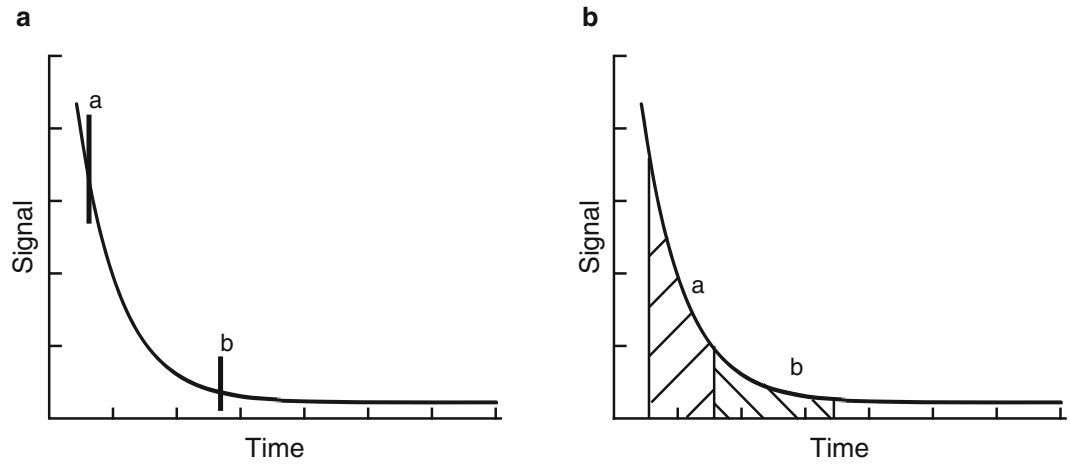

Fig. 3 Simplified method for measuring the lifetime of a phosphorescent oxygen sensor for use with the Stern-Volmer equation by determining log(*a*/*b*). (**a**) Using the ratio of two points along the decay curve. (**b**) Using the ratio of two integrated areas under the decay curve

4 Notes

1. It is also possible to use a combined Digital Delay/Pulse Generator (e.g., Model 577, Berkeley Nucleonics Corporation, Berkeley, CA).
2. Many power supplies and function generators have multiple outputs, so one of each for the system may be all that is required.
3. Depending on the specifications of the PMT, a preamplifier may improve the signal-to-noise ratio.
4. Some cavity well slides come with multiple wells. These can be separated from each other by scoring the slide and breaking them apart.
5. Plasma treating the slides can improve sensor bead adherence to the glass surface, although it may not be necessary depending on how thoroughly the slides are cleaned.
6. An excitation filter is normally not necessary if the spectrum of the LED light is very narrow.
7. Washing and filtering with an appropriately sized filter for the bead size (e.g., dialysis membrane) is an alternative method for cleaning the preservative off the beads.
8. This alignment is consistent with the design of a simple fluorimeter. The emission filter could also be a plastic film placed directly on the PMT which transmits light in the appropriate wavelength range.

9. An OD_{600} of 0.1 is a good starting point, but depending on the actual cellular rate of oxygen consumption, it may be necessary to adjust the cell density. Low O_2 consumption rates cannot be accurately measured, while high O_2 consumption rates will lead to rapid oxygen depletion in the sample.
10. The oil will not form a complete diffusional seal, but the rate of oxygen diffusion across the barrier will be significantly decreased. The cell density in the sample should be high enough so that oxygen consumption by cells in the sample is significantly larger than oxygen diffusing across the oil barrier into the sample. The thicker the layer of oil, the lower the diffusion rate into the sample. Testing by the MLSC showed that castor oil provided the best oxygen barrier. To characterize the diffusion of oxygen across the oil barrier, first sparge the media or buffer in a cuvette with N_2 to remove the oxygen. Apply the oil to the top of the media and monitor the oxygen concentration by making lifetime measurements over time.
11. The time needed to complete the experiment will depend on the oxygen consumption rate and the cell density of the sample.
12. Possible methods to determine the number of cells in a sample include standard cell plating, counting cells under a microscope, and flow cytometry techniques.
13. Humidifying the gas before bubbling it in the media for calibration will help minimize evaporation during the calibration.
14. It is best to start with the 0% O_2 calibration point and then use increasing oxygen concentrations for subsequent calibration points. Lowering the oxygen concentration in the media during calibration will result in a longer measured lifetime, while increasing the oxygen concentration gives shorter lifetimes.
15. For a three-point calibration curve, gas mixtures with 0%, 10%, and 20% O_2 are recommended. If using a sodium bicarbonate/CO_2 buffer, each mixture should also contain 5% CO_2. The balance of each gas mixture should be N_2. Additional O_2 concentrations may be added as other calibration points.
16. With a gated CCD camera, there are a number of options for measuring the lifetime, and subsequent steps depend on the specific method [10]. A recommended method uses an optimized rapid lifetime determination (ORLD) technique [12]. Following an initial LED pulse, the intensity of emitted light during a short time window is measured. After the subsequent LED pulse, the intensity of a longer, later time window is measured. For the commercial beads the best timings were a 10 μs window that begins 6 μs after the LED pulse and a 60 μs window that begins 8.5 μs after the LED pulse. Camera gain settings depend on the intensity of the LED light and amount of sensor.

17. If there are problems with sensor adhering to glass slides cleaned with standard glass cleaners, try submerging the slide in fuming sulfuric acid for 30 min. Make sure to carry out this step in a chemical hood and wear personal protective equipment, including rubber gloves, lab coats, and face shields.
18. When the coverslip is placed on the well slide, there will be enough glass-to-glass contact to provide a full diffusional seal for up to 80 min. The larger the surface area of the contact, the longer the seal will hold.
19. If the well slide cannot be placed in a petri dish on the microscope for calibration, the same amount of sensor can be prepared in a borosilicate glass vial (e.g., 60975L-5, Kimble Chase, Vineland, NJ). The vial would be filled with the media or buffer to cover the sensor and then used on the microscope for the calibration.
20. The fit can be done to determine K_Q explicitly or the entire constant term $K_Q\tau_0$ in front of $[O_2]$.

References

1. Otterstedt K, Larsson C, Bill RM et al (2004) Switching the mode of metabolism in the yeast *Saccharomyces cerevisiae*. EMBO Rep 5:532–537
2. Ramamoorthy R, Dutta PK, Akbar SA (2003) Oxygen sensors: materials, methods, designs, and applications. J Mater Sci 38:4271–4282
3. Strovas TJ, Dragavon JM, Hankins TJ, Callis JB, Burgess LW, Lidstrom ME (2006) Measurement of respiration rates of *Methylobacterium extorquens* AM1 cultures by use of a phosphorescence-based sensor. Appl Environ Microbiol 72:1692–1695
4. Arain S, John GT, Krause C, Gerlach J, Wolfbeis OS, Klimant I (2006) Characterization of microtiterplates with integrated optical sensors for oxygen and pH, and their applications to enzyme activity screening, respirometry, and toxicological assays. Sens Actuators B 113:639–648
5. Will Y, Hynes J, Ogurtsov VI, Papkovsky DB (2006) Analysis of mitochondrial function using phosphorescent oxygen-sensitive probes. Nat Protoc 1:2563–2572
6. Lopes AS, Greve T, Callesen H (2007) Quantification of embryo quality by respirometry. Theriogenology 67:21–31
7. Wilson DF, Vanderkooi JM, Green TJ, Maniara G, DeFeo SP, Bloomgarden DC (1987) A versatile and sensitive method for measuring oxygen. Adv Exp Med Biol 215:71–77
8. Han BH, Manners I, Winnik MA (2005) Phosphorescence quenching of dyes adsorbed to silica thin-layer chromatography plates. Anal Chem 77:8075–8085
9. O'Riordan TC, Buckley D, Ogurtsov V, O'Connor R, Papkovsky DB (2000) A cell viability assay based on monitoring respiration by optical oxygen sensing. Anal Biochem 278:221–227
10. Molter TW, Holl MR, Dragavon JM et al (2008) A new approach for measuring single-cell oxygen consumption rates. IEEE Trans Autom Sci Eng 5:32–42
11. Strovas TJ, McQuaide SC, Anderson JB et al (2010) Direct measurement of oxygen consumption rates from attached and unattached cells in a reversibly sealed, diffusionally isolated sample chamber. Adv Biosci Biotechnol 5:398–408
12. Chan SP, Fuller ZJ, Demas JN, DeGraff BA (2001) Optimized gating scheme for rapid lifetime determinations of single-exponential luminescence lifetimes. Anal Chem 73:4486–4490

Measuring the Impact of Hydrocarbons on Rates of Nitrogen Fixation

Florin Musat and Niculina Musat

Abstract

Crude oils consist of complex mixtures of hydrocarbons, chemicals which are composed exclusively of carbon and hydrogen atoms. With a very low nitrogen content, crude oil contamination through natural seepage or anthropogenic activities leads to an overload of the affected environment with organic carbon. Degradation of oil hydrocarbons by microorganisms is therefore limited by the availability of fixed nitrogen. Studies of bioremediation of crude oil spills have shown that addition of nitrogen fertilizers or nitrogen salts led to an enhancement of crude oil degradation. Fixed nitrogen in crude oil-contaminated environments could also be provided by N_2 fixation, a process carried out by diverse groups of chemoautotrophic, heterotrophic, and phototrophic microorganisms. N_2-fixing heterotrophic bacteria have been isolated from environments contaminated with crude oil. Some of these bacteria were able to fix N_2 while growing with hydrocarbons as sole substrates. Microcosm studies showed that crude oil alters the N_2-fixing microbial populations or offers a substratum for the growth of N_2-fixing phototrophic microorganisms. Also, crude oil can indirectly stimulate the growth of N_2-fixing microorganisms by reducing the grazing pressure. In this chapter we describe methods to measure N_2 fixation rates using sediment or water microcosms. We present methods for preparation of microcosms with addition of crude oil. We describe two methods to measure the bulk N_2 fixation by the entire microcosm: the acetylene reduction assay and the analysis of bulk N isotope ratios following incubations with $^{15}N_2$. Also, we present a method to determine N_2 fixation at cellular level, based on nanoSIMS analysis of individual cells from microcosms incubated with $^{15}N_2$.

Keywords: ^{15}N assimilation, ^{15}N isotope labeling, Acetylene reduction assay, Crude oil, NanoSIMS, Nitrogen fixation, Single cell

1 Introduction

Crude oils are composed of very complex mixtures of thousands to tens of thousands of individual compounds, the majority of which are aliphatic and aromatic hydrocarbons. By definition, hydrocarbons are composed solely of carbon and hydrogen atoms. Compounds containing other elements, for example, sulfur, nitrogen, or oxygen, are less abundant in crude oils [1]. Based on the analysis of over 9000 oil samples, the sulfur content was determined to be

T.J. McGenity et al. (eds.), *Hydrocarbon and Lipid Microbiology Protocols*, Springer Protocols Handbooks, (2017) 81–97,
DOI 10.1007/8623_2015_58, © Springer-Verlag Berlin Heidelberg 2015, Published online: 04 April 2015

around 1% by mass [1]. Sulfur is typically present in crude oil as thiol functional groups, as sulfides and thiophene derivatives. Nitrogen is even less abundant than sulfur, typically less than 0.2% by mass [1]. Nitrogen is normally found in N-heterocyclic compounds such as pyridine, quinoline, and benzoquinoline derivatives and in high-molecular-mass polycyclic aromatic structures (asphaltenes). Crude oil spills in the biosphere, as a result of anthropogenic activities or through natural seepage, will therefore lead to an overload of the environment affected with organic carbon. Growth of microorganisms able to degrade crude oil hydrocarbons will be consequently limited by the availability of other nutrients, most importantly nitrogen, followed by phosphorus and metals, notably iron [2, 3]. Availability of sulfur is usually not a limiting factor for the growth of crude oil-degrading microorganisms, since sulfate is abundant in many aquatic environments, for example, 28 mM in seawater.

Case studies of bioremediation of crude oil spills have shown that addition of nitrogen as oleophilic fertilizers (usually together with phosphorus) or inorganic nitrogen salts leads, in the majority of applications, to an enhancement of the biodegradation of crude oil or individual hydrocarbons [2, 4, 5]. In one of the most extensive applications of bioremediation efforts following a crude oil spill, that of Exxon Valdez, treatment of shorelines with nitrogen-containing fertilizers resulted in a significant enhancement of crude oil degradation [6]. It was concluded that the amount of nitrogen added per unit of crude oil was the most important factor controlling the extent of hydrocarbon biodegradation [6]. Enhancement of crude oil degradation by addition of inorganic nitrogen salts was also demonstrated in microcosm experiments, for example, with marine intertidal sediments [7] or with seawater following an accidental oil spill [8].

Biological nitrogen fixation, the reduction and assimilation of atmospheric N_2 by microorganisms, has been recognized to compensate for the strong limitation in available nitrogen, for example, in marine environments (e.g., [9]). N_2 fixation is carried out by diverse groups of chemoautotrophic, heterotrophic, and phototrophic microorganisms [10]. Nitrogen fixation is essentially an anaerobic process but many organisms have oxygen protection mechanisms which allow them to fix nitrogen under oxic conditions. These include controlled oxygen diffusion, increased respiration rates, or expression of hydrogenases which will consume oxygen, further enhancing the respiratory protection of nitrogenase [11]. In oxygenic phototrophic microorganisms, N_2 fixation is usually carried out by specialized, non-photosynthetic cells or is confined into the dark phase of a diurnal cycle [11]. N_2 fixation requires a very high input of energy and, in heterotrophic microorganisms, is therefore limited by the availability of an energy substrate. In principle, a high load of hydrocarbons as potential

substrates following natural or anthropogenic spills of natural gas or crude oil could alleviate such limitations and lead to a stimulation of heterotrophic N_2 fixation. Also, N_2 fixed by microorganisms not directly involved in hydrocarbon degradation (e.g., cyanobacteria) could be in principle transferred to heterotrophic hydrocarbon degraders, for example, by cell lysis or excretion of ammonia (e.g., [12, 13]). In marine sediment microcosms, it was shown that weathered oil provided a favorable substratum for the attachment and proliferation of layers of N_2-fixing microorganisms [13, 14].

Relatively few studies have addressed the effect of hydrocarbons or of crude oil on N_2 fixation. The earliest indications that hydrocarbon contamination may select for microbial communities able to fix atmospheric nitrogen were provided by chemical analyses of soils exposed to natural gas [15, 16]. These studies showed a higher nitrogen content in soils exposed to natural gas (mostly methane and ethane) compared with adjacent soils which have not been exposed to hydrocarbons [15, 16]. The increase in nitrogen content was attributed to nitrogen fixation, a hypothesis partly supported by the finding of microorganisms known to fix N_2 in the soils exposed to natural gas [15]. N_2 fixation and an increase in the total N content were also observed in soil microcosms amended with butane [17]. In contrast to the apparent stimulation of N_2 fixation by gaseous alkanes, a generally less coherent effect was reported with crude oil. In arctic marine sediments and in marine sediment microcosms, addition of crude oil did not significantly stimulated N_2 fixation, in comparison with pristine microcosms [13, 18], while a seasonal stimulation of N_2 fixation by addition of crude oil was observed in salt-marsh sediments [19].

In general, crude oil led to various degrees of changes in the diazotrophic populations, as shown by analyses of the *nifH* gene (coding a subunit of nitrogenase, the enzyme catalyzing N_2 fixation) diversity, abundance, and expression. Moderate effects of crude oil on *nifH* diversity were found in marine sediment microcosms [13] and in mudflat mesocosms [20]. In contrast, a significant reduction in the *nifH* diversity was found in crude oil-amended mangrove sediment mesocosms [21]. The first microorganisms reported to fix N_2 during growth with hydrocarbons were methane-oxidizing bacteria isolated from various soils, including soil exposed to natural gas [22]. Microorganisms able to fix N_2 while growing with *n*-alkanes, including butane, *n*-dodecane, and *n*-tetradecane, were isolated from soils contaminated with crude oil [23, 24]. Pure cultures able to fix N_2 while growing with aromatic hydrocarbons were also reported [23, 25, 26]. In addition, hydrocarbon-degrading, diazotrophic microorganisms have been isolated from oily sludge [27], fuel-contaminated Antarctic soils [28], and crude oil-contaminated desert soil and seawater [29]. However, these microorganisms were shown to fix N_2 while growing on polar substrates but not when grown on hydrocarbons.

In conclusion, contamination with crude oil can have variable effects on the rates of N_2 fixation. In principle, crude oil contamination may lead to an increase in the number of diazotrophs, by selecting those microorganisms able to fix N_2 and degrade hydrocarbons. In addition, crude oil can indirectly stimulate the growth of N_2-fixing microorganisms by decreasing the grazing pressure [20] or by providing a substratum for the growth of phototrophic microorganisms [13]. In the present chapter, we describe methods to study the effect of crude oil on nitrogen fixation using microcosm experiments. We describe methods for the preparation of microcosms with addition of crude oil and methods to quantify nitrogen fixation including:

1. Measurements of nitrogen fixation rates using the acetylene reduction assay. Acetylene is added to sealed microcosms and the ethylene formed is quantified by gas chromatography. The microcosms can be incubated in the light, in the dark, or under a diurnal cycle, depending on the source of the sample, in order to distinguish between phototrophic- and heterotrophic-driven nitrogen fixation. This method will provide an overall estimate of N_2 fixation. It enables one to distinguish between phototrophic- and heterotrophic-driven N_2 fixation. N_2 fixation rates of microcosms amended with crude oil can be compared with rates in pristine microcosms to determine the effect of crude oil on the diazotrophic microorganisms.
2. Measurements of N_2 fixation using incubations with $^{15}N_2$. Sealed microcosms are provided with $^{15}N_{2\ (g)}$ and incubated as described for the acetylene reduction assay. Defined amounts of samples are withdrawn and dried and the isotopic ratio $^{15}N/^{14}N$ is determined by mass spectrometry. Similar with the acetylene reduction assay, this method provides an overall quantification of the N_2 fixed, without distinguishing N_2-fixing from non-fixing microorganisms. Versus the acetylene reduction assay, this method has the advantage of providing a direct quantification of the amount of N_2 fixed.
3. Measurements of N_2 fixation at the cellular level using nanoscale secondary ion mass spectrometry (nanoSIMS) analysis. For this analysis, subsamples from the microcosms incubated with $^{15}N_2$ can be used. The samples are prepared by chemical fixation. The microbial cells are transferred on gold or gold-/palladium-coated polycarbonate filters and hybridized with oligonucleotide probes followed by the deposition of fluorine-containing tyramides using catalyzed reporter deposition-fluorescence in situ hybridization (CARD-FISH)-based protocols adapted for nanoSIMS analysis (e.g., halogen in situ hybridization, HISH) for phylogenetic identification of diazotrophic microorganisms. Subsequently, the filters are

analyzed by nanoSIMS. This method allows the specific phylogenetic identification of single cells enriched in ^{15}N. The data obtained can be correlated with the abundance of a particular phylogenetic group (determined by hybridization and epifluorescence microscopy; the F-containing tyramides are also fluorescent) and with the bulk quantification of assimilated ^{15}N determined by mass spectrometry to determine the contribution of a particular phylogenetic group to the total ^{15}N assimilation. In addition, analysis of time series samples could determine the flow of fixed nitrogen between members of the microbial community.

2 Materials

2.1 Preparation of Microcosms with Addition of Crude Oil

1. 30-ml serum bottles (Sigma-Aldrich, www.sigmaaldrich.com), outer diameter 36.6 mm, height 62.8 mm; the total volume of these bottles varies (approximately 37 ml); determine the exact total volume before starting the microcosms, as this will be needed for concentration calculations.
2. Sediment and/or water samples, crude oil.
3. Artificial freshwater (in g l^{-1}): KH_2PO_4 (0.5), NaCl (1.0), $MgSO_4 \times 7H_2O$ (0.4), $CaCl_2 \times 2H_2O$ (0.1).
4. Artificial seawater (in g l^{-1}): NaCl (26.4), $MgCl_2 \times 6H_2O$ (5.6), $MgSO_4 \times 7H_2O$ (6.8), $CaCl_2 \times 2H_2O$ (1.47), KCl (0.66), KBr (0.09).

2.2 Quantification of Nitrogen Fixation Using the Acetylene Reduction Assay

1. Teflon-coated rubber stoppers, aluminum crimp seals (Wheaton, www.wheaton.com).
2. Acetylene gas, purity ≥99.5% (Air Liquide, www.airliquide.com). Ethylene 99.99% for calibration (Sigma-Aldrich).
3. Syringes with luer lock tip (Sigma-Aldrich), stopcock valve with luer connection (Cole-Parmer).
4. Gas-tight syringe, 1 ml, with a push–pull closing valve with luer connection (Restek, www.restek.com).
5. Gas chromatograph (Shimadzu), HP-PLOT U column, 30 m length, 0.53 mm inner diameter, 20 μm film thickness (Agilent Technologies).

2.3 Quantification of Nitrogen Fixation by Analysis of Bulk N Isotope Ratios in Incubations with $^{15}N_2$

1. $^{15}N_2$ gas (98 atom % ^{15}N; Sigma-Aldrich).
2. Gas-tight syringes.
3. Microanalytical balance (Sartorius, www.sartorius.balances.com), tin cups (Heraeus).
4. Glass fiber filters Whatman GF/F (Sigma-Aldrich).

5. Peristaltic pump (Cole Parmer), swinnex filter holder (Merck Millipore, www.emdmillipore.com), hole-punch tool (www.hoffmann-group.com, Germany).
6. Elemental analyzer Thermo Flash EA, 1112 Series (Thermo Finnigan), mass spectrometer Thermo Delta Plus Advantage (Thermo Finnigan).

2.4 Quantification of Nitrogen Fixation by nanoSIMS Analysis of ^{15}N Incorporation by Individual Cells in Incubations with $^{15}N_2$

1. Phosphate-buffered saline (PBS) 10× (Life Technologies, www.lifetechnologies.com); ethanol 96% analytical grade (Sigma-Aldrich).
2. Paraformaldehyde (PFA) solution, 4% (v/v) in PBS 1×. Prepare from 16% (v/v) PFA stock (EM-grade, Electron Microscopy Sciences).
3. Gold-coated GTTP polycarbonate filters (Whatman GmbH); alternatively, coat GTTP polycarbonate filters with a pore size of 0.22 μm (Millipore) with a thin (20–40 nm) layer of gold:palladium (80:20) using a Sputter Coater instrument (Polaron).
4. Sonopuls HD 2070, microprobe MS73 (www.bandelin.com).
5. Low-gelling-temperature agarose (Sigma-Aldrich). Prepare a 0.1–0.2% (w/v) solution in deionized water.
6. Lysozyme (Fluka); prepare a lysozyme solution of 10 mg ml^{-1} in Tris:EDTA buffer (0.1 M Tris, 0.05 M EDTA, pH 7.5).
7. Hybridization buffer: 0.9 M NaCl, 40 mM TrisHCl (Sigma-Aldrich), 10% (w/v) dextran sulfate (Sigma-Aldrich), formamide (Sigma-Aldrich; concentration depending on the oligonucleotide probe used), 0.26 mg ml^{-1} sheared salmon sperm DNA (Life Technologies), 0.2 mg ml^{-1} yeast RNA (Life Technologies), blocking reagent (Roche), 1× Denhardt's reagent (Life Technologies), SDS (Sigma-Aldrich).

   Preparation of hybridization buffer for different formamide concentrations: in a 50-ml tube, add 3.6 ml NaCl 5 M, 0.8 ml TrisHCl 1 M, 2 g dextran sulfate, and 2 ml deionized water. Keep the mixture on a water bath at 60°C and vortex intermittently until the dextran sulfate is dissolved. Cool down on ice, then add formamide (amount depending on the concentration required by the oligonucleotide probe used), 516 μl sheared salmon sperm DNA, 400 μl yeast RNA, 2 ml blocking reagent, 400 μl Denhardt's reagent 50×, 10 μl SDS 20% (w/v). Add deionized water to a final volume of 20 ml. Mix well, aliquot in 2 ml portions, and store at −20°C.
8. HRP-labeled oligonucleotide probes (Biomers, www.biomers.net).

9. Washing buffer: NaCl (concentration depending on the formamide concentration in the hybridization buffer; see below), 20 mM TrisHCl, 5 mM EDTA (do not add EDTA in washing buffer for 0 to 20% formamide in hybridization buffer), 0.01% (w/v) SDS, in deionized water.

   Concentration on NaCl in washing buffer depending on the concentration of formamide (FA, in v/v %) in hybridization buffer: 0% FA – 0.9 M NaCl, 10% FA – 0.45 M NaCl, 20% FA – 0.225 M NaCl, 30% FA – 0.112 M NaCl, 40% FA – 0.056 NaCl, 50% FA – 0.028 M NaCl, 60% FA – 0.014 M NaCl.

10. Tyramide HCl, succinimidyl ester of Oregon Green 488, 5-isomer (Molecular Probes Inc., www.lifetechnologies.com). To prepare the F-containing tyramides, mix 500 µl of dye ester (16 mM) with 125.4 µl of tyramide HCl stock (58 mM) and incubate overnight at 4°C in the dark. Dilute with EtOH to a final concentration of active dye of 1 mg ml^{-1}, distribute in 50 µl aliquots, and desiccate under vacuum for 4–6 h. Keep the tyramides thus prepared at −20°C. Before use, dissolve the tyramides in dimethylformamide (1 mg ml^{-1}) containing 20 mg ml^{-1} p-iodophenylboronic acid.

11. Amplification buffer: 2 ml of 20 × PBS, 0.4 ml blocking reagent, 16 ml 5 M NaCl, add deionized water to a volume of 40 ml. Add 4 g dextran sulfate. Heat at 40–60°C with vigorous shaking until the dextran sulfate is dissolved. Store the aliquots at 4°C.

12. DAPI (4′,6-diamidino-2-phenylindole dihydrochloride, Life technologies), Citifluor-glycerol-PBS solution AF1 (Citifluor Ltd., www.citifluor.com), Vectashield (Vector Laboratories, www.vectorlabs.com).

13. Fluorescence microscope (Zeiss, www.zeiss.com).

14. NanoSIMS 50 l (www.cameca.com). The applications of the nanoSIMS-based methodologies in microbiology are relatively recent, and the prices of the nanoSIMS instruments are rather prohibitive for most laboratories. The nanoSIMS analysis can be performed in collaboration with a research institute where such instruments are available. For a list of laboratories and the most common application of the nanoSIMS instruments, see www.cameca.com.

15. Software for analysis of nanoSIMS data: WinImage (Cameca), Look@NanoSIMS (free software, available for download at magnum.mpi-bremen.de/~lpolerec/LANS/program/).

3 Methods

3.1 Preparation of Microcosms with Addition of Crude Oil

3.1.1 Preparation of Sediment Microcosms

In the following, the preparation of sediment microcosms contaminated with crude oil is described. To allow the preparation of a relatively large number of replicate microcosms, the protocol considers the use of 30-ml serum bottles. If larger amounts of sediment are desired to be tested, the procedure described here can be scaled up.

1. Add collected sediment to 30-ml serum bottles to achieve a layer of 1 cm thickness. The sediment should be moist. Remove any layer of water from the top sediment. Add 0.5 ml of crude oil to the sediment in order to achieve a layer as homogeneous as possible (Fig. 1). The amount of crude should not exceed 100 μl cm^{-2}; addition of a thick layer of oil will lead to the "sealing" of the sediment below, which will not have access to oxygen diffusion. We obtained very good results with addition of 70 μl cm^{-2} crude oil to 30-ml serum bottles. Add the crude oil with a Pasteur glass pipette or with a microliter pipette whose tip was cut to obtain a large opening (useful for addition of very viscous crude oils) (**Note 1**). Prepare a number of microcosms depending on the number of sampling points required. For each time point sampled, prepare replicate microcosms. For example, to follow the effect of crude oil on nitrogen fixation for an incubation time of 20 days, with sampling at time = 0, 10, and 20 days, prepare 9 microcosms, 3 for each sampling time.

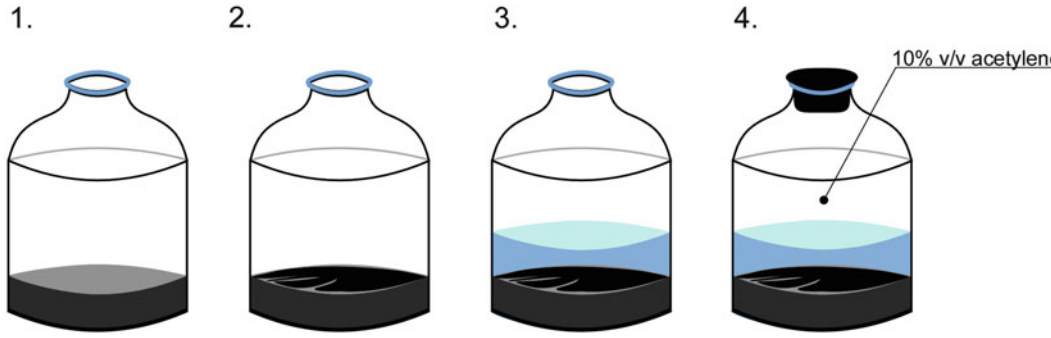

Fig. 1 Preparation of sediment microcosms with surface contamination of crude oil. (*1*) Add a layer of 1 cm of moist, fresh sediment to an open bottle; remove any overlaying water; (*2*) add a thin layer of crude oil over the sediment (100 μl cm^{-2}); allow the oil to soak onto the sediment and to loose the volatile fraction by evaporation for up to 5 days; (*3*) add water (freshwater or seawater, depending on the source of sediment) slowly to not dislodge the oil layer; incubate under defined conditions (temperature, light–dark regime); (*4*) to measure the N_2 fixation, at defined time intervals, seal triplicate microcosms with rubber stoppers, and replace a 10% v/v of the headspace with acetylene. Measure the production of ethylene at defined time intervals (e.g., 2, 4, 6 h). Avoid incubating the microcosms with acetylene for more than 24 h. Prepare pristine, reference microcosms in a similar way, by omitting the addition of crude oil

2. Incubate the bottles with crude oil in a flume hood, at room temperature, for up to 5 days, in order to evaporate the volatile fraction of the crude oil (weathering or aging). During this time, the crude oil will adhere to sediment. Check regularly the moisture of the sediment. If the upper sediment layers show signs of desiccation, add small amounts of sterile, distilled water. Let the water flow slowly on the glass walls of the bottle, in order to not disturb the crude oil layer (Fig. 1).
3. To prepare control microcosms, add a sediment layer of 1 cm thickness to an equal number of bottles as prepared in **step 1**. Incubate the control microcosms at room temperature for a similar period of time as the microcosms with crude oil. Check daily for desiccation of the upper sediment layers, and add sterile, distilled water if needed.
4. After crude oil weathering, add a layer of water of 1 cm thickness (Fig. 1; in the 30-ml serum bottles this corresponds to about 7.5 ml). Use seawater or freshwater from the same source as the sediment. For a more controlled environment, use artificial seawater or freshwater (*see* Sect. 2). In the microcosms with crude oil, add the water slowly on the glass walls, so as to not disturb the oil layer (**Note 2**).
5. Incubate all bottles for the desired time frame under light, dark, or light–dark conditions, depending on the sediment source. For incubations in the light or under a light–dark regime, to ensure that phototrophic microorganisms grow only on top of the sediment or oiled sediment layers and not on the side of the sediment column, wrap the bottles up to the upper sediment level in black paper. Alternatively, the bottles can be placed in larger vessels (e.g., aquaria) containing sediment and buried down to the upper sediment level. If the microcosms are incubated under aerobic conditions, the bottles are not closed unless they are amended with $^{15}N_2$ (*see* Sect. 3.3); compensate for evaporation by addition of sterile, distilled water.

3.1.2 Preparation of Water Microcosms

1. For preparation of microcosms with weathered crude oil, add a thin layer (1 ml) of sterile, distilled water to replicate 30-ml serum bottles. Add 0.5 ml crude oil and incubate for 5 days in a flume hood at room temperature. After weathering, add the water sample to achieve a layer of 2 cm (ca. 15 ml), and start the incubation. Compensate for evaporation by addition of sterile, distilled water.
2. For preparation of microcosms with fresh, non-weathered crude oil, add the water samples to replicate 30-ml serum bottles to achieve a layer of 2 cm (ca. 15 ml). Add 0.5 ml crude oil and start the incubation.

3.2 Quantification of Nitrogen Fixation Using the Acetylene Reduction Assay

1. At defined times of incubation (e.g., $t = 0$, 10, and 20 days), seal replicate microcosms with crude oil and replicate pristine microcosms with Teflon-coated butyl rubber stoppers and aluminum crimps.
2. Replace 10% v/v of the headspace volume with acetylene. Use a syringe with a luer lock tip, fitted with a gas-tight valve and needle (Fig. 1).
3. To quantify ethylene concentrations, withdraw 0.1 ml samples from the headspace using a 1-ml gas-tight syringe with a push–pull valve, and analyze them with a gas chromatograph (GC14A, Shimadzu) equipped with a HP-PLOT U column (0.53 mm inner diameter, 20 μm film thickness; Agilent Technologies) and an FID detector. GC operating conditions: injector 130°C, detector 150°C, oven 55°C. Use N_2 as a carrier gas, at a flow rate of 3 ml min^{-1}.
4. Ethylene measurement intervals. Take an initial ethylene measurement right after addition of acetylene. Continue measuring at regular intervals (e.g., 2, 4, 6 h), for up to 24 h since acetylene addition (**Note 3**).
5. Prepare an external calibration curve for ethylene. Using a gas-tight syringe, add defined amounts of ethylene (e.g., 0.01, 0.05, 0.1% v/v) into empty, sealed glass vials of known volume. Analyze the ethylene standards by GC, using the same conditions as in **step 4**.
6. Using the calibration curve for ethylene, calculate the ethylene concentration/rates in the microcosms. Acetylene reduction to ethylene is equimolar; the measured concentration of ethylene is equal to the concentration of acetylene reduced. The acetylene reduction rates can be expressed per surface area, per gram sediment, or per ml water (**Note 4**).

3.3 Quantification of Nitrogen Fixation by Analysis of Bulk N Isotope Ratios in Incubations with $^{15}N_2$

1. Preparation of microcosms for incubation with $^{15}N_2$.

   Sediment microcosms. Prepare pristine and crude oil-contaminated sediment microcosms as described in Sect. 3.1. Add freshwater or seawater to fill the serum bottles completely. Carefully seal all bottles with Teflon-lined butyl rubber stoppers.

   Water samples with weathered crude oil. Fill the bottles containing weathered oil completely with the water sample. To prevent the removal of floating oil layers during filling, seal the bottle before it is completely filled, and continue filling the water sample using a syringe; pass a needle through the stopper to remove the excess air.

Water samples with non-weathered crude oil. Fill the bottles completely with the water sample. Seal with Teflon-lined butyl rubber stoppers. Inject the crude oil while keeping the bottle inverted, and remove excess water through a second syringe.

2. Add 1 ml $^{15}N_2$ (Sigma-Aldrich) to all bottles (pristine and oil-amended) using a gas-tight syringe. Withdraw an equal volume of water to equalize the pressure. Mix the sediment microcosms by gentle horizontal shaking. Mix the water sample bottles by end-to-end inverting for a few times.
3. Incubate under conditions dictated by the sample source (e.g., light regime, temperature) for up to 12 h.
4. Sampling

   Sampling of sediment microcosms. Open a subset of bottles and remove most of the water column using a glass pipette to ease sampling. Collect sediment subsamples, and dry them overnight in a freeze-dryer or in an oven at 60°C. The samples can be stored at −20°C until further processing. Use a microanalytical balance (Sartorius) to weigh defined amounts of dry sediment, place the sediment into tin cups (Heraeus CHN cups), and press the tin cups into pellets.

   Sampling of water microcosms. Withdraw a defined amount of water using a syringe, and filter it onto pre-combusted (6 h at 450°C) 25-mm-diameter glass fiber filters (Whatman GF/F, Sigma-Aldrich) using a peristaltic pump (Cole-Parmer) and a swinnex filter holder. Dry the GF/F filters using a freeze-dryer or in an oven at 60°C. Decalcify the filters for 24 h in a desiccator in the presence of 37% HCl. Cut round pieces of 10 mm diameter from the GF/F filters using a punch-out tool, pack them into tin cups, and fold the tin cups into pellets (**Note 5**).
5. Analyze the tin cup samples for the N content and the N isotopic composition in an automated elemental analyzer (Thermo Flash EA, 1112 Series) coupled to a mass spectrometer (Thermo Delta Plus Advantage, Thermo Finnigan).

3.4 Quantification of Nitrogen Fixation by NanoSIMS Analysis of ^{15}N Incorporation by Individual Cells in Incubations with $^{15}N_2$

This method determines the assimilation of ^{15}N in individual cells (Fig. 2). The cells can be identified phylogenetically using hybridization with 16S rRNA oligonucleotide probes. This method leads to a precise identification of the N_2-fixing microorganisms. In addition, sampling of time series followed by nanoSIMS analysis offers the possibility to follow the transfer of fixed nitrogen within members of the microbial community. The N_2-fixation rates of individual cells can be correlated with the abundance of specific phylogenetic groups and with the overall $^{15}N_2$ fixation determined by analysis of bulk N isotope ratios (Sect. 3.3).

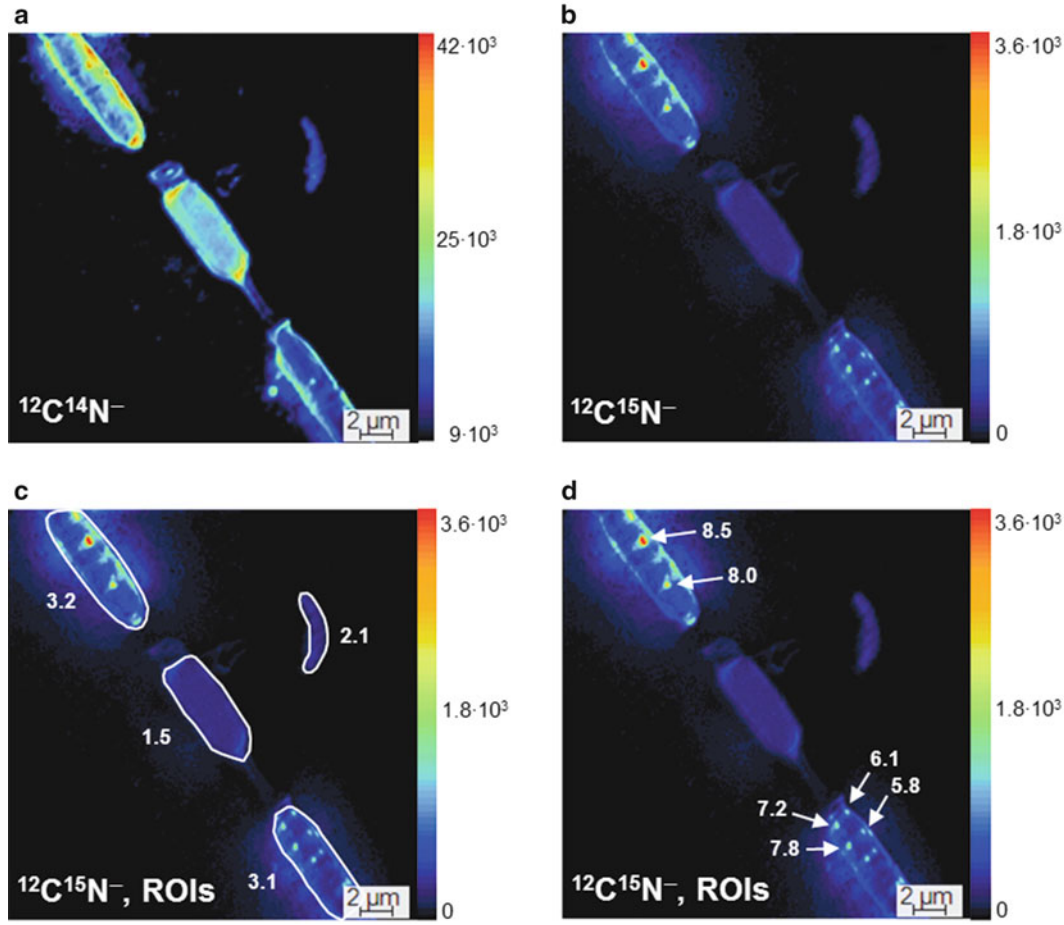

Fig. 2 Example of a nanoSIMS analysis of N_2 fixation in a marine environment. Seawater samples were incubated with $^{15}N_2$ for 6 h and chemically fixed. A field of 20 × 20 μm was analyzed at nanoSIMS, by acquiring $^{12}C^{14}N^-$ (**a**) and $^{12}C^{15}N^-$ (**b**) secondary ion images. The images show a part of a filamentous, heterocystous cyanobacterium (the central cell is a heterocyst) and a bacterial cell. Regions of interest (ROIs) can be defined around the entire cells (**c**) or around hot spots of intracellular ^{15}N accumulation (**d**) (in this particular case, interpreted as granules of cyanophycin). The ROIs are used to calculate $^{15}N/^{14}N$ ratios, thereby quantifying the enrichment in ^{15}N. Values on the images (in **c** and **d**) show $^{15}N/^{14}N$ ratios ($\times 10^{-2}$). The scale next to all images represents counts per second of secondary ions

1. Preparation of microcosms with addition of crude oil and of pristine microcosms, addition of $^{15}N_2$, and incubation conditions are similar to those described for the Sect. 3.3.
2. Incubate the microcosms for up to 12 h. Collect samples at $t = 0$ h (after addition of $^{15}N_2$), $t = n$ h ($0 < n < 12$, n is user defined), and $t = 12$ h. If correlation of this method with the bulk analysis of N isotope ratios (Sect. 3.3) is desired, collect samples at the same time points as for Sect. 3.3.

3. Chemically fix the samples by adding an equal volume of 4% (v/v) paraformaldehyde in PBS 1× (end concentration 2% v/v; for sediment samples, consider the equivalent volume of the sample including the interstitial water) (**Note 6**). Incubate for 1 h at room temperature or overnight at 4°C.
4. Removal of the PFA and sample storage

   Sediment samples. Centrifuge the sediment samples for 10 min at 10,000 rpm, 4°C, discard the aqueous phase, and wash with an equal volume of PBS 1×. Repeat three times. Store the sediment samples in a mix of 1× PBS:EtOH (1:1) at −20°C.

   Water samples. Transfer the water samples directly on Au or Au/Pd-coated GTTP filters using a peristaltic pump (Cole-Parmer) and a swinnex filter holder (**Note 7**). Wash the filters three times with 1× PBS, followed by 3 min each in 50, 80, and 96% v/v EtOH. Air-dry. Store at −20°C.
5. Addition of sediment samples on Au or Au/Pd-coated polycarbonate filters. Take a sediment subsample and sonicate it for 7 times on an ice bath at an amplitude of 42 μm, for 30 sec with a 30-sec pause. Withdraw samples from the supernatant and add them on coated filters using a peristaltic pump (Cole-Parmer) and a swinnex filter holder. The volume of supernatant to add on a filter depends on the cell density in the sample. Determine the cell density by adding various volumes of supernatant on GTTP polycarbonate filters, DAPI staining (*see* **step 15**), and microscopic investigation.
6. Immobilize the cells on filters by embedding in agarose. Dip the filters in 0.1–0.2% (w/v) low-gelling-point agarose prepared in deionized water (gel strength approximately 1,000 g cm^{-2}). Place the filter facing down onto glass slides and dry at 35°C. Add 1–2 ml of 96% v/v EtOH over the filters, at room temperature, to help detach the filters from the slides and to dehydrate them. Allow the filters to dry in air at room temperature.
7. Cell wall permeabilization. Incubate the filters in the lysozyme solution for 1 h at 37°C. Wash the filters twice with deionized water.
8. Inactivation of endogenous peroxidases. Incubate the filters in 0.01 M HCl for 10 min at room temperature. Alternatively, incubate the filters in 3% v/v H_2O_2 for 10 min at room temperature. Wash twice in deionized water, followed by 1 min each in 50, 80, and 96% EtOH (v/v in water). Allow the filters to dry. Continue with the following step, or store the filters at −20°C (**Note 8**).
9. Pre-hybridization. Incubate the filters for 1 h in hybridization buffer without the HRP-labeled probe at 46°C.

10. Add the HRP-labeled probe to a concentration of 50 ng μl^{-1}. Hybridize for 6 h at 46°C.
11. Wash off the unbound probe by incubating the filters for 15 min in 50 ml pre-warmed washing buffer at 48°C.
12. Transfer the filters in 1× PBS for 30 min. Do not allow the samples to dry before and during the tyramide amplification step.
13. Tyramide signal amplification. Incubate the filters for 20 min at 46°C in the dark in the reactant mixture containing amplification buffer, fluorine-labeled tyramides, and 0.015% v/v H_2O_2. The filters must be immersed in the solution mixture, or use a wet chamber to prevent the filters from drying. Prepare the reactant mixture right before use.
14. Wash the filters in the dark as follows: 15 min in 1× PBS, rinse twice with deionized water, and wash once for 1 min in 96% v/v EtOH.
15. Counterstaining with DAPI. Place the filters on glass slides, add 50 µl DAPI solution (1 µg ml^{-1}), and incubate for 10 min in the dark at 4°C. Wash twice in deionized water and once in 80% v/v EtOH for 1 min. Air-dry in the dark. Embed in Citifluor/Vectashield 4:1 (v/v). Inspect the filters by epifluorescence microscopy to verify the success of the hybridization procedure before running the samples at nanoSIMS.
16. Punch out round pieces of 5 mm diameter from the hybridized filters, using a hole-punch tool.
17. NanoSIMS analysis. Mount the filter pieces onto the nanoSIMS holder (**Note 9**). Sputter an area of 40 × 40 µm for approximately 10 min with a Cs^+ primary ion beam of 150 pA in order to pre-implant Cs^+ ions into the outermost layers of the sample [30]. After pre-sputtering, measure the sample using a Cs^+ primary ion beam of 0.3–0.8 pA focused onto a spot of ca. 100 nm. Scan fields of 30 × 30, 20 × 20, or 15 × 15 µm (typical for microbial cells of 1–10 µm) using a pixel size of 256 × 256 and a dwelling time of 1 ms per pixel repeatedly, creating 10 to 30 images of the same field; the images are combined (accumulated) to create the final image. Acquire parallel secondary images of $^{12}C^{14}N^-$, $^{12}C^{15}N^-$ (Fig. 2), and $^{19}F^-$ (usually during a nanoSIMS run, images of $^{12}C^-$ secondary ions and secondary electrons are also acquired; if labeling with ^{13}C is done at the same time with the ^{15}N labeling, $^{13}C^-$ or $^{13}C^{14}N^-$secondary ions can also be acquired). Use a mass resolution sufficient to separate isobars, e.g., $^{13}C^-$ from $^{12}CH^-$ and $^{12}C^{15}N^-$ from $^{13}C^{14}N^-$ (6,000 M/ΔM or above).

18. NanoSIMS image processing. NanoSIMS images can be processed with the CAMECA WinImage software or with the Look@NanoSIMS free software. Sum all scans of each scanned area, and apply image drift correction to obtain the final image. Manually draw regions of interest (ROIs) around individual cells recognized in the $^{12}C^{14}N^-$ secondary ion or in the secondary electron images (Fig. 2). For each ROI, calculate the $^{12}C^{15}N^-/^{12}C^{14}N^-$ ratio. This will provide the enrichment in ^{15}N of individual cells. Correlate the enrichment in ^{15}N with the cell identity (phylogenetic level depending on the probe chosen) given by the $^{19}F^-$ secondary ion or $^{19}F/^{12}C$ ratio image. Alternatively, fluorescence microscopy images can be used to ensure correct identification of cells.

4 Notes

1. Do not add the crude oil dissolved in solvents; addition of solvents will have a strong toxic effect on the microbial community.
2. After addition of water, even if the crude oil was weathered, some oil may still be removed from the sediment surface and will float on the water. Do not remove this crude oil, as the total amount per microcosm will be changed. Continue with the incubation as described in **step 5**.
3. Acetylene has a high solubility in water (ca. 45 mmol l^{-1} at 20°C) and can be used as a substrate by microorganisms (e.g., [31]). Prolonged incubations in the presence of acetylene are not recommended, since it may lead to changes in the microbial community structure, for example, by the enrichment of acetylene degraders.
4. The conversion of acetylene reduction rates to N_2 fixation rates in complex environments is difficult. Direct correlation of C_2H_2 and N_2 reduction rates with various species of cyanobacteria showed C_2H_2/N_2 ratios ranging from 2.58 to 9.29 [32]. We recommend using directly the C_2H_2 reduction rates.
5. The water microcosms can be sampled multiple times, if the sample withdrawn is relatively small with respect to the total volume and if an equal volume of water is injected after sampling; in this case, the same microcosm can be used for a time series; if the cell density is rather low and a large sample must be filtered, replicate microcosms must be prepared if a time series is desired.
6. Chemical fixation can be done with PFA concentration ranging from 1 to 2% v/v.

7. Choose the volume of sample to load on a filter depending on the cell density; care has to be taken to not overload the filters.
8. Filters can be safely stored at −20°C for up to 30 days before continuing with the hybridization.
9. The nanoSIMS holder is available at the nanoSIMS laboratory; the procedures to mount the filters onto the nanoSIMS holders and the loading of the holder into the nanoSIMS instrument are usually done by the nanoSIMS technician or operator and are not described here.

References

1. Tissot BP, Welte DH (1984) Petroleum formation and occurrence, 2nd edn. Springer, Berlin
2. Leahy JG, Colwell RR (1990) Microbial degradation of hydrocarbons in the environment. Microbiol Rev 54(3):305–315
3. Widdel F, Musat F (2010) Energetic and other quantitative aspects of microbial hydrocarbon utilization. In: Timmis KN (ed) Handbook of hydrocarbon and lipid microbiology. Springer, Heidelberg/Berlin pp 731–763
4. Atlas RM (1981) Microbial degradation of petroleum hydrocarbons: an environmental perspective. Microbiol Rev 45(1):180–209
5. Swannell RP, Lee K, Mcdonagh M (1996) Field evaluations of marine oil spill bioremediation. Microbiol Rev 60(2):342–365
6. Bragg JR, Prince RC, Harner EJ, Atlas RM (1994) Effectiveness of bioremediation for the Exxon Valdez oil spill. Nature 368:413–418
7. Röling WFM, Milner MG, Jones DM et al (2002) Robust hydrocarbon degradation and dynamics of bacterial communities during nutrient-enhanced oil spill bioremediation. Appl Environ Microbiol 68(11):5537–5548
8. Medina-Bellver JI, Marin P, Delgado A et al (2005) Evidence for in situ crude oil biodegradation after the Prestige oil spill. Environ Microbiol 7(6):773–779
9. Zehr JP, Waterbury JB, Turner PJ et al (2001) Unicellular cyanobacteria fix N_2 in the subtropical North Pacific Ocean. Nature 412 (6847):635–638
10. Zehr JP, Jenkins BD, Short SM, Steward GF (2003) Nitrogenase gene diversity and microbial community structure: a cross-system comparison. Environ Microbiol 5(7):539–554
11. Fay P (1992) Oxygen relations of nitrogen fixation in cyanobacteria. Microbiol Rev 56 (2):340–373
12. Ploug H, Musat N, Adam B et al (2010) Carbon and nitrogen fluxes associated with the cyanobacterium *Aphanizomenon* sp. in the Baltic Sea. ISME J 4(9):1215–1223
13. Musat F, Harder J, Widdel F (2006) Study of nitrogen fixation in microbial communities of oil-contaminated marine sediment microcosms. Environ Microbiol 8(10):1834–1843
14. Musat F, Wieland A, Widdel F (2004) Marine sediment with surface contamination by oil in microcosms for microbiological studies. Ophelia 58(3):217–222
15. Harper HJ (1939) The effect of natural gas on the growth of micro-organisms and the accumulation of nitrogen and organic matter in the soil. Soil Sci 48(6):461–466
16. Schollenberger CJ (1930) Effect of leaking natural gas upon the soil. Soil Sci 29 (4):261–266
17. Toccalino PL, Johnson RL, Boone DR (1993) Nitrogen limitation and nitrogen fixation during alkane biodegradation in a sandy soil. Appl Environ Microbiol 59(9):2977–2983
18. Knowles R, Wishart C (1977) Nitrogen fixation in arctic marine sediments: effect of oil and hydrocarbon fractions. Environ Pollut 13 (2):133–149
19. Thomson A, Webb K (1984) The effect of chronic oil pollution on salt-marsh nitrogen fixation (acetylene reduction). Estuaries 7(1):2–11
20. Chronopoulou P-M, Fahy A, Coulon F et al (2013) Impact of a simulated oil spill on benthic phototrophs and nitrogen-fixing bacteria in mudflat mesocosms. Environ Microbiol 15 (1):242–252
21. Taketani RG, Dos Santos HF, Van Elsas JD, Rosado AS (2009) Characterisation of the effect of a simulated hydrocarbon spill on diazotrophs in mangrove sediment mesocosm. Antonie Van Leeuwenhoek 96(3):343–354

22. Davis JB, Coty VF, Stanley JP (1964) Atmospheric nitrogen fixation by methane-oxidizing bacteria. J Bacteriol 88:468–472
23. Coty VF (1967) Atmospheric nitrogen fixation by hydrocarbon-oxidizing bacteria. Biotechnol Bioeng 9(1):25–32
24. Roy I, Shukla S, Mishra A (1988) n-Dodecane as a substrate for nitrogen fixation by an alkane-utilizing *Azospirillum* sp. Curr Microbiol 16 (6):303–309
25. Chen Y, Lopez-De-Victoria G, Lovell C (1993) Utilization of aromatic compounds as carbon and energy sources during growth and N_2-fixation by free-living nitrogen fixing bacteria. Arch Microbiol 159(3):207–212
26. Prantera M, Drozdowicz A, Gomes Leite S, Soares RA (2002) Degradation of gasoline aromatic hydrocarbons by two N_2-fixing soil bacteria. Biotechnol Lett 24(1):85–89
27. Laguerre G, Bossand B, Bardin R (1987) Free-living dinitrogen-fixing bacteria isolated from petroleum refinery oily sludge. Appl Environ Microbiol 53(7):1674–1678
28. Eckford R, Cook FD, Saul D, Aislabie J, Foght J (2002) Free-living heterotrophic nitrogen-fixing bacteria isolated from fuel-contaminated antarctic soils. Appl Environ Microbiol 68 (10):5181–5185
29. Al-Awadhi H, Al-Mailem D, Dashti N, Khanafer M, Radwan S (2012) Indigenous hydrocarbon-utilizing bacterioflora in oil-polluted habitats in Kuwait, two decades after the greatest man-made oil spill. Arch Microbiol 194(8):689–705
30. Audinot JN, Cabin-Flaman A, Philipp P, Legent G, Wirtz T, Migeon HN (2011) NanoSIMS50 imaging of thin samples coupled with neutral cesium deposition. Surf Interface Anal 43:302–305
31. Rosner BM, Rainey FA, Kroppenstedt RM, Schink B (1997) Acetylene degradation by new isolates of aerobic bacteria and comparison of acetylene hydratase enzymes. FEMS Microbiol Lett 148(2):175–180
32. Montoya JP, Voss M, Kahler P, Capone DG (1996) A simple, high-precision, high-sensitivity tracer assay for N_2 fixation. Appl Environ Microbiol 62(3):986–993

Protocols for Measuring Activity of Sulphate-Reducing Bacteria in Water Injection Systems by Radiorespirometric Assay

Gunhild Bødtker and Terje Torsvik

Abstract

Growth and activity of sulphate-reducing bacteria (SRB) is a problem for offshore oil fields injecting sea water for pressure support. Oxygen is traditionally removed before injection to reduce corrosion. The anoxic conditions and high sulphate content of sea water promotes growth and activity of SRB in the water injection system and in the reservoir. The major concern top side in the water injection system is microbiologically influenced corrosion (MIC) caused by SRB activity. Combined with the assessment of corrosion rates, monitoring of SRB activity is applied to evaluate treatment methods and optimize treatment regimens. The aim is to reduce corrosion and maintenance cost and ensure a healthy work environment for platform personnel. In the current chapter we will describe a radiorespirometric method for assessment of H_2S production rate in biofilm from water injection systems.

Keywords: Biofilm, H_2S production rate, MIC, Sea water injection, Sulphate, Sulphate-reducing bacteria, Sulphate-reduction rate

1 Introduction

Within the petroleum industry, growth and activity of sulphate-reducing bacteria (SRB) is generally associated with microbiologically influenced corrosion (MIC) and reservoir souring. Injection of sea water for pressure support during secondary oil recovery promotes growth and activity of SRB, which cause corrosion of steel and steel alloys. The theory of cathodic depolarization caused by H_2-scavenging SRB has traditionally been applied to explain high corrosion rates in sulphate-rich environments, but has not been proven experimentally [1]. More recent research suggests that SRB utilizing electrons directly from metal may be responsible for accelerating corrosion rates [1, 2]. In addition to the corrosive effect that SRB have by attacking the metal directly, they produce the highly corrosive gas hydrogen sulphide (H_2S) as end product of dissimilatory sulphate reduction.

T.J. McGenity et al. (eds.), *Hydrocarbon and Lipid Microbiology Protocols*, Springer Protocols Handbooks, (2017) 99–109, DOI 10.1007/8623_2015_166, © Springer-Verlag Berlin Heidelberg 2015, Published online: 04 May 2016

SRB also utilize a range of organic compounds as energy source, whereof organic acids and hydrocarbons [3–5] are particularly relevant in petroleum-related systems. Therefore, H_2S generated from organic components present in reservoir formation water and crude oil should be addressed in fields reinjecting produced water and when assessing MIC in oil–water transport pipelines or storage tanks. When injecting oligotrophic sea water, H_2S is generated mainly from the metal surface and associated biofilm structure. However, unintentional stimulation of SRB may occur by use of water additives containing growth-promoting components [6]. In systems rich in organic compounds, planktonic SRB will generate significant amounts of H_2S in the water phase and/or at oil–-water contacts.

The current chapter will concern sampling of biofilm from sea water injection systems and the subsequent measurement of H_2S production rate by a radiorespirometric method modified after Maxwell and Hamilton (1986) [7]. The method determines H_2S production rate in biofilm incubated with radioactive-labelled sulphate ($^{35}SO_4^{2-}$) by trapping H_2S produced and measuring of accumulated $H_2{}^{35}S$. Other diffusion-based methods for assessment of SRB reduction rates and reduced inorganic sulphur quantification have been described for sediment samples [8–11]. Although the principle of the methods are similar, the current method allows for real-time capture of H_2S during incubation of replicate sets of intact biofilm in addition to final capture of residual acid volatile sulphur species (AVS; H_2S, HS^-, S^{2-}, FeS) at end of incubation. The current method also includes an improved H_2S trap that eliminates bias due to carryover of labelled sulphate. The method is rapid, simple and sensitive (detects production rates down to ~0.1 μg H_2S/cm^2/day), but requires skills in anaerobic techniques to avoid oxidation of samples and inhibition of SRB activity.

Sampling and sampling procedures are a crucial part of microbial analyses in general and for anaerobic microbial analyses in particular. Biofilm from the water injection systems are sampled by mounting metal coupons (biocoupons) flush with the inside of the pipeline wall. The biocoupons are incubated for e.g. 3–12 months, depending on the need for sampling intervals. The minimum incubation time is determined by the time needed for biofilm formation on pristine coupons. In our experience regrowth occurs within a month. A major cause for sample compromising lies in the handling and transport of biofilm samples to the laboratory. Upon sampling, the anaerobic biofilm should be placed in an airtight container submerged in anoxic water from the sampling site and transferred to the laboratory for analysis as soon as possible. Storage at low temperature will reduce the change in biofilm composition before analysis. As a general rule mesophilic microorganisms are stored at refrigerator temperature to slow metabolic

activity and minimize growth before analysis. As for thermophilic microorganism, room temperature will have the same effect, as they generally do not grow below 40°C. However, room temperature may promote mesophilic growth in thermophilic samples, thus storage at low temperature is generally applied for all samples.

Determination of SRB activity is part of monitoring regimes in offshore water injection systems, often in combination with assessments of viable counts and real-time molecular quantification (qPCR) of SRB and other relevant metabolic groups, enrichments and total numbers of prokaryotic microorganisms [12–15]. The determination of SRB activity in intact biofilm has several advantages compared to quantitative culture-based and molecular methods, as it enables direct assessment of H_2S production rate for the whole SRB community. Viable counts of SRB are traditionally performed in medium targeting *Desulfovibrio* species, and although we have observed correlation between SRB activity levels and *Desulfovibrio* sp. numbers [12–13], it is not possible to generally link viable counts to in situ activity. For instance, during nitrate treatment SRB may be inhibited by nitrite [16] or the increased redox potential [17] but not killed. Some SRB may even reduce nitrate and/or nitrite [18, 19]. Cultivation outside the system in medium targeting SRB may thus give high viable counts indicating high SRB activity, when the in situ sulphate respiration is in fact inhibited by an active NRB community. The same argument is valid for DNA-based quantifications. The current method does not take into account the fate of total H_2S generated during incubation, only the net H_2S production is accounted for. During nitrate treatment chemolithotrophic NRB may oxidize $H_2{}^{35}S$ as it is generated in the biofilm, to either $^{35}S^0$ (not recovered by the current method) or back to $^{35}SO_4{}^{2-}$, possibly masking SRB activity completely. It is important to be aware of this limitation of the method; it was not designed to account for the cycling of inorganic sulphur. The aim is to assess in situ SRB activity by net H_2S production rates in offshore water injection systems and other relevant systems, as tool in the monitoring and mitigation of MIC. Although the current method only recovers AVS, it may probably be modified to also recover FeS_2 and S^0.

2 Materials

2.1 Sampling of Biofilm

1. Biopro 5 bio-probe system with 5 C-steel biocoupons assembled in a housing made of Polytetrafluoroethylene (PTFE) (Roxar, Stavanger, Norway) (Fig. 1). The biocoupons are prepared and analyzed by onshore laboratory personnel.
2. Transport container for biocoupon housing ("body with washer" Roxar, Stavanger, Norway) (Fig. 2).

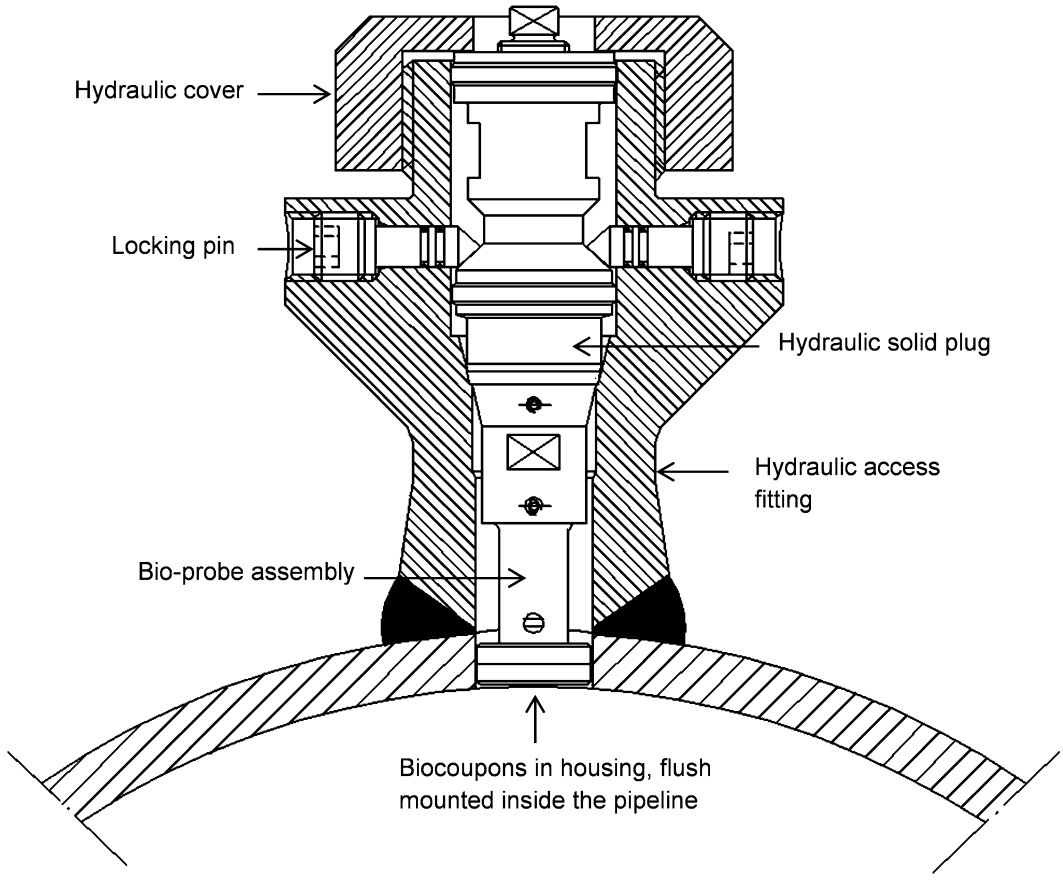

Fig. 1 The sketch shows a bio-probe in the access fitting, which provides the actual pressure seal and serves as the carrier for the equipment to be installed in the pipe. The sketch was provided by Roxar, Stavanger, Norway (http:/www2.emersonprocess.com/en-us/brands/roxar/pages/roxar.aspx) and modified by authors by labelling

Fig. 2 The picture shows a transport container for biocoupons. The biocoupon housing is mounted and secured in the container by a central corrosion-resistant screw. The container and lid is closed by screw threads. After closing the container, anoxic sample water is carefully flushed through the valves before they are closed

2.2 Placement and Retrieval of Biocoupons (Performed by Platform Personnel)

1. Holder body in stainless steel (holds housing with biocoupons).
2. Hydraulic access and retrieval system for standard mechanical 2″ system (Roxar, Stavanger, Norway).

2.3 Sampling of Water

1. Sterile anaerobic culture bottles with rubber stoppers and crimp seals for anoxic water samples.
2. Sterile tubing for sampling.
3. Forceps and crimper.

2.4 Radiorespirometric Analysis

1. Anoxic solutions of 6 M HCl and 1 M zinc acetate.
2. Radioactive sulphate ($^{35}SO_4^{2-}$), 1 mCi/37mBq, specific activity 100 mCi/mmol (Perkin Elmer, Waltham Mass., US). Solid salt is dissolved in 1 mL sterile distilled water (sdH_2O) (*see* **Note 1**).
3. Scintillation tubes (20 mL poly vials with cap).
4. Scintillation liquid (Ultima Gold™ F, Perkin Elmer, Waltham Mass., US).
5. Center well, polypropylene 10 mm (Kimble Chase, Vineland NJ., US).
6. Filter paper.
7. GR-2 Septa, 12.5 mm (Supelco, Bellefonte Pa., US) for side arm (Fig. 3c).
8. Syringes: 50, 5, 1 mL; needles: 0.5 × 25 mm, 0.8 × 50 mm.
9. Gas: N_2.
10. Custom glass tube-sets for incubation, with rubber stopper connection and cap (*see* Fig. 3 and **Note 2**).
11. Tube incubator without lid.

3 Methods

The current method description considers the type of biocoupons and biocoupon housing that has been described in previous publications [12–14]. The biocoupons, placed in the housing, are contained in a bio-probe that is mounted flush with the pipeline inner surface (Fig. 1, Sects. 2.1 and 2.2). With regard to sampling points along the water injection system, it is important to consider the system that you are studying so that you get relevant samples. A sketch of a generic sea water injection system with suggestion of sampling points is given in Fig. 4.

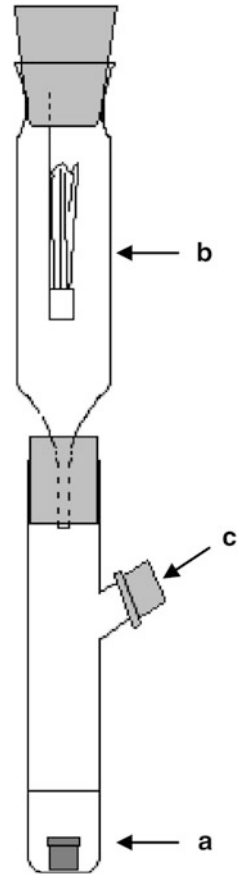

Fig. 3 Schematic drawing of experimental setup for radiorespirometric measurements of sulphate reduction rate. The biocoupon with biofilm is submerged in isotope solution (*a*). The H_2S filter-trap is placed in the upper tube, attached to the rubber stopper at the top of the tube (*b*). The lower and upper tubes are connected by a hollow rubber stopper. HCl is added the samples through the side port equipped with septum and screw cap (*c*)

3.1 Sampling of Biofilm

Biofilm is collected on C-steel biocoupons that are incubated flush mounted inside the water injection pipeline, embedded in a housing containing 5–6 biocoupons (*see* **Note 3**). After extraction from the pipeline, the biocoupon housing is placed in a transport container (Fig. 2) that ensures anoxic conditions during transport to the laboratory. The container has valves that allow for careful flushing and filling of anoxic sample water on site. Store the samples cold.

1. Extract biocoupon housing from pipeline (performed by platform personnel).
2. Place biocoupon housing in transport container, secure and mount the top end to the bottom.

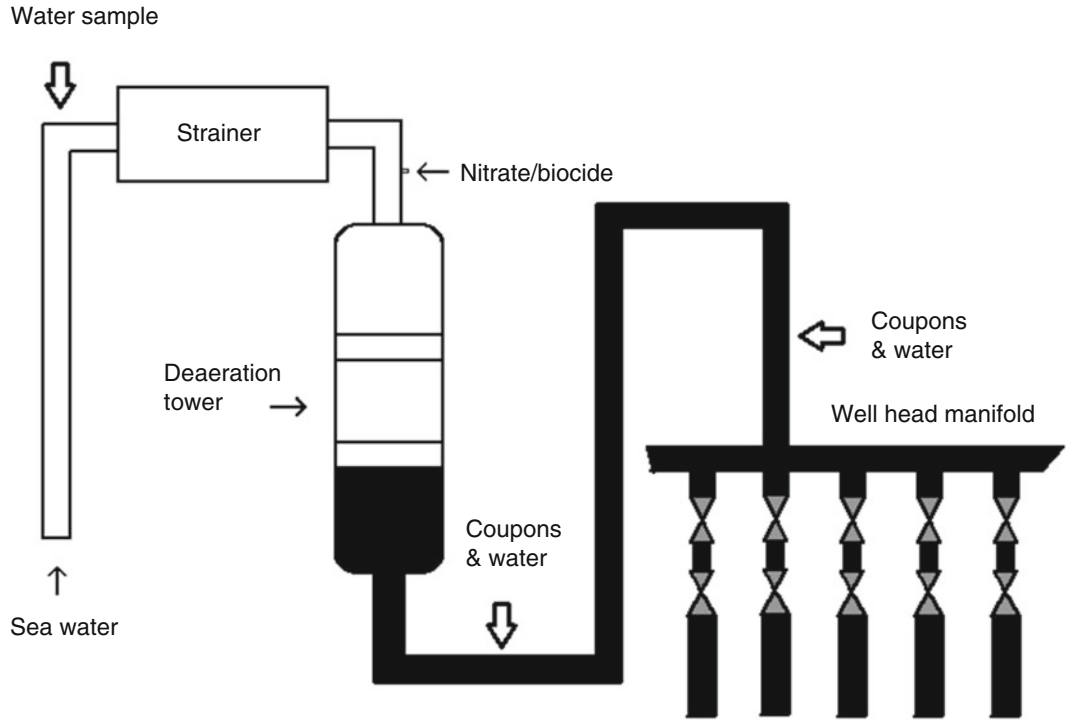

Fig. 4 A generic sketch of a sea water injection system equipped with a strainer for filtration of sea water and a deaeration tower for removal of oxygen. Sampling points are indicated along the system, after deaeration (low pressure) and at the well head (injection pressure)

3. Carefully flood through with anoxic sample water and seal container by closing the valves.
4. Store and transport at low temperature (e.g. 4–10°C).

3.2 Sampling of Water

Water samples are collected from the sampling point of biocoupons, or upstream of their incubation site (*see* **Note 4**). Fill anaerobic culture bottles completely before closing and sealing with rubber stoppers and crimp seals, respectively. In addition to using sterile bottles, it is important to ensure that sampling tubes and other sampling equipment is clean and sterile.

1. Prepare for sampling by flushing the sample line (*see* **Note 4**).
2. Connect sterile sampling tube to the sampling point and place the tubing at the bottom of the bottle and fill it completely with water before closing (*see* **Note 5**).
3. Store at low temperature during transport to the laboratory (e.g. 4–10°C).

3.3 Preparation for Analysis

Depending on the total number of biocoupons, 3 or 4 are used for the determination of sulphate reduction rate (1 for determination of background, 2(3) for activity measurements). The remaining

two biocoupons may be prepared by sonication for viable counts, enrichments and molecular-based analyses [12].

1. Prepare a radioactive working area in a fume cupboard according to regulations (bench coat, tape, shield, etc.).
2. Set the tube incubator at 30°C (*see* **Note 6**).
3. Mount and place 4 incubation tube-sets in a rack and start flushing with N_2 gas for 15 min (use side port, Fig. 3c).
4. Fold (*see* **Note 7**) and place filter paper in center well in upper tube (Fig. 3b).
5. Assemble the lower and upper tube according to Fig. 3.
6. Prepare an isotope user-solution for each sample series by sterile filtering 25 mL sample water into a 50 mL culture bottle under N_2-flushing. Use a 50 mL syringe with 0.2 µm filter attached. Add 125 µL ^{35}S-labelled sulphate prepared according to the manufacturer or the equivalent from another supplier (*see* **Note 1**).

3.4 Analysis

1. Add 4 mL isotope solution to each of the lower tubes by use of a 5 mL syringe with long needle, while still under N_2-flushing.
2. The biocoupons are separated from the housing (*see* **Note 8**) and added directly to the lower incubation tubes under N_2-flushing.
3. Secure the connection between lower and upper tube by tape (*see* **Note 9**).
4. Add 0.45 mL 1 M zinc acetate to the filter in the upper tube by using a 1 mL syringe with a long needle.
5. Stop N_2-flushing and seal upper rubber stopper with tape.
6. Add 0.5 mL 6 M HCl to one of the biocoupons by injection through the side port (Fig. 3c). Use this sample for background measurement. Note the time, as this is the time for start of incubation.
7. Incubate for 20–24 h.
8. At end of incubation, add 0.5 mL 6 M HCl to stop the SRB activity and convert dissolved and precipitated (FeS) sulphide to its gaseous phase (H_2S) for entrapment in the top filter. Leave for equilibration for 18–20 h.
9. Cut the center well from the rubber stopper directly into a scintillation tube.
10. Fill the tube completely with scintillation liquid.
11. Leave for minimum 3 h in the dark before counting.
12. For estimation of total activity, extract three parallels of 0.1 mL isotope user-solution and add 3 mL scintillation liquid, respectively.

13. Measure the activity (DPM) in filters and isotope solution according to respective instruments and protocols.

3.5 Calculations

The sulphate reduction rate is calculated according to the equation:

$$\Delta SO_4^{2-} = \frac{C \times 1.06 \times a}{T \times A}$$

where:

ΔSO_4^{2-} is the sulphate reduction rate in $nmolSO_4^{2-}$/biocoupon/h.

C is the total concentration of sulphate in the incubation tube in $nmolSO_4^{2-}$ (*see* **Note 10**).

1.06 is a factor that corrects for the microbiological partitioning of sulphur isotopes [20].

a is DPM $^{35}S^{2-}$ on filter minus background.

A is DPM $^{35}SO_4^{2-}$ added incubation tube (activity is measured in 0.1 mL isotope solution, thus multiply with 40 for total activity in 4 mL).

T is incubation time in hours.

Convert to production rate, μg H_2S/cm^2/day, by taking into account the surface area of the biocoupon, the molecular weight of H_2S and unit conversions.

4 Notes

1. The isotope user-solution is applied only for the one experiment and is thereafter put away for storage until it is cold and may be discharged. The remaining ^{35}S-labelled sulphate may be used for new samples series analyzed within the timeframe of a few weeks. As you always assess the total activity in each isotope user-solutions you prepare, the decay of ^{35}S is relevant only with regard to the sensitivity of the method. If using a decayed ^{35}S-sulphate batch is considered, you should assess the residual total DPM as well as the incubation time of your experiment (note that the half-life of ^{35}S is 87.4 days).
2. The original experimental design had only a bottom incubation tube. We added a top tube to avoid contamination of the filter by aerosol from the isotope solution (carryover of $^{35}SO_4^{2-}$) when adding the biocoupons or when adding acid at end of incubation.
3. The biocoupons used in previous studies had an exposed area of 0.5 cm^2 [12–14]. Different designs of biocoupons and housing are produced by different supplies.

4. Let the water flow at the sampling point for some time before sampling. This will flush the sampling line and ensure collection of water from the water injection system and not water that has been residing in the sampling line. The time needed to flush will be individual and needs to be considered for each systems.
5. By filling the bottles carefully from the bottom by use of a sterile tube, you will minimize mixing of the sample water with air and thus minimize the exposure to oxygen.
6. 30°C is here considered the general optimal growth temperature for mesophilic sea water bacteria, which is relevant for the current sea water injection systems that have water temperatures around 20–25°C. The incubation temperature should be adjusted for the sampling location in question.
7. Cut the filter paper into 4 × 8 cm pieces and fold to get maximum surface.
8. The separation of biocoupons from the housing may be performed in anoxic chamber. However, with experience the procedure goes quickly and the biofilm exposure to oxygen is limited before it is submerged in anoxic $^{35}SO_4^{2-}$ user-solution in the lower N_2-flushed incubation tube.
9. Development of gas during incubation and/or after acid addition at the end of incubation may cause the rubber stoppers to pop off. Secure the connections with a strong tape, such as, e.g. autoclaving or masking tape.
10. The sulphate content of sample water may be provided by the platform operators (ion analysis of injection water) or may have to be determined individually for other type of samples. Sulphate content may be determined by precipitation of SO_4^{2-} as $BaSO_4$, which may be measured gravimetrically [21] or turbidimetrically.

References

1. Enning D, Garrelfs J (2014) Corrosion of iron by sulfate-reducing bacteria: new views of an old problem. Appl Environ Microbiol 80:1226–1236
2. Dinh HT, Kuever J, Mussmann M, Hassel AW, Stratmann M, Widdel F (2004) Iron corrosion by novel anaerobic microorganisms. Nature 427:829–832
3. Muyzer G, Stams AJM (2008) The ecology and biotechnology of sulphate-reducing bacteria. Nat Rev Microbiol 6:441–454
4. Widdel F, Rabus R (2001) Anaerobic biodegradation of saturated and aromatic hydrocarbons. Curr Opin Biotechnol 12:259–276
5. Rueter P, Rabus R, Wilkes H et al (1994) Anaerobic oxidation of hydrocarbons in crude-oil by new types of sulfate-reducing bacteria. Nature 372:455–458
6. Sunde E, Thorstenson T, Torsvik T (1990) Growth of bacteria on water injection additives. Soc Pet Eng 20690:301–316
7. Maxwell S, Hamilton WA (1986) Modified radiorespirometric assay for determining the sulfate reduction activity of biofilms on metal-surfaces. J Microbiol Methods 5:83–91
8. Ulrich GA, Krumholz LR, Suflita JM (1997) A rapid and simple method for estimating sulfate reduction activity and quantifying

inorganic sulfides. Appl Environ Microbiol 63:1627–1630

9. Ulrich GA, Krumholz LR, Suflita JM (1997) A rapid and simple method for estimating sulfate reduction activity and quantifying inorganic sulfides. Appl Environ Microbiol 63:4626, 1627
10. Hsieh YP, Shieh YN (1997) Analysis of reduced inorganic sulfur by diffusion methods: Improved apparatus and evaluation for sulfur isotopic studies. Chem Geol 137:255–261
11. Meier J, Voigt A, Babenzien HD (2000) A comparison of S-35-SO42- radiotracer techniques to determine sulphate reduction rates in laminated sediments. J Microbiol Methods 41:9–18
12. Bødtker G, Thorstenson T, Lillebø B-LP et al (2008) The effect of long-term nitrate treatment on SRB activity, corrosion rate and bacterial community composition in offshore water injection systems. J Ind Microbiol Biotechnol 35:1625–1636
13. Sunde E, Lillebø BLP, Bødtker G, Torsvik T, Thorstenson T (2004) H_2S inhibition by nitrate injection on the Gullfaks field. Corrosion 2004:paper 04760
14. Thorstenson T, Bødtker G, Lillebø BLP, Torsvik T, Sunde E, Beeder J (2002) Biocide replacement by nitrate in sea water injection systems. Corrosion 2002:paper 02033
15. Drønen K, Roalkvam I, Beeder J et al (2014) Modeling of heavy nitrate corrosion in anaerobe aquifer injection water biofilm: a case study in a flow rig. Environ Sci Technol 48:8627–8635
16. Myhr S, Lillebø BLP, Sunde E, Beeder J, Torsvik T (2002) Inhibition of microbial H_2S production in an oil reservoir model column by nitrate injection. J Ind Microbiol Biotechnol 58:400–408
17. Jenneman GE, McInerney MJ, Knapp RM (1986) Effect of nitrate on biogenic sulfide production. Appl Environ Microbiol 51:1205–1211
18. Dunsmore B, Whitfield TB, Lawson PA, Collins MD (2004) Corrosion by sulfate-reducing bacteria that utilize nitrate. Corrosion 2004, NACE International, Houston TX, USA
19. Greene EA, Hubert C, Nemati M, Jenneman GE, Voordouw G (2003) Nitrite reductase activity of sulphate-reducing bacteria prevents their inhibition by nitrate-reducing, sulphide-oxidizing bacteria. Environ Microbiol 5:607–617
20. Jørgensen BB, Fenchel T (1974) Sulfur cycle of a marine sediment model system. Mar Biol 24:189–201
21. Kremling K (1983) Determination of the major constituents. In: Grasshoff K, Ehrhardt K, Kremling K (eds) Methods of seawater analysis, 2nd edn. Verlag Chemie, Weinheim, pp 247–268

Bacterial Solvent Responses and Tolerance: *Cis–Trans* Isomerization

Hermann J. Heipieper and Nancy Hachicho

Abstract

The protocol describes the application of the membrane adaptive mechanism of Gram-negative bacteria belonging to the genera *Pseudomonas* and *Vibrio*, the isomerization of *cis*- to *trans*-unsaturated membrane fatty acids as a tool for the measurement of the toxicity of membrane-disturbing compounds. The degree of isomerization directly depends on the toxicity and concentration of membrane-affecting agents. Synthesis of *trans* fatty acids is apparent within 30 min after addition of stressors by direct isomerization of the respective *cis* configuration of the double bond without shifting the position. The purpose of the conversion of the *cis* configuration to *trans* is apparently a rapid decrease of the membrane fluidity to rising temperature or the presence of toxic organic hydrocarbons. Therefore, for those bacteria in which this mechanism is present, it offers the possibilities to use the *trans/cis* ratio of unsaturated fatty acids as an elegant, reliable, and rapid bioindicator for membrane stress in experimental setups.

Keywords: Bacterial stress response, *Cis/trans* isomerization, Membrane fatty acids, Unsaturated fatty acids

1 Introduction

About 20 years ago, the conversion of *cis*- to *trans*-unsaturated fatty acids was found as a new adaptive mechanism enabling bacteria belonging to the genera *Vibrio* [1] and *Pseudomonas* [2] to decrease their membrane fluidity as a response to a rise in temperature as well as to the presence of toxic organic hydrocarbons.

P. putida cells increase the proportion of *trans*- to *cis*-unsaturated fatty acids in their membrane in response to phenol exposure to the cells [2]. *Cis–trans* conversion does not depend on culture growth since it also occurs in non-growing cells, which do not carry out de novo lipid biosynthesis [3]. *Cis–trans* conversion is an enzymatic process and typically reaches its final *trans* to *cis* ratio already 30 min after exposure to membrane-toxic agents. The process is carried out by an enzyme called the *cis–trans* isomerase, which is expressed constitutively in response to the membrane

T.J. McGenity et al. (eds.), *Hydrocarbon and Lipid Microbiology Protocols*, Springer Protocols Handbooks, (2017) 111–118,
DOI 10.1007/8623_2014_16, Published online: 20 November 2014

stress and does not depend on de novo protein or to fatty acid biosynthesis [2, 4–6]. Thus, *cis–trans* isomerization turned out to be a new adaptive response of bacteria allowing them to withstand rises in temperature or toxic concentrations of membrane active compounds, which otherwise would inhibit cell functions by causing an increase in membrane fluidity [7–9].

Gram-negative bacteria can also respond to an increase in membrane fluidity by increasing the degree of saturated phospholipid fatty acids [10–12]. In contrast to *cis–trans* isomerization, however, changing the degree of phospholipid fatty acid saturation is strictly dependent on growth and active fatty acid biosynthesis. Indeed, it has been reported that exposure to solvents causes a shift in the ratio of saturated to unsaturated fatty acids in the cell membrane. However, exposure to concentrations that completely inhibit cell growth will render the cells unable to adapt and part of them may die [5]. The isomerization of *cis*- to *trans*-unsaturated fatty acids offers an alternative solution to membrane protection in non-growing cells. The conversion from a *cis*- to *trans*-unsaturated double bond does not have the same quantitative effect on membrane fluidity as a conversion in the ratio of saturated to unsaturated fatty acids, but it still substantially influences the rigidity of the membrane and leads to a protective effect [13, 14].

Incited by results mainly obtained with phenolic compounds, a number of organic hydrocarbons were tested for their ability to cause *cis–trans* isomerization in exposed cells. It was seen that the degree of isomerization correlated with the toxicity and the hydrocarbon concentration [15]. The concentration of hydrocarbons in the membrane depends on their hydrophobicity, which can be described as the logarithm of the octanol–water partition coefficient ($\log P_{ow}$ or $\log K_{ow}$, or simply $\log P$) [16, 17]. Organic solvents with $\log P$ values between 1 and 4 are potentially more toxic for microorganisms because they partition preferentially into membranes [7, 16, 18]. Interestingly, a direct relation was found between the growth-inhibiting toxicity of organic solvents and their potential to cause *cis–trans* isomerization. This relation was independent from the chemical structure of the compound [8, 19].

Besides organic solvents or increase in temperature, also osmotic stress (e.g., those caused by NaCl and sucrose), exposure to heavy metals or related nanoparticles [20], and exposure to some antibiotics cause *cis–trans* isomerization [21, 22]. This indicates that *cis–trans* isomerization is part of a general stress-response adaptation mechanism of microorganisms [12, 23–25].

Recent BLAST analysis revealed that the *cis–trans* isomerase is likely present in other bacteria than *Pseudomonas* or *Vibrio*. Potential candidates are members of the genera *Methylococcus* and *Nitrosomonas*. In fact, the presence of *trans*-unsaturated fatty acids is long known in these bacteria. Recently the *cis–trans* isomerase activity was shown in *Methylococcus capsulatus* Bath [26] as well as

in *Alcanivorax borkumensis*, a marine hydrocarbonoclastic bacterium important for biodegradation of oil spills in marine environments; *cis–trans* isomerization was found to protect the cells against the toxicity of oil particles and toxic biodegradation intermediates [27, 28].

The *trans/cis* ratio of unsaturated fatty acids in bacteria (at least for those in which *cis–trans* isomerase activity is present) can thus be applied as a bioindicator for membrane stress as a result of toxicity exposure, either in experimental setups or in contaminated environments. The procedure to use the *trans/cis* ratio as biomarker will be described in the following protocol.

2 Materials

2.1 Solutions and Materials

Chloroform, methanol, hexane, and the methylation reagent: a BF_3/methanol solution can be obtained from Merck (Darmstadt, Germany). Solvent-resistant plastic (centrifugation) tubes (Nalgene, Rochester, USA) and GC-autosampler flasks (Nalgene, Rochester, USA) are the only special equipment needed. All extraction steps need to be performed under the fume hood and with the usage of nitrile gloves. Solvent-resistant pipet tips should be used to prevent contamination of samples with plastic components.

2.2 Time Considerations

Harvesting of the cells by centrifugation and additional washing step take about 30 min to 1 h of preparation. The disruption of the cells, lipid extraction, and FAME synthesis need about 2 h of work. In case of a GC–FID with autosampler capacity, the analysis of the FAME can be done overnight. Data analysis is regularly done by the GC-supporting hard- and software (e.g., ChemStation, Agilent).

3 Methods

3.1 Preparing Cells from Pure Cultures Containing Cis–Trans Isomerase Activity

Cis–trans conversion is typically maximal 30 min after addition of membrane-toxic agents to bacterial cells. As explained above, it is not necessary to have actively growing cells for this assay, and also resting cells can be taken for the analysis. For toxicity tests the measurement of the final *trans/cis* ratio is appropriate and no kinetic studies are necessary. Cells can be harvested about 30–60 min after the application of the stressor by centrifugation for 15 min at 10,000×*g*, and the cell pellet is suspended in 2 mL phosphate buffer (50 mM, pH 7.0). Afterwards, pellets are concentrated by centrifugation for 5 min at 10,000×*g* and stored at −20°C before starting the extraction. The amount of cell mass in the procedure should be at least 10 mg dry weight. 30 mL with a cell density of about 5×10^8 mL^{-1} or a culture turbidity of 0.5 at 600 nm should be sufficient for subsequent fatty acid analysis.

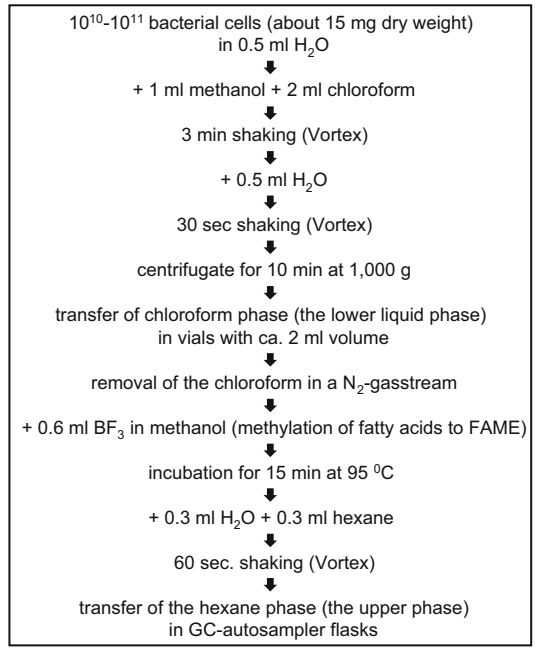

Fig. 1 Scheme of the lipid extraction of cell pellets and the conversion of fatty acids to fatty acid methyl esters (FAME) as routinely performed for analysis of membrane fatty acid contents of microorganisms

When using growing cells, it is necessary to harvest the cells in the exponential growth phase and not at the entry to stationary phase. Fatty acid composition changes when the cells enter the stationary phase [29].

3.1.1 Lipid Extraction and Methylation to Fatty Acid Methyl Esters

The lipids of the cell pellets are extracted subsequently with chloroform/methanol/water (1:1:1 v/v) as first described by Bligh and Dyer [30] and shown schematically in Fig. 1. The fatty acids in the resulting lipid extracts are methylated to the corresponding fatty acid methyl esters (FAME) in order to make them feasible for GC analysis by incubation for 15 min at 95°C in boron trifluoride/methanol (20% boron trifluoride in methanol, Merck, Darmstadt, Germany) [31]. Afterwards, the reaction is stopped by adding 300 µL H_2O as well as 300 µL hexane to extract the FAME for GC analysis. The procedure is very simple and summarized in the scheme shown in Fig. 1.

3.1.2 Analysis of Fatty Acid Composition by GC–FID

Analysis of FAME in hexane is performed using a quadrupole GC System (HP5890, Hewlett-Packard, Palo Alto, USA) equipped with a split/splitless injector and a flame ionization detector (GC–FID). The best column system in our hands for the separation of *cis*- and *trans*-unsaturated FAME is a CP-Sil 88 capillary column (Chrompack, Middelburg, the Netherlands; length, 50 m; inner

diameter, 0.25 mm; 0.25 μm film). GC conditions are the following: Injector temperature was held at 240°C and detector temperature was held at 270°C. The injection should be splitless and carrier gas is He at a flow rate of 2 mL min^{-1}. The temperature program is 40°C, 2 min isothermal; 8°C min^{-1} to 220°C; and 5 min isothermal at 220°C. The pressure program is 27.7 psi (=186.15 kPa), 2 min isobaric; 0.82 psi min^{-1} (5.65 kPa min^{-1}) to a final pressure of 45.7 psi; and 5.55 min isobaric at 45.7 psi (310.26 kPa). Fatty acids can be identified by GC from retention time of authentic reference compounds obtained from Supelco (Bellefonte, USA).

In our hands, the GC-column system applied for the FAME procedure of the Sherlock Microbial Identification System (MIDI Inc., Newark, Del.), which uses a GC–FID gas chromatography system and an Ultra2 nonpolar capillary column (length, 25 m; inside diameter, 0.20 mm; film thickness, 0.33 μm; Agilent), is functional but less effective regarding the separation properties of FAMEs than the Sil 88 capillary column.

3.2 Troubleshooting

In the Bligh and Dyer procedure of 1959, it is necessary to obtain a clear chloroform phase (the lower liquid phase). When high biomass content is used, this phase can be very small. This can be solved simply by adding more (about 0.5 mL) chloroform to the tubes and shaking once more for 1 min. After another centrifugation for 10 min at 1,000×*g*, the volume of the chloroform phase should be large enough.

For analysis of growing cultures, it is necessary to harvest the cells in the exponential growth phase, because the fatty acid composition changes when the cells enter the stationary phase [29].

Because *cis–trans* isomerase activity is constitutive and usually high, even mechanical stress on cell pellets can have an effect on the *trans/cis* ratios [29]. Therefore, the procedure after harvesting the cell pellets such as storage (at −20°C) and the time needed to start the Bligh and Dyer extraction after melting the pellets should be unified to avoid artificially high *trans/cis* values.

3.3 Data Analysis Regarding Trans/Cis Ratio of Unsaturated Fatty Acids

Regularly, the degree of *cis–trans* isomerization of unsaturated fatty acids is given as the ratio of all *trans*-unsaturated fatty acids divided by the corresponding *cis*-unsaturated fatty acids (see equation). In some strains, where the amount of C18:1*trans* fatty acids is very low, only the C16 *trans/cis* ratio can be used (C16:1*trans*/C16:1*cis*).

$$trans/cis \text{ ratio}: \frac{(\mathrm{C16:1}trans + \mathrm{C18:1}trans)}{(\mathrm{C16:1}cis + \mathrm{C18:1}cis)}$$

4 Notes

4.1 Application of the Obtained Trans/Cis Ratios as an Indicator for Membrane Toxicity Stress

The above-described protocol can be used to measure toxicity of any compound producing membrane damage. This is especially true for hydrocarbons. Figure 2 gives an example, here for toluene as toxicant. The toxicity of a hydrocarbon can be predicted by its hydrophobicity (log*P*) and water solubility [8, 19]. For toxic hydrocarbons a direct dose dependency between their aqueous phase concentration and the final *trans/cis* ratio occurs [15, 21, 32–34]. A direct relation between toxicity, given as the effective concentration (EC50) leading to 50% growth inhibition, and *cis/trans* isomerization was measured for a range of hydrocarbons and is described as the concentration causing a half-maximum increase in the *trans/cis* ratios (Fig. 3). In principle, the procedure can be

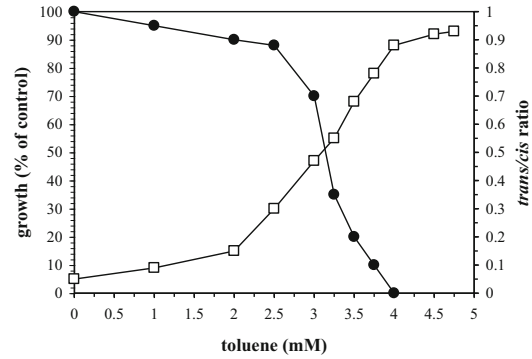

Fig. 2 Effect of toluene on growth rates (*filled circle*) and *trans/cis* ratio (*open square*) of *Pseudomonas putida* cells

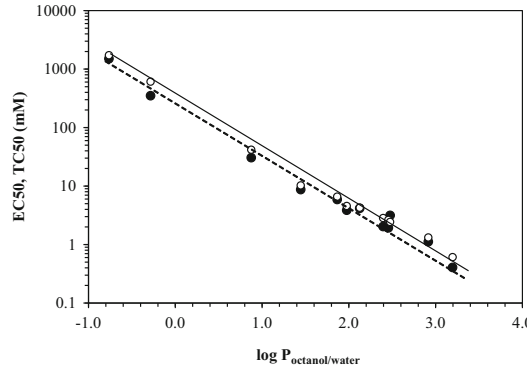

Fig. 3 Correlation between the hydrophobicity, given as the log*P* value of different organic hydrocarbons, growth inhibition, and *trans/cis* ratio of *Pseudomonas putida* cells. Growth inhibition (*open circle*) is given as the EC50 concentration, and the TC50 (*filled circle*) is given as the concentrations which caused an increase in the *trans/cis* ratio of unsaturated fatty acids to 50% of the maximum *trans/cis* level reached at saturating concentrations of the toxicant

used to assess the toxicity of unknown hydrocarbons in known pure cultures, the cellular fitness of mutants to those hydrocarbons, and hydrocarbon toxicity to new bacterial isolates. The limitation regarding the occurrence of the *cis–trans* isomerase will restrict the use of the *trans/cis* ratio to those genera which are able to express the enzyme and show the conversion.

4.2 Research Needs

An open question remains the use of the *trans/cis* ratio as a biomarker for membrane toxicity stress in environmental samples or contaminated sites. Such applications have been suggested; in fact, a *trans/cis* ratio greater than 0.1 was proposed to serve as an index for starvation or stress in environmental samples [35]. However, a clear knowledge about the behavior of bacteria containing the *cis–trans* isomerase, especially with respect to long-term application of stressors, and a statistical validation seem necessary, before the determination of the *trans/cis* index might be a valuable option in studying the toxicity status of natural samples [36, 37].

References

1. Okuyama H, Okajima N, Sasaki S, Higashi S, Murata N (1991) The *cis/trans* isomerization of the double bond of a fatty acid as a strategy for adaptation to changes in ambient temperature in the psychrophilic bacterium, *Vibrio* sp. strain ABE-1. Biochim Biophys Acta 1084:13–20
2. Heipieper HJ, Diefenbach R, Keweloh H (1992) Conversion of *cis* unsaturated fatty acids to *trans*, a possible mechanism for the protection of phenol-degrading *Pseudomonas putida* P8 from substrate toxicity. Appl Environ Microbiol 58:1847–1852
3. Morita N, Shibahara A, Yamamoto K, Shinkai K, Kajimoto G, Okuyama H (1993) Evidence for *cis-trans* isomerization of a double bond in the fatty acids of the psychrophilic bacterium *Vibrio* sp. strain ABE-1. J Bacteriol 175:916–918
4. Diefenbach R, Heipieper HJ, Keweloh H (1992) The conversion of *cis-* into *trans-* unsaturated fatty acids in *Pseudomonas putida* P8: evidence for a role in the regulation of membrane fluidity. Appl Microbiol Biotechnol 38:382–387
5. Heipieper HJ, de Bont JAM (1994) Adaptation of *Pseudomonas putida* S12 to ethanol and toluene at the level of fatty acid composition of membranes. Appl Environ Microbiol 60:4440–4444
6. Kiran MD, Annapoorni S, Suzuki I, Murata N, Shivaji S (2005) *Cis-trans* isomerase gene in psychrophilic *Pseudomonas syringae* is constitutively expressed during growth and under conditions of temperature and solvent stress. Extremophiles 9:117
7. Weber FJ, de Bont JAM (1996) Adaptation mechanisms of microorganisms to the toxic effects of organic solvents on membranes. Biochim Biophys Acta 1286:225–245
8. Heipieper HJ, Meinhardt F, Segura A (2003) The *cis-trans* isomerase of unsaturated fatty acids in *Pseudomonas* and *Vibrio*: biochemistry, molecular biology and physiological function of a unique stress adaptive mechanism. FEMS Microbiol Lett 229:1–7
9. Kiran MD et al (2004) Psychrophilic *Pseudomonas syringae* requires *trans*-monounsaturated fatty acid for growth at higher temperature. Extremophiles 8:401–410
10. Ingram LO (1977) Changes in lipid composition of *Escherichia coli* resulting from growth with organic solvents and with food additives. Appl Environ Microbiol 33:1233–1236
11. Kabelitz N, Santos PM, Heipieper HJ (2003) Effect of aliphatic alcohols on growth and degree of saturation of membrane lipids in *Acinetobacter calcoaceticus*. FEMS Microbiol Lett 220:223–227
12. Zhang YM, Rock CO (2008) Membrane lipid homeostasis in bacteria. Nat Rev Microbiol 6:222–233
13. MacDonald PM, Sykes BD, McElhaney RN (1985) Fluorine-19 nuclear magnetic resonance studies of lipid fatty acyl chain order and dynamics in *Acholeplasma laidlawii* b membranes. a direct comparison of the effects of *cis* and *trans* cyclopropane ring and double-

bond substituents on orientational order. Biochemistry 24:4651–4659

14. Roach C, Feller SE, Ward JA, Shaikh SR, Zerouga M, Stillwell W (2004) Comparison of *cis* and *trans* fatty acid containing phosphatidylcholines on membrane properties. Biochemistry 43:6344
15. Heipieper HJ, Loffeld B, Keweloh H, de Bont JAM (1995) The *cis/trans* isomerization of unsaturated fatty acids in *Pseudomonas putida* S12: an indicator for environmental stress due to organic compounds. Chemosphere 30:1041–1051
16. Sikkema J, de Bont JA, Poolman B (1995) Mechanisms of membrane toxicity of hydrocarbons. Microbiol Rev 59:201–222
17. Isken S, de Bont JAM (1998) Bacteria tolerant to organic solvents. Extremophiles 2:229–238
18. Heipieper HJ, Weber FJ, Sikkema J, Keweloh H, de Bont JAM (1994) Mechanisms behind resistance of whole cells to toxic organic solvents. Trends Biotechnol 12:409–415
19. Neumann G et al (2005) Prediction of the adaptability of *Pseudomonas putida* DOT-T1E to a second phase of a solvent for economically sound two-phase biotransformations. Appl Environ Microbiol 71:6606–6612
20. Hachicho N, Hoffmann P, Ahlert K, Heipieper HJ (2014) Effect of silver nanoparticles and silver ions on growth and adaptive response mechanisms of *Pseudomonas putida* mt-2. FEMS Microbiol Lett 355:71–77
21. Heipieper HJ, Meulenbeld G, VanOirschot Q, De Bont JAM (1996) Effect of environmental factors on the *trans/cis* ratio of unsaturated fatty acids in *Pseudomonas putida* S12. Appl Environ Microbiol 62:2773–2777
22. Isken S, Santos P, de Bont JAM (1997) Effect of solvent adaptation on the antibiotic resistance in *Pseudomonas putida* S12. Appl Microbiol Biotechnol 48:642–647
23. Segura A, Duque E, Mosqueda G, Ramos JL, Junker F (1999) Multiple responses of Gram-negative bacteria to organic solvents. Environ Microbiol 1:191–198
24. Ramos JL, Gallegos MT, Marques S, Ramos-Gonzalez MI, Espinosa-Urgel M, Segura A (2001) Responses of Gram-negative bacteria to certain environmental stressors. Curr Opin Microbiol 4:166–171
25. Ramos JL et al (2002) Mechanisms of solvent tolerance in gram-negative bacteria. Annu Rev Microbiol 56:743–768
26. Loffler C, Eberlein C, Mausezahl I, Kappelmeyer U, Heipieper HJ (2010) Physiological evidence for the presence of a *cis-trans* isomerase of unsaturated fatty acids in *Methylococcus capsulatus* Bath to adapt to the presence of toxic organic compounds. FEMS Microbiol Lett 308:68–75
27. Hara A, Syutsubo K, Harayama S (2003) *Alcanivorax* which prevails in oil-contaminated seawater exhibits broad substrate specificity for alkane degradation. Environ Microbiol 5:746–753
28. Naether DJ et al (2013) Adaptation of the hydrocarbonoclastic bacterium *Alcanivorax borkumensis* SK2 to alkanes and toxic organic compounds: a physiological and transcriptomic approach. Appl Environ Microbiol 79:4282–4293
29. Hartig C, Loffhagen N, Harms H (2005) Formation of *trans* fatty acids is not involved in growth-linked membrane adaptation of *Pseudomonas putida*. Appl Environ Microbiol 71:1915–1922
30. Bligh EG, Dyer WJ (1959) A rapid method of total lipid extraction and purification. Can J Biochem Physiol 37:911–917
31. Morrison WR, Smith LM (1964) Preparation of fatty acid methyl esters and dimethylacetals from lipids with boron fluoride-methanol. J Lipid Res 5:600–608
32. Weber FJ, Isken S, de Bont JA (1994) *Cis/trans* isomerization of fatty acids as a defence mechanism of *Pseudomonas putida* strains to toxic concentrations of toluene. Microbiology 140:2013–2017
33. Hage A, Schoemaker HE, Wever R, Zennaro E, Heipieper HJ (2001) Determination of the toxicity of several aromatic carbonylic compounds and their reduced derivatives on *Phanerochaete chrysosporium* using a *Pseudomonas putida* test system. Biotechnol Bioeng 73:69–73
34. Neumann G, Kabelitz N, Heipieper HJ (2003) The regulation of the *cis-trans* isomerase (cti) of unsaturated fatty acids in *Pseudomonas putida*: correlation between cti activity and K^+-uptake systems. Eur J Lipid Sci Technol 105:585–589
35. Guckert JB, Hood MA, White DC (1986) Phospholipid ester-linked fatty acid profile changes during nutrient deprivation of *Vibrio cholerae*: increases in the *trans/cis* ratio and proportions of cyclopropyl fatty acids. Appl Environ Microbiol 52:794–801
36. Fischer J, Schauer F, Heipieper HJ (2010) The *trans/cis* ratio of unsaturated fatty acids is not applicable as biomarker for environmental stress in case of long-term contaminated habitats. Appl Microbiol Biotechnol 87:365–371
37. Frostegård Å, Tunlid A, Bååth E (2011) Use and misuse of PLFA measurements in soils. Soil Biol Biochem 43:1621–1625

Protocols for Measuring Biosurfactant Production in Microbial Cultures

Roger Marchant and Ibrahim M. Banat

Abstract

Microbial biosurfactants have wide structural and functional diversity which consequently requires the adoption of a range of techniques to investigate these amphiphilic molecules. Literature on the production and analytical detection of biosurfactants is overwhelmed with assertions of high yields for such products which are mostly over exaggerated estimates due to the use of flawed or inaccurate analytical techniques. In this chapter we focus on quantitative methods available to allow accurate estimates of production and yield data to be generated.

Keywords Colorimetric methods, HPLC/MS, Rhamnolipid, Sophorolipid, Surface/interfacial tension, UPLC

1 Introduction

Biosurfactants are amphiphilic molecules mainly produced by bacteria, yeasts and fungi. They possess both hydrophilic and hydrophobic moieties and are able to display a variety of surface activities that, among other roles, help solubilising hydrophobic substrates and are the subject of intense investigation [1, 2]. One of the major potential applications is their use as replacements for synthetic surfactants in many existing and future industrial and environmental applications [3]. Diverse functional properties, viz. emulsification, wetting, foaming, cleansing, phase separation, surface activity and reduction in viscosity of crude oil, makes it feasible to utilise them for numerous environmental, food, pharmaceutical, medical, cleaning and other industrial application purposes [4–9].

Accurate measurement of biosurfactant production and determination of final yields from microbial fermentations are things which have been rarely or never achieved by researchers up to the present time. The reasons for this are complex but are due to factors such as the diversity of the congeners produced and their chemical

T.J. McGenity et al. (eds.), *Hydrocarbon and Lipid Microbiology Protocols*, Springer Protocols Handbooks, (2017) 119–128,
DOI 10.1007/8623_2014_10, Published online: 04 December 2014

similarity plus the need for sophisticated methodology for analysis. There have been many publications describing several qualitative methods for the screening and detection of biosurfactant producing cultures and product in cell culture broths. Such methods include haemolysis of erythrocytes, axisymmetric drop shape analysis, cell surface hydrophobicity, drop collapse, oil spread on surfaces, tilted glass slide, blue agar plate method, emulsification activity, agar plate method and direct colony or broth chromatographic technique. All these methods have been adequately reviewed by Satpute et al. [10].

In this chapter we will not deal with these varied methods that have traditionally been employed for screening for biosurfactant production as they are generally indirect methods using the physicochemical properties of surfactants and emulsifiers as indicators of production rather than direct quantitative measures. There are also a number of methods that have been used quantitatively to asses production, but which in reality are only semi-quantitative at best, these methods will be described and evaluated. Finally we will focus on the critical quantitative methods that are now being developed to allow accurate production and yield data to be generated. The field of microbial biosurfactant research is beset with claims for efficient and large product yields which on closer examination can be shown to be massive overestimates based on the use of flawed methodology.

2 Materials

Bradford Reagent: Dissolve 100 mg Coomassie Brilliant Blue G-250 in 50 ml 95 % (v/v) ethanol, and add 100 ml 85 % (w/v) phosphoric acid. Dilute to 1 l when the dye has completely dissolved and then filter through Whatman Number 1 filter paper just before use. 1 M NaOH can be used in the assay mixture if the lipopeptide is not completely soluble in the Bradford Reagent.

3 Methods

3.1 Semi-quantitative Methods

3.1.1 Surface Tension

The reduction in surface tension of a culture broth as the organism grows is indicative that the organism may be producing a specific surface active compound, although many molecules show the same characteristic and may only be subsidiary metabolites. It is a relatively simple procedure to measure the surface tension (ST) of a culture broth during the growth cycle using the the Du Nouy method using a digital tensiometer equipped with a platinum-iridium ring. Distilled water is used to calibrate the instrument and mean values of replicates are necessary for reproducible results.

The ST value for pure water is 72.8 mN/m at 20°C and microbial biosurfactants may reduce the value to around 27 mN/m. Although ST measurements do give numerical values, the data are of limited use in quantifying the biosurfactant production for the following reasons:

1. The ST value falls to a minimum at the Critical Micelle Concentration (CMC) for a specific biosurfactant molecule and any further increases in biosurfactant concentration produce no further decline in ST value. For the most active biosurfactants, the CMC value may be very low, e.g. rhamnolipid CMC values have been variously determined as in the range 24–65 mg/L. Since biosurfactant production may be in the range of tens to hundreds of grams per litre, the initial decline in ST in a culture covers only a small portion of the production cycle. The value of the method can be extended, however, by using a dilution series and calculating approximate yields on the basis of titre.
2. Microbial biosurfactants are not produced as a single molecular species but as a mixture of different congeners. Very often this mixture is exceedingly complex and the variations in structure lead to each congener having different surface-active properties. A further complication is that different culture conditions may alter the proportion of the individual congeners. It is clear therefore that an overall measurement like ST can only give an indication of biosurfactant production and no specific quantitative information concerning individual congeners.
3. Measuring the ST of a culture broth also fails to take account of the contribution to the ST value by constituents of the growth medium and the changes that take place during microbial growth. For example, the use of oleic acid as a carbon source may lead to its emulsification and reduction of surface tension measurements in the broth culture.
4. Theoretically isolating and purifying the individual congeners from the mixture should allow true CMC values to be determined, however, separation of a complex mixture of different but similar congeners is seldom feasible [11].

3.1.2 *Interfacial Tension*

Interfacial tension (IFT) is a measure of the cohesive energy present at an interface, e.g. liquid/liquid or gas/liquid phases. The surface activity of biosurfactants reduces the IFT in a similar fashion to the ST effect. The IFT can be measured using specific pieces of equipment, or through examination of the axisymmetric shape of a hanging or supine drop [12], the units of measurement for IFT are the same as ST, i.e. mN/m. The same comments made about the limitations of ST measurement apply to IFT.

3.2 Colorimetric Methods

3.2.1 Orcinol Method

Colorimetric methods to determine the production of biosurfactants in microbial cultures have many immediate attractions. They offer the prospect of a simple, rapid, reproducible and accurate methodology; however, in the case of biosurfactants, this prospect is not one that is fulfilled. The orcinol method for the determination of rhamnolipids [13] is one that has been used extensively in the literature to report production and yields of rhamnolipids; unfortunately in most applications, it is fatally flawed as we will discuss later. The method is carried out as follows: cell-free supernatant from a microbial culture is diluted 10 times and 100 μl of this sample added to 900 μl of fresh orcinol reagent (0.19% orcinol in 53% sulphuric acid). The sample is then incubated in a water bath at 80°C for 30 min, cooled to room temperature for 15 min and finally the absorbance measured at 421 nm (Abs_{421nm}). The rhamnose content is calculated by comparison with a standard curve prepared with L-rhamnose at concentrations of 0–50 μg/ml. Rhamnolipid concentration is obtained by multiplying the rhamnose content by 3.0, which represents the rhamnolipid/rhamnose correlation [14]. The measurements should be carried out in duplicate and may be expected to consistently show less than 5% variation. The underlying problems with the orcinol method for the determination of glycolipid biosurfactants is that the reagent reacts with any pentose sugar and is not specific for rhamnose; indeed orcinol has been used for the quantification of both DNA and RNA. The second point is that it is in any case an indirect method for rhamnolipid determination, and the final calculation of rhamnolipid concentration depends on an estimated proportion of rhamnose to total glycolipid quantity which will vary from culture to culture and between different fermentation runs in addition to variations of sugar content and proportions between the different biosurfactant congeners such as mono- and di-rhamnose sugar containing rhamnolipids. The effect of these problems is that the orcinol method always overestimates the quantity of rhamnolipid present, sometimes to an alarming degree. Carrying out the determination on the culture broth will compound the error, but even using an extraction and purification protocol as described by Smyth et al. [11, 15] will not remove the errors. Some workers have attempted to improve the accuracy of the method by using a standard of rhamnolipid rather than pure rhamnose; however, this does not prevent the interference of contaminating pentoses in the sample. In conclusion we can say that the orcinol method is really only of value in a comparative quantitative role within a single experiment and should not be used where absolute values are required to make comparisons between different studies.

3.2.2 Bradford Method

Just as orcinol can be used as an indirect method to measure the pentose portion of a glycolipid biosurfactant, the Bradford method [16] to estimate protein can used as an indirect method for lipopeptide biosurfactant quantification. The assay is carried out as follows:

Samples should contain between 5 and 100 μg protein in a volume of 100 μl. If the lipopeptide to be assayed is not soluble in the Bradford reagent, add an equal volume of 1 M NaOH to each sample and vortex (if this option is used, the NaOH should also be added to the standards). Standards containing 5–100 μg of a suitable protein, e.g. albumin, should be prepared for calibration of the method. Add 5 ml of the Bradford Reagent to each sample and incubate for 5 min and then measure the absorbance at 595 nm.

The Bradford Reagent reacts primarily with arginine residues and less so with histidine, lysine tyrosine, tryptophan and phenylalanine residues. This means that the overall reaction is very dependent on the composition of the peptide being assayed. It is therefore obvious that this method, like the orcinol method, has severe limitations for the quantification of biosurfactant production and should only be used to obtain relative yields under one set of conditions rather than as an absolute quantification method.

3.3 Gravimetric Methods

The most obvious and perhaps the simplest quantification method is gravimetric analysis, i.e. isolating/separating and then directly weighing the amount of product. While this approach has a great deal of merit, there are significant problems in applying it to biosurfactant production. Methods for the isolation and purification of a range of low molecular weight and high molecular weight biosurfactants have been detailed by Smyth et al. [11, 15]. One major complication for the isolation of the 'pure' biosurfactant is the type of substrate used for the growth of the microbial producer. Very often this takes the form of an excess amount of a pure fatty acid or fatty acid mixture such as rapeseed oil, which has to be removed before the further purification of the biosurfactant can take place. Solvent extraction, e.g. hexane, can be used for this removal; however, it can be difficult to determine whether excess fatty acid removal has been effectively achieved. The purity of the finally isolated biosurfactant can be checked before gravimetric analysis using analytical methods such as direct injection mass spectrometry; however, not all contaminating molecules will give a signal and this methodology can only really be used in a negative mode; i.e. if a contaminant is seen then the surfactant preparation is not pure, but if no contaminants are seen this does not necessarily mean the preparation is pure. Despite the drawbacks of the gravimetric method, it does provide a reasonably good comparative measure providing care is taken with the isolation and purification steps.

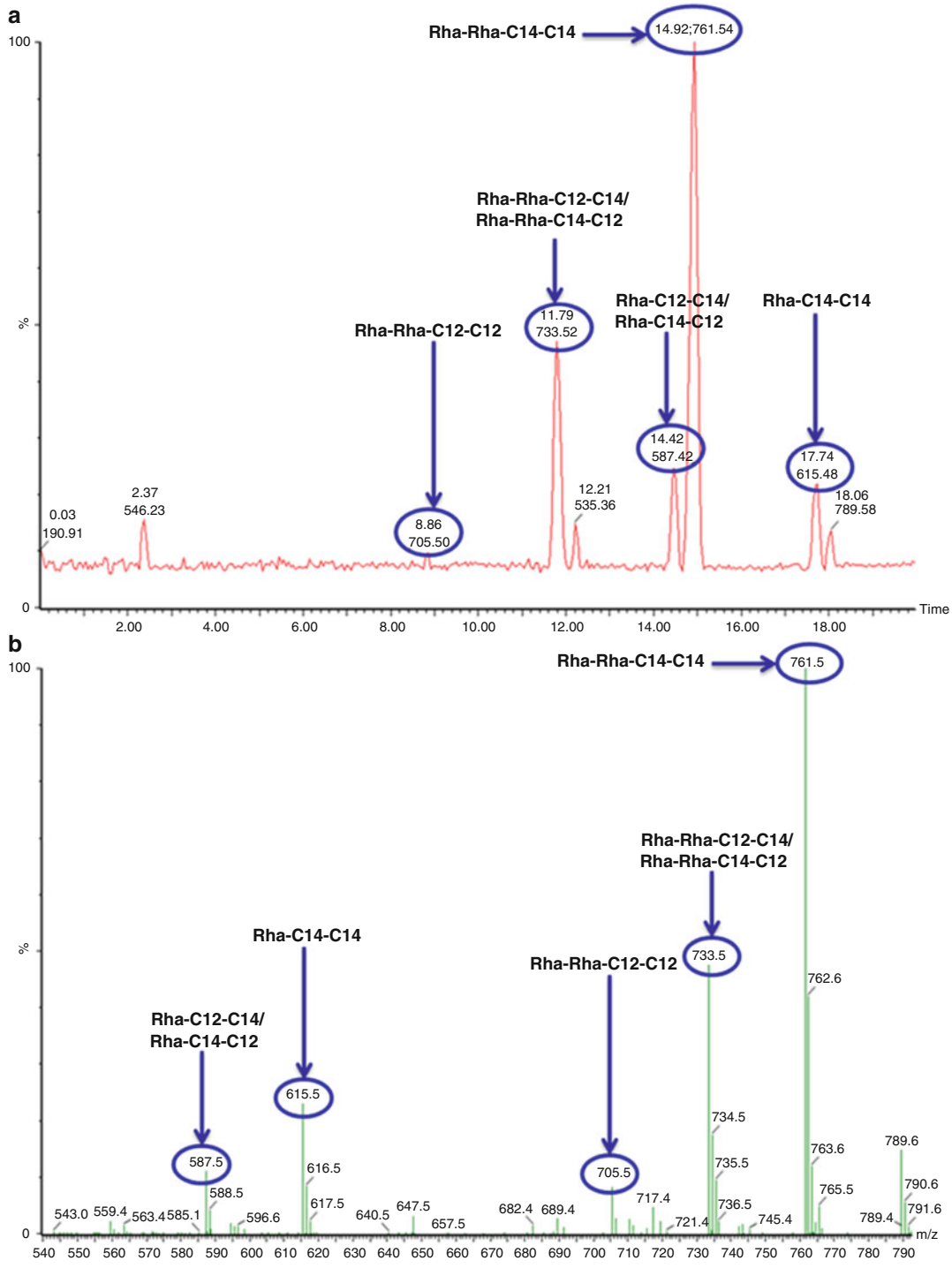

Fig. 1 Separation of rhamnolipid congeners produced by *B. thailandensis* E264. (**a**) LC-QToF-MS of rhamnolipid crude extract after SPE purification. Static phase, Agilent poroshell SB-C3, 2.1 × 100 mm, particle size 2.7 μm. Mobile phase 1, H_2O (4 mM ammonium acetate), and mobile phase 2, MeCN, were used for chromatographic separation as follows: 0–17 min 50–70% mobile phase 2, 17.0–17.5 min 70% mobile

3.4 Rigorous Quantitative Methods

The very nature of most biosurfactants produced by microorganisms makes absolute quantification a very difficult task. The mixtures of different congeners differing only slightly in structure, but with possibly widely variant functionalities, provide a major obstacle to accurate differential quantification. As we have seen with the indirect methods or the measurement of a fractional component of the molecules, these techniques can produce grossly misleading results which are usually overestimates of quantity. An effective approach therefore must include separation and characterisation technologies which allow individual components of the mixtures to be identified and quantified. These requirements effectively limit the possible methods to combinations of HPLC and mass spectrometry; see Fig. 1 which shows an example of such separation for rhamnolipid congeners produced by *B. thailandensis*.

HPLC is a practical and efficient method for separating individual components of biosurfactant mixtures, particularly glycolipids. The precise conditions which need to be used for complete separation of a specific set of biosurfactant congeners have to be determined experimentally each time, but we can give the conditions for separation of some of the systems that have already been developed.

3.4.1 Rhamnolipids and Sophorolipids

The first step in the process of analysing a culture broth involves the removal of the cells by centrifuging followed by some measure of purifying the biosurfactant through acidification to precipitate the glycolipids combined with solvent extraction [11]. The purified extract (5 μl of a 1 mg/mL solution) of the glycolipid is then diluted in methanol (95 μl) and 10 μl used for HPLC analyses coupled to a tandem quadrupole mass spectrometer. Analysis of mixtures containing predominantly $C_{10}C_{10}$ rhamnolipids can be performed using a Luna C_{18} 250 × 4.6 mm 5 μm column (Phenomenex, Cheshire, UK) with a mobile phase consisting of water + 4 mM ammonium acetate (phase A) and acetonitrile (phase B) and the operating conditions as follows: 70:30 (A:B) to 30:70 (A:B) over 50 min and back to 70:30 (A:B) over 5 min with hold for 5 min.

Analysis of sophorolipids can be carried out using a similar C_{18} column with the same mobile phases and chromatographic conditions as above. Flow rates of 0.5 ml/min are appropriate. The mass

Fig. 1 (continued) phase 2, 17.5–18.0 min 70%–50% mobile phase 2 and 18–20 min 50% mobile phase 2. (**b**) QToF-MS profile of rhamnolipid crude extract after SPE purification. SPE purification was carried out using Strata SI-1 silica (55 μm, 70 A) 2 g/12 ml Giga Tubes. $CHCl_3$ was used to clean the column before the sample was added. The sample was then dissolved in $CHCl_3$ and added to the column; pure $CHCl_3$ was ran through the column to clean and remove any unwanted products from the sample. Finally, the purified rhamnolipid was eluted using a 1:1, *v/v* solution of $CHCl_3$:MeOH

spectrometer should be operated in ionisation negative mode with a scanning range of 50–1,200 Da. Using these conditions, good separation of congeners should be achieved and relative abundance of the individual congeners will be observable from the HPLC peak areas. The MS data will also allow each peak to be directly identified. Ideally for fully accurate quantification, a glycolipid standard should be run for each congener to calibrate the peak areas from the HPLC trace. This approach, however, is not practicable since it is probably only realistic to obtain pure samples of the major components of any mixture in useable quantities. An alternative approach is to use an internal standard with each glycolipid sample run. Costa et al. [17] used this technique for the analysis of rhamnolipids from *Burkholderia glumae*, adding 16-hydroxyhexadecanoic acid or 5,6,7,8-tetradeutero-4-hydroxy-2-heptylquinoline at a final concentration of 10 mg/L. *Burkholderia glumae* produces mono and di-rhamnolipids with alkyl chains ranging in length between $C_{12}C_{12}$ and $C_{16}C_{16}$ with the most abundant congener Rha-Rha-$C_{14}C_{14}$; effective separation of these congeners was achieved using a 4.6 × 50 mm 300SB-C3 Zorbax 5 μm reverse-phase column using a water/acetonitrile gradient with a constant 2 mM concentration of ammonium acetate. The choice of internal standard to use in this system is governed by the ability to obtain a good signal in the MS system. The examples of HPLC separation conditions given above cannot be applied directly to separation and quantification of other glycolipid biosurfactants without selecting an appropriate column and suitable elution phases and gradients. Each new type of surfactant mixture will require careful optimisation of the conditions.

Although the system outlined above for quantification of biosurfactant produced in a microbial culture is accurate and reproducible, it does have disadvantages, notably the length of time required to run each sample means that monitoring of the progress of a fermentation run can only be carried out off-line and at relatively infrequent intervals. More recently an improved technique has been developed (Rudden, Smyth, Marchant, & Banat) which uses UPLC technology with much improved separation of congeners achieved in 3 min with a further 2 min conditioning of the column between runs; this compares to a normal run time of 55 min using HPLC. This method potentially allows accurate quantification to be carried out at short time intervals during a fermentation run. The UPLC system operates at ultrahigh pressure (600 bar) through a narrow bore column (21 x 100 mm) and for separation of $C_{10}C_{10}$ rhamnolipids uses water plus 4 mM ammonium acetate as mobile phase A and acetonitrile as phase B with a gradient from 50% A to 90% B over 2.2 min. The peaks produced are analysed as with the HPLC system using a tandem quadrupole

mass spectrometer. Rhamnolipid standards used for calibration and validation of the system were prepared from a mixture of up to 14 different congeners by separating the congeners into two fractions: one containing mono-rhamnolipids and the other di-rhamnolipids. Since separation of the fractions into individual congeners was impracticable (some congeners are present in very low amounts), the relative proportion of each congener was established from the % peak area from the mixed sample, and then 1 mg/mL of the most abundant rhamnolipid congener present in each of the purified fractions was analytically weighed to obtain standard solutions; i.e. in fraction R1, Rha-C_{10}-C_{10} (503 m/z $[M\text{-}H]^-$) was the most abundant congener comprising 83.8% of the total sample, and in fraction R2, Rha-Rha-C_{10}-C_{10} (649 m/z $[M\text{-}H]^-$) was the most abundant congener comprising 85.1% of the total sample. Standard curves could then be constructed to allow accurate quantification of all the congeners present in the initial sample. The major advantages of the UPLC method are the approximately 12-fold reduction in run time for the separation of the rhamnolipid congeners compared to the HPLC method, and with the use of multiple reaction monitoring (MRM), which eliminates other interfering compounds in the sample, preliminary preparation of the sample can be reduced to the removal of particulate material, i.e. microbial cells.

4 Conclusion

The overall conclusion at present is that published data on the yields of biosurfactant from different fermentation systems cannot be directly compared and that great care should be exercised in evaluating claims for high production yields. The fact that micro-organisms produce a mixture of very similar congeners also means that absolute quantification of yield is always going to be difficult to achieve. The use of appropriate standards in conjunction with techniques that allow accurate quantification, e.g. HPLC or UPLC, is most likely to give the accurate and reproducible yield data that are required to evaluate the economic feasibility of any process.

Acknowledgement

We would like to thank Dr Thomas J.P. Smyth and Mr Scot Funston for valuable comments and results from analytical methods.

References

1. Marchant R, Banat IM (2012) Biosurfactants: a sustainable replacement for chemical surfactants? Biotechnol Lett 34:1597–1605
2. Marchant R, Banat IM (2012) Microbial biosurfactants: challenges and opportunities for future exploitation. Trends in Biotechnol 30:558–565
3. Banat IM, Franzetti A, Gandolfi I, Bestetti G, Martinotti MG, Fracchia L, Smyth TJP, Marchant R (2010) Microbial biosurfactants production, applications and future potential. Appl Microbiol Biotechnol 87:427–444
4. Perfumo A, Smyth TJP, Marchant R, Banat, IM (2010) Production and roles of biosurfactants and bioemulsifiers in accessing hydrophobic substrates. In: Timmis KN (ed) Handbook of hydrocarbon and lipid microbiology, Chap 47, vol 2, part 7. Springer-Verlag, Berlin Heidelberg, pp 1501–1512
5. Fracchia L, Cavallo M, Martinotti MG and Banat IM (2012) Biosurfactants and bioemulsifiers biomedical and related applications – present status and future potentials. In: Ghista DN (ed) Biomedical science, engineering and technology, Chap 14. InTech Open Access Publisher, pp 325–370. ISBN: 978-953-307-471-9
6. Franzetti A, Gandolfi I, Raimondi C, Bestetti G, Banat IM, Smyth TJP, Papacchini M, Cavallo M, Fracchia L (2012) Environmental fate, toxicity, characteristics and potential applications of novel bioemulsifiers produced by *Variovorax paradoxus* 7bCT5. Bioresource Technol 108:245–51
7. Mueller MM, Kugler JH, Henkel M, Gerlitzki M, Hormann B, Pohnlein M, Syldatk C, Hausmann R (2012) Rhamnolipids-next generation surfactants? J Biotechnol 162:366–380
8. Campos JM, Montenegro Stamford TL, Sarubbo LA, de Luna JM, Rufino RD, Banat IM (2013) Microbial biosurfactants as additives for food industries; a review. Biotechnol Prog 29:1097–1108
9. Quinn GA, Maloy AP, Banat MM, Banat IM (2013) A comparison of effects of broad-spectrum antibiotics and biosurfactants on established bacterial biofilms. Curr Microbiol 67:614–623
10. Satpute SK, Banpurkar AG, Dhakephalkar PK, Banat IM, Chopade BA (2010) Methods for investigating biosurfactants and bioemulsifiers: a review. Crit Rev Biotechnol 30:127–144
11. Smyth TJP, Perfumo A, Marchant R, Banat IM (2010) Isolation and analysis of low molecular weight microbial glycolipids. In: Timmis KN (ed) Handbook of hydrocarbon and lipid microbiology, vol 5, part 2, Chap 28. Springer-Verlag, Berlin Heidelberg, pp 3705–3723
12. Van der Vegt W, van der Mei HC, Noordmans J, Busscher HJ (1991) Assessment of bacterial biosurfactant production through axisymmetric drop shape analysis by profile. Appl Microbiol Biotechnol 35:766–770
13. Chandrasekaran EV, Bemiller JN (1980) Constituent analysis of glycosaminoglycans. In: Whistler RL (ed) Methods in carbohydrate chemistry. Academic, New Jersey, pp 89–96
14. Abalos A, Pinazo A, Infante MR, Casals M, Garcia F, Manresa A (2001) Physicochemical and antimicrobial properties of new rhamnolipids produced by *Pseudomonas aeruginosa* AT10 from soybean oil refinery wastes. Langmuir 17:1367–1371
15. Smyth TJP, Perfumo A, McClean S, Marchant R, Banat IM (2010) Isolation and analysis of lipopeptides and high molecular weight biosurfactants. In: Timmis KN (ed) Handbook of hydrocarbon and lipid microbiology, vol 5, part 2, Chap 27. Springer-Verlag, Berlin Heidelberg, pp 3688–3704
16. Bradford MM (1976) A rapid and sensitive method for the quantitation of microgram quantities of protein utilizing the principle of protein-dye binding. Anal Biochem 72:248–254
17. Costa SGVAO, Déziel E, Lépine F (2011) Characterization of rhamnolipid production by *Burkholderia glumae*. Lett Appl Microbiol 53:620–627

Analysis of PHB Metabolism Applying Tn*5* Mutagenesis in *Ralstonia eutropha*

Matthias Raberg, Daniel Heinrich, and Alexander Steinbüchel

Abstract

Transposon mutagenesis presents a powerful and practicable method to generate single-gene disruption mutants of microorganisms. As naturally occurring transposons "jump" within the genome, molecular biology uses plasmid-bound transposons, which randomly disrupt genomic regions of the target organism. Obtained transposon mutants help to elucidate metabolic pathways and to identify essential genes, which are involved in syntheses or degradation of compounds or are important for other cell processes or cell structures. The best-known transposon, Tn*5*, codes for different antibiotic resistances as well as for a transposase mediating transposition and a transposase inhibitor protein. A notable example of applied Tn*5* mutagenesis is the identification and localization of genes, which are involved in the synthesis of the industrially relevant biopolymer poly(3-hydroxybutyrate) (PHB) in *Ralstonia eutropha* H16. PHB is synthesized in a three-step pathway, and the key genes of *R. eutropha* were found to be organized as a single operon. In this chapter, the generation and analysis of Tn*5*-induced mutants of *R. eutropha* is described. This procedure starts with the transfer of the Tn*5*-harboring plasmid pSUP5011 into *R. eutropha* by conjugation, is followed by the screening of mutants defective in PHB accumulation, and is then completed by identifying genes, which have been disrupted by Tn*5* by sequence analyses.

Keywords: Conjugation, PHB metabolism, *Ralstonia eutropha*, Suicide plasmid technique, Tn*5* mutagenesis, Two-step gene walking

1 Introduction

The betaproteobacterium *Ralstonia eutropha* H16 serves as a model organism for H_2- and CO_2-based lithotrophy, as well as the synthesis of the industrially relevant bacterial storage compound poly (3-hydroxybutyrate) (PHB). The metabolically versatile inhabitant of soil and freshwater can gain energy by oxidizing molecular hydrogen or formate and fix CO_2 via the Calvin–Benson–Bassham cycle under autotrophic conditions [1]. Besides heterotrophic utilization of organic acids or fructose, which is catabolized through the Entner–Doudoroff pathway, it is also able to utilize aromatic compounds [2]. In limited presence of another macroelement, e.g., nitrogen, excess carbon is stored as intracellular granule-bound

T.J. McGenity et al. (eds.), *Hydrocarbon and Lipid Microbiology Protocols*, Springer Protocols Handbooks, (2017) 129–148, DOI 10.1007/8623_2015_110, © Springer-Verlag Berlin Heidelberg 2015, Published online: 26 June 2015

PHB, a biodegradable polyester that was first produced commercially by ICI (Zeneca) in 1970 [3]. Synthesis of PHB requires three steps, starting with the condensation of two molecules of acetyl-CoA to acetoacetyl-CoA, which is catalyzed by a betaketothiolase PhaA [4]. Upon the reduction by an NADPH-dependent acetoacetyl-CoA reductase (PhaB) leading to the formation of (*R*)-3-hydroxybutyryl-CoA (3HB-CoA), the PHA synthase PhaC catalyzes the polymerization of the 3HB moieties to PHB [5, 6]. The genes for the three enzymes are located in the PHA-operon *phaCAB* [6–8]. Whereas PhaC is essential for PHA biosynthesis in *R. eutropha* H16, PhaA and PhaB can be replaced by isoenzymes [9, 10]. A second PHA synthase gene was identified within the *R. eutropha* H16 genome sequence project [11], which putatively encodes an additional PHA synthase in this bacterium. However, this *phaC2* annotated gene is obviously not transcribed in H16 [12]. The genome of *R. eutropha* H16 is organized on two chromosomes consisting of 4.1 Mbp (chromosome 1) and 2.9 Mbp (chromosome 2) and the megaplasmid pHG1 (0.5 Mbp). Besides the *phaCAB* operon which is localized on chromosome 1, isologues of *phaA* (15) and *phaB* (39) are spread over the two chromosomes [11].

The genomic organization of the PHB biosynthetic genes of *R. eutropha* H16 was first elucidated in 1988 by applying transposon Tn*5* mutagenesis [6]. Transposable elements (transposons) are fragments of DNA, which usually code for phenotypic markers, as for example, antibiotic resistance genes. Naturally occurring transposons change their position within the genome employing a transposase, which is encoded by the transposon. This mechanism can be exploited in order to generate disruption mutants through transposon-containing plasmids, which are introduced into the respective microorganism.

Tn*5*, which is one of the best characterized transposons, consists of three major segments. The 2,748 base pair (bp) central region of the Tn*5* transposon harbors the three antibiotic resistance genes *kan*, *str*, and *ble* (kanamycin^r, streptomycin^r, and bleomycin^r; [13]). This region is flanked by two nearly identical 1,535 bp sequences referred to as IS*50*L and IS*50*R, of which only IS*50*R codes for an active transposase and a transposase inhibitor both requiring different gene transcription initiation sites [14]. The ratio of transposase to inhibitor proteins determines the rate of transposition. Terminal 9 bp inverted repeats, which act as transposase recognition sites, complete the 5,818-bp-long Tn*5* sequence [15].

Different approaches to determine the location of the transposon insertion are available. The flanking regions of the Tn*5* insertion can directly be amplified and sequenced by applying the two-step gene walking method [16]. In this polymerase chain reaction (PCR)-based technique, a walking primer, which specifically hybridizes with the IS*50*L or the IS*50*R element, is used to amplify the

complimentary single-strand DNA (ssDNA) of the unknown sequence downstream of the IS*50* element. The walking primer then binds nonspecifically to different sites of the generated ssDNA in a second stage with a decreased annealing temperature, which results in double-strand DNA (dsDNA) of different lengths with attached walking primers at the 5′ ends. In the final stage of the PCR, the annealing temperature is raised again to amplify the dsDNA exponentially. The amplified and isolated dsDNA can then be sequenced when using a primer, which binds to the IS*50* element downstream of the walking primer. Employing the BLAST algorithm [17], the position of the Tn*5* and the respective disrupted gene can be directly determined if the organism's genome sequence is known. Furthermore, the function of the respective protein can be analyzed.

Alternatively, the gene, which is disrupted by Tn*5*, can be identified by employing a gene bank of the respective wild-type organism. This method was especially relevant, when PCR methods such as the two-step gene walking approach were not advanced. Gene banks are generated by enzymatically digesting genomic DNA and ligating the resulting fragments into separate vectors, which are then transferred into a host organism, as for example, *Escherichia coli*. This results in a population of different *E. coli* strains, each containing a different DNA fragment of the originating organisms' genomic DNA. The Tn*5*-containing genomic fragment can be obtained by digestion of the mutant DNA with subsequent subcloning of the fragment and isolation of kanamycin-resistant *E. coli* clones. It is important to use a restriction enzyme, which does not cut inside of Tn*5* (e.g., *Eco*RI). By DNA–DNA hybridization of the Tn*5*-inserted fragment with the wild-type gene bank, the original DNA fragment can be identified and sequenced.

In order to identify key genes for certain metabolic or biosynthesis pathways, transposon mutagenesis is superior to other methods as, for example, the use of chemical reagents or radiation, since it leads to mutants showing only single-gene mutations. Moreover, the arrangement of genes within a single operon can be determined, if polar effects prevent transcription of genes, which are located downstream of transposon insertions. However, the benefit of generating single-gene mutants also limits transposon mutagenesis in cases, where multiple isoenzymes catalyze the same reaction step. For example, the analysis of the genome sequence of *R. eutropha* H16 revealed multiple genes coding for isoenzymes of the betaketothiolase PhaA as mentioned above. Consequently, transposon mutants with a PhaA-negative phenotype were not identified [10, 11].

Advances in DNA sequencing during the last decades have further increased the potential of transposon mutagenesis, as widely available genome sequences and genomic maps provide instant and

comprehensive information about disrupted genomic regions. Therefore, Tn*5* mutagenesis is a powerful method for analyzing the genome of various microorganisms up to this day [18, 19]. Furthermore, the application of Tn*5* mutagenesis is not limited to identifying key genes of certain pathways, but can also enhance different biosyntheses. In 2012, Brandt et al. identified Tn*5* mutants of *R. eutropha* H16 with increased PHB synthesis when genes involved in the synthesis of liposaccharides were disrupted. Those mutations apparently lead to an increased uptake of carbon substrates [20].

In this chapter, we describe the procedure of generating, isolating, and characterizing single-gene mutants of *R. eutropha* by Tn*5*::*mob* mutagenesis by using the suicide plasmid pSUP5011 ([21]; Fig. 1). The pSUP5011 plasmid contains a pMBI origin of replication, which is not functional in *R. eutropha*, but leads to replication of the plasmid in the donor strain *E. coli* S17-1. In order to transfer the vector from *E. coli* S17-1 to the recipient *R. eutropha* via conjugation, the plasmid pSUP5011 contains a *mob* site, which codes for a mobilizing protein that breaks the plasmid strand at a specific site. Furthermore, *E. coli* S17-1 was engineered to chromosomally harbor *tra* genes, which encode the formation of a pilus mediating the transfer of the 10-kbp plasmid to the acceptor cell [22]. As the plasmid itself cannot replicate in *R. eutropha*, only cells in which Tn*5* has transposed into the genome are viable in the

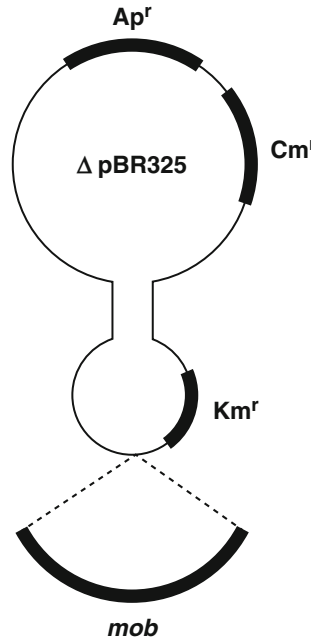

Fig. 1 Schematic structure of plasmid pSUP5011 [21]. For details, see text

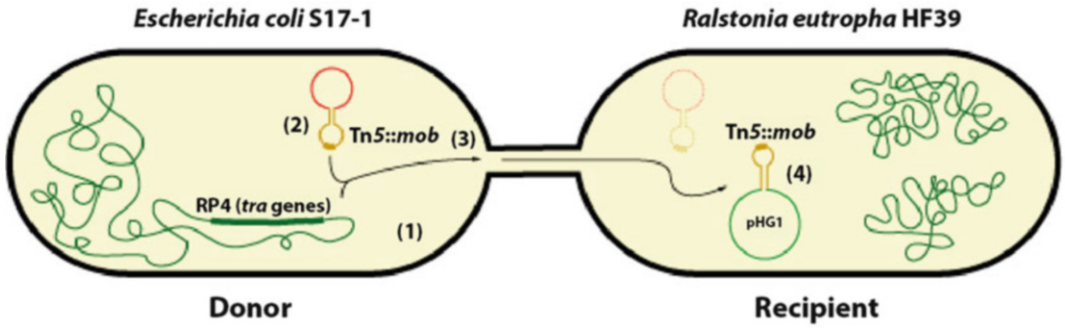

Fig. 2 Schematic representation of Tn*5* mutagenesis in *R. eutropha*. (1) Synthesis of proteins necessary for conjugation. (2) Transfer of suicide plasmid pSUP5011 from *E. coli* S17-1 (donor) to *R. eutropha* HF39 (recipient), which is not replicated in *R. eutropha* (3) and is therefore lost during cell division. (4) Integration of Tn*5* into the genome (here: megaplasmid pHG1) (Fig. 2 which is based on data previously provided by [23] and an illustration by [22] was adapted and modified from [24])

presence of kanamycin. After cultivating the donor and recipient cells, a spot mating is carried out with concentrated cell suspension on an agar plate to allow plasmid transfer via conjugation ([23]; Fig. 2). In order to isolate Tn*5*-induced mutants of *R eutropha* after the spot mating, dilutions of the cells are plated onto selective media. In this applied protocol, the strain *R. eutropha* HF39 is used, as it is resistant to higher concentrations of streptomycin [25]. Therefore, cells of *R. eutropha* HF39 can grow on streptomycin-containing solid media that prevents the streptomycin-sensitive donor *E. coli* S17-1 from growing. Furthermore, the medium contains kanamycin so that only Tn*5* mutants of *R. eutropha* HF39 are viable. With respect to the PHB metabolism and its biosynthesis route, the phenotype and genotype of generated Tn*5* mutants are then analyzed. For this, cells are cultivated on different solid media, including a medium, which promotes PHB accumulation (reduced nitrogen) to screen for phenotypes. Thereby PHA-"leaky" or PHA-negative phenotypes can be recognized by observing the opacity of the colonies. The location of the Tn*5* insertion of several mutants is then determined by the two-step gene walking method.

2 Materials

2.1 Cultivation of the Recipient

1. Strain: *Ralstonia eutropha* HF39 (DSM 15444).
2. Sterile saline: (*see* Sect. 2.11).
3. Growth media: Nutrient broth (NB) medium (*see* Sect. 2.12), liquid and solid media.
4. Antibiotics: Streptomycin (500 µg/ml) (*see* Sect. 2.11).

2.2 Cultivation of the Donor

1. Strain: *Escherichia coli* S17-1 (pSUP5011) (DSM 5167).
2. Sterile saline: (*see* Sect. 2.11).
3. Growth media: Lysogeny broth (LB) medium (*see* Sect. 2.12), liquid and solid media.
4. Antibiotics: Kanamycin (50 μg/ml) (*see* Sect. 2.11).

2.3 Cell Harvest

1. Sterile saline: (*see* Sect. 2.11).
2. 50 ml reaction tubes.

2.4 Conjugation

1. NB agar plates (*see* Sect. 2.12).

2.5 Selection of Transconjugants

1. Sterile saline: (*see* Sect. 2.11).
2. NB agar plates supplemented with kanamycin (300 μg/ml) and streptomycin (500 μg/ml) (*see* Sects. 2.11 and 2.12).
3. 50-ml reaction tubes.

2.6 Identification of Mutants of Interest

1. Nile red-containing mineral salt medium (MSM) agar plates with 0.5% (w/v) fructose and reduced nitrogen content (0.02% [w/v], NH_4Cl) (*see* Sects. 2.11 and 2.12).
2. NB agar plates with kanamycin (300 μg/ml) and streptomycin (500 μg/ml) (*see* Sects. 2.11 and 2.12).

2.7 Screening of Mutants

1. NB agar plates with kanamycin (300 μg/ml) and streptomycin (500 μg/ml) (*see* Sects. 2.11 and 2.12).

2.8 Phenotypic Characterization of Mutants

1. 1.5 ml reaction tubes.
2. Sterile saline: (*see* Sect. 2.11).
3. Nile red-containing mineral salt medium (MSM) agar plates with 0.5% (w/v) fructose and reduced nitrogen content (0.02 % [w/v], NH_4Cl) (*see* Sects. 2.11 and 2.12).

2.9 Selection of Mutants for Determination of Tn*5* Insertion Loci

1. Phase contrast microscope.
2. Microscope slides, cover glasses, and immersion oil.

2.10 Genomic Characterization for Determination of Tn*5* Insertion Loci

1. Growth media: Nutrient broth (NB) medium with kanamycin (300 μg/ml) and streptomycin (500 μg/ml) (*see* Sects. 2.11 and 2.12).
2. 1.5-ml reaction tubes.

2.10.1 Isolation of Genomic DNA (gDNA)

3. Isolation of gDNA: Apply an appropriate extraction kit, for example, "NucleoSpin® Tissue" kit, Macherey-Nagel, #740952.50.

2.10.2 Two-Step Gene Walking

1. Walking PCR: BioMix™ (Bioline GmbH, Luckenwalde, Germany, #BIO-25012). Walking primer "IS50 walking": 5′-TCG GCC GCA CGA TGA AGA GC-3′.

2.10.3 Agarose Gel Electrophoresis

1. TBE buffer: Tris (50 mM), boric acid (50 mM), disodium ethylenediaminetetraacetate (EDTA) (2.5 mM). Prepare at least 2 l of buffer.
2. Loading dye: EDTA (50 mM), sucrose (50 % [w/v]), bromophenol blue (0.1 % [w/v]).

2.10.4 Sequencing

1. Removal of walking primers: Apply an appropriate extraction kit, for example, "GeneJET Gel Extraction and DNA Cleanup Micro Kit," Thermo Scientific, # K083.
2. IS50 sequencing primer: 5′-CGT TAC CAT GTT AGG TCA CAT GG-3′.

2.11 General Buffers and Reagents

1. Sterile saline: 0.9 % (w/v) NaCl; sterilize by autoclaving or by filtration.
2. Streptomycin stock solution: 500 mg/ml streptomycin sulfate in $H_2O_{demin.}$; sterilize by filtration.
3. Kanamycin stock solution: 150 mg/ml kanamycin sulfate in $H_2O_{demin.}$; sterilize by filtration.
4. Nile red stock solution: 0.25 mg/ml Nile red in dimethyl sulfoxide (DMSO); Add to solid media to a final concentration of 0.5 μg/ml.
5. Fructose stock solution: 40% (w/v) in $H_2O_{demin.}$; sterilize by filtration. Add to MSM to a final concentration of 0.5 % (w/v).

2.12 Bacteria Growth Media

These may be purchased from any supplier of common bacterial growth medium components or prepared media:

1. Nutrient broth (NB) medium: 5 g peptone, 3 g meat extract/l $H_2O_{demin.}$; for solid media, add 1.5% (w/v) agar. Sterilize by autoclaving.
2. Lysogeny broth (LB) medium [26]: 10 g tryptone, 5 g yeast extract, 10 g NaCl/l $H_2O_{demin.}$; for solid media, add 1.5% (w/v) agar. Sterilize by autoclaving.
3. Mineral salt medium (MSM) [27] agar plates: Mineral salt component and agar component have to be autoclaved separately (*see* **Note** 4). Unify both components when cooled to 50°C. Then add sterilized carbon source and if required antibiotics and Nile red.

Mineral salt component		
$Na_2HPO_4 \times 12\ H_2O$	9.0	g
KH_2PO_4	1.5	g
NH_4Cl	0.2	g
$MgSO_4 \times 7\ H_2O$	0.2	g
$CaCl_2 \times 2\ H_2O$	0.02	g
Fe(III)NH_4 citrate	1.2	mg
Trace element solution SL6 (10,000-fold)	0.1	ml
$H_2O_{demin.}$	ad 500	ml, pH 6.9
SL6 (10,000-fold)		
$ZnSO_4 \times 7\ H_2O$	0.1	g
$MnCl_2 \times 4\ H_2O$	30	mg
H_3BO_3	0.3	g
$CoCl_2 \times 6\ H_2O$	0.2	g
$CuCl_2 \times 2\ H_2O$	10	mg
$NiCl_2 \times 6\ H_2O$	20	mg
$Na_2MoO_4 \times 2\ H_2O$	30	mg
$H_2O_{demin.}$	ad 100	ml
Agar component		
Agar	15	g
H_2O_{demin}	ad 500	ml

3 Methods

The protocol below provides a detailed description of all necessary laboratory steps to conduct a transposon mutagenesis in *Ralstonia eutropha* including a precise timetable of the daily experimental setup. In this chapter, transposon Tn*5* will be transferred by a suicide plasmid (pSUP5011) from *Escherichia coli* S 17-1 to *R. eutropha* HF39 via conjugation in order to cause transposon-induced mutations in *Ralstonia*'s genome. In the second step, transconjugants showing defects in PHB biosynthesis should be identified and analyzed at a molecular level applying the two-step gene walking method.

In preparation for the experiments, both strains are suspended in sterile saline and spread on NB solid media containing 500 μg/ml streptomycin (*R. eutropha*) or LB solid containing 50 μg/ml kanamycin (*E. coli*) (*see* Sects. 2.11 and 2.12). These agar plates are incubated for 1–2 days at 30°C (*R. eutropha*) or 37°C (*E. coli*), respectively, and stored at 4°C until further use.

3.1 Cultivation of the Recipient (Day 1)

Inoculate four 100 ml Erlenmeyer flasks (preferably baffled) filled with 10 ml liquid NB medium (500 μg/ml streptomycin) (*see* Sects. 2.11 and 2.12) with single colonies of *R. eutropha* HF39 (*see* Sect. 2.1) and incubate for 20 h at 30°C on a rotary shaker (~120 rpm).

3.2 Cultivation of the Donor (Day 1)

Inoculate four 100 ml Erlenmeyer flasks filled with 10 ml liquid LB medium (50 μg/ml kanamycin) (*see* Sects. 2.11 and 2.12) with single colonies of *E. coli* S 17-1 (pSUP5011) (*see* Sect. 2.2) and incubate for 15 h at 30°C on a rotary shaker (~120 rpm).

3.3 Cell Harvest (Day 2)

Cells of the donor and the recipient are harvested by centrifugation in sterile 50 ml tubes:

1. Centrifuge culture broth of donor and the recipient (15 min, 3,500 × *g*, 4°C).
2. Discard the supernatant.
3. Suspend cell pellets in 1 ml saline solution (*see* Sect. 2.11). Donor or recipient aliquots, respectively, may be combined in one tube each.

3.4 Conjugation (Mating, Day 2)

1. Place five (relatively thick) NB agar plates (mating plates) on the bench.
2. Unite donor and recipient by successively dripping 0.2 ml donor suspension, then 0.2 ml of the recipient suspension in the middle of each plate to allow conjugative plasmid transfer (*see* **Note** 1).
3. Transfer the mating plates carefully to the incubator avoiding diffluence of the suspensions and incubate at 30°C overnight (*see* **Note** 2).
4. Also prepare two control plates solely with 0.2 ml donor suspension or 0.2 ml recipient suspension, respectively.

3.5 Selection of Transconjugants (Day 3)

In order to discriminate transconjugants of *R. eutropha*, which have successfully received transposon Tn*5* from *E. coli* S 17-1 via suicide plasmid pSUP5011, from donor cells and nonconjugated recipient cells, cells have to be washed from the mating plates and transferred to selective NB solid medium harboring kanamycin as well as streptomycin. Exclusively transconjugants are able to grow on these agar plates as strain *R. eutropha* HF39 is mutatively streptomycin resistant while the integrated Tn*5* mediates kanamycin resistance. In contrast, growth of donor cells is repressed although Tn*5* harbors a streptomycin resistance gene. However, this streptomycin resistance gene is expressed in *E. coli* only at a very low level. Therefore, also donor cells harboring Tn*5* cannot survive the applied high streptomycin concentration of 500 μg/ml:

1. Suspend/wash the cell layer from the middle of the mating plates with 3 ml sterile saline.
2. Transfer cell suspension to sterile reaction tubes with lid (*see* **Note** 3).
3. Evenly spread 0.1 ml of cell suspensions using a sterilized spreader rod over the complete surface of NB agar plates which contain 300 μg/ml kanamycin and 500 μg/ml streptomycin until all of the liquid is absorbed by the agar plate.

4. Incubate the agar plates at 30°C for 2 to 3 days at the maximum. Thereafter, the cells must be subjected to the next step, or the agar plates can be stored for a limited time (1 week at the maximum) in the refrigerator.

Prepare as much plates as possible from these mating solutions. For the controls, one plate is sufficient for each.

3.6 Identification of Mutants of Interest (Day 5–6)

After 2 or 3 days of incubation, a distinct colony-forming unit (cfu) should be apparent on the selective NB agar plates while no growth is expected on the control plates (*see* **Note** 6). Each cfu represents cells of an individual transconjugant which had received pSUP5011 by conjugation and actually harbors transposon Tn*5* its genome. In order to identify mutants with defects in PHB synthesis, cells from a large number of transconjugant colonies should be transferred in an ordered manner on two different solid media (*see* Sects. 2.11 and 2.12):

1. Nile red-containing mineral salt medium (MSM) agar plates with 0.5% (w/v) fructose and reduced nitrogen content (0.02 % [w/v], NH_4Cl).
2. NB agar plates with kanamycin (300 μg/ml) and streptomycin (500 μg/ml).

Application of Nile red and nitrogen limitation allows an in vivo staining of PHB (*see* **Note** 7). It is advantageous to perform the transfer applying a picking scheme as provided in Fig. 3.

1. Print two colony transfer ("picking") arrays (Fig. 3) on one paper sheet.

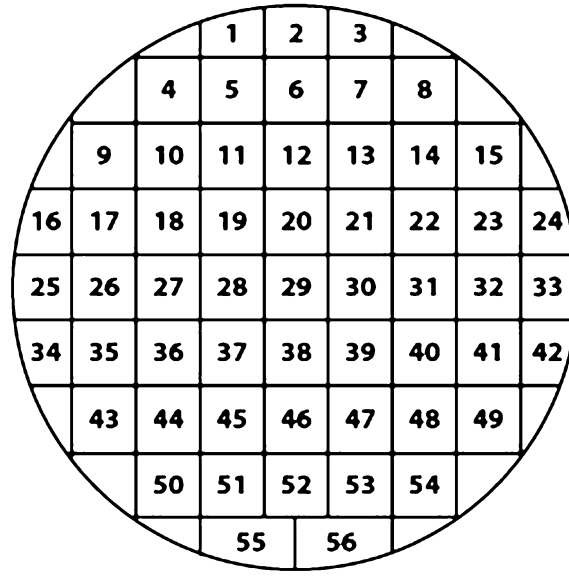

Fig. 3 "Picking" array to transfer mutants onto selective media in an ordered manner

2. Place one of the abovementioned Nile red-containing mineral salt medium (MSM) agar plates (left) and one of the selective NB agar plates (right) on top of the schemes.
3. Mark the plates similarly in relation to their orientation to ensure transfer colonies on the same location on both plates.
4. Take little cell material from one cfu with a sterile toothpick and streak out (approximately 5 mm long), first on the MSM agar plate and then on the NB agar plate (*see* **Note** 5).
5. Continue and transfer cells from as much cfu as possible as the picking scheme allows on both plates.
6. Incubate the agar plates at 30°C for 2 to 3 days.

This procedure is essential to generate sorted patterns with identical orientation of each transconjugant on both plates to allow subsequent comparison of mutants.

3.7 Screening of Mutants (Day 8)

Screen the agar plates for mutants which are putatively impaired in PHB biosynthesis. Such mutants appear translucent on Nile red-containing agar plates with reduced nitrogen content. Additionally, check Nile red plates under UV light (312 nm) for fluorescence: Nile red accumulates in PHB granules stored in the cells, so only PHB-accumulating cells can show fluorescence. Mutants of interest with impaired or disabled PHB synthesis will show lower or no fluorescence at all. Prepare purity plates (Fig. 4) for these mutants on NB agar plates with kanamycin (300 µg/ml) and streptomycin (500 µg/ml). Incubate the agar plates at 30°C for 2 days.

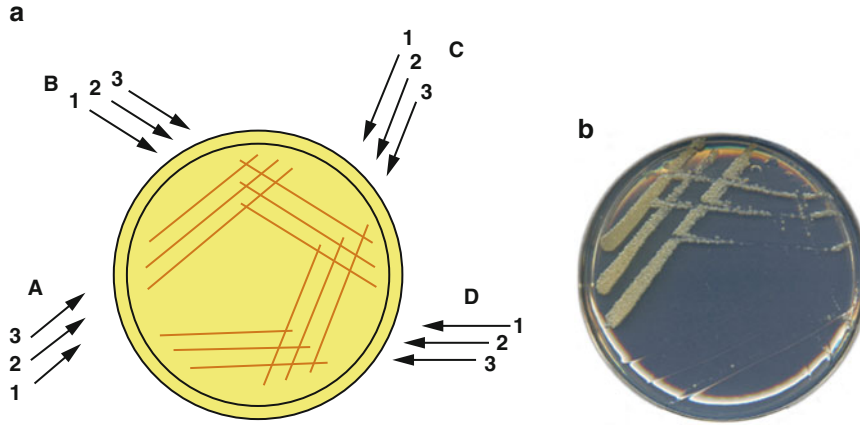

Fig. 4 Technique to gain isolated colonies by successive threefold streaking. (**a**) Schematic presentation: Take cell material with a sterile inoculation loop from one cfu and streak it threefold on the agar plate (**a**). Continue with strokes B, C, and D as shown in the scheme. Do not forget to burn out the inoculation loop for sterilization after the three A strokes, B strokes, and C strokes, respectively. (**b**) Agar plate showing isolated colonies of *R. eutropha* obtained by applying mentioned technique and incubation of 2 days at 30°C

3.8 Phenotypic Characterization of Mutants (Day 10)

Prepare sectorial strokes from purified mutants on Nile red containing MSM agar plates with reduced nitrogen content:

1. Suspend 1 cfu of each mutant's purity plate in 100 µl sterile saline in sterile 1.5 ml reaction tubes.
2. Spread the suspensions in triangle shapes onto the plates employing an inoculation loop. Do not forget to flame the inoculation loop for sterilization before continuing.
3. Include strain HF 39 as reference.
4. Incubate the agar plates at 30°C for 2 days.

3.9 Selection of Mutants for Determination of Tn5 Insertion Loci (Day 12)

Conduct a final analysis of the mutants:

1. Accurately compare phenotypes on the agar types (Fig. 5) and observe noticeable mutants in the phase contrast of a light microscope (Fig. 6) in comparison to control strain HF39 (*see* **Note** 8). Are PHB granules detectable?
2. Select mutants with an obvious defect in PHB synthesis for further genomic characterization.

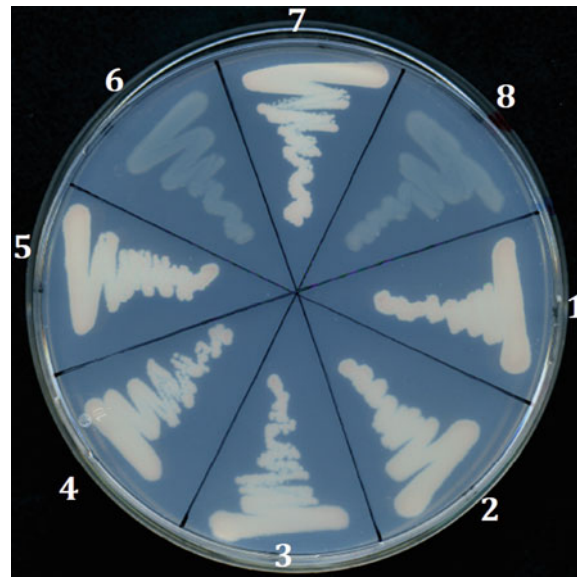

Fig. 5 Screening for mutants impaired in PHB biosynthesis. Investigated strains were spread as sectorial strokes from purified mutants on Nile red-containing MSM agar plates with reduced nitrogen content. Strains 6 and 8 appear translucent and therefore show clear PHB-negative phenotypes. All other tested strains are not impaired in PHB biosynthesis but store significant amounts of PHB as indicated by their reddish opaque phenotype

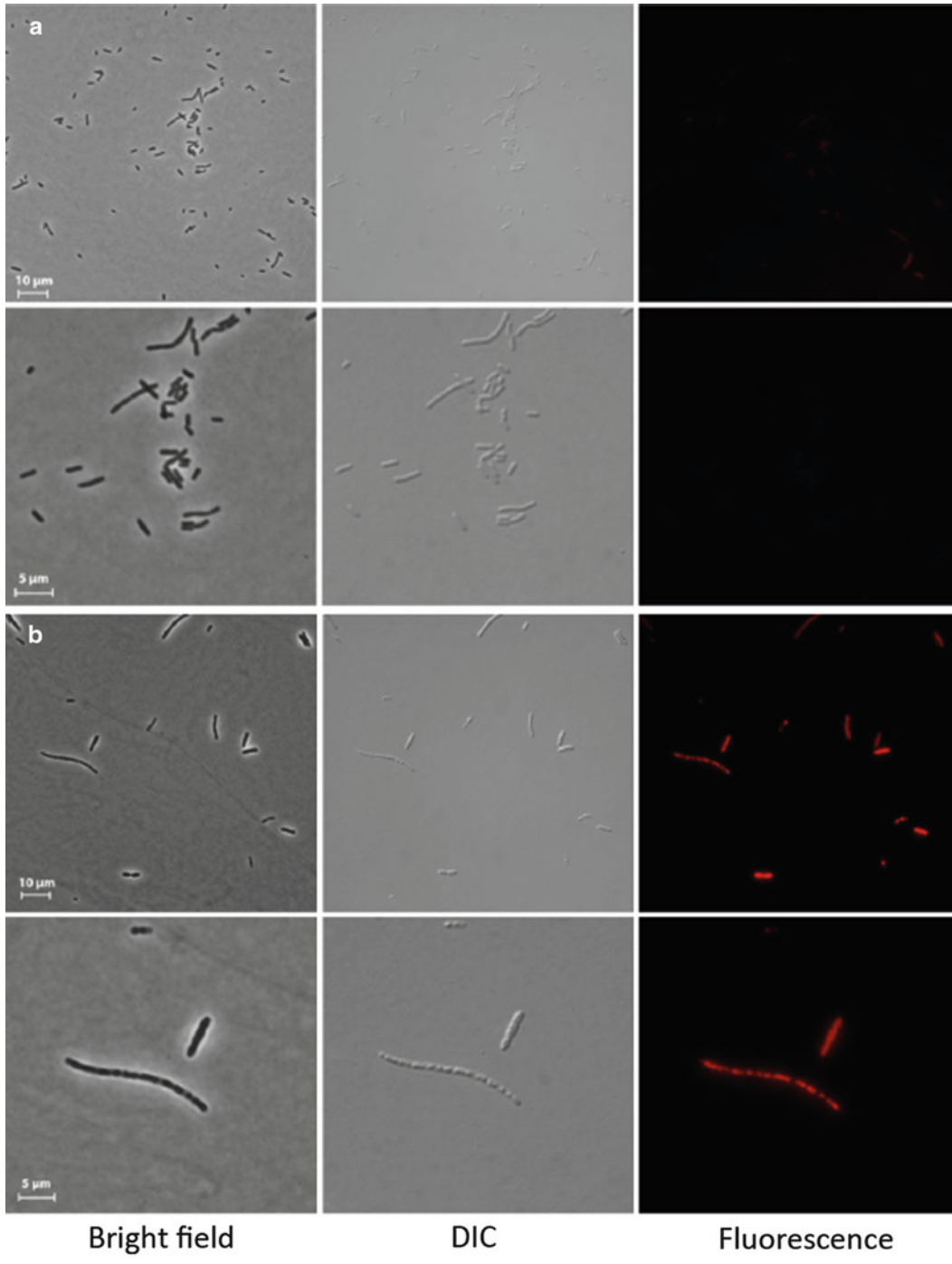

Fig. 6 Microscopic pictures of PHB-negative Tn*5* mutant (**a**) and a *R. eutropha* HF39 control strain (**b**). *Left*, bright field; *Middle*, differential interference contrast (DIC); *Right*, fluorescent light ($\lambda = 234$ nm). Cells were cultivated for 48h in MSM media (*see* Sect. 2.12). For both strains, samples of 200 µl were diluted 1:10 with saline and incubated with 4 µl of Nile red solution (*see* Sect. 2.11) for 30 min on ice. Cells were fixed on the microscope slides with 100 µl of agarose (1% [w/v])

3.10 Genomic Characterization for Determination of Tn*5* Insertion Loci (Day 12–14)

At first, genomic DNA (gDNA) of selected mutants is isolated. Samples of these gDNAs serve as templates for the "two-step gene walking" method [16]. This technique is based on a randomly primed polymerase reaction and comprises only two major steps: (1) a walking PCR with a single specific outward pointing primer (**step 1**) and the (2) direct sequencing of its product using a nested specific primer (**step 2**) which is shown in Fig. 7 (*see* **Note** 10). Finally, the precise insertion loci of Tn5::*mob* can be determined by sequence comparison with *Ralstonia*'s genome via BLAST search (*see* **Note** 11).

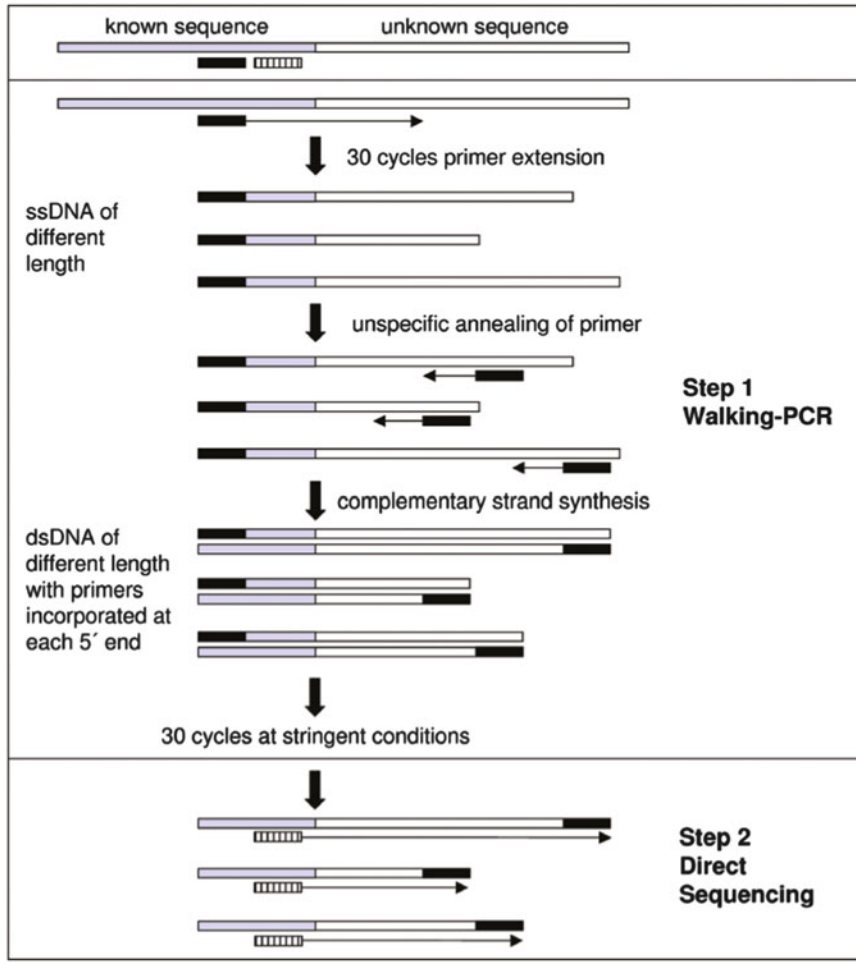

Fig. 7 Basic principle of the two-step gene walking procedure. The known sequence stretch is shown in gray; unknown sequence stretches are shown in white; the walking PCR primer is shown in black; the specific nested sequencing primer is shown as striped. During the first 30 cycles, the PCR primer binds at stringent conditions and specific ssDNA of different length (caused by different drop-off sites of polymerase) is produced. One subsequent cycle at low annealing temperature allows unspecific binding of primer at different sites on ssDNA as reverse primer. dsDNA of different length with primer sequence incorporated at each 5-prime end is produced. Thirty cycles at stringent conditions specifically and exponentially amplify dsDNA. The PCR product is sequenced directly by using a specific nested primer. Taken from [16]

3.10.1 Isolation of gDNA (Day 12–13)

1. For each mutant, inoculate one Erlenmeyer flask filled with 20 ml of NB medium (containing 300 μg/ml kanamycin and 500 μg/ml streptomycin) from cells of 1 cfu.
2. Incubate overnight at 30°C on a rotary shaker.
3. Harvest cells by repeated centrifugation steps in 1.5 ml reaction tubes (5 min, 16,000 × *g*, 4°C).
4. Isolate gDNA applying a commercially available DNA extraction kit according to the manufacturer's instructions (*see* Sect. 2.10.1).
5. Check successful gDNA isolation with a UV-vis spectrophotometer following the instructions of the manufacturer. Determine the concentration of gDNA samples and calculate the volume corresponding to 50 ng gDNA which is the amount needed for walking PCR. If necessary, dilute gDNA samples.

3.10.2 Two-Step Gene Walking (Day 13)

1. Pipette and mix the following samples into 200 μl PCR tubes (*see* Sect 2.10.2):

Biomix (Bioline GmbH, Luckenwalde, Germany)	15 μl
Walking primer (10 μM)	3 μl
DNA template (50 ng)	×μl
H_2O	ad 30 μl

2. Conduct the walking PCR according to the cycling program mentioned below:

Round	Cycles	Temperature (°C)	Time	Action
		94	4 min	Primary denaturation
1	30	94 56 72	30 s 30 s 2 min	Specific primer extension; ssDNA synthesis
2	1	94 40 72	30 s 30 s 2 min	Unspecific binding of primer; dsDNA synthesis
3	30	94 56 72	30 s 30 s 2 min	Specific exponential amplification
		72	10 min	Final elongation

3.10.3 Agarose Gel Electrophoresis (Day 13)

To control the products of the walking PCR, analyze aliquots of the reaction mix after cycling via agarose gel electrophoresis:

1. Prepare an agarose gel (1% agarose [w/v] in TAE buffer, boiled up; *see* Sect. 2.10.3) in an electrophoresis chamber.
2. Mix 3 µl walking PCR sample each with 2 µl loading dye (*see* Sect. 2.10.3).
3. Transfer samples to the agarose gel
4. Run gel at 140 V
5. Stain with ethidium bromide
6. Analyze and document walking PCR product patterns under UV light (*see* **Notes** 9 and 10).

Remove primers from the residual walking PCR aliquots applying a Gene Clean kit (*see* Sect. 2.10.3) according to the manufacturer's instructions (*see* **Note** 10).

3.10.4 Sequencing (Day 14)

Carry out direct sequencing at a company providing commercial DNA sequencing:

1. For each mutant, mix a required aliquot of purified walking PCR products (usually 5–10 µl) with the specific unmodified nested primer (*see* Sect. 2.10.4) according to the provider's instructions and send it to the company.
2. Analyze received nucleotide sequences via BLAST search (http://www.ncbi.nkm.nih.gov/BLAST/).
3. Determine Tn*5* insertion loci in comparison to *Ralstonia*'s genome (*see* **Notes** 11 and 12).

4 Notes

1. Ad 2.4/3.4: It is favorable to have a donor-to-recipient cell ratio of 1:1 in the mating process. For this, the optical densities of the overnight cultures of *E. coli* S17-1 and *R. eutropha* HF39 can be adjusted by sterile saline.
2. Ad 3.4: To ensure fast absorption of bacteria suspensions and to gain a concentrated spot with efficient donor/recipient contact, it is highly recommended to apply thick agar plates, which have been left to dry at room temperature for 2 days prior to the spot mating. To additionally prevent the spot mating from flowing all over the agar, it might be helpful to incubate the opened plate under the laminar flow or near the Bunsen burner for 30 min to allow drying of the spot suspension before carrying the plate to the incubator.
3. Ad 2.5/3.5: The easiest way to wash the cells from the mating agar plates is to incline the respective plate while carefully

splashing the saline against the cell layer on the mating plate with a pipette. Suck the rinsed fluid from the bottom of the plate back into the pipette tip and splash the solution against the cell layer again. Repeat this procedure till the entire cell layer has been suspended in the saline.

4. Ad 2.12: To avoid precipitation of agar components with the mineral salts, the solid MSM should be autoclaved in two separate parts of equal volumes: (1) a flask containing the agar and (2) a flask containing the medium component. Both parts therefore contain the twofold component concentration of the final medium. Sugars should be sterile filtered and added separately to the medium. This also applies to antibiotics, which should be added after the agar is warm to the touch as most of them are sensitive to heat.
5. Ad 2.6/3.6: It is favorable to burn the tips of the toothpicks with a Bunsen burner before first use. Doing so, the toothpick tips get round ends which do not scratch the agar plate surface. Afterwards, toothpicks are vertically packed into small beakers, covered with aluminum foil, and autoclaved. After sterilization, toothpicks should be stored for at least one hour for drying at 60°C.
6. Ad 2.6/3.6: It must be noted that the rich NB medium accounts for much quicker growth as compared to the defined MSM, which is why it might take a day longer for colonies of *R. eutropha* to appear on MSM plates. As stated above, a large number of generated mutants should be screened in order to obtain a significant percentage distribution of mutants. As the *R. eutropha* genome comprises 7.7 Mbp with an average target gene size of 1.2 kbp, the probability of Tn*5* disrupting a certain gene of interest is 0.016%, which results in approximately only one desired mutant of 6,250 transconjugants showing a certain genotype.
7. Ad 2.6/3.6: Nile red presents a favorable compound to stain lipophilic substances. Therefore, staining with Nile red to monitor PHB accumulation of cells is quite sensitive. As other lipophilic compounds can be stained as well, it is essential to avoid too long Nile red incubation and exposure time under the microscope. Otherwise, even cell membranes may fluoresce so that false-positive results are possible. This is even more severe if this method is applied to gram-positive bacteria.
8. Ad 3.9: The microscopic observation of *R. eutropha* cells is crucial to ensure that the right cells are isolated after the spot mating and also provides impressive images of the PHB producer. PHB-synthesizing cells of *R. eutropha* are rod shaped and usually contain between eight and 13 granules. If cells are stained with Nile red, only the PHB granules should appear when viewed under the fluorescence microscope. This requires adequate staining of the cells (*see* Sect. 2.11).

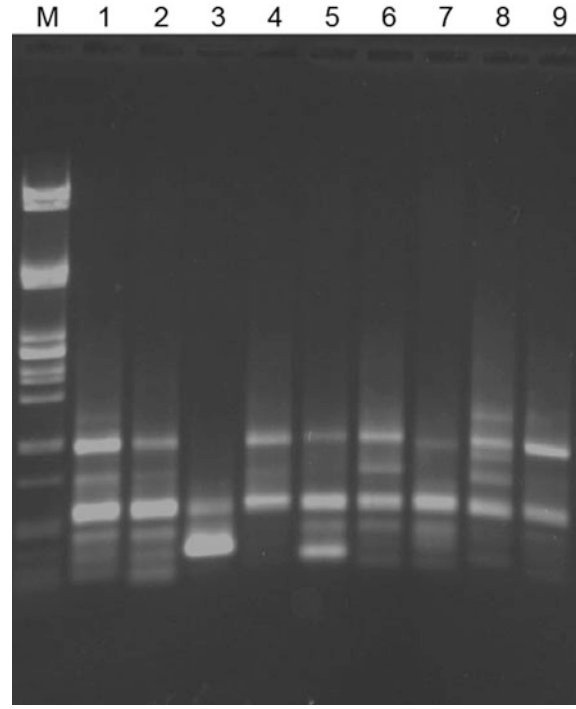

Fig. 8 Analysis of walking PCR via agarose gel electrophoresis. The gel picture shows typical walking PCR product patterns. Aliquots of 3 μl of different PCR samples and 2 μl of loading dye were separated in 1% (w/v) agarose with TBE buffer. Marker (lane M) shows λ DNA/*Pst*I-ladder for determination of fragment lengths

9. Ad 3.10.3: Only samples, which show distinct fragments as in lanes 1–9 in the gel picture (Fig. 8), are purified and subjected to sequence analysis (3.10.4). Discard samples showing smear or weak signals in the gel.
10. Ad 3.10.3: In order to view the result of the two-step gene walking PCR, only 3 μl of the sample needs to be subjected to agarose gel electrophoresis. The remaining part of the sample can be directly mixed with the binding buffer of the respective commercial gel extraction kit and transferred onto the column for the first centrifugation step. The manufacturer's protocol can then be followed as if the DNA was extracted from the gel matrix.
11. Ad 3.10.4: While using the BLAST algorithm, certain statistical rules of thumb should be kept in mind. A significant sequence similarity requires a maximum identity value of at least 30%. Depending on the sequence length, the e-value should be as low as possible ($\leq$ e-50 for sequences longer than 300 bp) in order to minimize the probability of a random alignment result.

12. Ad 3.10.4: Mutants, which are not able to grow on MSM agar plates, will appear at a relatively high frequency. These mutants display an auxotrophy, a phenotype which is not in the focus of this book chapter. A smaller number will show a PHB-"leaky" phenotype. Only very few of the *R. eutropha* mutants will be PHB negative (*see* **Note** 6). In all cases, PHA-negative mutants should show a disruption of the *phaC1* gene, since the second gene coding for a PHA synthase, *phaC2*, codes for an inactive enzyme. As there are numerous isoenzymes of PhaA and PhaB in *R. eutropha*, disruptions of their respective genes will not be noticed phenotypically. PHB-"leaky" mutants will harbor mutations in different genes, which do not code for the three proteins involved in the PHB synthesis pathway (PhaCAB) but indirectly influence accumulation of PHB.

References

1. Bowien B, Schlegel HG (1981) Physiology and biochemistry of aerobic hydrogen oxidizing bacteria. Annu Rev Microbiol 35:405–452
2. Wilde E (1962) Untersuchungen über Wachstum und Speicherstoffsynthese von *Hydrogenomas eutropha*. Arch Mikrobiol 43:109–137
3. Anderson AJ, Dawes AE (1990) Occurrence, metabolism, metabolic role, and industrial uses of bacterial polyhydroxyalkanoates. Microbiol Rev 54:450–472
4. Oeding V, Schlegel HG (1973) β-Ketothiolase from *Hydrogenomonas eutropha* H16 and its significance in the regulation of poly-β-hydroxybutyrate metabolism. Biochem J 134:239–248
5. Haywood GW, Anderson AJ, Chu L, Dawes EA (1988) The role of NADH- and NADPH-linked acetoacetyl-CoA reductases in the poly-3-hydroxybutyrate synthesizing organism *Alcaligenes eutrophus*. FEMS Microbiol Lett 52:259–264
6. Schubert PA, Steinbüchel A, Schlegel HG (1988) Cloning of the *Alcaligenes eutrophus* genes for synthesis of poly-β-hydroxybutyrate. J Bacteriol 170:5837–5847
7. Peoples OP, Sinskey AJ (1989) Poly-β-hydroxybutyrate biosynthesis *in Alcaligenes eutrophus* H16. Characterization of the genes encoding β-ketothiolase and acetoacetyl-CoA reductase. J Biol Chem 263:15293–15297
8. Peoples OP, Sinskey AJ (1989) Poly-β-hydroxybutyrate biosynthesis in *Alcaligenes eutrophus* H16. Identification and characterization of the PHB polymerase gene (*phbC*). J Biol Chem 264:15298–15303
9. Slater T, Houmiel KL, Tran M, Mitsky TA, Taylor NB, Padgette SR, Gruys KJ (1998) Multiple β-ketothiolases mediate poly(β-hydroxyalkanoate) copolymer synthesis in *Ralstonia eutropha*. J Bacteriol 180:1979–1987
10. Lindenkamp N, Peplinski K, Volodina E, Ehrenreich A, Steinbüchel A (2010) Impact of multiple β-ketothiolase deletion mutations in *Ralstonia eutropha* H16 on the composition of 3-mercaptopropionic acid-containing copolymers. Appl Environ Microbiol 76:5373–5382
11. Pohlmann A, Fricke WF, Reinecke F, Kusian B, Liesegang H, Cramm R, Eitinger T, Ewering C, Pötter M, Schwarz E, Strittmatter A, Voss I, Gottschalk G, Steinbüchel A, Friedrich B, Bowien B (2006) Genome sequence of the bioplastic-producing "Knallgas" bacterium *Ralstonia eutropha* H16. Nat Biotechnol 10:1257–1262
12. Peplinski K, Ehrenreich A, Döring C, Bömeke M, Reinecke F, Hutmacher C, Steinbüchel A (2010) Genome-wide transcriptome analyses of the "Knallgas" bacterium *Ralstonia eutropha* H16 with regard to polyhydroxyalkanoate metabolism. Microbiology (SGM) 156:2136–2152
13. Genilloud O, Garrido MC, Moreno F (1984) The transposon Tn*5* carries a neomycin-resistance determinant. Gene 32:225–233
14. Lowe JB, Berg DE (1983) A product of the Tn*5* transposase gene inhibits transposition. Genetics 103:603–615
15. Berg DE, Johnsrud L, McDivitt L, Ramabhadran R, Hirschel BJ (1982) Inverted repeats of

Tn*5* are transposable elements. Genetics 79:2632–2635

16. Pilhofer M, Bauer AP, Schrallhammer M, Richter L, Ludwig W, Schleifer KH, Petroni G (2007) Characterization of bacterial operons consisting of two tubulins and a kinesin-linke gene by the novel two-step gene walking method. Nucleic Acids Res 35, e135
17. Altschul SF, Madden TL, Schäffer AA, Zhang J, Zhang Z, Miller W, Lipman DJ (1997) "Gapped BLAST and PSI-BLAST": a new generation of protein database search programs. Nucleic Acid Res 25:3389–3402
18. Schürmann M, Wübbeler JH, Grote J, Steinüchel A (2011) Novel Reaction of succinyl coenzyme A (Succinyl-CoA) synthetase: Activation of 3-sulfinopropionate to 3-sulfinopropionyl-CoA in *Advenella mimigardefordensis* strain DPN7^{T} during degradation of 3,3′-dithiodipropionic acid. J Bacteriol 193:3078–3089
19. Deng Y, Nagachar N, Xiao C, Tien M, Kao TH (2013) Identification and characterization of non-cellulose-producing mutants of *Gluconobacter hansenii* generated by Tn*5* transposon mutagenesis. J Bacteriol 195:5072–5083
20. Brandt U, Raberg M, Voigt B, Hecker M, Steinbüchel A (2012) Elevated poly(3-hydroxybutyrate) synthesis in mutants of *Ralstonia eutropha* H16 defective in lipopolysaccharide biosynthesis. Appl Microbiol Biotechnol 95:471–483
21. Simon R (1984) High frequency mobilization of gram-negative bacterial replicons by the in vitro constructed Tn*5*-Mob transposon. Mol Gen Genet 196:413–420
22. Simon R, Priefer U, Pühler A (1983) A broad host range mobilization system for in vivo genetic engineering: Transposon mutagenesis in Gram-negative bacteria. Biotechnology 1:784–791
23. Friedrich B, Hogrefe C, Schlegel HG (1981) Naturally occurring genetic transfer of hydrogen-oxidizing ability between strains of *Alcaligenes eutrophus.* J Bacteriol 147:198–205
24. Steinbüchel A, Oppermann-Sanio FB, Ewering C, Pötter M (2013) Mikrobiologisches Praktikum. Springer Verlag, Berlin
25. Srivastava S, Urban M, Friedrich B (1982) Mutagenesis of *Alcaligenes eutrophus* by insertion of the drug-resistance transposon Tn*5.* Arch Microbiol 131:203–207
26. Sambrook J, Fritsch EF, Maniatis T (1989) Molecular cloning: a laboratory manual, 2nd edn. Cold Spring Harbor Laboratory, New York
27. Schlegel HG, Kaltwasser H, Gottschalk G (1961) Ein Submersverfahren zur Kultur wasserstoffoxidierender Bakterien: Wachstumsphysiologische Untersuchungen. Arch Mikrobiol 38:209–222

Microbial Control of the Concentrations of Dissolved Aquatic Hydrocarbons

D.K. Button

Abstract

Hydrocarbon oxidizing bacteria have a major effect on the chemistry of natural water systems, particularly with increased inputs of anthropogenic petroleum products. We review the basic kinetics helpful in understanding the equilibrium between nutrient concentrations and microbial populations, and describe some techniques useful in establishing that equilibrium with emphasis on hydrocarbons. Topics include oil spills, naturally occurring hydrocarbons such as terpenes, and some peculiarities of the metabolism of these hydrophilic solutes, isolation of ambient hydrocarbon-using bacteria, liberation of partly oxidized products of their metabolism, some environmental effects, and presumed peculiarities of the associated membrane transport mechanisms. Analysis techniques include radionuclide methods, autoradiography, microbial isolations and identification, quantitative high-resolution flow cytometry, and methods for tracking down the sources of aquatic hydrocarbons. The need for improved instrumentation and theoretical approaches is demonstrated.

Keywords: Flow cytometry, Hydrocarbons, Kinetics, Microbial populations

1 Introduction

Hydrocarbons are ubiquitous components of natural water systems including lakes and marine systems [1]. Most were formed by rearrangement of biogenic organic carbon in deep anaerobic systems. Now extracted and used as a source of energy, significant amounts reenter the aquatic environment as byproducts of these anthropogenic activities. All organics that dissolve, including even the heavier fraction of crude oil, are represented. Many bacteria (about 10% in Alaskan seawater) have the ability to use hydrocarbons for energy and carbon [2]. The resulting standing concentrations of these highly reduced organics are reflected by their kinetics of removal as demonstrated by radiotracers [3]. Growth rates of bacteria (including archaea) tend toward the minimum sustainable, perhaps generation times of hours to days [4] and likely longer in cold water (in preparation). The degree of approach to a particular

T.J. McGenity et al. (eds.), *Hydrocarbon and Lipid Microbiology Protocols*, Springer Protocols Handbooks, (2017) 149–166,
DOI 10.1007/8623_2016_224, © Springer-Verlag Berlin Heidelberg 2016, Published online: 10 September 2016

concentration depends on the rate of removal, typically by predation from various classes of filter feeders and viral infection [5]. Population persistence depends on organism ability to effect a flow of nutrients into their cytoplasm. Nutrient use by these oligotrophs (transthreptic or surface-feeding organisms) remains perpetually nutrient-limited by the biophysics of nutrient capture. Increased concentrations of nutrients give faster growth until capacity is saturated. With increasing growth or use of a particular species comes an increase in the rate of consumption of that species because they contribute to the biomass of the user. The balance describes a steady state toward which natural water systems tend to approach. The resulting biomass reaches a quasi-equilibrium with the limiting nutrients, an equilibrium set by the kinetics of nutrient capture by the microbes.

At steady state, any increase in biomass is followed by a decrease in substrate concentration arising from increased demand. Over time frames of a few generations, concentrations remain rather stable. This propensity toward an equilibrium concentration set by nutrient input together with the affinity of organisms for the nutrient and the rate of removal of those produced was demonstrated in continuous cultures or chemostats. It led to early descriptions of the kinetics of microbial growth [6] due to similarities with the saturation curves observed for enzymatic activity. Here, saturation means that concentrations are sufficient to give rates that approach maximal rates. In these nutrient-limited continuous cultures, growth rates are set at some rate below saturation, i.e. the maximal, μ_{max}, by the influent rate of fresh medium containing substrate. Population is set by the concentration of substrate in the influent medium. Both may be operator-controlled. Growth in the environment is basically similar except that the loss of biomass is through predation rather than dilution.

Because hydrocarbon transport appears to be unusual in mechanism, and because formulations can be ambiguous due to differing definitions of affinity, key terms [7] that describe the kinetics are reviewed. They describe the balance between transthreptic microbes, nutrient concentrations S, and rate. Included is the conversion of maximal rates of substrate uptake $V_{max} = gS/gX\,t$ where X is cells, t is time to growth. Cell yield $\Upsilon (= dX/d\Upsilon)$ is needed to convert V_{max} to maximal growth rate μ_{max} to cell yield: $V_{max}, = \mu_{max}/\Upsilon$. Substrate sequestering is described by the associated rate and kinetic constants as described in the literature on enzyme kinetics [8]. Ability to collect substrate is generally described by affinity as expressed by the Michaelis constant K_m where K_m is the concentration of substrate restricting uptake rate to half-maximal; $K_m = V_{max}/2$. But μ_{max} varies greatly depending on properties other than ability to collect substrate. These properties include the rate of macromolecule synthesis, whether the particular substrate in question is a major component of the nutrient mix, and

metabolome control. V_{max} is a capacity factor that usually depends on the population density of transporters or other molecular pumps on the cell surfaces. Other factors can include the concentration of cytoplasmic enzymes, or the ability to assemble macromolecular structures. However hydrocarbons, due to their solubility in limit membranes as indicated by Bunsen coefficients, may have other constraints as described below. All these are cytoarchitectural parameters and ones that affect terms describing the relationship between rate and activity.

Multiple substrate use by aquatic microflora is the rule [9]. Specific growth rate μ is the rate of microbial growth per unit biomass invoking the steady-state approximation. It is also the loss rate of used substrates $dS/\Upsilon dt$ where S is substrate, Υ is cell yield, and t is time. For rich systems, it is near the grazing or consumption rate by bacterivores. Base values for the specific affinity a_S^o of a particular substrate within a group *A, B, C...* are designated a_A^o, a_B^o, a_C^o, so that $a_{total}^o = \Sigma a_A^o, a_B^o, a_C^o$ For aquatic or oligobacteria, the number of substrates must be very large because the product of the concentration of any one and the associated specific affinity is small compared with the rate of population growth. The small affinities may be for reasons of economy of permeases. This is particularly true for use of hydrocarbons by pelagic bacterial populations where the number of chemical species tends to be large. Various hydrocarbon oxidizing isolates fed a menu of crude oil left leave unique patterns of unused components on chromatograms [10] demonstrating that a diversity of metabolic systems is necessary for the metabolism of homologs. Many metabolic systems for hydrocarbons have been described [11], including some from aquatic oligobacteria. Affinities for toluene ranged from 84 L/g-cells hr in the ballast water treatment facility plume near Port Valdez, Alaska down to 0.05 L/g-cells hr 15 km west. By comparison, the value for an isolate designated *Pseudomonas* T2 was 87 L/g-cells h. Half-maximal transport concentrations K_t for toluene oxidation rates by the Port Valdez microflora were in the range of 0.5–1.5 μg/L. Still, in the environment, affinities are generally comparable to oxygen-containing organics so that simultaneous use of multiple substrates is required for growth at expected rates. The presence of oil in the water increases affinities; pre-spill oxidation rates of dodecane in Port Valdez were 0.1 μg/liter-day but only 0.001 μg/liter-day under the Arctic Ocean ice [12].

Kinetic constants usually derive from the rectangular hyperbolic relationship (Fig. 1), but they are sometimes erratic, as often noticed for phosphate [13, 14] as shown. Note the continued upward drift of uptake rate with the concentration of phosphate. Often cell yield, and the rate constant or ability to collect substrate, and induction both increase with K_m because transport activity can affect both the rate constant and $V_{max.}$ Thus such changes can leave

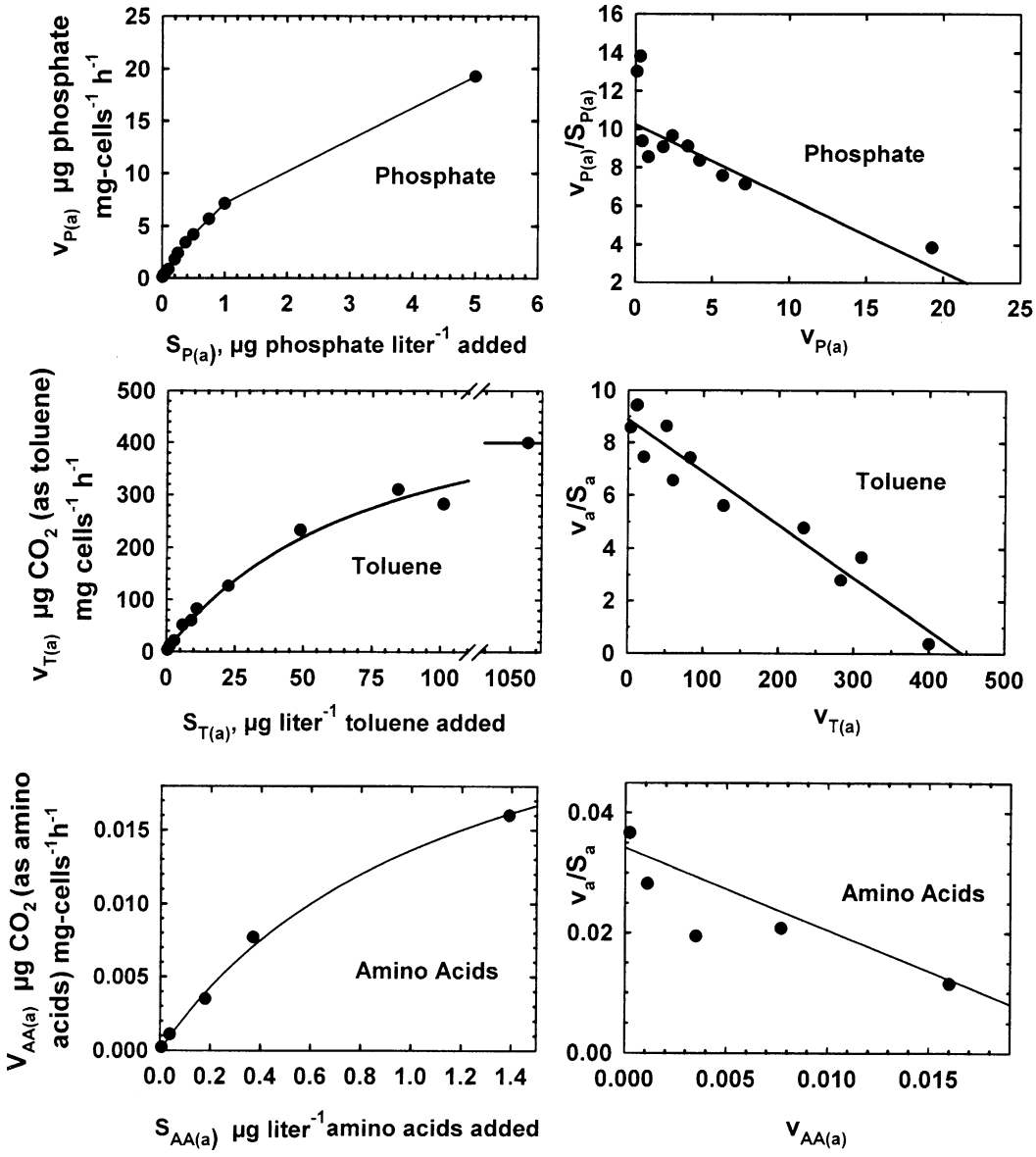

Fig. 1 Left: kinetics of uptake for phosphate, toluene, and amino acids in East Twin Lake, Alaska. Right: affinity plots

K_m, the putative measure of ability to collect substrate unchanged. For example, V_{max} for methane use by a methanotroph can increase 100-fold upon induction while leaving the affinity unchanged [15]. And K_m can increase with cell yield by over a factor of 10^7 [16], too much to be accounted for by kinetic theory alone. These observations contradict the concept that a small K_m reflects high affinity, although a search of Science Citations Index suggests that the paradigm is the custom in at least 10,000 publications. Secondly

rate may be restricted in a concentration-dependent way by the amount of energy available for transport. While Michaelian concepts may be empirically accurate for single enzymes, they are incompatible with operation of the substrate accumulation sequence within a complete organism. Further the theoretical accuracy is called into question by Kou [17], as well as by us, because K_m can reflect the distribution of waiting times for a receptive active site rather than the probability of ineffective binding by a permease. For these reasons, we first tried to replace affinity with a rate constant [13], then by the term specific affinity, and now for both historical and thermodynamic reasons, by affinity alone. It reflects the nutrient sequestering ability of the cell according to the sum total of its individual nutrient accumulating nutrients as affected by their total molecular environment [18].

For the base hyperbolic or Michaelian uptake, the base relationship between uptake rate v_S, maximal rate, affinity a_S, and substrate concentration is given by Eq. (1).

$$v_S = \frac{V_{max} a_S S}{V_{max} + a_S S} \tag{1}$$

Anthropogenic hydrocarbons are a significant component of the pollutants introduced into both lakes and the marine system. Large oil spills into the marine environment [19] have been chronicled for decades, and effects reported [20]. Sources such as exhaust from two-stroke outboard engines are now recommending cleaner burning engines for boats. Pollution is often cited as a reason for the decline in the water quality of lakes. The mayfly hatch in Wisconsin has obviously declined, and to such an extent that there is a new program to seed Green Bay off Lake Michigan with mayfly eggs. This is because their larvae are a major source of food for fish (Associated Press release Aug 20, 2015). Such reports are abundant but linkages are difficult to establish. This author has observed the failure of marine pseudomonads to grow in the presence of terpene vapors. Toluene to 1 mg/l would still support growth, but visible blebs apparently from disrupted membrane lipids, appear. At the low concentration end, toluene begins to induce the ability of the natural microflora of seawater to oxidize radiolabeled toluene at 10 nM [21]. Physical effects from the heavier hydrocarbons before weathering in seawater are widely reported to affect wildlife and could be easily found as large sticky globs in the subsurface gravel 5 years after the Port Valdez oil spill (unpublished).

Populations of marine hydrocarbon oxidizing bacteria can be located in real time with the help of an onboard scintillation counter. Those in Port Valdez, Alaska from the oil-tanker ballast water treatment plant were claimed to be strongly mixed and diluted throughout the ocean by plant engineers. However on site measurement of toluene oxidizing capacity in the fjord

revealed a layer of hydrocarbon oxidizing organisms with capacity 1,000-fold larger than in the ocean nearby [22]. It was trapped below less saline but cooler water, and above by more dense salty water in a layer about 30 m deep. Yet rates far from the plant were no lower than those near the impacted layer. This indicated alternative sources of hydrocarbons. The layer would have gone unnoticed without radioactive hydrocarbons and a scintillation counter onboard to home in on the population of active hydrocarbon metabolism. This involved simply amending samples from various depths and locations, with radiolabeled toluene, incubating, and measuring filtered organisms for radioactivity.

How the ambient population of hydrocarbon oxidizers was maintained away from the hydrocarbon source was then in question. Data suggested another supply of hydrocarbons in the rather pristine Alaska coastal environment. Heavy loads of floating pollen on the seawater from streams draining Alaska's vast conifer forests suggested the presence of this plant hydrocarbon [23]. Seasonally and depth-dependent concentrations of terpenes, common to conifers, were detected by MS/GC at the predicted μg/L concentrations, together with brominated hydrocarbons from algae, confirmed the presence of biogenic hydrocarbons in the coastal ocean.

Floating slicks from spills tend to aggregate in turbulent seawater, aided by wind action, increase in density, and sink. Factors include microbial oxidation to a more dense suspension of clumps, along with dissolution and evaporation of the lighter fraction. Clay is quite effective in outcompeting bacteria for organics such as glucose [24]. However suggested use of clay to sink oil slicks, abundant in Alaskan glacial plumes, was not supported by laboratory trials [25]. But natural populations of bacteria were quite effective, as compared to sterile controls, in removing oil slicks from slowly rotating seawater in carboys. It collected into small black hydrophilic particles that settled out in a way that revealed the process of oil spill degradation in the oceans. Oil oxidizing bacteria are quite good at dispersing oil slicks; however, commercial dispersants can actually inhibit the process [26].

Although a large portion of the marine microflora can metabolize petroleum hydrocarbons, affinities are generally only sufficient for them to supplement the many other organics used from natural waters. Enrichment cultures tend to select for high capacity to use the amended substrate, but they bias the selection toward copiotrophic (rich) environments. Extinction cultures, where ambient populations are diluted to single-digit numbers and allowed to develop in unamended lake or seawater, produce oligobacteria. These are low-nutrient concentration adapted organisms more typical of the environment. The first culture developed by this procedure, *Cycloclasticus oligotrophus*, was particularly good at using acetate [25]. However genomic analysis showed the presence

of gene sequences that are consistent with the metabolism of hydrocarbons [27] as well. Tests with toluene showed that this acetate user was also quite good at using a hydrocarbon, and was perhaps a more typical marine bacterium than previous isolates due to small size and low specific gravity. These and other data above underscore the ubiquity of hydrocarbons in the environment, and as a significant substrate for typical aquatic bacteria.

One of the most common classes of environmental hydrocarbons is terpenes [23]. They are ubiquitous products of biosynthesis in plants. Unlike lipids, terpenes have an isoprene backbone, and can contain minor amounts of oxygen. At least 10% of the organisms present in the Gulf of Alaska actively accumulated terpenes extracted from $^{14}CO_2$-grown spruce seedlings as determined by autoradiography [28]. Results were the same for ^{3}H-toluene, while controls using active *Escherichia coli* cells showed none of the telltail black spots. The indigenous organisms had a relatively large specific affinity for hydrocarbons giving a turnover time of 4–19 days (Table 1), a large value for Alaskan seawater where values for toluene can approach 100 years. Sufficient quantities appear to be washed from conifers in Southeast Alaska to help base a food chain. The most abundant terpenes were α-pinene, β-pinene, and other conifer constituents. Bromoform a related macrophyte constituent was abundant as well. These were discovered in a search for compounds that sustained ability of the microflora to metabolize hydrocarbons. Such plant hydrocarbons undoubtedly supported seed populations of bacteria able to help dissipate oil spills.

Hydrocarbons are used for carbon and energy by many species of bacteria. Oxidation of ^{14}C-dodecane was observed in the Arctic Ocean in the 1970s [12, 29] and oxidation of light hydrocarbons such as toluene and benzene was apparent in all of the many natural water systems later examined. Affinities were much higher than for amino acids and nearly as high as for phosphate in East Twin Lake near Fairbanks, Alaska (Fig. 1, v/S axis intercepts). Hydrocarbons have a high-energy level in oxidative environments due to a large hydrogen content and also contain carbon for use as cell material. Most substrates are transported at the expense of a chemical and electrical potential generated across the limit cell membrane usually generated by the ejection of protons. However bacterial membranes have a high lipid content, and thus are subject to disruption by hydrocarbons like toluene. This unique feature is explored below by the use of inhibitors. Blebs or outcrops likely comprised of disrupted cell membranes appear on the cell surface as mentioned and the organisms die. Thus metabolism is limited to concentrations that are low.

However, hydrocarbons are high-energy substrates that require oxygen with twice the stoichiometry as carbohydrates. Cell yields therefore are large, to 80% dry weight [30] or 400% wet weight for oligotrophs at only 20% dry weight [31]. This, along with small

size, allows aquatic bacteria to maximize surface to mass ratio for better substrate collection, called streamlining [32]. Most cultivars have more solids and are about a third dry weight. Recent values for amino acids are about 25% wet mass for in situ lakewater populations. Other reports are much lower but measurements of in situ values [33] contain uncertainties. An additional factor is that at large concentrations of hydrocarbons, large amounts can be excreted, reducing cell yields by a factor of five [2].

The reduction of yields from hydrocarbons is due to metabolism that is initially incomplete. When toluene concentrations exceeded the transport constant K_t, large amounts of partly oxidized products including catechols [34] and ring cleavage products such as 2-hydroxy-6-oxohepta-2,4-dienoic acid [35] can be released. These often appear in batch cultures, both mixed and pure, turning the medium a bright yellow. Product leakage is thought to result from initial cleavage of the hydrocarbon by enzymes in the cell membrane due to "vectorial partitioning" (see mechanisms below). This can result in a ratio of initial pathway enzymes in the bacterial membrane to cytoplasmic catabolic enzymes, and result in large affinities and maximal growth rates as well. Affinities for three-methyl catechol and toluene dihydrodiol were 0.14 and 1.7 mg/L as compared with only about 1 μg/L for the parent toluene. The environmental significance of these electrophilic alkylating agents is unknown.

Some of the ambiguity in describing microbial activity with K_m, it was argued, can be avoided by use of affinity (formerly specific affinity) particularly where concentrations are small as they are for environmental hydrocarbons. Here affinity is taken as the second order rate constant relating the net uptake rate v_s of a population to the concentration of a particular substrate S and population is given by wet rather than dry weight. This is because it reflects size together with the surface area available to collect substrate. Also water is a functional part of cytoplasmic function. The maximal value of the affinity is a kinetic constant and the initial slope of the kinetic (v_S *vs* S) curve. In enzymatic terms, it is the effective catalytic constant of the organism. As saturation ensues, specific affinity decreases from its base or maximal value a_S^o to the rate constant a_S with increasing concentration of substrate. The concentration-dependent affinity for uptake a_S is always uptake rate divided by substrate concentration from the rate equation $v_S = a_S S$ and is typically a monotonic increasing function of S up to inhibitory concentrations for fully energized cultures. It however may be sigmoidal in the case of positive cooperativity among substrates in energy-poor systems. In the experience of the author, most (but not all) uptake data that depend on uptake kinetics alone conform to a rectangular hyperbola. Moreover single molecule kinetic data agree with this when tested according to a variety of constraining forces [17]. For hydrocarbons, low solubility may preclude

concentrations sufficient to saturate the capacity of cytoplasmic enzymes. Larger concentrations of the lighter fraction may be achieved in water due to increased solubility [36], and a greater presence in the membrane-lipid phase, but this can lead to toxicity, particularly in the C_6–C_{10} range. For toluene, concentrations shift from stimulatory to inhibitory at about 70 mg/L [37]. Monoterpenes, plant hydrocarbons located in coastal seawater (vide supra), were surprisingly inhibitory toward toluene uptake. However benzene added at 50 times the concentration of toluene was ineffectual as a competitive inhibitor of toluene metabolism and the induction constants for toluene were much larger [9]. These observations, along with the selective use of alkane homologs from the mixture found in crude oil, indicated metabolic pathways with unique enzymatic components [3].

2 Materials

2.1 Flow Cytometry

1. Flow cytometry greatly improved evaluations of both activity of natural populations (Fig. 2) as well as in isolates of environmental bacteria. However instruments with the required sensitivity are not widely available. One reason is the cost of suitable instruments with the required sensitivity. Those in current production give no indication of the sensitivity of the dual 5-watt lasers used here, and may not be easily modified to attain this sensitivity. Secondly flow cytometry received some negative

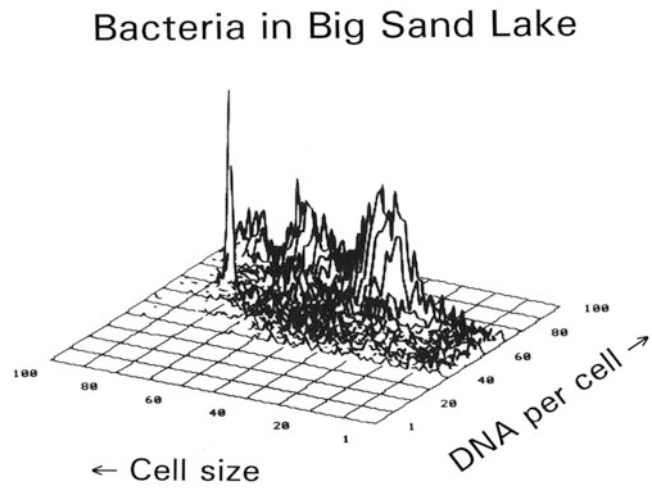

Fig. 2 Cytogram of lakewater bacteria from Harding Lake, Alaska. The sharp peak at left is standard spheres. Three major bacterial populations appear to the right. The corresponding *dot plot* (not shown) indicates a mean DNA content of 1.8 fg/cell. A major population appears at 10 fg DNA per cell, and two (one hidden) at 48 fg/cell. The corresponding volumes are 0.08 and 2.8 μm^3

comments due to non-linearity of the light scatter signal with particle mass of large size compared with aquatic bacteria. However we had previously shown that forward light scatter is a reliable property of small particle dry mass when size is small and refractive index is low, both by theory and by experiment [33]. Experimentally the dry weight of a small marine isolate measured by radioactivity from ^{14}C-acetate and CHN-content by analysis was within 12 % of that predicted from small glass beads after correcting for refractive index. Moreover the carbon content computed from dry weight according to flow cytometry agreed with values obtained from coal standards.

2. The DNA content of bacteria easily resolved by flow cytometry [38] helps distinguish bacteria from other particles. Further, genome size of aquatic bacteria can be extremely small helping define a group first cultured only rather recently [39]. Third, the number of chromosomes, $1n$, $2n$, and $4n$, is easily resolved giving an indication of the rate of growth because fast growing organisms tend to start additional rounds of replication before they divide.
3. The difference in cytoarchitecture between aquatic bacteria and commonly used species is huge. For example, sizes of typical marine bacteria are only 6% of that of *E. coli*, as sharply resolved by flow cytometry. Those of lakewater are in between. There can be an annual shift in physical properties of the bacterial population in northern lakes because size tends to increase with temperature, likely due to faster growth. Total populations tend to be fairly constant around the year as numbers reflect the ability of grazers and filter feeders to sweep them from the water. There is also an increase in microbial size; organisms are generally larger in nutritionally rich systems. Cell size increases with growth rate, and larger species may do better in rich systems, both likely to give space for the required increase in enzyme content. Suspended natural populations of aquatic appear to be most accurately enumerated by flow cytometry due to their small and varied size. Further, analysis of their dry or wet weight provides a solid base for evaluating their affinities for substrates in question. Thus it is important to base kinetic constants on a more conservative parameter than population. Cell volume, dry mass, and total surface area are all useful choices. We prefer cell volume because water is a functional component of microbes and provides additional space for transporters required to enhance their affinity for most nutrients.
4. Flow cytometry was with a Cytofluorograf IIs equipped with a model 2151 computer system, high sensitivity photomultiplier tubes, 3.5-decade logarithmic circuitry, quartz flow-cell and 75-pm orifice, custom adjustable beam-shaping lens assembly, and two 5 W argon lasers (Coherent, Inc., Palo Alto, CA). Data were

supplemented with a Model ZBI Coulter counter with 30-pm orifice (Coulter Electronics, Hialeah, FL) and a Leitz Dialux 20-EB fluorescence microscope (E. Leitz, Inc., Rockleigh, NC) equipped with a 100 W mercury arc lamp and filter cubes A and I2 to accommodate excitation and emission wavelengths for DAPI and acridine orange.

5. Flow cytometry requires the means for adding internal standards for both numbers of organisms and as a reference for their dry mass and density [21, 31]. Latex beads are useful for both. Use care to consider particle size because those much larger than bacteria loose linearity S with particle mass as apparent from the theory of Raleigh scattering. Specific gravities are corroborated with particles of standard density in solutions of gradient density.

2.2 Sampling and Supplies

1. A means for quick transfer of samples from the environment to the analytical laboratory is useful to assess in situ activities because substrate turnover times of labile nutrients can be very short. Thus, separation from the environment and nutrient sources contained within can affect the kinetics. To minimize this artifact, we used a seaside laboratory, a shipboard laboratory, and rapid sample transport by ski or float plane to a laboratory at the University of Alaska, Fairbanks.
2. Radioactive tracers are often central to the analysis of microbial kinetics. Impurities acquired during synthesis often contaminate commercial radioisotopes and can confound the results. For hydrocarbons, sublimation onto chilled glass works well. A refrigerated cold finger in an alcohol bath can provide cooling. Purified toluene can be thawed and pipetted into ampules and sealed with little loss.
3. Micropipettes provide an accurate means of diluting radioisotopes and applying standards and other low-volume reagents.
4. A walk-in constant temperature room is useful for subdividing environmental samples and subsequent incubation.
5. Manifolds with vacuum driven filter chambers are useful for quick separation of radiolabeled cells from solution when using small volumes (~5 milliliters) and small pore size (0.08 μm) filters needed to remove the small but difficult to culture bacteria.

3 Methods

3.1 Chemical Concentrations

1. Relative rates of ^{14}C-hydrocarbon uptake compared to concentration v can be calculated from the rate of evolution of $^{14}CO_2$ [21] as corrected for cell yield. Initial concentrations of hydrocarbon can be determined from specific radioactivity along with

high-resolution chromatography. The hydrocarbon should first be purified to eliminate residual impurities from the chemosynthesis. Otherwise $^{14}CO_2$ from isotope precursors can indicate metabolism where there is none. For ^{14}C-toluene, the isotope is treated with NaOH to sequester $^{14}CO_2$ and sublimed onto a cold finger. This eliminates most of the abscissa intercept in the time courses for $^{14}CO_2$ liberation by eliminating the more polar sources of radioactivity used in ^{14}C-toluene synthesis. Where glassware has been previously exposed to $^{14}CO_2$, heating to 550°C is necessary to further reduce background.

Microbiologically evolved $^{14}CO_2$ from purified ^{14}C-toluene amendments is dried by bubbling through concentrated H_2SO_4 and remaining water removed with a cold trap of glass beads in a dry-ice acetone bath. This is followed by a hydrophobic (Tenax) trap cooled in the same way. Biogenic $^{14}CO_2$ in the effluent gas stream is bubbled through in a series of three small phenethylamine containing traps to insure complete recovery. A procedure such as this is necessary for accurate measurements in the oligotrophic environment where concentrations are small.

2. Radioactivity in the cells is collected on atomic nuclei perforated filters. Holes in many of the filters commonly used such as 0.45 μm are too large to retain most marine bacteria, and gentle filtration through 0.08 μm filters is recommended. Sample volumes must be small, just a few milliliters.
3. Concentrations of organic products are determined from the radioactivity of the spent incubation medium after purging to remove substrate toluene and filtering off the cells.
4. Absolute uptake rate v_s is given by filter plus CO_2 plus organic product radioactivity and converted to units of substrate mass.
5. Affinities can be determined from the initial slope of the kinetic curve. If perfectly hyperbolic, it is also V_{max}/K_m. However the base affinity as well as K_m is compromised by any unlabeled background substrate that may be present. Presumably this can be accounted for by applying the kinetics of competitive inhibition of radioactive substrate by that which is not, proof in progress.

3.2 Populations

1. Isolation of the more typical aquatic microbes, sometimes called oligobacteria, can be accomplished by extinction culture. This technique is also called dilution culture, but terminology is ambiguous with a technique for eliminating the effect of bacterivores on kinetics. The population of natural water samples is determined by flow cytometry, diluted to give ten or so organisms in a container of filtered autoclaved source water, the inoculated vessel incubated for a few weeks, and examined for culture development [39].

2. Populations of hydrocarbon oxidizing organisms can be estimated from the rates of hydrocarbon uptake compared with the affinity of isolates, appropriate genes for hydrocarbon oxidation in them, or by autoradiography. These organisms are mostly bacteria but taken here to include the functionally similar archaea. ^{14}C-dodecane added to fresh seawater from the Arctic Ocean and incubated in situ produced radioactive CO_2 within 1.5 days [12].
3. Hydrocarbon oxidizing microorganisms were more easily isolated from Cook Inlet than from Port Valdez, Alaska in 1977 when oil production was limited to the inlet [40]. Later, following the operation of the ballast water treatment plant in Port Valdez, bacterial populations of 0.7 mg/L appeared at a density trap-depth for the discharge of 50 m depth as mentioned [22]. Populations, located and mapped with onboard toluene oxidation rate measurements in near real time, were a factor of 10^4 larger than elsewhere. Those bacteria able to metabolize toluene are necessarily substantial but variable as determined by autoradiography [41]. The populations of hydrocarbon oxidizers can be distinguished from others by autoradiography. Water samples are incubated with ^{3}H-toluene, and filtered onto 0.2-μm Nuclepore polycarbonate membranes. The filters are quartered, fixed onto glass slides, coated with NTB-2 nuclear track emulsion (Kodak), and exposed to the radiation for about a week. After photographic development, the autoradiographs are stained with acridine orange and examined by epifluorescence microscopy. The organisms become visible with this DNA stain, and toluene-derived protons appear as obvious black spots.
4. Samples for flow cytometry of the microflora were preserved with the addition of formaldehyde to 0.5%, stored on ice, and processed within a day or so. Formaldehyde speeds dye penetration. Dry weight was computed from forward light scatter intensities obtained by flow cytometer [42]. Formaldehyde combines with protein adding to the dry weight, and must be corrected for; however, glutaraldehyde is much more problematic due to its larger molecular weight. Volumes are calculated from density constructed with sucrose gradients calibrated with standard density beads. Calibration [25] was confirmed with *C. oligotrophus* grown on ^{14}C-acetate by determining the ratio of carbon to dry weight. To determine the ratio of cell carbon to dry weight, a culture was grown on acetate and pelleted by centrifugation. The pellet was washed with saline, dried, weighed, and analyzed for carbon content with a CHN 600 analyzer.
5. DNA was determined from DAPI-DNA fluorescence intensity and standardized with the signal from a single chromosome of *E. coli* of known genome size and GC content. For seawater,

there is a 10–30% correction for salt. Volumes of the larger organisms were measured with a Coulter Counter model Z_{BI} with a Channelyzer; Coulter Electronics, Inc. Instrument calibration was done with 1.942 μm-mean-diameter spheres and corroborated by data from a Coulter Multisizer II.

3.3 Metabolic Products and Transport Mechanism

1. Cultures often turn yellow due to the escape of partly oxidized products of metabolism, such as catechols and ring-cleavage products, as mentioned. Amounts are reflected by the radioactivity of culture filtrate grown on radioactive toluene after stripping off the remaining substrate with nitrogen. Some can be identified by chromatography. Amounts can exceed the amount of CO_2 liberated by a factor of three, but re-metabolism of some often occurs and the color is lost. This raised questions about the fate of hydrocarbons from lightly treated tanker ballast water following a quick trip and aeration through a "microbial treatment" pond. The discharge produced a large population of bacteria from labeled toluene that quickly revealed their presence onboard ship, using a scintillation counter and radioactive toluene for detection.
2. For *Marinobacter* sp. (designated "*M. arcticus*"), the low oxidation state and high carbon content of hydrocarbons make them high-energy substrates in an oxidative environment. With added CCCP (carbonyl cyanide *m*-chlorophenylhydrazone), 45% of the radioactive toluene supplied turned up as non-volatile products after adding acid to purge the CO_2. Product formation in batch culture was initially about equal to that of CO_2, but their radioactivity was resorbed after a few minutes. With both *Marinobacter* sp. and *Pseudomonas* sp. T2, transport of strongly polar substrates like alanine is completely inhibited by protonophores such as CCCP. Even for the ampholyte leucine, only about 1% of the affinity remained after treatment. By comparison, for the hydrophilic hydrocarbon toluene 99% of the affinity was retained (unpublished). Neither did the Na^+/H^+ transport inhibitor monensin [43], and therefore ATP-dependent transport, have any effect. Uncoupling oxidative phosphorylation by dinitrophenol slowed, but did not stop the accumulation of toluene, while metabolic functions like CO_2 production were reversed. For in situ populations, the yield of cell dry weight from radioactive toluene was particularly high. So it appears that little energy is devoted to transport for the metabolism of hydrocarbons leaving more available for subsequent metabolism. Some of these metabolic products are lost before complete utilization as mentioned, perhaps due to location of the responsible enzymes near the cell surface where their retention within the cell is limited; see mechanisms below.

3. Embedded permeases or molecular pumps of bacteria can retain highly water soluble solutes once actively accumulated. However low molecular weight hydrocarbons are soluble in the limit membrane including the inner membrane for gram-negative bacteria, due to a high lipid content. Thus hydrocarbons like toluene can disrupt the membrane and inhibit the transport of more polar substrates including sugars and amino acids. Cell damage can be observed by microscopy as blebs. Clearly this dissolution is not problematic for methane, benzene, toluene, or dodecane at small concentrations because they support growth when the concentration is low. Affinities for natural populations of lakewater bacteria for toluene are similar to those for phosphate and much higher than those for amino acids (Fig. 2). These observations offer a means to help understand how hydrocarbons are transported into bacteria.
4. Transport mechanisms for hydrocarbons appear to be unique and can be examined by the use of mechanism-specific inhibitors such as CCCP. According to the vectorial partitioning hypothesis described here, hydrocarbon transport depends on high concentrations within the cytoplasmic membrane that result from the large partition coefficient between water and membrane lipids near where the initial oxidative enzymes are located. The resulting polar products are produced near the limit membrane and trapped by low solubility inside the cell for further metabolism. The result is high affinity for hydrocarbon because the enzymatic process involves a substrate that is concentrated by physical partitioning rather than active transport requiring specific permeases that set rate according to their number density. The polar products of hydrocarbon metabolism require conventional permeases for retransport when lost. This may result in smaller affinities and Michaelis constants depending on the abundance of rate-limiting process downstream. Diffusion shells can limit transport rates to high-affinity organisms. These are probably reduced in the oceans by currents that generate turbulence. But with the small affinities characteristic for hydrocarbon oxidizers in most natural waters, applied diffusion barriers formed by casting them in millimeter-sized blocks of agar made no significant difference in the kinetic constants [2]. That affinities are very large for hydrocarbons (Table 1) is a likely consequence of partitioning. Membrane concentrations are increased over those external according to the size of the partition coefficient. Values from octanol as a membrane surrogate are of the order of 10^2–10^5. Membrane-bound oxidases may then use the large concentration to accelerate production of membrane insoluble products which are trapped inside for further use. Thus unlike amino acids, hydrocarbon transport by *Pseudomonas* T2 was unaffected by high pH

Table 1
Comparison of chemical and physical properties of environmental bacteria[a]

Organism	Dry wt. fg/cell	Solids (%)	Density (%)	Genome, MBP	DNA (%)	Operons	Memb/Cyt proteins	Affinity (L/mg cells wet hr)
Cryptococcus oligotrophus	43 ± 12	15	1.04	1	14	1	210/170	20
Marinobacter sp. T2	52 ± 12	20	1.07	2	11	2	300/290	0.32
Escherichia coli	275 ± 17	27	1.10	7	2.2	7	800 total	0.21

[a]Column headings include dry weight, buoyant density, ribosome operon number, membrane to cytoplasmic protein ratio, and affinity for amino acids

(small concentration of co-transporting ions) and was resistant to proton ionophores such as carbonyl *m*-chlorophenylhydrazone and monensin. Moreover liberation of metabolic products was increased by these antagonists, consistent with hydrocarbons being transported differently than they are for amino acids. Thus use of inhibitors provides an important tool for understanding how bacteria accumulate substrates. Another conclusion is that the use of low molecular weight hydrocarbons is limited by their concentration in the cell at the active site of the first enzyme for metabolism such as toluene dioxygenase, and not the concentration-dependent rate of diffusion to a membrane-bound transporter. It could even be enhanced if that enzyme were membrane bound which gives rise to the term vectorial partitioning for the transport of low molecular weight polar substrates. Such models can help suggest strategies for understanding the effect of natural populations in the environment.

References

1. Shaw DG, Part I (1989) Hydrocarbon C5 to C7. Pergamon Press, Oxford
2. Button DK, Robertson BR (1986) Dissolved hydrocarbon metabolism. Limnol Oceanogr 31:101–111
3. Button DK, Robertson BR, McIntosh D, Jüttner F (1992) Interactions between marine bacteria and dissolved phase and beached hydrocarbons after the *Exxon Valdez* oil spill. Appl Environ Microbiol 58:243–251
4. Kemp PF, Lee S, LaRaoche J (1993) Estimating the growth rate of slowly growing marine bacteria from RNA content. Appl Environ Microbiol 59:2594–2601
5. Zhao Y, Temperton B et al (2013) Abundant SAR11 viruses in the ocean. Nature 494:357–360
6. Monod J (1950) La technique de culture continue. Théory et applications. Ann Inst Pasteur Paris 79:390–410
7. Button DK (1998) Nutrient uptake by microorganisms according to kinetic parameters from theory as related to cytoarchitecture. Microbiol Mol Biol Rev 62:636–645
8. Cook PF, Cleland WW (2007) Enzyme kinetics and mechanisms. Garland Science, New York
9. Law AT, Button DK (1977) Multiple-carbon-source-limited growth kinetics of a marine

coryneform bacterium. J Bacteriol 129:115–123
10. Robertson BR, Schell DW, Button DK (1979) Dissolved hydrocarbon rates. University of Alaska, Fairbanks, Port Valdez, Alaska, pp 109–123
11. Zystra GJ, Gibson DT (1989) Toluene degradation by *Pseudomonas putida* F1. Nucleotide sequence of the todC1C2BADE genes and their expression in Escherichia coli. J Biol Chem 264:14940–14946
12. Arhelger SD, Robertson BR, Button DK (1976) Arctic hydrocarbon biodegradation. In: Wolfe DA (ed) Fate and effects on petroleum hydrocarbons in marine ecosystems and organisms. Pergamon, Oxford, pp 270–275
13. Robertson BR, Button DK (1979) Phosphate-limited continuous culture of *Rhodotorula rubra:* kinetics of transport, leakage, and growth. J Bacteriol 138:884–895
14. Brown EJ, Button DK (1979) Phosphate limited growth kinetics of *Selenastrum Capricornutum (Chlorophyceae)*. J Phycol 15:305–311
15. Dunfield PF, Conrad R (2000) Starvation alters the apparent half-saturation constant for methane in the type II *methanotroph methylocystis* strain LR1. Appl Environ Microbiol 66:4136–4138
16. Button DK (1985) Kinetics of nutrient-limited transport and microbial growth. Microbiol Rev 49:270–297
17. Kou SC, Cherayil BJ, Min W, English BP, Xie XSB (2005) Single-molecule Michaelis-Menten equations. J Phys Chem 109:19068–19081
18. Eigen M (2013) From strange simplicity to complex familiarity. Oxford University Press, Oxford
19. Shrope MA (2011) Deep wounds. Nature 472:154
20. Peterson CH, Rice SD (2003) Long-term ecosystem response to the Exxon Valdez oil spill. Science 302:2082–2086
21. Button DK, Robertson BR (1987) Toluene induction and uptake kinetics and their inclusion into the specific affinity equation for describing rates of hydrocarbon metabolism. Appl Environ Microbiol 53:2193–2205
22. Button DK, Robertson BR, Craig KS (1981) Dissolved hydrocarbons and related microflora in a fjordal seaport: sources, sinks, concentrations, and kinetics. Appl Environ Microbiol 42:708–719
23. Button DK, Jüttner F (1989) Terpenes in Alaskan waters: concentrations, sources, and the microbial kinetics used in their prediction. Mar Chem 26:57–66
24. Button DK (1969) Effect of clay on the availability of dilute organic nutrients to steady state heterotrophic populations. Limnol Oceanogr 14:95–100
25. Button DK (1976) The influence of clay and bacteria on the concentration of dissolved hydrocarbon in saline solution. Geochim Cosmochim Acta 40:435–440
26. Kleindiensta S, Seidela M, Ziervogelb K (2015) Chemical dispersants can suppress the activity of natural oil-degrading microorganisms. Proc Natl Acad Sci U S A 112:14900–14905
27. Wang Y, Lau PC, Button DK (1996) A marine oligobacterium harboring genes known to be part of aromatic hydrocarbon degradation pathways of soil pseudomonads. Appl Environ Microbiol 62:2169–2173
28. Button DK (1984) Evidence for a terpene-based food chain in the Gulf of Alaska. Appl Environ Microbiol 48:1004–1011
29. Button DK (1971) Biological effects in the marine environment. In: Hood DW (ed) Impingement of man on the oceans. University of Alaska Press, Fairbanks Alaska, pp 421–429
30. Johnson MJ (1967) Growth of microbial cells on hydrocarbons. Science 3769:1515–1519
31. Robertson BR, Button DK, Koch AL (1998) Determination of the biomasses of small bacteria at low concentrations in a mixture of species with forward light scatter measurements by flow cytometry. Appl Environ Microbiol 64:3900–3909
32. Giovannoni SJ, Tripp HJ, Givan S (2005) Genome streamlining in a cosmopolitan oceanic bacterium. Science 309:1242–1245
33. Robertson BR, Button DK (1989) Characterizing aquatic bacteria according to population, cell size, and apparent DNA content by flow cytometry. Cytometry 10:70–76
34. Heider J, Spormann AM, Beller HR (1999) Anaerobic bacterial metabolism of hydrocarbons. FEMS Microbiol Rev 22:459–473
35. Button DK, Robertson BR (1988) Hydrocarbon bioconversions: sources, dynamics, products and populations. In: Shaw DG, Hameedi MJ (eds) Environmental studies in Port Valdez, Alaska: a basis for management. Springer, New York, pp 267–291
36. Shreve GS, Vogel TM (1992) Comparison of substrate utilization rates and growth kinetics between immobilized and suspended *Pseudomonas* cells. Biotechnol Bioeng 41:370–379
37. Robertson BR, Arhelger S, Kinney PJ, Button DK (1981) Hydrocarbon biodegradation in Alaskan waters. In: Wolf D (ed) Microbial degradation of oil pollutants. Center for Wetland

Resources, Louisiana State University, pp 171–184

38. Button DK, Robertson BR (2001) Determination of DNA content of aquatic bacteria by flow cytometry. Appl Environ Microbiol 67:1636–1645
39. Button DK, Robertson BR, Lepp PW, Schmidt TM (1998) A small, dilute-cytoplasm, high-affinity, novel bacterium isolated by extinction culture and having kinetic constants compatible with growth at ambient concentrations of dissolved nutrients in seawater. Appl Environ Microbiol 64:4467–4476
40. Kinney PJ, Button DK, Schell DM (1969) Kinetics of dissipation and biodegradation of crude oil in Alaska's Cook Inlet. In: Proceedings of the 1969 Joint Conferences on Prevention and Control of Oil Spills. American Petroleum Institute, Washington, pp 333–340
41. Button DK (1971) Biological effects in the marine environment. In: Hood DW (ed) Impingement of man on the oceans. University of Alaska Press, Fairbanks, Alaska, pp 421–429
42. Button DK, Robertson BR (1989) Kinetics of bacterial processes in natural aquatic systems based on biomass as determined by high-resolution flow cytometry. Cytometry 10:558–563
43. Chen GI, Russell JB (1990) Transport and deamination of amino acids by a gram-positive, monensin-sensitive ruminal bacterium. Appl Environ Microbiol 56:186–192

Phenotyping Microarrays for the Characterization of Environmental Microorganisms

Etienne Low-Décarie, Andrea Lofano, and Pedram Samani

Abstract

Culture-based methods for the characterization of microorganisms remain essential to advances in microbiology. Phenotyping arrays and microplates in which each well represents a different selective growth environment are important tools (1) in the identification of microbial isolates, (2) in the characterization of the phenotypic fingerprint of microbial communities, (3) for linking specific functions with specific organisms or genes, and (4) for the identification of evolutionary trade-offs in the establishment of phenotypes. The use of phenotyping arrays in the study of hydrocarbon and lipid degradation by microbial isolates or communities is an emerging application. The application of phenotyping arrays requires careful selection of substrates, growth medium, and dyes and consideration of the intrinsic limitations of the approach. The use of phenotyping arrays leads to the production of large amounts of data, which require specific approaches for summarization and analysis. Liquid handling automation will increase the feasibility of custom phenotyping arrays that include hydrocarbons and lipids.

Keywords: Biodegradation, Biolog™, Culturomics, Ecotype, High throughput, Microtiter, Phenomics, Phenotyping microarray (PM), Substrate

1 Introduction

1.1 Phenotype Characterization and Microtiter Plate-Based Arrays

Selective and restrictive growth substrates have played a central role in the taxonomy and isolation of microorganisms and represent an important early step in the development of the field of microbiology [1]. Growth properties of microorganisms continue to play an important role in the identification and characterization of microorganisms and their communities. Microtiter plates and plate readers now allow the rapid testing of cultures in hundreds of selective growth conditions (variously described as high-throughput phenotyping, phenomics [2], or culturomics [3]). The pattern of substrates that can be metabolized by an organism or the experimental environments in which an organism can thrive can provide a diagnostic physiological fingerprint for the identification of the studied organism. Biolog™ commercialized a method for the identification

T.J. McGenity et al. (eds.), *Hydrocarbon and Lipid Microbiology Protocols*, Springer Protocols Handbooks, (2017) 167–181, DOI 10.1007/8623_2015_106, © Springer-Verlag Berlin Heidelberg 2015, Published online: 20 June 2015

of microorganisms based on their capacity to catabolize specific substrates [4] as measured using a reducible indicator dye [5]. Biolog™ Phenotype MicroArray panels (Biolog™ plates) consist of 96-well plastic microtiter plates, each well containing a specific substrate to be catabolized, as well as a proprietary tetrazolium-based redox dye mix. The line of Biolog™ plates currently surveys microorganismal catabolic activity in the context of carbon, nitrogen, phosphorus, and sulfur sources as well as pH and osmotic pressure. The use of custom-assembled phenotyping arrays, including arrays that contain various types of hydrocarbons and lipids as target substrates, will undoubtedly increase with the growing availability of liquid handling automation and robotics that facilitate and increase the replicability of the distribution of defined selective medium to specific wells on the complex array.

1.2 Applications

Biolog™ plates are widely used phenotyping arrays. Biolog™ plate use has been reported in over 1,650 articles (as of September 2014). This technique is not only useful for characterizing the metabolic capabilities of a single sample, but based on the distinctive utilization of metabolites, Biolog™ plates can be used to identify species based on their metabolic fingerprint. They can also be used for comparing the rate of respiration and diversity between samples, providing a spatial and temporal map to track changes in the microbial communities [6, 7]. The utilization of Biolog™ plates in the context of the characterization of communities has grown to represent around 50% of the reported usage (Fig. 1a). The use of Biolog™ plates has focused on the characterization of bacteria and their communities, though fungi and diverse communities have also been characterized [8] (Fig. 1b). Biolog™ plates specifically designed for fungi and yeast exist; however their use is still rare. Most of the studies involve soil organisms (Fig. 1c). A growing, but small, number of articles are characterizing strains and communities that are cable of degrading hydrocarbons or lipids using Biolog™ plates (Fig. 1d). Studies using Biolog™ plates in the context of hydrocarbons and lipids from oil spills and pollution tend to use these phenotyping arrays to identify change in microbial communities due to petroleum pollution (e.g., [9–13]). Determining the types of hydrocarbons that can be degraded by microbial communities or by specific species is essential to monitoring the impact of oil in the environment and its bioremediation. The type of community that thrives and degrades oil depends on the hydrocarbon substrate present [14]. A plate-based method for the measurement of microbial catabolism of polycyclic aromatic hydrocarbons has been developed [15]. However, a phenotype panel to characterize strains and communities specifically in terms of their capacity to degrade hydrocarbons and lipids has yet to be commercialized, despite its feasibility.

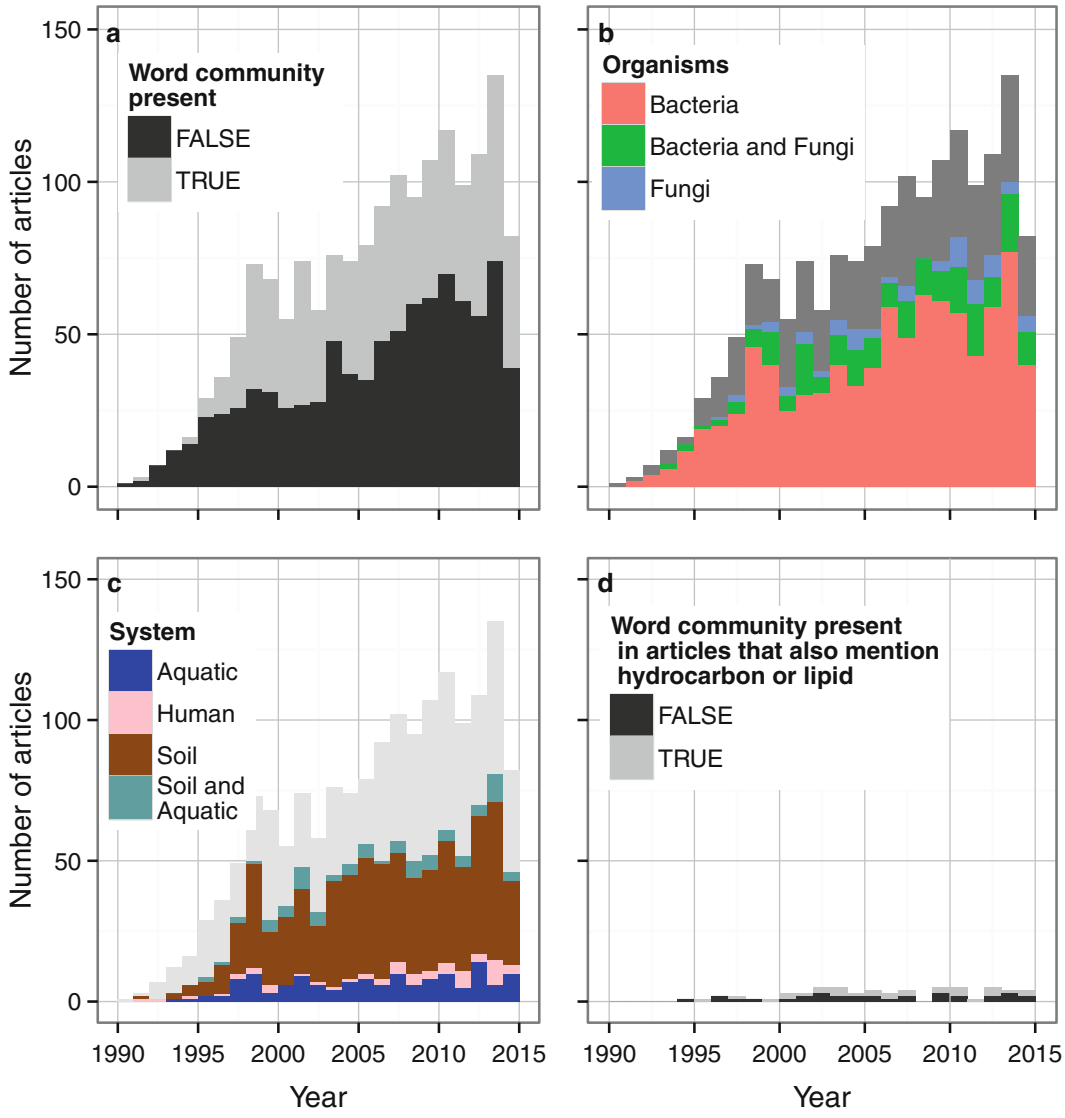

Fig. 1 The number of publications that mention "Biolog" and (**a**) those that also mention community. (**b**) Those that also mention bacteria, fungi or bacteria, and fungi. (**c**) Those that also mention keywords associated with specific biomes. (**d**) Those that also mention keywords relating to hydrocarbon and lipids and whether they also include the word "community." Search was conducted on Thomson Reuters "Web of Science" on September 9, 2014. Search was for documents of type article and review. Mention of "biolog " (**a**–**d**), "hydrocarbon" (**d**), and "lipid" (**d**) could be found within title, abstract, author keywords, and "Keywords Plus." Further keyword searches were done in the abstract of the documents containing the word "biolog." Search for the mention of community was done with the "communit*" root. For organisms, the following roots were used for the search: bacteria: bacter*, fungi:fung*, phytoplankton:phytopl*, protozoan:protozo*. Search for soil was with the roots soil*, sand*, clay*, rhizosphere; for aquatic with marine, lake*, river*, pond*, stream*, groundwater*; for human with human*, clinic*

In addition to allowing the characterization of strains and communities based on their substrate metabolism or growth condition preferences and capacities, microtiter plate-based phenotype arrays can help establish intrinsic physiological trade-offs in microorganism [16] and help characterize metabolic pathways [17]. Furthermore, using Biolog™ plates could help discover ecotypes that can have specific biodegradation capacities, within microorganism species [18].

1.3 Limitations and Critique

The use of culture-based characterization of microorganisms, including with Biolog™ plates, has faced widespread criticism, given the rise of genomic techniques for identification and characterization of microbial communities. The central critique revolves around our inability to culture most microorganisms in laboratory conditions [19, 20]. Therefore, our knowledge of communities arising from phenotyping arrays may be biased, since only types adapted to culturing conditions dominate the growth-based survey. In the future, in situ culture techniques [21] may extend the application of phenotyping arrays to recalcitrant microorganisms. Preston-Mafham et al. provide a thorough critique of the utilization of Biolog™ in the context of community characterization [19].

Firstly, the use of tetrazolium dye provides a measure of cellular respiration. It does not provide a measure of growth. This may be an advantage of dye-based assays, as catabolism by organisms that cannot grow in culture may still be detected. Reduction of the dye requires either cell surface reductase activity, in the case of net negatively charged dye molecules, or transportation of the dye into and back out of the cell, as in positively charged tetrazolium. Reduction of the dye 103 requires either cell surface reductase activity, in the case of net 104 negatively charged dye molecules, or transportation of the dye 105 into and back out of the cell, as in positively charged tetrazolium [24, 25]. Additional factors affecting the reduction of tetrazolium include the type of organism being assayed, the nature of its growth phase, metabolism, nutrient availability, as well as the overall growth conditions [11]. Different organisms can also experience different levels of dye toxicity and reduction capabilities that are unrelated to their growth, viability, and fitness in a particular test condition. Alternatives to the use of dyes include the measurement of cell density to measure growth and novel techniques directly measuring respiration in microplate wells [22, 23].

A further complication arises when dealing with the differential reduction capabilities of a community of microorganisms. This community analysis must take into account how each individual species of the community is able to reduce tetrazolium and how interspecies interactions and competition can be a confounding variable. Additionally, when dealing with soil samples, biological contaminants in these environmental samples can positively or negatively influence the reduction of the dye. Given the

multitude of possible confounding variables, it is paramount that these dye reduction-based approximations be adequately and independently verified.

An additional critique not often addressed in the utilization of Biolog™ is the proprietary nature of the technology, including substrate mixes and dye mixes, which hamper replicability and add unknown variables that may affect the overall results (*see* **Notes**).

2 Materials

2.1 Growth Vessel

2.1.1 Microtiter Plate

A large variety of microtiter plates exist in which custom phenotyping arrays can be assembled. Biolog™ assays are provided in polystyrene microtiter plates. Glass-coated or polypropylene (not optically transparent) microtiter plates should be used when a substrate included in the assay can dissolve polystyrene, such as chlorinated and aromatic hydrocarbon solvents. Optical transparency of the microplate is required for direct reading on a microplate reader and culture in nontransparent microplates (including polypropylene) requires transfer to adequate transparent plates, such as glass-coated polystyrene or quartz microplates.

2.1.2 Seal

To minimize edge effect in the microplate, the plate should be sealed with a gas-permeable membrane during growth (e.g., Aera-Seal™ and Breathe-Easy™ film). The membrane is removed and replaced with the optically transparent plate lid during optical density readings with the plate reader.

2.2 Chemicals

2.2.1 Substrates

Commercially available plates currently assay the ability of a strain to utilize metabolites such as common carbon sources, nitrogen sources (including peptides), phosphorus and sulfur sources, as well as nutrient supplements, osmolytes, and utilization of carbon sources in a range of pH conditions. Custom microplates can be assembled using target hydrocarbons and lipids in relevant concentrations.

2.2.2 Defined Growth Medium

Growth medium must be chemically defined and designed specifically for particular microplates, such that the fluid does not contain the target substrates. For example, the medium does not contain a carbon substrate if the microplate assay is surveying the inoculum's ability to utilize various carbon sources. The medium must not contain a reducing agent that could interact with the redox dye. For bacteria, the Biolog™ BUG medium is commonly used [2]; yeast nitrogen base with no carbon source (modified YNB) has been used for yeast [16] and Bold's Basal Medium (BBM) for the growth of heterotrophic algae (but *see* **Note** 2.1). Biolog™ provides a variety of inoculation fluids (IF) depending on the nature of the individual species or community being tested: media are available for gram-positive and gram-negative bacteria, filamentous fungus, anaerobic bacterium, yeast, and generalized communities.

2.2.3 Dyes

Most phenotype arrays rely on a redox dye to indicate hydrolytic activity on a given substrate. Most of these dyes are reduced to a form of formazan. Positively charged dyes are likely reduced within the cell, whereas negatively charged dye requires an intermediate electron donor and is reduced at the cell surface [24, 25]. Dye mix should be stored at −20°C and kept away from a light source.

2.3 Data Collection

2.3.1 Plate Reader

For Dye-Based Assays

A plate reader with filters or monochromator set to the specific wavelength of the formazan produced by the reduction of the dye indicated in Table 1. A second reading can be taken at 750 nm to account for background absorbance.

For Cell Density Approximation

The wavelength of optimal absorption will depend on the organisms studied and the substrates used. A wavelength around 660 nm is correlated with cell counts in yeast [16]. A wavelength of 700 nm was used for the measurement of fungal hyphae [8]. See Notes for use in algae. Alternative plate-based devices including particle counters and flow cytometer can provide direct measurement of cell counts and are not sensitive to the optical properties of the substrate.

3 Methods

Methods will vary based on cell types and phenotype array class. A generalized protocol that applies to most assays is presented.

3.1 Assay Preparation

Preparation of the assay environment includes preparation of the cells to be assayed, finding the optimal redox dye (*see* Table 1) and preparing the correct inoculation fluid mix for the type of assay being conducted. Defrost and prepare the dyes only immediately prior to use. Keep the dyes away from light.

3.1.1 Acclimation

Prior to inoculation into the phenotyping microarray, samples, especially ones taken directly from the field, should be acclimated to laboratory and microtiter liquid culture conditions. Samples should be cultured in similar 96-well microplates on permissive medium prior to the assay.

3.1.2 Starvation and Washing

Cells should be starved for the substrate category of interest prior to inoculation of array. This can be achieved by growing the cells in medium in which the substrate category is absent. To accelerate the starvation process, the cells can be washed using the impoverished media. Samples are placed in 5 ml micro-centrifuge tubes and pelleted down at 2,000 rpm for 10 min as to not damage the cellular integrity. The medium is then decanted and the cell

Table 1
Example redox indicator dyes

Name	Formula	Charge	[References] Read wavelength (nm)	Note
Tetrazolium violet (TV)	2,5-Diphenyl-3-(α-naphthyl) tetrazolium chloride	None	[25] 480 [26] 595 [27] 570 [28] 525	–
Nitroblue tetrazolium (NBT)	2,2-bis(4-Nitrophenyl) -5,5-diphenyl-3, 3-(3,3-dimethoxy-4, 4-diphenylene) ditetrazolium chloride	Positive	[29] 690 [28] 730 [30]	
Methylthiazolyldiphenyl-tetrazolium bromide (MTT)	2-(4,5-Dimethyl-2-thiazolyl) -3,5-diphenyl-2H-tetrazolium bromide	Positive	[24, 30] 570 [28] 575 [31] 540	
XTT	Sodium 2,3-bis (2-methoxy-4-nitro-5-sulfophenyl)-5-[(phenylamino)-tetrazolium inner salt	Negative	[24, 31, 32] 450 [33] 492	
WST-1	Sodium 5-(2,4-disulfophenyl) -2-(4-iodophenyl)-3 -(4-nitrophenyl)-2H-tetrazolium inner salt	Negative	[24] 450	–
Biolog™ Redox Dye Mix MA	Undisclosed	Depends on pH (reported by Biolog™)	590	Proprietary
Biolog™ Redox Dye Mix MB	Undisclosed	Depends on pH (reported by Biolog™)	590	Proprietary

resuspended in fresh medium or water. This process is repeated 3 times after which the cells are incubated in the impoverished medium or water. Cellular reserves naturally depend on cell type being assayed, but generally a 6–24 h starvation period applies to most microorganisms [17].

3.2 Inoculation

Low cell concentrations should be used as the redox dye reaction is very sensitive and the signal of the assays measuring growth in cell density directly will be enhanced by the number of cell divisions that can occur before carrying capacity is reached. The inoculum density should be known and kept stable between replicate experiments. For accurate cell densities, a hemocytometer, flow cytometer, or particle counter should be used.

3.3 Growth

Phenotyping arrays should be incubated in conditions near the organism's optimal growth conditions, including temperature range and adequate oxygen and carbon dioxide concentrations.

Incubation times vary with the species inoculated. Sufficient reduction of the dyes can generally be detected within 72 h. Measurements should be taken twice daily until maximum absorbance in each well has been maintained for at least two measurements at which point incubation can stop.

3.4 Measurement

Phenotyping arrays are measured using a microplate reader set to the dye read wavelength (Table 1). A second reading at 700 nm, where the reduced dye shows little absorption, measures absorption not related to the dye and this second reading is subtracted from the primary reading at the dye specific wavelength.

3.5 Analysis

3.5.1 Summarizing the Data

The first step in phenotyping array analysis is summarizing the data collected over time from each well. For arrays containing a dye, this is best done by calculating the area under the curve [34], though length of lag phase, slope of the increase in optical density and maximal optical density have all been used. When analyzing optical density data representing cell density in the absence of a dye, fitting a logistic growth curve to the data and extracting the biologically relevant parameters of growth rate (r) and carrying capacity (K) are the preferred summary methods.

3.5.2 Standardization

To account for variations between microplates, data can be standardized as deviations from the mean optical density across the plate or through standardization against a positive control substrate.

3.5.3 Analysis for Interpretation

The statistical analysis method used to interpret phenotyping array data depends on the purpose of the analysis. For the identification of species, the optical density pattern is compared to databases of patterns for known organisms, which can be done through least-squares optimization. In the study of communities using Biolog™ plates, principal component analysis (PCA) is the dominant analysis approach [19], though other multivariate methods can be used to compare communities, including linear discriminant analysis and random forest algorithms [35]. Phenotyping array data can be used in the calculation of phenotypic distance and thus construction of phenotype-based phylogenies.

3.5.4 Analysis Software

Biolog™ instruments provide analysis and identification software. Complete analysis solutions are available in the R language and environment for statistical computing [36]. The R package OPM [37] provides functions for the extraction of parameters from curves (lag phase, slope, maximum optical density, and area under the curve, including confidence intervals based on bootstrapping or

replication), the visualization of plates (plots for diagnostics on raw data, kinetic curve plots, diagnostic plots highlighting positive and negative controls, and heat map, and plots for interpretation of extracted data, correlation heat maps including innovative plotting methods [38, 39]), and information on substrates included in the Biolog™ plates with links to major chemical and biological annotation databases (CAS, KEGG, MeSH, and MetaCyc). For studies looking to link genomic (or metagenomic) data with phenotyping array data, the software suite DuctApe provides tools to summarize curve parameters (as an "activity" based on cluster analysis of curve shape parameters) and tools to correlate differential activity on specific substrates with the presence and absence of genes [2, 40].

4 Notes

4.1 An Example Experiment Comparing Biolog™ Results to In-House Phenotyping Array for the Characterization of Heterotrophic Microalgae

4.1.1 Introduction

This example experiment demonstrates the modifications required to phenotyping array protocols and some of the limitations of the approach. Results from Biolog™ plates were compared to equivalent phenotyping arrays we prepared for the characterization of divergently selected lines of *Chlamydomonas reinhardtii*, microalgae capable of autotrophic, mixotrophic, and heterotrophic growth.

Source samples arose from the experiments described by Bell 2012 [41] where replicate populations of *C. reinhardtii* were selected in purely heterotrophic conditions for several hundred generations. Cultures were grown in complete darkness and supplemented with the carbon source acetate. Ancestral strains have a rudimentary ability to metabolize acetate and their efficiency increases over time.

We investigated if these heterotrophically adapted lines could exploit carbon sources other than acetate, on which they had evolved. We used Biolog™ PM1 and PM2A plates, which contain a unique carbon source in each well. For a subset of substrates contained in the PM1 and PM2A plates, growth of the *C. reinhardtii* lines was also tested in non-Biolog™ microtiter plates.

4.1.2 Methods

Since Biolog™ plates are tailored to bacteria, testing the evolved lines of *C. reinhardtii* required the modification of Biolog™ published protocols.

Six *C. reinhardtii* evolve to grow heterotrophically on acetate in the dark were used in this experiment. Lines set aside for inoculation were transferred into 24-well microtiter plates and grown on acetate supplemented Bold's Basal Medium (BBM) in the dark [42]. Two transfers were done at 14-day intervals prior to testing. Samples were starved and washed per Sect. 3.1.2. Following resource starvation, lines were used to create an inoculation

suspension of 24 ml total volume in order to inoculate both PM1 and PM2A plates for each line being analyzed. 25 µl of starved cells and 320 µl of Dye mix D were added to 23.65 ml BBM. After adequately homogenizing the mixture, 100 µl of suspension was inoculated into both Biolog™ plates. A set of PM1 and PM2 plates were also inoculated with one of the lines, but without the addition of the dye, to allow the direct detection of growth. Plates were then placed in a dark chamber and optical density measurements taken after 14 days of incubation using BioTek instruments ELx800 microplate reader set at wavelength 620 nm for plates containing dye and at 405 nm for plates that did not contain the dye.

A subset of eight carbon sources was selected from the 190 surveyed for inclusion in the in-house assay. All eight carbon sources led to a reduction signal in the Biolog plate containing the dye. Acetate (acetic acid) was one of the eight carbon sources assayed both by Biolog™ and in-house assay. Acetate serves as a positive control as all lines used in this experiment are known to grow well when acetate is provided as sole carbon source. A gradient of concentrations ranging from 0 to 10 g/l for each carbon source was constructed on the 96-well plate. Results are presented for the 10 g/l of each carbon substrate, but the growth pattern across substrates was the same at all concentrations. BBM supplemented with the carbon sources was filter-sterilized using a Millex syringe-driven filter unit 33 mm size. Plates were read using a 405 nm absorption filter, which has been used for the measurement of cell density in *C. reinhardtii* [43].

Change in optical density from inoculation to after 14 days of incubation was used in analysis and figures.

4.1.3 Results

A reduction signal was detected across a large variety of carbon sources in Biolog™ plates containing the tetrazolium dye (Figs. 2a and 3). Growth was also detected across a large variety of carbon sources in Biolog™ plates that did not contain the tetrazolium dye (Figs. 2b and 3). Though there was no correlation between reduction and growth for the eight substrates also tested in the in-house assay (Fig. 2a, b), values in plates containing the dye and in plates not containing the dye were correlated across all 190 substrates in the PM1 and PM2 plates (Fig. 3, $F_{1,190} = 173.7$, $P < 0.0001$, $R^2 = 0.48$). However, no growth was consistently detected in the in-house microplates, independent of concentration of substrate, with the exception of growth detected in acetate (acetate; Fig. 2c). There was therefore no correlation between Biolog™ plate measurements of reduction, or growth, and in-house plate measurements of growth for the eight substrates tested.

4.1.4 Discussion

One of the potential issues with Biolog™ assays is that the biological activity detected using the tetrazolium dye is not an

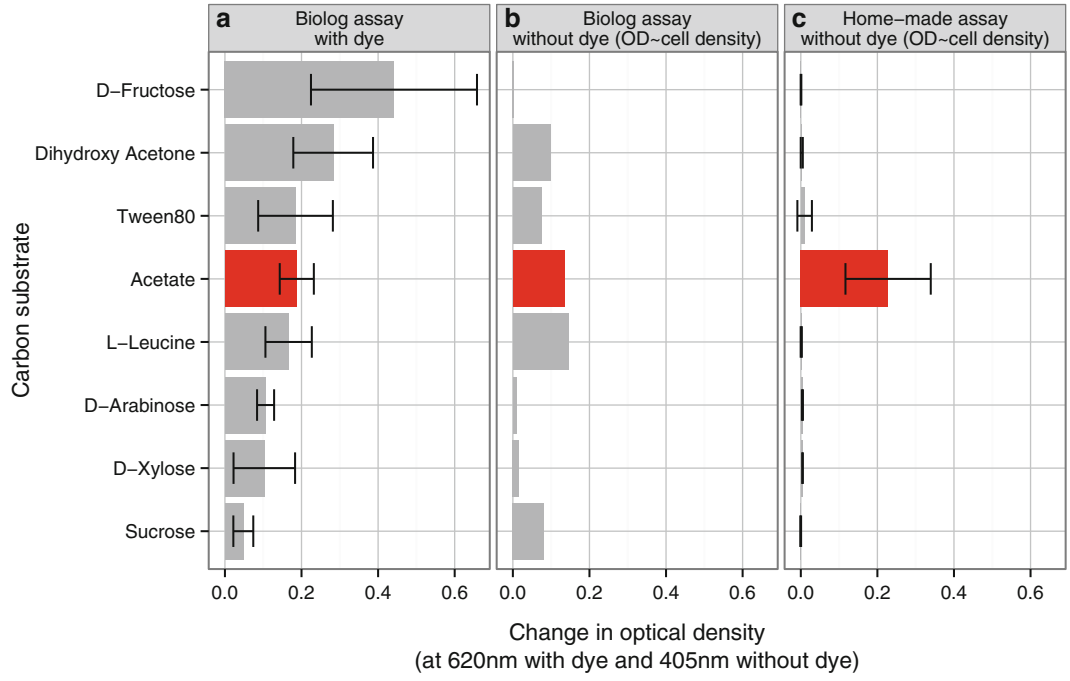

Fig. 2 Change in optical density for microalgae lines evolved for heterotrophic growth on acetate (values for acetate are highlighted in *red*) tested (**a**) in a commercial Biolog™ array containing the reduction detection dye, (**b**) a line tested in a commercial Biolog™ array in the absence of the reduction dye, (**c**) lines tested in a custom assemble "homemade" array. Substrates are in descending order of the average change in optical density in a commercial Biolog™ array containing the reduction detection dye. The average values are presented with error bars representing the 95% confidence intervals across lines

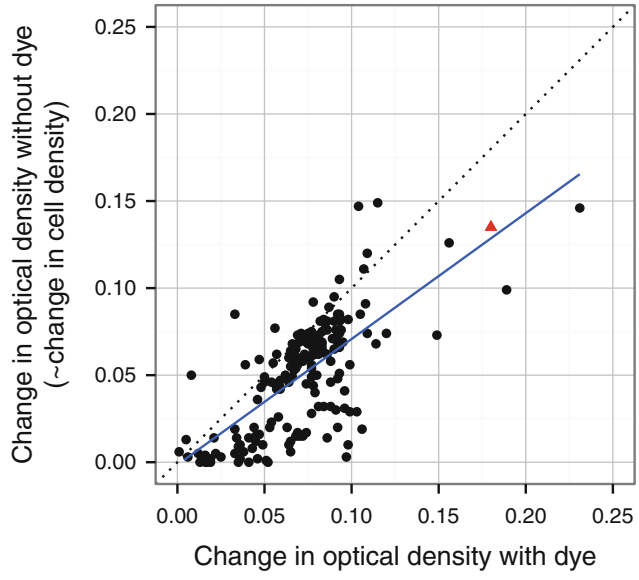

Fig. 3 Optical density in Biolog™ plates containing the reduction detection dye read at 620 nm (measurement of reduction) and in the absence of dye read at 405 nm (measurement of change in cell density). Each point is one of the 190 carbon substrates present in the PM1 and PM2 Biolog™ plates. The *red triangle* is the value for acetate. The *dotted line* represents the 1:1 line. The *full blue line* is the linear regression with $R^2 = 0.48$

indicator of the capacity of the organism to metabolize the substrate and grow. The correlation between measurements in plates containing the tetrazolium dye and those that did not contain the dye indicates that the measurement of reduction is at least a partial indicator of the potential for *C. reinhardtii* growth on a particular substrate.

A second potential limitation of Biolog plates is the proprietary nature of the substrate and dye mixes. The *C. reinhardtii* lines tested were evolved to grow heterotrophically on acetate, which could thus serve as positive control in our assays. All assays detected activity on acetate. However, both Biolog™ plates containing the reduction detection dye and those not containing the dye detected activity of the *C. reinhardtii* lines in substrates in which the lines did not grow in the homemade assay.

To date, we are unaware of literature using Biolog™ plates for the characterization of heterotrophic substrate utilization in algae. It is therefore possible that false-positive results may occur given the necessary experimental modifications to accommodate this new model organism. These modifications included use of an untested inoculation fluid (Bold's Basal Medium) and prolonged incubation periods.

The incubation time needed to be drastically increased, since these particular strains of *C. reinhardtii* require 1–2 weeks to reach carrying capacity in the dark. Seventy-two-hour incubation is usually used for Biolog™ plates and associated dye mix. There was a significant difference (t-test, $p < 0.001$, initial mean OD 0.12 SD 0.02 and final mean OD 0.16 SD 0.03) in the mean OD readings of the negative control, containing no substrate but containing the dye. However, the magnitude of this difference (0.04 OD units) represents only 1% of the average increase in optical density in wells containing a substrate. The effect of prolonged incubation times on the degradation of the tetrazolium dye therefore does not explain the extended activity detected in the Biolog™ plates. Furthermore, any changes in the dye would not provide an explanation for the expanded capacity of *C. reinhardtii* to grow on a diversity of substrates as indicated in the Biolog™ plates that did not contain the dye.

Without further information on the composition of Biolog™ plates, the determination of the discrepancy between findings in Biolog™ and in homemade assays will be difficult to determine.

5 Conclusion

Phenotyping assays, including Biolog™ plates, continue to be an invaluable tool in characterizing the unique chemical utilization or survival fingerprints of various strains of fungi and bacteria and may eventually be adapted for use with other microorganisms. Despite

its recent popularity and multiple uses, caution should be employed when analyzing results and applying the approach to organisms beyond bacteria and fungi. Ideally, a noncommercial phenotyping array should be assembled with defined chemical compositions to ensure replicability and mechanistic understanding of the response.

Acknowledgments

We thank Graham Bell, from McGill University, for supporting this research. Andrea Lofano and Pedram Samani were supported by a Discovery Grant from NSERC awarded to Graham Bell. Pedram Samani was also supported by a scholarship from FRQNT.

References

1. Wainwright M, Lederberg J (1992) History of microbiology. In: Encyclopedia of microbiology. Academic Press, Waltham, Massachusetts, pp 358–362
2. Viti C, Decorosi F, Marchi E, Galardini M, Giovannetti L (2015) High-throughput phenomics. In: Bacterial pangenomics. Springer, New York, pp 99–123. doi:10.1007/978-1-4939-1720-4_7
3. Lagier J-C, Hugon P, Khelaifia S, Fournier P-E, La Scola B, Raoult D (2015) The rebirth of culture in microbiology through the example of culturomics to study human gut microbiota. Clin Microbiol Rev 28(1):237–264
4. Bochner B (1989) Sleuthing out bacterial identities. Nature 339:157–158
5. Bochner BR, Savageau MA (1977) Generalized indicator plate for genetic, metabolic, and taxonomic studies with microorganisms. Appl Environ Microbiol 33(2):434–444
6. Garland JL, Mills AL (1991) Classification and characterization of heterotrophic microbial communities on the basis of patterns of community-level sole-carbon-source utilization. Appl Environ Microbiol 57 (8):2351–2359
7. Garland J (1997) Analysis and interpretation of community level physiological profiles in microbial ecology. FEMS Microbiol Ecol 24 (4):289–300
8. Atanasova L, Druzhinina IS (2010) Review: global nutrient profiling by Phenotype MicroArrays: a tool complementing genomic and proteomic studies in conidial fungi. J Zhejiang Univ Sci B 11(3):151–168
9. Maila MP, Randima P, Drønen K, Cloete TE (2006) Soil microbial communities: influence of geographic location and hydrocarbon pollutants. Soil Biol Biochem 38:303–310
10. Kaufmann K, Christophersen M, Buttler A, Harms H, Höhener P (2004) Microbial community response to petroleum hydrocarbon contamination in the unsaturated zone at the experimental field site Værløse, Denmark. FEMS Microbiol Ecol 48:387–399
11. Wünsche L, Brüggemann L, Babel W (1995) Determination of substrate utilization patterns of soil microbial communities: an approach to assess population changes after hydrocarbon pollution. FEMS Microbiol Ecol 17:295–305
12. Juck D, Charles T, Whyte LG, Greer CW (2000) Polyphasic microbial community analysis of petroleum hydrocarbon-contaminated soils from two northern Canadian communities. FEMS Microbiol Ecol 33:241–249
13. Mansur A, Adetutu EM, Kadali KK, Morrison PD, Nurulita Y, Ball AS (2014) Assessing the hydrocarbon degrading potential of indigenous bacteria isolated from crude oil tank bottom sludge and hydrocarbon-contaminated soil of Azzawiya oil refinery, Libya. Environ Sci Pollut Res 2014:10725–10735
14. McKew B, Coulon F, Osborn M, Timmis KN, McGenity TJ (2007) Determining the identity and roles of oil-metabolizing marine bacteria from the Thames estuary, UK. Environ Microbiol 9(1):165–176
15. Johnsen AR, Bendixen K, Karlson U (2002) Detection of microbial growth on polycyclic aromatic hydrocarbons in microtiter plates by using the respiration indicator WST-1. Applied and Environmental Microbiology 68(6):2683–2689. doi:10.1128/AEM.68.6.2683-2689.2002
16. Samani P, Low-Decarie E, McKelvey K et al (2015) Metabolic variation in natural populations of wild yeast. Ecol Evol 5 (3):722–732

17. Lee C, Russell NJ, White GF (1995) Rapid screening for bacterial phenotypes capable of biodegrading anionic surfactants: development and validation of a microtitre plate method. Microbiology 141(11):2801–2810
18. Oberhardt M, Puchałka J, Fryer KE, Martins dos Santos VP, Papin J (2008) Genome-scale metabolic network analysis of the opportunistic pathogen *Pseudomonas aeruginosa* PAO1. J Bacteriol 190(8):2790–2803
19. Preston-Mafham J, Boddy L, Randerson PF (2002) Analysis of microbial community functional diversity using sole-carbon-source utilisation profiles – a critique. FEMS Microbiol Ecol 42(1):1–14
20. Ritz K (2007) The plate debate: cultivable communities have no utility in contemporary environmental microbial ecology. FEMS Microbiol Ecol 60(3):358–362
21. Ling LL, Schneider T, Peoples AJ et al (2015) A new antibiotic kills pathogens without detectable resistance. Nature 517:455–459
22. Rogers GW, Brand MD, Petrosyan S et al (2011) High throughput microplate respiratory measurements using minimal quantities of isolated mitochondria. PLoS One 6(7), e21746
23. Deshpande RR, Koch-Kirsch Y, Maas R, John GT, Krause C, Heinzle E (2005) Microplates with integrated oxygen sensors for kinetic cell respiration measurement and cytotoxicity testing in primary and secondary cell lines. Assay Drug Dev Technol 3(3):299–307
24. Berridge MV, Herst PM, Tan AS (2005) Tetrazolium dyes as tools in cell biology: new insights into their cellular reduction. Biotechnol Annu Rev 11(05):127–152
25. Tachon S, Michelon D, Chambellon E et al (2009) Experimental conditions affect the site of tetrazolium violet reduction in the electron transport chain of *Lactococcus lactis*. Microbiology 155(Pt 9):2941–2948
26. Anderson SA, Sissons CH, Coleman MJ, Wong L (2002) Application of carbon source utilization patterns to measure the metabolic similarity of complex dental plaque biofilm microcosms. Appl Environ Microbiol 68 (11):5779–5783
27. Tracy BS, Edwards KK, Eisenstark A (2002) Carbon and nitrogen substrate utilization by archival Salmonella typhimurium LT2 cells. BMC Evol Biol 2:14
28. Altmann FP (1969) The use of eight different tetrazolium salts for a quantitative study of pentose shunt dehydrogenation. Histochemie 19(4):363–374
29. Vera-Jimenez NI, Pietretti D, Wiegertjes GF, Nielsen ME (2013) Comparative study of β-glucan induced respiratory burst measured by nitroblue tetrazolium assay and real-time luminol-enhanced chemiluminescence assay in common carp (*Cyprinus carpio* L.). Fish Shellfish Immunol 34(5):1216–1222
30. Mosmann T (1983) Rapid colorimetric assay for cellular growth and survival: application to proliferation and cytotoxicity assays. J Immunol Methods 65(1-2):55–63
31. Scudiero DA, Shoemaker RH, Paull KD et al (1988) Evaluation of a soluble tetrazolium/formazan assay for cell growth and drug sensitivity in culture using human and other tumor cell lines. Cancer Res 48 (17):4827–4833
32. Meshulam T, Levitz SM, Christin L, Diamond RD (1995) A simplified new assay for assessment of fungal cell damage with the tetrazolium dye, (2,3)-bis-(2-methoxy-4-nitro-5-sulphenyl)-(2H)-tetrazolium-5-carboxanil ide (XTT). J Infect Dis 172(4):1153–1156
33. Kuhn DM, Balkis M, Chandra J, Mukherjee PK, Ghannoum MA (2003) Uses and limitations of the XTT assay in studies of Candida growth and metabolism. J Clin Microbiol 41 (1):506–508
34. Guckert J, Carr G, Johnson T (1996) Community analysis by Biolog: curve integration for statistical analysis of activated sludge microbial habitats. J Microbiol Methods 27:183–197
35. Smith A, Sterba-Boatwright B, Mott J (2010) Novel application of a statistical technique, Random Forests, in a bacterial source tracking study. Water Res 44(14):4067–4076
36. R Development Core Team (2009) R: a language and environment for statistical computing. R Development Core Team. Is software. Vienna, Austria
37. Vaas LI, Sikorski J, Hofner B et al (2013) Opm: an R package for analysing OmniLog® phenotype microarray data. Bioinformatics 29(14):1823–1824
38. Jacobsen JS, Joyner DC, Borglin SE, Hazen TC, Arkin AP, Bethel EW (2007) Visualization of growth curve data from phenotype microarray experiments. In: Proceedings of the international conference on information visualisation. Zürich, Switzerland, pp 535–544
39. Vaas LI, Sikorski J, Michael V, Göker M, Klenk H-P (2012) Visualization and curve-parameter estimation strategies for efficient exploration of phenotype microarray kinetics. PLoS One 7 (4):e34846

40. Galardini M, Mengoni A, Biondi EG et al (2014) DuctApe : a suite for the analysis and correlation of genomes and Omnilog TM phenotype microarray data. Genomics 103 (1):1–10
41. Bell G (2013) Experimental evolution of heterotrophy in a green alga. Evolution 67 (2):468–476
42. Stein JR (1979) Handbook of physiological methods: culture methods and growth measurements. Cambridge University Press, Cambridge
43. De Visser JGM, Hoekstra RF, Van Ende H Den, De Visser A (1997) An experimental test for synergistic epistasis and its application in *Chlamydomonas*. Genetics 145(3): 815–819

Laboratory Protocols for Investigating Microbial Souring and Potential Treatments in Crude Oil Reservoirs

Yuan Xue, Gerrit Voordouw, and Lisa M. Gieg

Abstract

Oilfield souring is most frequently caused by the activities of sulfate-reducing microorganisms as they reduce sulfate to sulfide as their terminal electron-accepting process. Souring poses serious health and safety hazards to oilfield workers and can be detrimental to oil production processes by potentially plugging reservoirs and/or leading to infrastructure corrosion. Oilfield souring often occurs during secondary recovery operations based on waterflooding, especially when the water source contains an ample amount of sulfate that can stimulate sulfate reducers associated with the reservoir or other locations within an oil recovery operation (such as topside facilities). Water chemistry, temperature, potential carbon sources, and microbial communities all play a role in determining whether souring will occur in a given field. Approaches such as biocide, nitrate, or, most recently, perchlorate treatments have shown good success in controlling souring in laboratory experiments and/or in field applications. This chapter outlines a variety of protocols that can be used in a laboratory setting to study souring potential in a given oilfield and to test methods of souring control that may be applied to that field or oilfields in general. Methods of field sample collection, water chemistry analyses, microbiological analyses, and laboratory incubation strategies are described.

Keywords: Biocides, Column studies, Crude oil reservoir, Microcosms, Nitrate, Souring, Sulfate reducers, Sulfide

1 Introduction

Souring, the production of sulfide (that exists as S^{2-}, HS^-, and/or H_2S depending upon pH) by sulfate-reducing microorganisms, is a detrimental process that commonly occurs during crude oil recovery operations [1, 2]. These sulfide-producing anaerobic microorganisms can be *Bacteria* (referred to as SRB) or *Archaea* (referred to as SRA) and are often collectively referred to as sulfate-reducing prokaryotes (SRP) to account for sulfate reducers in both domains [3]. When sulfate is present in oil reservoirs, these microbes reduce sulfate as their terminal electron accepter to sulfide [4, 5] coupled with the oxidation of various electron donors such as H_2, volatile fatty acids (VFA) such as acetate, and crude oil hydrocarbons [2, 6, 7]. Souring can also arise from abiotic phenomena

T.J. McGenity et al. (eds.), *Hydrocarbon and Lipid Microbiology Protocols*, Springer Protocols Handbooks, (2017) 183–210, DOI 10.1007/8623_2015_115, © Springer-Verlag Berlin Heidelberg 2015, Published online: 15 July 2015

including thermochemical sulfate reduction [8], hydrolysis of S-containing organic compounds [9], or dissolution of pyrite [2]. However, most reports and studies attribute souring to biotic processes [6, 10].

Sulfide production in oilfield operations poses a serious safety and health hazard for oilfield personnel and the surrounding environment [11]. Operationally, produced sulfide increases total sulfur content in produced oil and can lead to plugging problems [6]. Souring can also lead to microbially influenced corrosion due to the corrosivity of formed iron sulfides and related sulfur compounds on oil operation infrastructure [12] and often requires specialized and costly sour service infrastructure materials. Souring occurs mainly as the result of waterflooding during secondary oil recovery wherein water is injected into a reservoir to sustain pressure and help mobilize crude oil [2, 6, 10]. Before waterflooding, souring is not obvious because SRP are dormant or act as fermenters with little sulfide production due to the scarcity of sulfate [13]. However, waterflooding may initiate souring, especially if seawater is used that contains a high concentration of sulfate (up to 25–30 mM). In addition, injection water can add carbon sources and nutrients including nitrogen and phosphate, as well as exogenous sulfate reducers into the reservoir [14]. As the injected electron acceptors mix with the electron donors in the formation water in the near-injection wellbore region, SRP are activated and reduce sulfate to sulfide to cause souring [15, 16]. Therefore, the chemistry of the injection water is a major factor that can influence the onset of souring [17, 18]. All seawater-flooded fields examined have been deemed sour to some degree [19].

Temperature is also an important factor influencing souring as it may impact microbial growth. In general, SRB are most active at temperatures below 80°C; thus, reservoirs with higher downhole temperatures (e.g., >100°C) should in principle not experience souring. However, the risks of souring in high-temperature reservoirs are not negligible, because the mixing of cold injection water containing sulfate (such as seawater) with hot formation waters in these reservoirs creates a temperature gradient that may be suitable for SRB growth, especially in the near-injection wellbore region. In general, low-temperature oil reservoirs are more prone to be sour than high-temperature oil reservoirs. Souring can also be a problem in topside (surface) facilities if sulfate-containing water/oil mixtures are stored at mesothermic conditions [20].

To control souring in oilfields, many methods have been developed including physical, chemical, and mechanical approaches. Chemical treatment is most frequently used and involves the addition of biocides or nitrate to control microbial growth and thus mitigate souring [2, 21]. Biocides are broad-spectrum antimicrobial agents, specially designed to kill bacteria in a very efficient way. Biocides used in the oil industry can be divided into

two classes: (1) nonoxidizing biocides such as glutaraldehyde, quaternary ammonium compounds (quats), cocodiamine, and THPS and (2) oxidizing biocides such as chlorine dioxide, hypochlorite, peracetic acid, and ozone [22]. In spite of their high efficiency, the application of biocides is usually limited to aboveground infrastructure to control biocorrosion and biofouling and is rarely implemented in oil reservoirs to control souring because biocides are poorly transported in reservoirs. In addition, repeating dosing of biocides over long periods of time is very costly and increases microbial resistance [2]. Compared to biocides, nitrate injection is relatively cheap and environmental friendly as nitrate is water-soluble, compatible with other chemicals, and does not bind to reservoir rocks, which enables nitrate to penetrate deeper into reservoirs. There are several mechanisms accounting for the control of souring by nitrate: (1) biocompetitive exclusion driven by the competition between heterotrophic nitrate-reducing bacteria (hNRB) stimulated by nitrate addition and SRB for the same electron donors [23]; (2) scavenging of sulfide by sulfide-oxidizing nitrate-reducing bacteria (soNRB) [24, 25] and by nitrite, the intermediate of nitrate reduction [26, 27]; and (3) the inhibition of sulfite reduction by nitrite [25, 28, 29]. Recently, perchlorate has been shown to be an effective alternate electron acceptor that may be used to control souring [30].

Field trials using nitrate and/or biocides to control souring have shown great success in both offshore and onshore oilfields. For example, in the Skjold oilfield located in the Danish sector of the North Sea, souring was first observed in the same year as waterflooding (primarily seawater) was initiated in 1985. Nitrate injection reduced up to 80 % of sulfide production in an individual well pair, and field-wide nitrate injection was successful in preventing increased sulfide production expected based on a logistical growth model [18]. The Medicine Hat Glauconitic C (MHGC) oilfield, located in Western Canada, is a shallow, low-temperature, and land-locked oil reservoir, in which souring was first detected 6 years after the onset of waterflooding. Field-wide injection of 2 mM nitrate decreased sulfide production by 70 % in the first 7 weeks following injection. However, a recovery of sulfide production was observed following the initial inhibition, which was explained by the establishment of microbial zonation, where NRB reduce nitrate in the near-injection wellbore region followed by SRB reducing sulfate to sulfide deeper into the reservoir [31]. A subsequent pulsed injection involving higher nitrate concentrations was shown to overcome this zonation to control souring in an individual production well [31].

Many of the successes of field trials were initially based on laboratory experiments using produced oilfield waters designed to understand and control souring. While key microorganisms to identify and monitor for souring studies are sulfate reducers,

other organisms whose activities often require monitoring when nitrate is used are hNRB and soNRB, for example; other microbes such as metal or perchlorate reducers can also be monitored if needed [21]. This chapter describes sampling protocols, produced water analysis, and various laboratory-based approaches that can be used to assess biological souring potential in crude oil reservoirs and methods of its control that may ultimately help inform field operations to control souring. Please note that these protocols are largely based on our own experiences and may not reflect the entire suite of tools used by all researchers worldwide to study biological souring of reservoirs, e.g., radiolabeled assays [16].

2 Materials (*See* Note 1)

2.1 Sampling Produced Waters from Crude Oil Reservoirs

Produced water samples can readily be obtained from most oilfield operations in order to study microbial souring and its control in laboratory experiments. To obtain such samples, it is necessary to collaborate with industry partners and to work with field-trained oilfield operators, as rigorous, mandated safety protocols are in place. To accompany operators at a field site to view and potentially help with sampling, hazard safety training (e.g., "H_2S Alive" in Canada) and appropriate personal protective gear such as safety glasses, hard hats, fire-resistant coveralls, and steel-toed boots are required. In many cases, however, field locations are remote and in-person sampling cannot be arranged; thus, materials (e.g., sampling bottles) can be shipped to field operators along with detailed written protocols (*see* Sect. 3.1) for sample collection:

1. Larger-sized sterile sampling bottles with screw-capped lids having blank affixed labels for sampling larger volumes of produced water to establish laboratory incubations (e.g., 1 L); bottles can be glass or Nalgene™. If shipping samples is required, Nalgene™ bottles are preferred in order to maintain sample integrity (e.g., minimize bottle breakage).
2. Smaller-sized vessels with screw-capped lids having blank affixed labels for collecting smaller volumes of produced water that can be frozen immediately to store for DNA analysis (e.g., 50–250 mL) such as Falcon™ tubes.
3. Ice or dry ice (preferable) in a cooler for sample storage.
4. Gloves and other specified safety gear
5. Optional: Commercially available analytical field kit to do immediate on-site sulfide determinations (*see* **Note 2**).

2.2 Sample Water Chemistry Analysis

It is recommended that a well-working anaerobic glove bag be used to process field samples and for the preparation of some reagents (indicated below). However, if a glove bag is not available, samples

can be opened and processed in a fume hood (due to potential sulfide and hydrocarbon vapors) under a blanket of N_2. Similarly, reagents can be prepared on the bench (ideally in a fume hood) under an N_2 blanket. Please note that unless specified, the majority of chemicals used for the various assays can be purchased from any chemical supplier of choice.

2.2.1 Sulfide Analysis by Spectrophotometric Determination ***(See Note 3)***

1. Anaerobic glove bag (e.g., from Coy Laboratories, www.coylab.com)
2. Glass tubes with rubber-lined screw caps for solution preparation and assay (e.g., 16 × 150 mm, Fisher Scientific, #14-959-25D)
3. Glass serum bottles (e.g., 160-mL bottle for preparation of sulfide stock solution; 40-mL bottles for sulfide calibration standards) (Wheaton, www.wheaton.com)
4. Sodium sulfide ($Na_2S{\cdot}9H_2O$) (keep stored in a dessicator)
5. Sodium hydroxide (NaOH)
6. *N*-, *N*-Dimethyl-*p*-phenylenediamine HCl solution (DMPD)
7. Concentrated sulfuric acid
8. Zinc acetate dihydrate
9. Ferric chloride ($FeCl_3$)
10. Deionized water (such as MilliQ™ or NanoPure™ water)
11. UV/VIS spectrophotometer (e.g., Shimadzu Model UV-1800)
12. Disposable plastic cuvettes
13. Glass pipets
14. Sterile forceps
15. Automatic, adjustable volume pipettors (e.g., Gilson, Eppendorf, 100/200 and 1,000 μL capacities) and pipet tips
16. Kimwipes™

2.2.2 Ammonium Analysis by Spectrophotometric Determination

1. Deionized water (such as MilliQ™ or NanoPure™ water)
2. Phenol
3. Sodium nitroprusside (e.g., RICCA Chemical Co. #7498-32)
4. Sodium hydroxide (NaOH)
5. Sodium hypochlorite (10–14 %, NaClO, Sigma #425044-200 mL)
6. Ammonium chloride (NH_4Cl)
7. UV/VIS spectrophotometer (e.g., Shimadzu Model UV-1800)
8. Disposable plastic cuvettes

9. Automatic, adjustable volume pipettors (e.g., Gilson, Eppendorf, 100/200 and 1,000 μL capacities) and pipet tips
10. Microfuge tubes (1.5 mL)

2.2.3 Sulfate Analysis by Spectrophotometric Determination

1. Deionized water (such as MilliQ™ or NanoPure™ water)
2. Barium chloride ($BaCl_2$) dihydrate
3. Ethanol, 95 %
4. Concentrated HCl
5. Sodium chloride (NaCl)
6. Glycerol
7. Anhydrous sodium sulfate
8. UV/VIS spectrophotometer (e.g., Shimadzu Model UV-1800)
9. Disposable plastic cuvettes
10. Automatic, adjustable volume pipettors (e.g., Eppendorf, 100/200 and 1,000 μL capacities) and pipet tips
11. Microfuge tubes (1.5 mL)

2.2.4 Liquid Chromatography Analysis to Determine Sulfate, Nitrate, Nitrite, Chloride, and VFA Concentrations ***(See Note 4)***

1. Liquid chromatograph (LC) system equipped with a conductivity detector and a UV detector (e.g., Thermo Scientific™ Dionex™ Model ICS-5000)
2. Appropriate column for analyzing anions such as sulfate, nitrate, nitrite, chloride (e.g., IonPac AS18 column, #060549, Thermo Scientific)
3. Appropriate column for analyzing volatile fatty acids such as acetate, propionate, butyrate (e.g., Acclaim OA column, #062902, Thermo Scientific)
4. Appropriate solvents to prepare mobile phases (e.g., MilliQ™ or NanoPure™ water, buffers of various salt compositions, HPLC-grade solvents such as acetonitrile, methanol, etc.)
5. Appropriate autosampler vials
6. Automatic, adjustable volume pipettors (e.g., Gilson, Eppendorf, 100/200 and 1,000 μL capacities) and pipet tips
7. Disposable plastic syringes, 1 mL (e.g., from BD, Franklin Lakes, NJ, www.bd.com)
8. Microfuge tubes
9. Microcentrifuge (e.g., Eppendorf model 5424).
10. Syringe filters (e.g., 13 mm, 0.2 μm PTFE membranes, e.g., from VWR # 28145-491)
11. Appropriate stock solutions for analytes (e.g., for sulfate, nitrate, nitrite, chloride, acetate, usually prepared from the sodium salts of these compounds in deionized water). For the particular columns listed above, calibration curves for these are prepared ranging from 0 to 500 μM

2.3 Sample Microbiological Activity and Composition

2.3.1 Enumeration by the Most-Probable-Number (MPN) Method

Commercially available media bottles are available for determining microbial counts for SRB (e.g., ZAPI-5, Dalynn Biologicals, www.dalynn.com/dyn). Alternatively, MPN tubes for SRB assays (or for other microbial groups) can be prepared in the laboratory using the following materials:

1. Balch tubes (18 × 150 mm anaerobic glass tubes) (e.g., Bellco, #2048-00150)
2. Blue butyl rubber septum stoppers (20 mm) (e.g., Bellco, #2048-11800A)
3. Aluminum crimp seals and crimper (Wheaton, # 229193-01, #225303)
4. Anoxic medium for SRB (or media for enumerating other groups) (*see* **Note 5**)
5. Syringes and needles for inoculating and sampling incubations (e.g., 21G × 2 [0.8 mm × 50 mm] PrecisionGlide™ needles and 1–5-mL disposable plastic syringes e.g., from BD, Franklin Lakes, NJ, www.bd.com)

2.3.2 Microbial Activity Determination (**See Note 6**)

1. Glass serum bottles (recommended, 120- or 160-mL size, Wheaton, www.wheaton.com)
2. Anoxic medium for SRB or other microbial groups (*see* **Note 5**)
3. Blue butyl rubber septum stoppers (20 mm) (e.g., Bellco, # 2048-11800A)
4. Aluminum seals and crimper (Wheaton, # 229193-01, #225303)
5. Syringes and needles for inoculating and sampling incubations (e.g., 21G × 2 [0.8 mm × 50 mm] PrecisionGlide™ needles and 1–5-mL disposable plastic syringes e.g., from BD, Franklin Lakes, NJ, www.bd.com)
6. Reagents and supplies for measuring sulfate, sulfide, and other microbial indicators (depending on experiment) as outlined in this chapter
7. Incubators at appropriate temperatures

2.3.3 DNA Extraction and PCR Amplification for Total Microbial Community Composition

1. Commercially available DNA extraction kit (e.g., Fast DNA Spin Kit for Soil, MP Biomedicals, Solon, OH, www.mpbio.com)
2. Sample homogenizer (bead beater) (e.g., FastPrep® Instrument, MP Biomedicals, Solon, OH, www.mpbio.com)
3. Microcentrifuge (e.g., Eppendorf model 5424)
4. Instrument for measuring DNA concentration (e.g., such as a fluorometer [Qubit®, www.lifetechnologies.com]) and required reagents (for Qubit®, Quant-iT™ dsDNA HS kit, #Q32854, Invitrogen™, Life Technologies, Burlington, ON, www.lifetechnologies.com)

5. Thermocycler (e.g., BioRad Model S1000)
6. TopTaq PCR kit (e.g., from Qiagen, #200205) (includes Taq, buffers, and salt solutions for PCR amplification)
7. dNTPs, PCR grade (100 mM each dNTP, Qiagen #201913)
8. Nuclease-free water (e.g., from Invitrogen™, Life Technologies, Burlington, ON, www.lifetechnologies.com)
9. Agarose
10. SYBR®safe gel stain (10,000X conc. in DMSO, Invitrogen #533102)
11. QIAquick PCR Purification Kit (Qiagen, #28106)
12. DNA concentration cups (Amicon Ultra-0.5 Centrifugal Filters Ultracel-30K, EMDMillipore)

2.4 Laboratory Incubations to Assess Microbial Souring and Its Control

The materials listed below are for establishing either serum bottle or column incubations. Please note that other supplies needed to monitor souring and treatment experiments such as for sulfide analysis, microbial community analysis, etc. are described above.

2.4.1 Serum Bottle Incubations

1. Glass serum bottles (recommended, 120- or 160-mL size, Wheaton, www.wheaton.com)
2. Blue butyl rubber septum stoppers (20 mm) (e.g., Bellco, #2048-11800A)
3. Aluminum seals and crimper (Wheaton, # 229193-01, #225303)
4. Sterile pipets for sample distribution into serum bottles
5. Anoxic sulfate (Na_2SO_4) and/or substrate stock solutions
6. Anoxic solutions of treatment chemicals (e.g., $NaNO_3$, biocides)
7. Syringes and needles for adding stock solutions and sampling incubations (e.g., 21G × 2 [0.8 mm × 50 mm] Precision-Glide™ needles and 1–5-mL disposable plastic syringes e.g., from BD, Franklin Lakes, NJ, www.bd.com)

2.4.2 Column Incubations

Column Assembly

1. Glass or plastic columns (e.g., 20- or 30-cc glass tip syringes, Cadence Science #5036; 20- or 30-mL disposable plastic syringes, from BD, Franklin Lakes, NJ, www.bd.com) (*see* **Note 7**)
2. Polymeric mesh
3. Cutting tool (e.g., scissors)
4. Glass wool
5. Forceps
6. Sand of appropriate grain size (e.g., from Sigma-Aldrich, www.sigmaaldrich.com with the size of 50–70 mesh particle; *see* **Note 8**)

7. Scoop utensil (e.g., metal spoon) for loading the sand into columns
8. Perforated rubber stoppers tightly fitted with a glass or plastic connector
9. Three-way Luer-Lock valves (e.g., from Cole-Parmer, #RK-30600-02)
10. Zip ties
11. Weighing balance and weight boats

Flow Path Setup

1. Retort stands attached with clamps
2. Multichannel pump (e.g., peristaltic pump MINIPULS® 3, Gilson Inc., Middleton, WI, www.gilson.com) (*see* **Note 9**)
3. Tubing and tubing connectors (e.g., from Gilson Inc., Middleton, WI, www.gilson.com) (*see* **Note 10**)
4. Autoclavable glass bottles for acting as medium storage and waste containers (e.g., PYREXPLUS® media bottles, VWR International, www.vwr.com)
5. Metal fittings/connecters for connecting medium containers, waste vessels, or column with the end of tubing path
6. Perforated rubber stoppers
7. Equipment for anoxic maintenance of columns (e.g., anaerobic chamber containing 90 % N_2 and 10 % CO_2, N_2–CO_2 gas cylinders containing 90 % N_2 and 10 % CO_2 or syringes filled up with anaerobic gas and attached with needles able to penetrate rubber stoppers capping the medium/waste containers)

Biofilm Establishment

1. Sterile anoxic minimal medium (*see* **Note 11**)
2. Sulfate-reducing culture or production well fluids (*see* **Note 12**)
3. Syringes with gradient for inoculation of sulfate-reducing culture
4. Instruments and reagents for sulfate and sulfide assays (and/or nitrate, nitrite, ammonium, VFA analysis) as outlined in this chapter

3 Methods

3.1 Sampling Produced Waters from Crude Oil Reservoirs

Whether sampling in person in conjunction with an oilfield operator or sending supplies to remote locations for sampling to be conducted by operator personnel, the sampling protocol outline below is recommended to maintain anoxic samples so that accurate sulfide measurements can be made and microbial communities are as representative of the sampled field as possible (*see* **Note 13**).

These protocols can be used to collect produced waters from any oilfield for a wide variety of microbiological studies.

1. Open the sampling valve at a production well and allow approximately 1 L of fluids to flow out into a waste vessel in order to flush stagnant fluids from the line.
2. Open a large sterile sampling bottle, taking care not to touch the inside of the screw cap lid or threads on the bottle to help maintain sterility. To minimize collecting air bubbles into the sample, slowly add production water fluid into the bottle and allow sample to fill to the brim (even to overflowing if possible) and immediately close the sample bottle with the sterile lid. Filling to the brim helps to maintain an anoxic sample. Some crude oil may also be collected in the bottle (*see* **Note 14**).
3. Label the sample bottle with the well number, sampling dates, type of sample, etc., with a non-water-soluble marker.
4. Record any available metadata regarding the samples such as temperature, depth, pH, location, etc., as this information can help with data interpretation.
5. Collect fluids in a similar manner into smaller sterile vessels.
6. Place the smaller sample vessels on ice/dry ice for shipment or transport back to the laboratory. Larger sample vessels can be transported/shipped at ambient temperatures.

3.2 Sample Water Chemistry

Upon arrival in the laboratory, samples should be placed immediately into an anaerobic glove bag for processing and analysis. Sulfide should be measured immediately following the opening of samples so as to minimize sulfide volatilization that would result in an underestimation of sulfide concentrations. Ammonium analysis, if desired, should also be done as soon as possible after opening the sample bottles as concentrations of this analyte may also change with storage at ambient temperatures (*see* **Note 15**). Subsamples for other analyses (e.g., sulfate, nitrate, nitrite, chloride, VFA, microbial communities) can be removed at this time as well and can be frozen at −20°C until analyses can be performed (*see* **Note 15**). Subsamples for microbial community analysis should be placed into sterile tubes (e.g., 2-mL microfuge tubes or larger tubes such as 50-mL Falcon™ tubes) as required.

3.2.1 Sulfide Analysis by Spectrophotometric Determination

Preparation of Reagents and Calibration Standards

Sulfide stock solution (e.g., to prepare a 1,000 mg/L stock solution in a 100-mL volume)

1. To prepare an anoxic 0.01 M NaOH stock solution, first boil approximately 120-mL deionized water to remove dissolved oxygen and cool (on ice) under a N_2 blanket.
2. While the water is cooling, weigh out 0.04-g NaOH, place into a 160-mL serum bottle, and flush with N_2.

3. Also while water is cooling, gently rinse crystals of $Na_2S{\cdot}9H_2O$ with deionized water and blot dry with a Kimwipe™. Weigh out 0.0749 g into a weigh boat and cover with foil.
4. Once water has cooled to the touch, dispense 100-mL aliquot into the N_2-flushed serum bottle containing the pre-weighed NaOH and close with a butyl rubber stopper. Bring this NaOH solution and the pre-weighed sodium sulfide into an anaerobic glove bag.
5. Open serum bottle and add pre-weighed sodium sulfide. Close bottle with butyl rubber stopper and remove from glove bag. Crimp-seal with aluminum seals and autoclave. Sulfide stock solutions can be stored up to 1 year in an anaerobic glove bag.

Sulfide Calibration Standards

1. Sterilize serum bottles (e.g., 40-mL size) wrapped with aluminum foil at the opening along with the correct number of butyl rubber stoppers (added to a beaker and wrapped with foil at the opening).
2. To prepare anoxic water, boil deionized water to help remove dissolved oxygen and cool under N_2. Transfer an appropriate amount of water into N_2-flushed serum bottles, close with butyl rubber stoppers, crimp-seal, and autoclave.
3. Once all autoclaved materials are cool, bring into an anaerobic glove bag at least a day ahead of time. These include sterile serum bottles, butyl rubber stoppers, sulfide stock solution, and anoxic water. Also ensure there are ample needles and syringes of appropriate volumes in the glove bag. These will be used to transfer volumes from the sulfide stock solution into the calibration standard bottles.
4. Calculate how much water and anoxic stock solution volumes will be needed to dilute the sulfide stock solution (1,000 mg/L) to amounts needed for the calibration curve. The assay is linear up to 4 μg sulfide.
5. To empty serum bottles, add appropriate amounts of water to each serum bottle to prepare standards. Close bottles with butyl rubber stoppers.
6. Using a needle and syringe, transfer an appropriate amount of sulfide stock solution into each bottle (*see* **Note 16**).
7. Remove sulfide calibration standards from glove bag, and crimp-seal with aluminum seals. These will be used to prepare sulfide calibration standards for the spectrophotometric assay described below.

DMPD Reagent (1 L)

1. Add 950-mL deionized water to a glass bottle. Slowly add 50-mL concentrated sulfuric acid while stirring. It is highly recommended that this be done in a fume hood.

2. Add 1.0-g DMPD and 1.0-g zinc acetate and ensure that reagents are dissolved.
3. Dispense 4.9-mL DMPD reagent into a series of glass tubes and close with rubber-lined screw caps. Cover racks of tubes with foil and store in the dark at room temperature until needed for sulfide assay.

Ferric Chloride Reagent (20 mL)

1. Dissolve 5.0-g $FeCl_3 \cdot 6H_2O$ in 20-mL deionized water. Store at room temperature.

Performing the Sulfide Assay

1. Remove only as many DMPD tubes from dark storage as needed for the sulfide assay. Add 5-mL deionized water to each tube using a clean glass or plastic pipet.
2. Add 0.1-mL (100 μL) sample or calibration standard.
3. Immediately add 100 μL $FeCl_3$.
4. Vortex solution, and let stand for at least 10 min.
5. Prepare a blank sample to zero the spectrophotometer by preparing a tube in the same way as the samples except add 100 μL deionized water instead of a sample.
6. Set the spectrophotometer to A_{660}, blank the spectrophotometer with the blank sample, then analyze the samples at this wavelength. Tubes will be blue if sulfide is present. For this assay, we have analyzed the samples within 1 h of preparation (following the 10 min incubation, step 4), and during this time, the color (e.g., A_{660} values for calibration standards) remains stable.

3.2.2 Ammonium Analysis by Spectrophotometric Determination

Preparation of Reagents and Calibration Standards

Reagents A and B

1. *To prepare Reagent A*: With stirring, add 2.9-mL phenol and 6 mL of a 0.5-g/L solution of sodium nitroprusside to 91-mL deionized water. Gloves should be worn, and a fume hood is recommended for the preparation of this reagent due to the toxicity of these compounds. This reagent is stable for approximately 1 month [32].
2. *To prepare Reagent B*: With stirring, dissolve 10-g NaOH to 495-mL deionized water and then add 5 mL of 10–14 % NaClO. A fume hood is recommended for the preparation of this reagent.

Preparation of Ammonium Calibration Standards

1. To prepare a 20 mM stock solution of NH_4Cl, dissolve 0.107-g of NH_4Cl in a 100-mL volumetric flask, topping water up to the 100-mL line. Mix well by gently inverting the volumetric flask.

2. Prepare appropriate dilutions of this stock in microfuge tubes to achieve standards ranging from 0 to 10 mM.

Performing the Ammonium Assay

1. Add 30 μL sample or calibration standard to a 1.5-mL microfuge tube.
2. Add 950 μL milliQ water.
3. Add 100 μL Reagent A.
4. Add 100 μL Reagent B; mix all together gently (e.g., by inverting tube).
5. Store samples for 1 h in the dark at room temperature.
6. Read absorbance at 635 nm (A_{635}) on a spectrophotometer. We have always analyzed the samples for this assay for up to 30 min following the 1 h incubation (step 5) and have found the absorbance readings (e.g., A_{635} of the calibration standards) to be consistent within this time.

3.2.3 Sulfate Analysis by Spectrophotometric Analysis (Turbidometric Assay) ***(See Note 17)***

Preparation of Reagents and Calibration Standards

Conditioning Reagent

1. In a fume hood, combine 100-mL 95 % ethanol, 30-mL concentrated HCl, 75-g NaCl, and 50-mL glycerol in a glass bottle with stirring.
2. Dilute 180-fold in deionized water.

Preparation of Sulfate Calibration Standards

1. Weigh 2.84-g Na_2SO_4 into a 100-mL volumetric flask and top up to volume line with deionized water to prepare a 200 mM stock solution. Mix well by gently inverting the volumetric flask.
2. From this stock solution, prepare sulfate standards ranging from 1 to 20 mM in 1.5-mL microfuge tubes by diluting stock solution with deionized water (e.g., to prepare a 20 mM standard, add 100 μL stock solution to 900 μL water). The assay is linear up to 20 mM sulfate.

Performing the Sulfate Assay

1. Add 50 μL of standard or sample to a microfuge tube.
2. Add 950 μL conditioning agent.
3. Add a small "scoop" of $BaCl_2$ (e.g., 1/3 the area of a standard weighing spatula). As this is a toxic compound, it is suggested that this step be done in a fume hood.
4. Vortex until mixed, and let stand for approximately 30 min.
5. Measure the samples at A_{420} on a spectrophotometer, blanking with water. Use plastic cuvettes. Samples will be turbid (cloudy) if sulfate is present; no color change will occur. As with the other colorimetric assays described above (for sulfide and ammonium), we have always analyzed samples within an hour following their preparation and have not observed changes in the A_{420} of the calibration standards during this time.

3.2.4 LC Analysis for Anions and VFA

1. Prepare appropriate buffers (mobile phases) for analyte analysis. As mentioned in the Methods section, specific protocols for conducting analyses by HPLC will depend on the model of the instrument being used and the types of columns that are specified for that instrument. Regardless of the model, once the buffers are prepared, start up the HPLC system to achieve the appropriate flow rate (typically 1 mL/min), pressure, and a stable baseline.
2. Prepare samples for analysis. If samples were frozen, thaw before dilution. Samples for HPLC analysis should be completely free of particulates, as these can clog inlet lines. Samples should be centrifuged (e.g., on a microcentrifuge) at ~14,000 rpm for at least 5 min.
3. The resulting supernatants can then be diluted at this point, but for even cleaner samples, samples should then be filtered through 13 mm syringe filters. This can be done by withdrawing approximately 0.5 mL of sample using a 1-mL syringe, then attaching the syringe to the syringe filter and expelling the fluid through the filter into a clean microfuge tube.
4. This clean sample can now be diluted to within an appropriate concentration range (e.g., 0–500 μM range) into an autosampler vial.
5. Following this sample preparation, the samples can then be analyzed according to the conditions specified for a given column and instrument.

3.3 Sample Microbiological Activity and Composition

3.3.1 Most Probable Number (MPN) Analysis (See Note 18)

1. This cultivation-based method of determining numbers of SRB (or other microbial groups) involves serial tenfold dilutions of a given sample in a selective medium (*see* **Note 5** for examples of SRB media). After incubation, the highest dilution showing the most growth (or the most pronounced indicator) can be used to statistically estimate the number of cells per unit volume in the original volume. A minimum of three replicates of each dilution should be prepared for proper statistical analysis of the data [33].
2. To conduct MPN analysis for SRB, a selective medium for SRB such as CSB-K containing lactate and sulfate (*see* **Note 5**) is typically used. In many cases, an iron nail is included in the medium to readily observe the formation of black FeS as a clear indicator of sulfate reduction. Anoxically prepare 300 mL of such a medium and dispense 9 mL into each of 30 Balch tubes (for a 3-tube MPN out to 10^{-10} dilutions) flushed with N_2/CO_2, close with butyl rubber stoppers, crimp-seal with aluminum seals, and autoclave.
3. Once tubes have cooled, add 1 mL of sample into each of the first three tubes (10^{-1} dilution) and then repeat such 1 in 10

dilutions out to a desired end point (e.g., 10^{-6} to 10^{-10}). Incubate the tubes at an appropriate temperature. Once growth has occurred and black FeS has formed in higher dilutions, published MPN tables can be used to interpret the data to get an estimate of microbial numbers in the original sample [33].

3.3.2 Microbial Activity

1. Prepare anoxic medium (e.g., CSB-K medium; *see* **Note 5**) and dispense 50 mL into sterile 120-mL serum bottles. Close with butyl rubber stoppers and, crimp-seal. Depending on which microbial activity is of interest, the following components can be added as electron donors and electron acceptors, respectively: (1) lactate-using SRB (20 mM sulfate, 10 mM lactate), (2) VFA-using SRB (20 mM sulfate, 3 mM VFA), (3) hNRB (10 mM nitrate, 3 mM VFA), and (4) soNRB (10 mM nitrate, 4 mM sulfide). Inoculate with 5–10% produced water or enrichment culture.
2. Incubate at appropriate temperature conditions (e.g., close to field temperatures).
3. Monitor sulfate, sulfide, nitrate, and/or nitrite concentrations (depending on the kind of incubation set up) to determine the rates of consumption and/or production of these components.
4. Calculate microbial activities in the arbitrary units $= 100/t_{1/2}$ (units/day), wherein $t_{1/2}$ (days) is the time needed for 50 % of the electron acceptor (sulfate or nitrate) to be reduced under the stated conditions.

3.3.3 DNA Extraction and PCR Amplification for Analyzing Total Microbial Community Composition

DNA Extraction

1. In general, isolating DNA from oilfield produced waters is straightforward. We have frequently used commercially available DNA extraction kits that include a bead-beating step (in particular, the DNA Fast Spin Kit has been successfully used to extract DNA from produced waters).
2. Ideally, DNA should be extracted from three replicate samples, starting with a 0.5-mL sample for each replicate. Aliquot 0.5 mL into each of three sterile lysis tubes (that come with the kit). For all DNA extraction and PCR protocols, a negative control that contains no DNA should be processed in parallel to ensure that there is no contamination of reagents.
3. To extract DNA, follow the stepwise instructions provided with the commercially available kit.
4. Prepare a 1 % agarose gel (containing SYBR®Safe, 1X, 30 μL per 30-mL agarose gel) and load with extracted DNA to ensure successful DNA extraction. If needed, the DNA can be concentrated using centrifugal filters (e.g., Amicon concentration cups), which also aids with purification (*see* **Note 19**).
5. Combine replicate DNA extractions prior to the PCR amplification protocol described below.

PCR Amplification of 16S rRNA Genes

Once DNA is obtained, polymerase chain reaction (PCR) amplification of 16S rRNA genes is performed to determine total microbial community composition (*see* **Note 20**). This protocol describes amplification of the 16S rRNA gene for pyrotag sequencing analysis (using 454 pyrosequencing) (*see* **Note 21**) using a two-step PCR process. The first PCR step has more cycles and amplifies conserved regions (V6 – V8) of the 16S rRNA gene using non-barcoded primers (forward primer, 926f: AAACTYAAAGAATTGACGG; and reverse primer, 1392r: ACGGGCGGTGTGTRC) in order to "universally" amplify prokaryotic taxa [34]. The secondary PCR uses barcoded primers and 10 cycles [34].

1. Set up the first PCR on ice using the suggested following master mix (e.g., as per TopTaq kit instructions): 10X buffer (5 μL), 10 mM dNTPs (1.0 μL), 20 pmol/μL forward primer (0.5 μL); 20 pmol/μL reverse primer (0.5 μL), TopTaq (0.25 μL), template DNA (1–4 μL), and PCR-grade water (to make PCR reaction volume up to 50 μL).
2. Using a thermocycler, amplify the DNA according to the following program that is specific to the recommended primers: 5 min at 95°C; then 25 cycles of 95°C for 30 s, 55°C for 45 s, and 72°C for 1.5 min; and finally, 10 min at 72°C.
3. Verify the correct amplicon size (~500 bp) by analyzing the PCR products on a 1 % agarose gel.
4. Purify amplicons using the QIAquick PCR Purification kit according to the manufacturer's instructions. Run on a 1 % agarose gel to verify that DNA has not been lost and that primer dimers are minimal.
5. Use the purified amplicons from the first PCR step for the second PCR step. Set up the amplification reaction using the same master mix as outlined above. Amplify using the same program as above, but run for only 10 cycles.
6. Verify correct amplification on a 1 % agarose gel.
7. Purify the successful amplicons with the QIAquick PCR Purification kit according to the manufacturer's instructions. Run on a 1 % agarose gel to verify that primer dimers have disappeared and that multiple bands are not present.
8. Quantify the PCR product (e.g., using a fluorometer and associated reagents according to manufacturer's instructions). 454-Pyrotag sequencing requires ~400 ng of DNA. Combine replicates of a sample as need to obtain the necessary amount of DNA for sequencing. Store the products at −20 °C until sequencing. For longer storage, −80 °C storage is recommended. Immediately before shipping (e.g., within 24 h) for sequencing, amplicons should be re-quantified and rerun and a

1.75 % agarose gel to ensure proper concentrations and the absence of primer dimers and multiple bands.

9. Several commercial labs can be used for pyrotag sequencing analysis. Ship the amplicons to the appropriate sequencing facility on dry ice to ensure that they remain frozen.

3.4 Laboratory Incubations to Study Microbial Souring and Its Control

Laboratory incubations containing produced water fluids to study microbial souring and its control can be established in a variety of different ways but in general use either serum bottle-based or column-based incubations. Serum bottle incubations can contain produced water amended only with sulfate and a suitable substrate (lactate, VFAs, hydrocarbons) or can contain a mixture of produced water and a defined minimal medium. Various concentrations of sulfate and substrates can be tested, and incubations can be done at a variety of temperatures and/or salinities to determine effects on sulfide production. In addition, different concentrations of known souring inhibitors such as nitrate, nitrite, perchlorate, or biocides can be added to serum bottle incubations to determine their effects on rates of sulfide production. Column-based incubations that more closely simulate a reservoir are more complex to establish but can allow for researchers to determine microbial souring and treatment under flow conditions. As with serum bottle incubations, columns can be inoculated with production water fluids or sulfate-reducing cultures, and once sulfide production is observed, various treatment chemicals (nitrate, nitrite, biocides) can be added at various doses to determine effects on sulfide production.

3.4.1 Serum Bottle Incubations

1. In general, establishing serum bottle incubations, which are essentially batch cultures, follow a similar protocol to that of microbial activity tests (Sect. 3.3.2) except that multiple replicates and appropriate controls are established for each experiment. A minimum of three replicates for each test condition should be established along with triplicate sterile controls (usually achieved by autoclaving) and unamended controls (substrate-unamended and/or sulfate-unamended controls).
2. If medium is to be added to production water fluids for experiments, anoxically prepare a minimal salts medium such as that described in **Note 5**. There is no hard and fast rule for combining produced fluids with medium, but combining these in a 50:50 ratio is a reasonable way to start souring experiments.
3. As mentioned above, a multitude of experiments can be conducted to study souring and its treatment (e.g., challenging produced water fluid microbial communities with a variety of electron donors, acceptors, or treatment agents). Serum bottle incubations provide a simple way of studying souring and its mitigation in a well-defined system but may provide an over- or underestimation of souring and treatment rates given that they do not accurately represent the flowing system of a reservoir.

3.4.2 Column Incubations

Column-based incubations more closely mimic a flowing reservoir system but are more challenging to set up than serum bottle incubations. There are three stages for preparing columns in order to study souring. In the first stage, columns are assembled and sterilized. In the second stage, a flow path is established, and the third stage allows for the formation of a microbial biofilm and the creation of sour conditions that can then be used to study souring treatments.

Column Assembly

1. Measure the inside diameter (recorded as *d*) of the syringe column for future calculation of column parameters (e.g., total volume). If a syringe barrel is used as the column, take out the piston and measure the inside diameter (Fig. 1).
2. Use scissors to cut the polymeric mesh into small pieces of a thin layer (2–3 mm thickness) and round shape with the size completely fitting onto the bottom of the column and push down the polymeric mesh with tweezers, ensuring that it is tightly attached to the bottom and the wall of the column.
3. Place a thin layer (~2 mm thickness) of glass wool on top of the polymeric mesh to enhance its ability to contain sand.

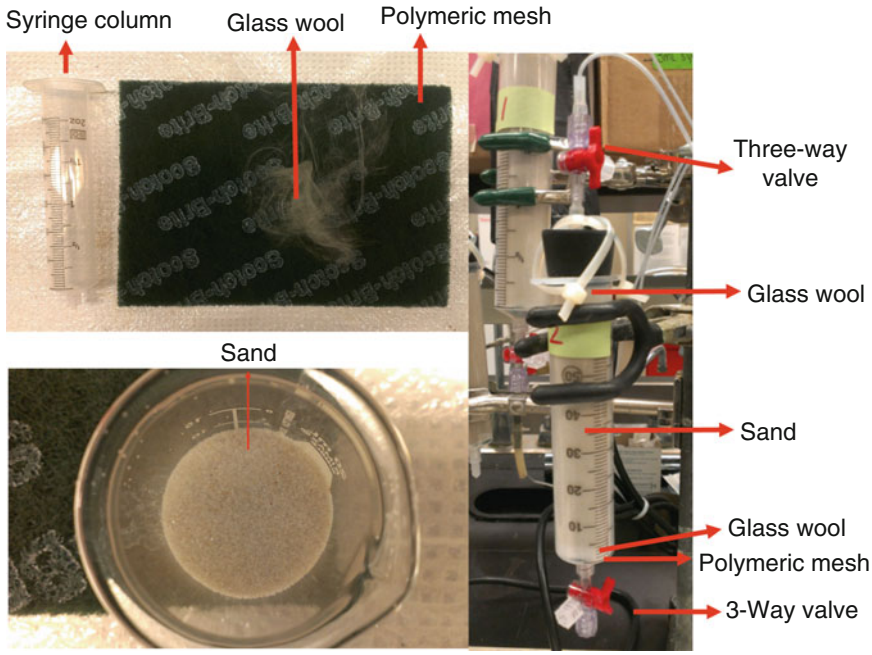

Fig. 1 Materials used to assemble column incubations for studying souring in a flow system

4. Load the sand into the column. As the sand is loaded into the column, tap the column to ensure that the sand is tightly packed.
5. Once the sand has been loaded close to the edge of the column, place another layer of glass wool on top of the sand to prevent the sand from flowing out of the column.
6. Close the column tightly with a perforated rubber stopper fitted with a glass or plastic connector, through which fluid can flow out of the column.
7. Attach a three-way valve to both the inlet and the outlet of the column. From the inlet valve, a sulfate-reducing culture or produced water sample will be inoculated into the column, while from the outlet valve, samples can be taken for chemical assays.
8. Wrap the zip ties around the rubber stopper to tighten the seal of the column.
9. Measure the actual length (recorded as L) of the sand bed (e.g., area of the column occupied by sand) used for flow path to calculate the total volume of the column with the following formula:

$$\text{Total volume} = \pi(d/2)^2 \text{L}$$

10. Autoclave the assembled column (*see* **Note 22**).
11. After autoclaving the column, weigh the dry assembled column and record the weight as $m_{\text{dry column}}$ (for future calculation of the pore volume of the column).

Flow Path Setup

1. Clamp the autoclaved column to a retort stand.
2. Thread the pump tubing through the pump head and connect the pump tubing with other connecting tubing to construct a tubing path.
3. Connect one end of the tubing path with the inlet three-way valve attached to the column (while keeping the other end with a medium container capped tightly with a perforated rubber stopper) through which the tubing can reach the medium.
4. Use another piece of tubing to connect the outlet three-way valve attached to the column with a waste container also closed tightly with a perforated rubber stopper, through which the effluent can be collected in the container.
5. Keep the whole system as anoxic as possible throughout the experiments. Three main options are available for achieving and maintaining an anoxic system. (1) The whole system can be set up in an anaerobic glove bag. The main disadvantage of using this option is that it can be quite inconvenient in general

to operate and monitor the system. (2) Connect a N_2/CO_2 (80/20) gas cylinder to the medium reservoir to keep the whole system anoxic while providing a positive pressure. This strategy is easier than the first option from an operational point of view; however, disadvantages are that consistent gas flow can be difficult to achieve and leads to high levels of gas consumption (higher cost). (3) Attach a syringe filled with anoxic gas (such as N_2/CO_2, 80/20) to the medium inlet bottle and an empty syringe to the waste bottle in order to maintain anoxic conditions and balance the pressure (Fig. 2). This is the most convenient method for column operation and most economic in terms of gas consumption compared to the other two. However, it has a high requirement for syringes.

Biofilm Establishment

1. Pump sterile water into the column (or minimal medium with known density, ρ_{fluid}, in this case ρ_{water}), ensuring the whole column is wet and the effluent is flowing out of the column.
2. Stop the pump and close both inlet and outlet three-way valves.
3. Disconnect the assembled column from the whole bioreactor system and weigh it, recording the weight of the wet column ($m_{\text{wet column}}$).
4. Calculate pore volume (PV) and porosity of the column by using the following formulae:

   (i) $\text{PV} = \left[m_{\text{wet column}} - m_{\text{dry column}}\right]/\rho_{\text{water}}$

   (ii) $\text{Porosity}(\%) = \text{PV}/\text{total volume}$
5. After weighing the wet column, reconnect the column.
6. Inject half a pore volume of sulfate-reducing culture or produced water into the column (*see* **Note 23**) through the inlet three-way valve.
7. Close the 2 three-way valves again and incubate the column as a batch culture without flow of medium at an appropriate temperature for a period of time, which can vary with the different incubation conditions (e.g., temperature, salinity, or the type of electron donors), in order to develop a microbial sulfide-producing biofilm. Sulfide production can usually be observed visually as the sand pack begins to blacken due to the production of iron sulfide.
8. Once sulfide production is suspected, start the pump and consistently deliver medium into the column starting at a very low flow rate, progressively increasing the flow rate to a desired level.
9. Monitor sulfate until it is at low levels or is no longer detected in the effluent. At the same time, sulfide should steadily be

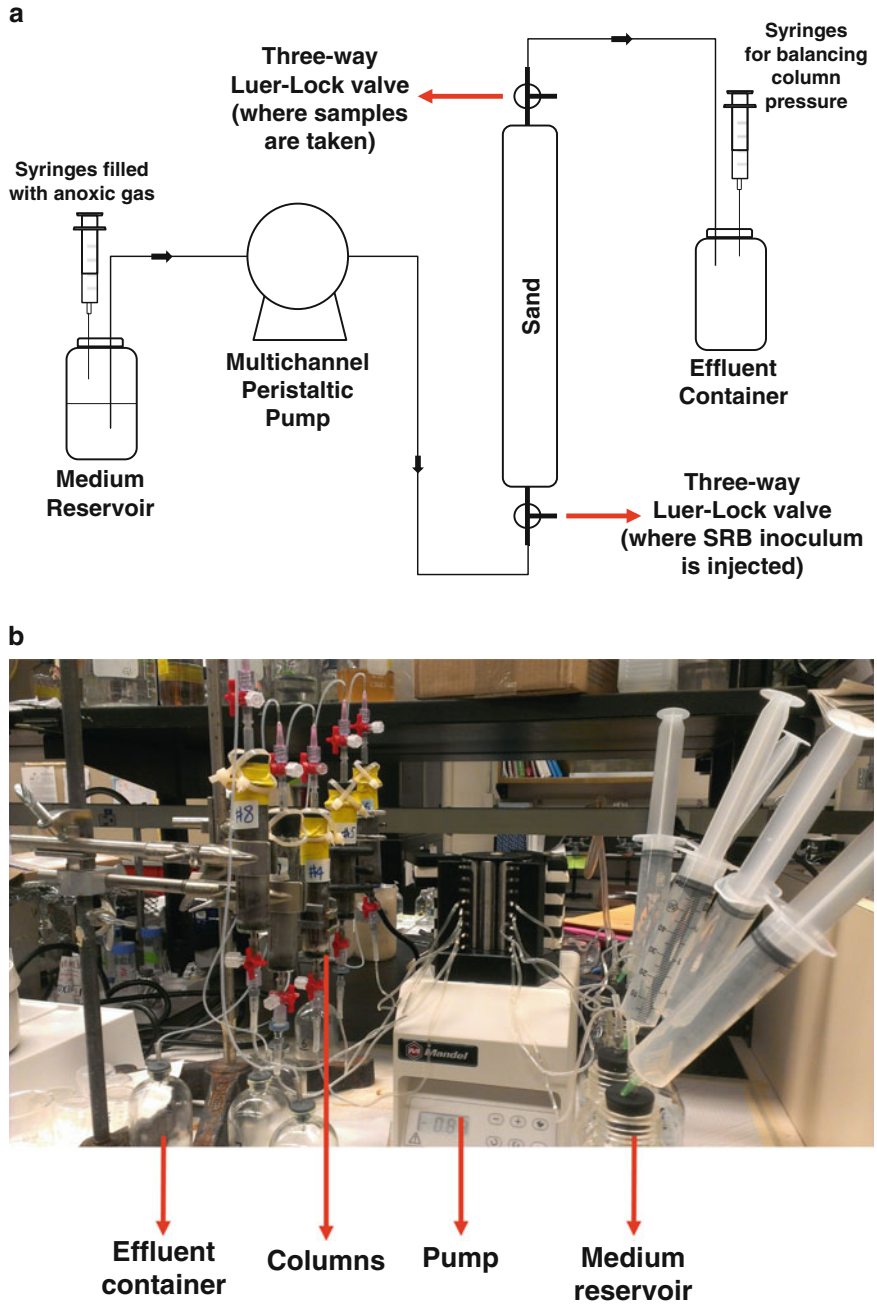

Fig. 2 (**a**) Schematic of column incubation set up. (**b**) Photograph of actual column system used to study souring and its treatment in a flow system

detected in the effluent. The column is now sour and can be used to test for a variety of treatment agents.

10. Throughout the column flow experiments, samples can be taken from the influent and effluent ports to monitor for

changes in relevant parameters such as sulfate and sulfide and other analytes that may be important to monitor during treatment experiments (e.g., nitrate, nitrite, perchlorate, VFA, biocide concentrations, etc.). In addition, effluent samples can be analyzed for any shifts in microbial community composition before and after treatment.

4 Notes

1. The products and vendors that we routinely use for our protocols are listed in the Materials section, but our intent is not to endorse these particular vendors; similar products from other vendors used for the same purpose can likely be substituted.
2. In some cases, it may be appropriate or desired that produced fluids are tested immediately for soluble sulfide concentrations (or the concentrations of other analytes such as ammonium). Commercially available kits are readily transported in robust cases to field sites and are quick and easy to use to obtain real-time measurements. An example of a field kit that can be used for in-field sulfide measurements is available through Hach (#223801).
3. This method is based on that of Cline [35]. Slightly different protocols for sulfide analysis have been described [36] and can also be used.
4. There are many different suppliers for HPLCs (e.g., Waters, Agilent), and any other unit can readily be used for anion and VFA analyses. Columns and reagents (e.g., mobile phases) will be different when using instruments from other suppliers but can be used for equivalent analysis.
5. There are many different media compositions that can be used for establishing SRB incubations. Some common ones that we have used include Postgate B [37], CSB-K, and CSB-A [20, 31, 38, 39]. The composition of CSB-A medium is as follows (per L): 7.0-g NaCl, 0.2-g KH_2PO_4, 0.25-g NH_4Cl, 0.15-g $CaCl_2{\cdot}2H_2O$, 0.4-g $MgCl_2{\cdot}6H_2O$, 0.5-g KCl, and 100-μL 1 % resazurin as redox indicator. Adjust the pH to 7.4–7.6; after autoclaving and cooling down to room temperature, add 30-mL 1 M $NaHCO_3$, 1-mL trace element solution (per L containing 5.20-g Na_2EDTA, 2.10-g $FeSO_4{\cdot}7H_2O$, 30.0-mg H_3BO_3, 100-mg $MnCl_2{\cdot}4H_2O$, 190-mg $CoCl_2{\cdot}6H_2O$, 24.0-mg $NiCl_2{\cdot}6H_2O$, 3.00-mg $CuSO_4{\cdot}5H_2O$, 68.0-mg $ZnCl_2$, and 36.0-mg $NaMoO_4{\cdot}H_2O$, adjust pH to 7.0), and 1-mL selenate/tungstate solution (400-mg NaOH, 6.0-mg $Na_2Se_2O_3{\cdot}5H_2O$, 8.0-mg $Na_2WO_4{\cdot}H_2O$, per L). CSB-K is half-strength CSB-A. Amendment of the medium with different

electron acceptors (e.g., sulfate, nitrate) and electron donors (e.g., VFA, lactate, H_2, crude oil) is dependent on the need of experiments. For oil column incubations, crude oil is contained in the column together with sand thus no oil is needed in the medium.

6. The microbial activity method has been successfully used for evaluating anoxic activities in oilfields in lieu of MPN counts (e.g., [31]). This method can be used when growth rates are slow, multiple cells are needed to establish a positive reading, and/or when cells are clumped or attached which is typically the case for microbiota present in oilfield samples. The method involves doing a single dilution and measuring the time required to score the tube as positive. This time is inversely proportional to the logarithm of the MPN of microorganisms in the original sample [31].
7. The columns can be glass or plastic with appropriate dimensions. However, the plastic has to be impermeable or have low gas permeability so as to prevent O_2 in the ambient air from diffusing into the column and disrupting the anoxic environment. More importantly, if O_2 is diffused into the column, the O_2 may consistently react with sulfide forming elemental sulfur that will deposit in the column resulting in an increase of the permeability of the column or even block the column, and the sulfur species measured at the effluent will be out of balance as well. For these reasons, we strongly recommend that all tubing, connectors, and other plastic materials used to construct a bioreactor system for souring study are impermeable to O_2. Alternatively, glass syringe barrels can also be used as columns which are more impermeable to air but are more costly.
8. The type of sand used in experiments depends on the type of rock in the oil reservoir that the investigator wants to mimic. For example, to set up columns simulating a low-temperature oilfield consisting of glauconitic sandstone oil-containing rocks, sand with the size of 50–70 mesh particle was used as the matrix to pack the bioreactor columns [39]. The size of the sand particles influences the permeability of the packed column thus can be altered depending on the requirements of the experiments.
9. A high-quality pump that can deliver reliable, consistent flow rates for consistent fluid delivery is imperative for the column experiments. This particular pump is highly recommended as it can deliver samples at a high resolution and precision speed and allows for low pulse flows without sample shearing or degradation.
10. The tubing used for the pump head is different from the others; therefore, tubing connectors are necessary. The size of the

tubing and connectors determine the flow rate range of the system controlled by a given pump. Thus, choosing the appropriate size of the tubing is very important and the information can typically be gathered from the pump manual.

11. There are several recipes to make the minimal salts medium for souring bioreactor experiments, which have been previously described [15, 28, 29, 38]. In our column incubation studies, we have most frequently used CSB-A [38] or CSB-K [39] as described in **Note 5**. As above, amendment of the medium with different electron acceptors (e.g., sulfate, nitrate) and electron donors (e.g., VFA, lactate, H_2, or even crude oil) is dependent on the need of experiments. If crude oil is to be used as the electron donor, crude oil is contained in the column together with sand; as a result, no oil is needed in the medium (a description of how oil is added to a sand-pack column can be found in [40]).
12. A sulfate-reducing culture/enrichment is made by adding produced waters from oilfield into medium (*see* **Note 5**) amended with sulfate and the desired electron donor in an anoxic serum bottle. Incubation is conducted at the desired temperature. Once most of the sulfate has been consumed (or the culture becomes turbid), transfer the culture into fresh medium. After two transfers, the sulfate-reducing enrichment is ready for inoculation into the column.
13. It has been documented that the microbial community composition of environmental samples can change substantially during storage [41]; thus it is best to process samples (or freeze samples) as soon as possible to obtain the most accurate community composition.
14. It can be very useful to have an oil sample associated with a given field. This oil can be used for many experiments to help determine what electron donors may be driving microbial processes like souring in oilfields.
15. Ammonium concentrations in samples have been found to be most stable with storage at −20°C; storage at ambient temperatures for several hours can result in increased levels of ammonium [42]. Other components such as volatile fatty acids have low volatility at neutral pH and higher; thus if samples are from more acidic environments, they should be made neutral or alkaline using a basic solution (e.g., of NaOH). If this is done, volumes of added solution should be recorded so that any dilutions can be accounted for in calculating final analyte concentrations. Overall, we recommend freezing samples at −20°C if immediate analysis will not be possible. We have noted that VFA standards can be stored at −20°C for up to a year without any significant changes in concentrations

compared with freshly prepared standards when analyzed by ion chromatography.

16. We have successfully used needles and syringes (e.g., 1-mL disposable syringes) to prepare sulfide calibration standard solutions that yield linear calibration curves. Micropipettors could also be used (and are considered more accurate for most applications); however, their use requires opening the sulfide stock solution, risking some volatilization of sulfide.
17. This turbidometric assay for sulfate is based on a method outlined previously [43, 44]. In general, we prefer to analyze sulfate concentrations by HPLC as more accurate sulfate concentrations can be achieved at low sulfate concentrations, but the turbidometric method also works well and can be used as a back-up method when LC instruments are under repair.
18. The preparation of anoxic medium for cultivating anaerobic microorganisms has been well described in other publications [45, 46] and thus is not described in great detail here. In general, medium components are mixed, then boiled to remove dissolved oxygen, cooled under O_2-free gas (usually an N_2/CO_2 mixture), and dispensed into N_2/CO_2-flushed glass vessels which are then capped and aluminum crimp-sealed before autoclaving. Reductants are typically added (before or after autoclaving), and some heat-sensitive reagents are added from sterile stock solutions after autoclaving.
19. Following genomic DNA extraction from low biomass samples, a band is often not observed on a gel. However, proceeding with the first PCR step generally results in the observation of amplified DNA.
20. Although this chapter focuses on analyzing for total microbial community composition (based on amplifying the 16S rRNA genes in a given sample), it should be noted that primers specific to sulfate reducers (e.g., primers specific to the *dsrAB* gene) can readily be used to target this microbial group specifically. Many such primers and protocols can be found in the literature (e.g., [16]).
21. To date, we have successfully used pyrotag sequencing (using the Roche 454 FLX Titanium sequencer, www.454.com) as the sequencing technology for analyzing produced water samples and laboratory experiments related to souring [20, 39]. However, with the announcement that this technology will cease to be supported in 2016, other technology platforms (such as Illumina, www.illumina.com) can also be routinely and reliably used for rapid, low-cost sequencing [47].
22. Since the sand is tightly packed in the column, it may be difficult for the heat from autoclaving to reach the center of the sand-packed column. Thus, to achieve thorough sterilization, each

item needed for assembling the column can be autoclaved (e.g., wrapped in foil) separately before assembling.

23. If water is used initially to wet the column prior to inoculation, medium should first be injected into the column to provide a nourishing environment for enhancing the growth and establishment of the cells in the column.

Acknowledgments

We thank Johanna Voordouw, Yin Shen, Dr. Rhonda Clark, Dr. Dongshan An, Dr. Chuan Chen, and Dr. Sandra Wilson for their roles in developing and optimizing many of the protocols described in this chapter. LMG was supported by a Natural Sciences and Engineering Research Council (NSERC) Discovery grant, while YX and GV were supported by an NSERC Industrial Research Chair Award (to GV) which is also funded by Baker Hughes, BP, Computer Modelling Group Limited, ConocoPhillips Company, Intertek, Dow Microbial Control, Enbridge, Enerplus Corporation, Oil Search Limited, Shell Global Solutions International BV, Suncor Energy Inc., and Yara Norge AS, as well as by Alberta Innovates Energy and Environment Solutions.

References

1. Hao OJ, Chen JM, Huang L, Buglass RL (1996) Sulfate-reducing bacteria. Crit Rev Environ Sci Technol 26:155–187
2. Gieg LM, Jack TR, Foght JM (2011) Biological souring and mitigation in oil reservoirs. Appl Microbiol Biotechnol 92:263–282
3. Bødtker G, Thorstenson T, Lillebø BL, Thorbjørnsen BE, Ulvøen RH, Sunde E, Torsvik T (2008) The effect of long-term nitrate treatment on SRB activity, corrosion rate and bacterial community composition in offshore water injection systems. J Ind Microbiol Biotechnol 35:1625–1636
4. Barton LL, Fauque GD (2009) Biochemistry, physiology and biotechnology of sulfate-reducing bacteria. Adv Appl Microbiol 68:41–98
5. Wolicka D, Borkowski A (2012) Microorganisms and crude oil. In: Romero-Zerón L (ed) Introduction to enhance oil recovery (EOR) processes and bioremediation of oil-contaminated sites. In Tech, Rijeka, Croatia
6. Vance I, Thrasher DR (2005) Reservoir souring: mechanisms and prevention. In: Ollivier B, Magot M (eds) Petroleum microbiology. ASM, Washington, DC
7. Liamleam W, Annachhatre AP (2007) Electron donors for biological sulfate reduction. Biotechnol Adv 25:452–463
8. Machel HG (2001) Bacterial and thermochemical sulfate reduction in diagenetic settings - old and new insights. Sediment Geol 140:143–175
9. Zhang S, Zhu G, Liang Y, Dai J, Liang H, Li M (2005) Geochemical characteristics of the Zhaolanzhuang sour gas accumulation and thermochemical sulfate reduction in the Jixian Sag of Bohai Bay Basin. Org Geochem 36:1717–1730
10. Jones C, Downward B, Edmunds S, Hernandez K, Curtis T, Smith F (2011) A novel approach to using THPS for controlling reservoir souring. Paper #11219, Corrosion 2011 conference, Houston, 13–17 Mar
11. Beauchamp RO, Bus JS, Popp JA, Boreiko CJ, Andjelkovich DA (1984) A critical review of the literature on hydrogen sulfide toxicity. CRC Crit Rev Toxicol 13:25–97
12. Enning D, Garrelfs J (2014) Corrosion of iron by sulfate-reducing bacteria: new views of an old problem. Appl Environ Microbiol 80:1226–1236

13. Magot M (2005) Indigenous microbial communities in oil fields. In: Ollivier B, Magot M (eds) Petroleum microbiology. ASM press, Washington, DC
14. Struchtemeyer CG, Davis JP, Elshahed MS (2011) Influence of the drilling mud formulation process on the bacterial communities in thermogenic natural gas wells of the Barnett Shale. Appl Environ Microbiol 77:4744–4753
15. Chen C-I, Reinsel MA, Mueller RF (1994) Kinetic investigation of microbial souring in porous media using microbial consortia from oil reservoirs. Biotechnol Bioeng 44:263–269
16. Gittel A, Sorensen KB, Skovhus TL, Ingvorsen K, Schramm A (2009) Prokaryotic community structure and sulfate reducer activity in water from high-temperature oil reservoirs with and without nitrate treatment. Appl Environ Microbiol 75:7086–7096
17. Jenneman GE, Moffitt PD, Bala GA, Webb RH (1999) Sulfide removal in reservoir brine by indigenous bacteria. SPE Prod Facil 14:219–225
18. Larsen J (2002) Downhole nitrate applications to control sulfate reducing bacteria activity and reservoir souring. Paper #02025, Corrosion 2002 conference, Denver, 7–11 Apr
19. Khatib ZI, Salanitro JP (1997) Reservoir souring: analysis of surveys and experience in sour waterfloods. SPE Paper #38795, SPE annual technical conference and exhibition, San Antonio, 5–8 Oct
20. Agrawal A, An D, Cavallaro A, Voordouw G (2014) Souring in low-temperature surface facilities of two high-temperature Argentinian oil fields. Appl Microbiol Biotechnol 98:8017–8029
21. Liebensteiner MG, Tsesmetzis N, Stams AJ, Lomans BP (2014) Microbial redox processes in deep subsurface environments and the potential application of (per)chlorate in oil reservoirs. Front Microbiol 5:428. doi:10.3389/fmicb.2014.00428
22. Williams TM, Cooper LE (2014) The environmental fate of oil and gas biocides: a review. Paper #3876, Corrosion 2014 NACE conference, San Antonio, 9–13 Mar
23. Giangiacomo LA, Dennis DM (1997) Field testing of the biocompetitive exclusion process for control of iron and hydrogen sulfides. SPE #38351, SPE rocky mountain regional meeting, Casper, 18–21 May
24. Voordouw G, Nemati M, Jenneman GE (2002) Use of nitrate reducing, sulfide oxidizing bacteria to reduce souring in oil fields: interactions with SRB and effects on corrosion. Paper #02034, Corrosion 2002 NACE conference, Denver, 7–11 Apr
25. Greene EA, Hubert C, Nemati M, Jenneman GE, Voordouw G (2003) Nitrite reductase activity of sulphate-reducing bacteria prevents their inhibition by nitrate-reducing, sulphide-oxidizing bacteria. Environ Microbiol 5:607–617
26. Sturman PJ, Goeres DM, Winters MA (1999) Control of hydrogen sulfide in oil and gas wells with nitrite injection. SPE #56772, SPE annual technical conference and exhibition. Houston, 3–6 Oct
27. Davidova I, Hicks MS, Fedorak PM, Suflita JM (2001) The influence of nitrate on microbial processes in oil industry production waters. J Ind Microbiol Biotechnol 27:80–86
28. Reinsel MA, Sears JT, Stewart PS, Mclnerney MJ (1996) Control of microbial souring by nitrate, nitrite or glutaraldehyde injection in a sandstone column. J Ind Microbiol 17:128–136
29. Myhr S, Lillebø BLP, Sunde E, Beeder J, Torsvik T (2002) Inhibition of microbial H_2S production in an oil reservoir model column by nitrate injection. Appl Microbiol Biotechnol 58:400–408
30. Engelbrektson A, Hubbard CG, Tom LM, Boussina A, Jin YT, Wong H, Piceno YM, Carlson HK, Conrad ME, Anderson G, Coates JD (2014) Inhibition of microbial sulfate reduction in a flow-through column system by (per)chlorate treatment. Front Microbiol 5:315. doi:10.3389/fmicb.2014.00315
31. Voordouw G, Grigoryan AA, Lambo A, Lin S, Park HS, Jack TR, Coombe D (2009) Sulfide remediation by pulsed injection of nitrate into a low temperature Canadian heavy oil reservoir. Environ Sci Technol 43:9512–9518
32. Solórzano L (1969) Determination of ammonia in natural waters by the phenolhypochlorite method. Limnol Oceanogr 14:799–801
33. Oblinger JL, Koburger JA (1975) Understanding and teaching the most probable number technique. J Milk Food Technol 38:540–545
34. Ramos-Padrón E, Bordenave S, Lin S, Bhaskar IM, Dong X, Sensen CW, Fournier J, Voordouw G, Gieg LM (2011) Carbon and sulfur cycling by microbial communities in a gypsum-treated oil sands tailings pond. Environ Sci Technol 45:439–446
35. Cline JD (1969) Spectrophotometric determination of hydrogen sulfide in natural waters. Limnol Oceanogr 14:454–458
36. Cord-Ruwisch R (1985) A quick method for determination of dissolved and precipitated

sulfides in cultures of sulfate-reducing bacteria. J Microbiol Methods 4:33–36

37. Postgate JR (1963) Versatile medium for the enumeration of sulfate-reducing bacteria. Appl Microbiol 11:265–267
38. Hubert C, Nemati M, Jenneman G, Voordouw G (2003) Containment of biogenic sulfide production in continuous up flow packed bioreactors. Biotechnol Prog 19:338–345
39. Callbeck CM, Dong X, Chatterjee I, Agrawal A, Caffrey SM, Sensen CW, Voordouw G (2011) Microbial community succession in a bioreactor modeling a souring low-temperature oil reservoir subjected to nitrate injection. Appl Microbiol Biotechnol 91:799–810
40. Berdugo-Clavijo C, Gieg LM (2014) Conversion of crude oil to methane by a microbial consortium enriched from oil reservoir production waters. Front Microbiol 5:197. doi:10.3389/fmicb.2014.00197
41. Hulecki JC, Foght JM, Fedorak PM (2010) Storage of oil field produced waters alters their chemical and microbiological characteristics. J Ind Microbiol Biotechnol 37:471–481
42. Linder A, Bauer S (1993) Effect of temperature during storage and sampling procedure on ammonia concentration in equine blood plasma. Eur J Clin Chem Clin Biochem 31:473–476
43. Tabatabai MA (1974) A rapid method for the determination of sulfate in water samples. Environ Lett 7:237–243
44. APHA (American Public Health Association) (1992) Standard methods for the examination of wastewater. American Water Works Association and Water Pollution Control Federation, Washington, DC, pp 439–440
45. Widdel F (2010) Cultivation of anaerobic microoorganisms with hydrocarbons as growth substrates. In: Timmis KN (ed) Handbook of hydrocarbon and lipid microbiology. Springer, Berlin, pp 3787–3798
46. Wolfe RS (2011) Techniques for cultivating methanogens. Methods Enzymol 494:1–22
47. Luo C, Tsementzi D, Kyrpides N, Read T, Konstantinidis KT (2012) Direct comparisons of Illumina vs. Roche 454 sequencing technologies on the same microbial community DNA sample. PLoS One. doi:10.1371/journal.pone.0030087

Protocol for Evaluating the Biological Stability of Fuel Formulations and Their Relationship to Carbon Steel Biocorrosion

Renxing Liang and Joseph M. Suflita

Abstract

The microbial metabolism of conventional and alternative fuels can be associated with the biocorrosion of the mostly carbon steel energy infrastructure. This phenomenon is particularly acute in anaerobic sulfate-rich environments. It is therefore important to reliably assess the inherent susceptibility of fuels to anaerobic biodegradation in marine waters as well as provide a measure of the impact of this metabolism on the integrity of steel. Such an assessment of fuels is increasingly important since the exact chemical makeup of both traditional and biofuels can vary and even subtle changes have a profound impact on steel biocorrosion. Herein, we describe a simple protocol involving the incubation of carbon steel coupons in seawater under anaerobic conditions. The increased depletion of sulfate in fuel-amended seawater incubations relative to both autoclaved and fuel-unamended negative controls is monitored as a function of time. We also recommend the incorporation of a known hydrocarbon-degrading sulfate-reducing bacterium as a positive control in the assay to verify that the protocol is not predisposed to failure for unrecognized reasons. At the end of the incubation, corrosion is assessed by both coupon weight loss and a mass balance of the total iron released. Lastly, three-dimension noncontact profilometry is used to assess the degree of damage (e.g., pitting) to the coupons. The integration of the interdisciplinary approaches in this protocol allows for a critical assessment of the biological stability of both traditional and alternative fuel formulations and their potential in exacerbating biocorrosion.

Keywords: Alternative fuels, Biocorrosion, Biodegradation, Biofuel, Carbon steel, Hydrocarbons, Petroleum fuels, Pitting, Sulfate reduction

1 Introduction

It is well known that the major hydrocarbon classes that make up petroleum-derived fuels are susceptible to biodegradation. When the rate of oxygen depletion exceeds the rate of oxygen supply, anaerobic conditions develop. In the absence of oxygen, hydrocarbon metabolism can be coupled to the reduction of a variety of other terminal electron acceptors [1–3]. For instance, hydrocarbons and other constituents that make up fuels can be biodegraded

T.J. McGenity et al. (eds.), *Hydrocarbon and Lipid Microbiology Protocols*, Springer Protocols Handbooks, (2017) 211–226, DOI 10.1007/8623_2015_76, © Springer-Verlag Berlin Heidelberg 2015, Published online: 23 April 2015

under sulfate-reducing conditions or even by pure cultures of sulfate-reducing bacteria [4–7]. Recent evidence has shown that this microbial activity can result in the production of reduced sulfides and the corrosion of carbon steel [8–10]. Such consequences are particularly important since the infrastructure used to explore, store, transport, and use hydrocarbons worldwide is largely one of carbon steel. Thus, it is reasonable to expect that the severest corrosion problems are likely to occur in portions of the infrastructure where hydrocarbons and sulfate are particularly abundant. In this regard, seawater-compensated diesel fuel ballast tanks onboard some Navy ships are particularly noteworthy [8]. The biological stability of diverse range of fuel formulations and their potential impact on the biocorrosion of carbon steel needs to be critically assessed [11, 12].

This assessment is particularly important given the rapid worldwide integration of various biofuels into the existing carbon steel infrastructure. Decisions on the introduction and use of biofuels are often made by regulatory mandate rather than by careful consideration of what makes a fuel compatible (or incompatible) with the prevailing infrastructure. Societies across the globe embrace alternate fuels in an effort to extend the fuel supply and to be environmentally greener. However, first-generation methylester biofuels are not stable, and the anaerobic biodegradation of these components can exacerbate biocorrosion problems [9].

Alternative fuels are considered more carbon neutral fuels since they are produced largely from renewable biomass and typically possess performance characteristics that are compatible with traditional fuels. However, since various feedstocks and processing technologies are employed in their manufacture [13, 14], the specific chemical composition of alternative fuels can vary greatly and thereby exhibit different stability characteristics. For example, first-generation biodiesels are typically produced via the transesterification of fatty acids obtained from plants or animals. The resulting esters contain oxygen in addition to carbon and hydrogen and by definition are not hydrocarbons at all [15, 16]. Such fuel components are relatively easily hydrolyzed and the resulting fatty acids used as electron donors to support corrosive biofilm formation [9]. Other biofuels (sometimes referred to as renewable or green diesels) are made into more conventional hydrocarbons via biomass hydrogenation processes. These fuels typically contain a complex alkane mixture, but the size and range of these components tend to be narrower than conventional petroleum-based fuels [11, 17]. Consequently, the fuels are typically blended (e.g., 50/50 renewable/petroleum fuel) to evaluate overall performance characteristics [18, 19]. Although the biological stability of such blended fuel formulations is unknown, the resulting products are destined to be transported and stored within existing pipeline, storage tank, and ballast tank infrastructure [20, 21]. This recognition prompted us

to develop a protocol to assess the relationship between the biological stability of fuels and their propensity to exacerbate carbon steel biocorrosion in order to select fuels that are most compatible with the fueling infrastructure.

While numerous studies have documented the susceptibility of fuel components to decay under defined conditions [8, 22–24], only a few focused on the relationship between fuel biodegradation and metal surface corrosion [9, 10, 25]. For instance, first-generation methylester biodiesel was relatively easily biodegraded and accelerated the corrosion of carbon steel materials [9]. Although a variety of seminal studies help pave the way for evaluating the biological stability and corrosiveness of fuels [10, 26, 27], a standardized protocol that could be easily adapted to not only account for first-generation fuels but also any future-generation fuel is lacking. Our goal is to put forward a scientifically defensible protocol that (1) is inexpensive and convenient to construct and operate, (2) is capable of incorporating multiple technical replicates, (3) includes both positive and negative controls, (4) integrates the ability to monitor multiple parameters that provide direct and convincing evidence of both biodegradation and biocorrosion, and (5) be adaptable to test any fuel with the selected inoculum.

To be most environmentally conservative, the assay employs strict anaerobic techniques and uses coastal seawaters or ship ballast waters as the inoculum source. Substrate (fuel) decay is routinely deduced based on the consumption of the sulfate in fuel-amended incubations relative to both sterile and fuel-unamended negative controls. These results are interpreted relative to both the aforementioned negative controls and a positive control consisting of the source inoculum amended with a known hydrocarbon-degrading marine sulfate-reducing bacterium with and without growth substrates. General and pitting corrosion is assessed on a pre-weighed metal coupon suspended in the incubation and recovered for analysis at the end of the assessment period. The protocol can be extrapolated to assess the risks associated with a variety of fuel and fuel formulations and thereby provide basis to determine the overall compatibility with the prevailing infrastructure. Moreover, the protocol can be easily adapted to also monitor the impact of mitigation efforts.

2 Materials

2.1 Construction of Incubations

1. Fuel and fuel mixtures
   The example fuels illustrated in this protocol include two typical petroleum-based (petro-) military fuels, F76 and JP5, as well as two biofuels, including a Fischer–Tropsch (FT)-F76 and a camelina-JP5 (Naval Fuels and Lubes Cross Functional Team, NAVAIR) [11]. The fuel blends include a

50/50 mixture of either (a) the FT- and petro-F76 or (b) the camelina and petroleum-JP5. These fuel combinations are used based on military plans to incorporate increasing amounts of biofuels for tactical vehicle use [18, 19]. Given the fundamental similarity in fuel composition, the same assay has also been used with commercial ultra-low sulfur diesel formulations [8].

2. Alkane preparation
   Since the composition of substrates available to the positive control inoculum can vary from fuel to fuel, an equimolar mixture of C_6-C_{12} *n*-alkanes (hexane, heptane, octane, nonane, decane, undecane, and dodecane; Sigma-Aldrich, St. Louis, MO, USA) is used to ensure an excess supply of available potential electron donors.
3. Seawater (*see* **Notes 1** and **2**)
   Typically coastal seawater is used as the assay medium as well as the inoculum of choice in this protocol. Thus, seawaters from different locations can be readily compared. However, the protocol can be easily adapted when particular hydrocarbon-laden marine waters are desired (e.g., seawater-compensated fuel ballast tanks, offshore oil production waters) as the inoculum of interest. For the purpose of illustrating this protocol, coastal seawaters from Key West (KW, Florida, USA), San Diego Bay (SDB, California, USA), and shipboard oily ballast water (Sicily, Italy) were collected and shipped to the laboratory in 50 l plastic carboys or other smaller containers. The seawater samples were stored in a cold room at 4°C until used.
4. Positive control inoculum (*see* **Notes 3** and **4**)
   Desulfoglaeba alkanexedens, strain ALDC was selected as a positive control inoculum for the assay. This marine alkane-degrading sulfate-reducing bacterium was originally isolated from a Navy facility treating shipboard oily wastewater [5]. The organism can anaerobically biodegrade *n*-alkanes from C_6–C_{12} in chain length via the fumarate addition activation mechanism. We typically cultivate the positive control inoculum on decane as a source of carbon and energy as previously described [5].
5. Mild carbon steel
   Carbon steel (type 1018) is comprised of 0.15–0.20% C, 0.6–0.9% Mn, 0.035% maximum S, 0.03% maximum P, and the remainder elemental Fe. We used a commercial facility to cut carbon steel rods into round coupons of 9.53 mm diameter and 1 mm thickness. The coupons are used without polishing (*see* **Note 5**), and the average surface roughness of the two sides before exposure is approximately 10.13 ± 3.26 μm and 9.78 ± 0.82 μm, respectively.

6. The incubation vessels are 120 ml serum bottles (Wheaton, Millville, NJ, USA) closed with 1 cm thick stoppers that are held in place with and aluminum crimp seals.
7. PTFE (polytetrafluoroethylene)-coated quartz sewing thread (Glens Falls, NY, USA) is used to suspend coupons in the incubations.
8. Schott bottle (Schott Duran, Germany) with a modified closure to maintain anaerobic conditions.
9. Resazurin (0.1%) is routinely employed as a sensitive indicator of anaerobic conditions (*see* **Note 6**).
10. Sterile stock solution of $Na_2S \cdot 9H_2O$ (12.5 g/L).

2.2 Monitoring Sulfate Depletion

1. ICS-3000 ion chromatography (Dionex, Sunnyvale, CA, USA)
2. AS4S eluent concentrate (100× concentrate containing 0.18 M carbonate/0.17 M bicarbonate; Thermo Scientific, Sunnyvale, CA, USA)
3. Nanopure water (>17.5 MΩ/cm; Barnstead Nanopure Water Purification System, Thermo Fisher Scientific, Waltham, MA, USA)
4. Syringe filter (0.2 μm; polytetrafluoroethylene membrane; VWR International, West Chester, PA, USA)
5. Dionex™ IonPac™ AS4A-SC column (Thermo Scientific, Sunnyvale, CA, USA)

2.3 Weight Loss Measurement and Pitting Corrosion Analysis

1. Ultrasonic cleaner (Branson model 1210, Danbury, CT, USA)
2. Hexamethylenetetramine (Acros Organics, NJ, USA)
3. Nanopure water (same as Sect. 2.2)
4. Reagent-grade 12 N HCl (same as Sect. 2.3)
5. Acetone (99%, BDH Chemicals; VWR International, West Chester, PA, USA)
6. Methanol (99%, BDH Chemicals; VWR International, West Chester, PA, USA)
7. Precision weighing scale (±0.1 mg, Sartorius, Bohemia, NY, USA)
8. Nanovea noncontact optical profilometer PS50 with a 400 μm optical pen (Nanovea, CA, USA).

2.4 Total Iron Analysis

1. 10% hydroxylamine hydrochloride (Sigma-Aldrich, St. Louis, MO, USA)
2. Nanopure water (same as Sect. 2.2)
3. Ferrozine reagent (Acros Organics, NJ, USA)

4. HEPES buffer (4-(2-Hydroxyethyl)piperazine-1-ethanesulfonic acid, Acros Organics, NJ, USA)
5. Disposable Borosilicate Glass Culture Tubes (VWR International, West Chester, PA, USA)
6. Spectrophotometer (Thermo Spectronic, GENESYS™ 200, Rochester, NY, USA)

3 Methods

3.1 Incubation Assembly

1. Resazurin is added from a sterile stock solution (0.1%) to bulk seawater (1 ml/l) as a redox indicator and to monitor the maintenance of anaerobic condition throughout the incubation.
2. For sterile negative controls, the seawater and the culture of *Desulfoglaeba alkanexedens*, strain ALDC, (when used) are autoclaved (20 min at 121°C and 20 psi) and aseptic conditions employed.
3. The seawater is dispensed into sterile glass Schott bottles that are fitted with a closure capable of maintaining anaerobic conditions and bubbled with N_2 for at least 30 min prior to sealing with a 1 cm thick rubber septum.
4. Change the headspace in the now partially filled Schott bottles three times with N_2/CO_2 (80:20).
5. Immediately reduce the bulk seawater in the Schott bottles with 10 to 20 ml per liter (depending on the seawater source) of a sterile stock solution of $Na_2S \cdot 9H_2O$ (12.5 g/l).
6. Distribute 40 ml of reduced seawater into sterile 120 ml serum bottles (Fig. 1) while inside an oxygen-free atmosphere provided by a well-working anaerobic glove bag. The preweighed and sterilized coupons are then placed in the bottles (*see* **Note 7**).
7. For the incubations with *Desulfoglaeba alkanexedens*, strain ALDC, 35 ml seawater and 5 ml of a mature culture are used instead of seawater alone. All the bottles should be closed with butyl rubber septa and sealed with aluminum crimps.
8. Remove the incubations from the glove box and immediately exchange the headspace in the serum bottles three times with N_2/CO_2 (80:20) and adjust to atmospheric pressure before fuel addition.
9. Aseptically amend the closed incubations with the fuel of choice (0.1 ml fuel over 40 ml of seawater) by sterile syringe.

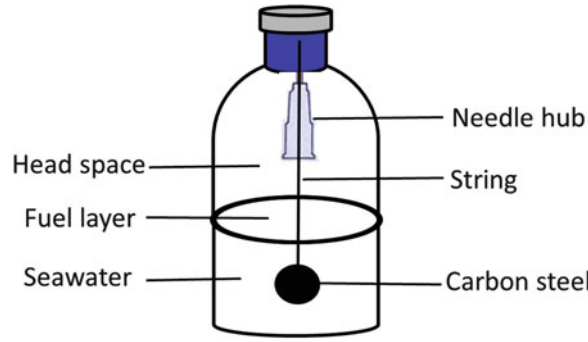

Fig. 1 Schematic of the serum bottle incubation system currently used to evaluate the relationship between anaerobic biodegradation of fuels and biocorrosion of carbon steel. In earlier iterations of this protocol, the coupon was simply placed on the bottom of the bottle. The suspension of the coupon in the medium with a PTFE-coated string (*see* Subsection 7 of Sect. 2.1) attached to the 1 cm thick stopper through a syringe needle that does not completely penetrate the closure (*see* **Note 7**)

10. For the incubations amended with the C_6-C_{12} *n*-alkanes, add 0.1 ml of the alkane mixture alone or with a particular fuel to each bottle as indicated in step 9.
11. Fuel-unamended and sterile controls should be incorporated, and all treatments should be conducted in triplicate and incubation should be in the dark at room temperature (21 ± 2°C).

3.2 Monitoring Sulfate Depletion (see Note 8)

1. Invert incubation bottles and withdraw ~0.3 ml aqueous phase periodically (generally every 30 days) with a sterile N_2-flushed syringe.
2. Freeze samples at (−20°C) prior to analysis by ion chromatography.
3. Thaw the frozen samples to room temperature and filter with 0.2 μm filters.
4. Dilute the samples (50 times for most seawaters) to target the linear range of analysis and load diluted samples into autosampler vials for subsequent analysis.
5. Prepare the ion chromatographic eluent by diluting a commercial available stock solution of sodium carbonate/bicarbonate buffer 100 times.
6. Operate the ion chromatographic system at 27 mA at a flow rate of 2.0 ml/min.
7. The standards are prepared by serial dilution (100, 200, 300, 400, and 500 μM) from 1 mM stock solution of sodium sulfate to quantify the amount of sulfate in the samples.
8. The concentration of sulfate in the various incubations is monitored over time and depicted in Fig. 2.

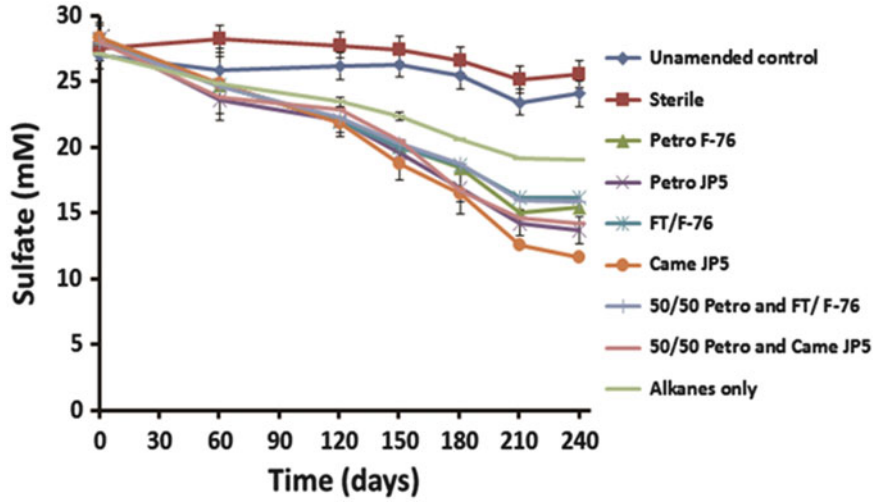

Fig. 2 Sulfate depletion with time (*see* **Note 9**) in anaerobic seawater incubations amended with various petroleum-based fuels (Petro JP5 and Petro F-76), hydroprocessed biofuels (Came JP5 and FT/F76), and blends of the petroleum-based and alternative fuels (50/50 JP5: 50% Petro and 50% Camelina; 50/50 F76: 50% Petro and 50% FT). The seawater incubations were also inoculated with the positive control organism, *Desulfoglaeba alkanexedens*, strain ALDC, and augmented with a series of low molecular weight (C_6–C_{12}) *n*-alkanes. No fuel or exogenously added electron donor were in the fuel-unamended control. Alkanes only indicated that no fuel was amended and *n*-alkanes served as the sole source of carbon. The sterile control incubations received the same amount of seawater and a culture of the positive control organism, but only after autoclaving

3.3 Corrosion Assay

1. The carbon steel coupons should be thoroughly cleaned before experimental use by washing with deionized water and sonication in water bath for 15 min followed by two successive acetone washes.
2. Dry the coupons with gentle stream of N_2, place in sealed serum bottles under N_2, and autoclave.
3. Weigh the coupons individually inside the glove bag and place the coupons on the bottom of the corresponding culture bottles prepared in Sect. 3.1.
4. Prepare acid cleaning solution (3.5 g l^{-1} of hexamethylenetetramine in 6 M HCl) to remove accumulated corrosion product from the coupon surface (*see* **Note 10**) based on the modification of ASTM G1-G3 [28].
5. Add 10–40 ml (depending on the amounts of corrosion products) of acid cleaning solution to the culture bottles with coupons and sonicate for 15 min (*see* **Note 11**) until all the corrosion products are dissolved.
6. Then withdraw the coupons and rinse (in order) with deionized water, acetone, and methanol.
7. The cleaned coupons should be dried and stored under N_2 prior to analysis (*see* **Note 12**).

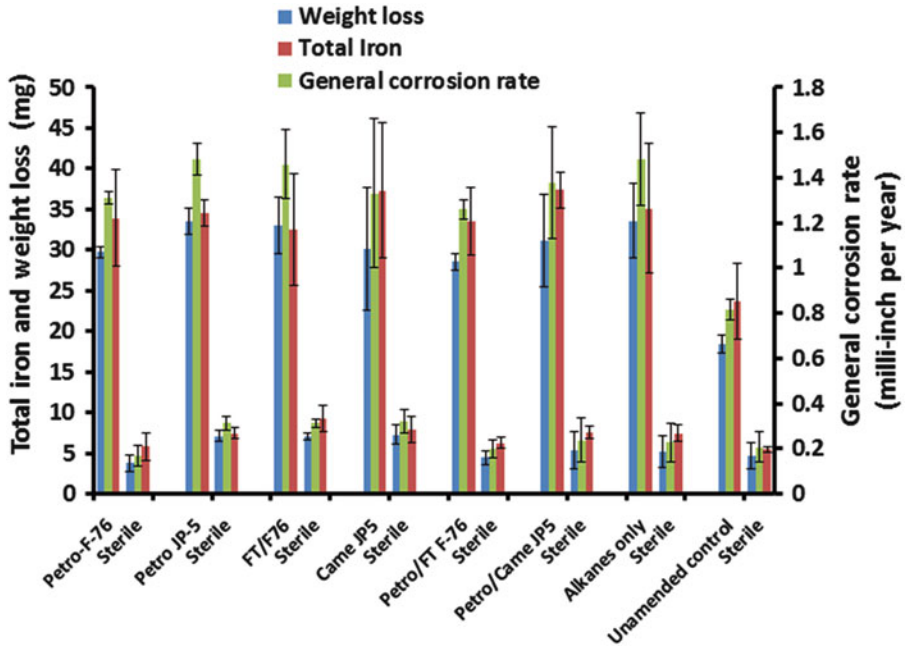

Fig. 3 Weight loss, general corrosion rate (*see* Subsection 8 of Sect. 3.3), and total iron analysis determined at the end of the incubations illustrated in Fig. 1. The total iron analysis largely accounts for the measured weight loss and thus serves as a complementary method for quantifying general biocorrosion activity. The general corrosion rate is much higher (5 to 10 times) than the corresponding sterile controls regardless of the nature of the fuel amendment

8. Weigh the cleaned coupons similarly inside the glove bag to obtain weight loss (Fig. 3), and the corresponding general corrosion rate can be calculated from weight loss according to ASTM G1-G3 standard [28].
9. Then the analyzed coupons should be kept under N_2 for subsequent analysis by profilometry (Sect. 3.5)

3.4 Total Iron Analysis

This analysis is performed to quantify the total iron removed via corrosion from the surface of the carbon steel coupons. As such, it helps close the iron mass balances and can be considered a complementary corrosion quantification analysis.

1. Prepare the ferrozine reagent (1 g/l ferrozine in 50 mM HEPES) with the pH adjusted to 7.
2. The acid cleaning solution in Sect. 3.3 should be diluted appropriately. The working range of the ferrous iron analysis is between 0.05 and 2 mM.
3. The diluted samples should be treated with 10% hydroxylamine hydrochloride to reduce any ferric iron to the ferrous state [29].
4. Add 10–100 μl samples into 5 ml prepared ferrozine reagent, and the iron can be quantified spectrophotometrically at 562 nm [30].

5. Prepare stock solution (10 mM) of ferrous ammonium sulfate in 0.5 mM HCl and then make serial dilutions from 0.05 to 2 mM with 0.5 mM HCl to construct a calibration curve.
6. The total iron could be calculated based on the dilution factors and final volume of the samples (Fig. 3).

3.5 Pitting Analysis

An important aspect of the protocol is the quantification of localized or pitting corrosion. This seemingly random nature of this type of damage is often of greater concern to the integrity of the fuel infrastructure than is general corrosion damage. Therefore, the exploration of this type of corrosion needs be carefully characterized in order to get better understanding of the underlying mechanisms. We recommend profilometry as it is both a sensitive and quantitative approach that has been successfully applied to assess pitting corrosion, e.g., [31].

1. The coupons after removing corrosion products with acid washing (Sect. 3.3) are scanned with a Nanovea noncontact optical profilometer PS50 with a 4 μm step size.
2. The electronically recorded raw data are then analyzed using the manufacturer supplied MountainsMap Topography XT6.2 software. The corrosion pattern can thus be visualized as a 3-D image (Fig. 4).
3. While there are several selectable options with the software, we define pits (*see* **Notes 13** and **14**) as damaged regions that are 20 μm below the mean plane and with an equivalent diameter ≥50 μm.

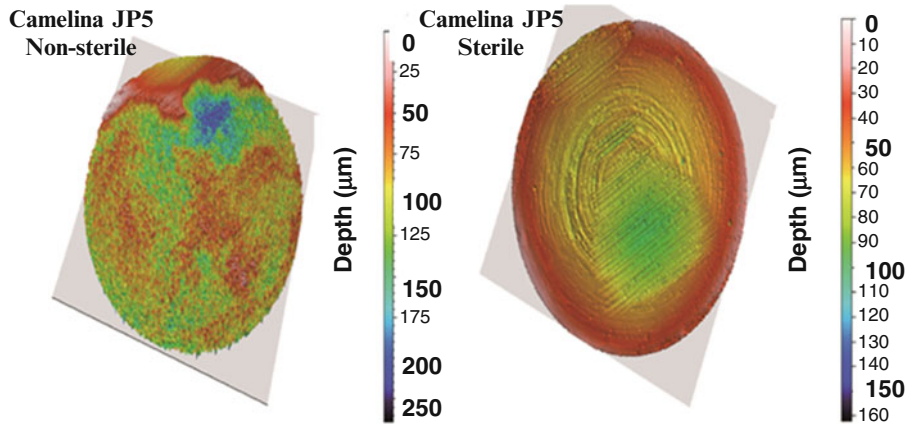

Fig. 4 Profilometry images of carbon steel coupons incubated in the seawater–fuel incubations containing camelina JP5. The degree of damage to the coupon in a nonsterile incubation is illustrated on the left, while the right image is a corresponding sterile control. Note the scales to the right of both images are not the same. Milling marks on the sterile control coupon are still obvious, while these have been removed from the nonsterile coupon. There were 598 pits in the coupon associated with microbial activity (*left*), while only 14 pits were evident in the sterile control. The pits (*see* **Note 13**) are defined as the regions that were ≥20 μm below the mean plane of the surface and had a diameter ≥50 μm

4. Other important parameters like average surface roughness and maximum pitting rate can also be obtained to characterize localized corrosion.

4 Notes

1. The seawater can be replaced with a defined microbiological medium [32] when desired. The procedure can be adapted to test any fuel exposed as well as different aqueous environments of varying salinity and electron acceptor characteristics.
2. We routinely use pristine oxygenated seawater in this protocol as this reflects the initial fill of seawater-compensated fuel ballast tanks. After a variable dark incubation period onboard ship, fuel is eventually added and the seawater gets displaced – but not from all ballast tanks in the ship network. There is direct contact between the seawater and fuel, and the rate of oxygen consumption via microbial heterotrophic respiration typically exceeds the rate of oxygen diffusion and anaerobic conditions develop. Upon ship deployment, fuel is consumed and the volume is replaced by new seawater, and transitory oxygenation of inflow ballast tanks can occur. However, the bulk of the ballast water can be retained in the tanks for months ($\geq$6 mo) at a time.
3. We recommend that a positive control organism be incorporated into the protocol to ensure that the assay is not predisposed to failure due to unrecognized inhibitory agents that might most likely be in either the fuel or aqueous environmental sample employed. To that end, we routinely use a known hydrocarbon-degrading sulfate-reducing bacterium, *Desulfoglaeba alkanexedens*, strain ALDC, as a positive control organism. When desired or necessary (depending on the fuel), we also add the preferred substrates for this organism (a mixture of C_6–C_{12} *n*-alkanes) so that excess suitable electron donors are available to the control organism.
4. Although *D. alkanexedens* serves as the recommended positive control bacterium, other marine hydrocarbon-degrading sulfate-reducing bacteria can fulfill this role. However, molecular surveys reveal that *D. alkanexedens* can be detected even at the end of rather lengthy incubations (>200 days). We currently have specific PCR primers to more fully monitor the fate of this positive control inoculum in the test protocol.
5. We used unpolished coupons in this protocol since the carbon steel employed in the infrastructure facilities (e.g., pipelines, ballast tanks, storage tanks, etc.) is unpolished carbon steel. However, coupons can be polished to varying degrees when more elaborate corrosion-monitoring efforts than the ones described here are desired.

6. The color of the resazurin-amended seawater should turn from blue to pink and eventually clear during this operation. This process may take several hours or even overnight depending on the dissolved oxygen in the seawater sample.
7. Merely placing the coupons on the bottom of the incubations, while simple, can be problematic when assessing corrosion. We use a 1 cm thick butyl rubber septum to suspend the coupon inside the incubation with a PTFE-coated quartz string (*see* Fig. 1). The suspended coupon approach allows for the evaluation of corrosion on both sides of the coupon, and assays have been proven to be more reproducible.
8. Additionally, gas chromatography–mass spectrometry (GC-MS) and/or advanced liquid chromatography coupled with electrospray ionization quadrupole time-of-flight mass spectrometry (LC-ETS-QTOF-MS) can be used to detect metabolites and thus confirm biodegradation of fuel constituents. For example, the detection of signature intermediates such as the alkyl- and arylsuccinates transiently produced during hydrocarbon biodegradation experiments can unequivocally attest to the metabolism of the fuel components [33].
9. It should be noted that the protocol-testing period, while commensurate with the residence time of seawater in navy ballast tanks, represents a rather prolonged laboratory-based evaluation procedure. This is due in part to the relatively slow anaerobic hydrocarbon biodegradation in the initially pristine oxygenated seawater used as an inoculum (*see* Fig. 2). For perspective, first-generation methylester biodiesel would consume the available sulfate and exhibit metal biocorrosion in less than 60 days [9]. We are attempting to develop an accelerated biodegradation/biocorrosion protocol that will provide comparable and environmentally conservative conclusions. To that end, we have tried incorporating marine sediment as source of additional inoculum in the test procedure. We are also trying to concentrate the seawater microorganisms using a variety of filtration, centrifugation, or cell trapping protocols. These procedures have the promise of greatly shortening the period of time needed to assess the stability of various fuel formulations.
10. The hexamethylenetetramine acts as a corrosion inhibitor to prevent the zerovalent iron from further oxidization during the cleaning process. The solution is used to remove only the corrosion product but not to cause excessive damage to the underlying metal.
11. If necessary, the carbon steel coupons can be scrubbed with bristle brush in order to remove the tightly attached corrosion products. It should be noted that for long-term corrosion experiments ($\geq$3 months incubation), that corrosion products

are so adherent that it can be nearly impossible to completely remove corrosion deposition even with sonicating while in the acid cleaning solution.

12. It's critical to store the acid-cleaned coupons under N_2 since carbon steel will rapidly oxidize upon exposure to air.
13. The quantification of pit number can be somewhat subjective, depending on the morphology severity of corrosion damage to the metal surface. The recommended parameters to define pits are arbitrary and ones that we have employed previously. However, different parameters or other approaches (*see* **Note 14**) can be employed to best evaluate pitting corrosion.
14. The profilometry analysis can be problematic if one is interested in studying the initiation and propagation of pitting. Initial pitting events are typically too small ($\leq$1 μm) to be well defined by profilometry. Complimentary approaches such as high-resolution field emission microscopy and atomic force microscopy are very powerful for characterizing nanoscale pitting during the early stages of corrosion, but these approaches are typically nonquantitative.
15. Obviously, any assessment of the biodegradation and biocorrosion processes associated with any fuel formulation must incorporate the use of appropriate negative controls. We recommend that minimally the two negative controls (and one positive control) be utilized faithfully as an essential part of the protocol. The fuel-unamended controls will provide an assessment of the endogenous rate of electron acceptor consumption in the absence of a hydrocarbon source. This rate or amount can be dismissed as baseline microbial activity and corrected from the fuel-amended experimental treatments. Similarly, the amount of corrosion in the negative control incubations can also be dismissed as background and not in any way linked with fuel consumption. Sterile controls would seem to be rather obvious to include in the protocol. However, inactivation of the requisite biology also eliminates the capacity of the control incubations to maintain highly reducing conditions that are characteristic of active sulfate-reducing conditions. Nevertheless, the provision of sterile controls allows for the correction of spurious and unanticipated abiotic loss mechanisms (e.g., differential adsorption of some hydrocarbon components to the stopper). If further metabolite profiling will be performed, the GC-MS analysis of sterile controls is essential to be certain that resolvable chromatographic peaks detected in nonsterile incubation are not mistaken as putative metabolites. The comparable peaks in the sterile controls confirm that compound was already present in the incubations and not worth further identification attempts.

Table 1
The impact of petroleum and biobased diesel fuels on carbon steel corrosion. Data was collected after >300 day incubations using the described protocol. A positive control bacterium was not included

Inoculum	Incubation condition[a]	Sulfate (mM)		Coupon weight loss (mg)	General corrosion rate (milli-inch year^{-1})[b]	Localized corrosion (number of pits)
		Initial	Loss			
San Diego Bay seawater and sediment	Fuel-unamended	28.54 ± 0.31	12.72 ± 0.38	63.6 ± 7.21	5.34 ± 0.6	277 ± 72
San Diego Bay seawater and sediment	Fuel-amended	28.42 ± 0.90	19.72 ± 1.44	80.55 ± 8.83	6.76 ± 0.76	351 ± 114
San Diego Bay seawater and sediment	Sterile (*see* **Note 15**)	28.31 ± 0.41	−0.83[c] ± 0.13	8.9 ± 2.26	0.74 ± 0.79	38 ± 5.65
Shipboard oily ballast water	Fuel-unamended	9.77 ± 0.30	6.44 ± 0.18	37.5 ± 4.03	2.83 ± 0.33	432 ± 24
Shipboard oily ballast water	Fuel-amended	9.55 ± 0.72	8.46 ± 0.57	40.3 ± 4.1	3.07 ± 0.34	932 ± 224
Shipboard oily ballast water	Sterile	9.60 ± 0.27	−1.42 ± 0.30[c]	4.55 ± 0.21	0.34 ± 0.01	1

[a]San Diego Bay and the oily ballast water (*see* **Note 16**) experiments received camelina-JP5 or petroleum F76, respectively, as example diesel fuels where indicated
[b]The general corrosion rate was calculated from the weight loss data according to ASTM procedures [28]
[c]Negative sulfate loss in sterile controls reflects experimental variability in replicate incubation

16. The bulk of the results presented in this chapter were obtained using seawater incubations obtained from Key West, FL, and incorporating where appropriate the positive control bacterium *D. alkanexedens* strain ALDC. However, the protocol can be successfully employed to assess both petroleum-based (e.g., petroleum-F76) and biomass-derived (camelina-JP5) fuels in incubations that were not amended with the positive control bacterium. Examples of seawater/sediment incubations from the San Diego Bay as well as oily ballast water incubations are shown in Table 1. The inocula in these samples were able to biodegrade fuel components as evidenced by sulfate utilization and corrode metal coupons as indicated by both weight loss and profilometry. The success of these inocula suggests that they already possessed a metabolically capable microflora that was functional under the assay conditions. In effect, the exogenous addition of a positive control bacterium proved unnecessary in these cases, but rarely is this information known a priori. We are currently using the protocol to examine biodegradation, metal corrosion, and the succession of microbial communities in seawater-compensated fuel ballast tanks from navy ships.

Acknowledgement

We acknowledge the financial support from the Office of Naval Research (Award no. N0001408WX20857) and the advice and expertise of the many investigators on this project who contributed to the development of this protocol.

References

1. Widdel F, Rabus R (2001) Anaerobic biodegradation of saturated and aromatic hydrocarbons. Curr Opin Biotechnol 12(3):259–276
2. Rabus R (2005) Functional genomics of an anaerobic aromatic-degrading denitrifying bacterium, strain EbN1. Appl Microbiol Biotechnol 68(5):580–587
3. Gieg LM, Duncan KE, Suflita JM (2008) Bioenergy production via microbial conversion of residual oil to natural gas. Appl Environ Microbiol 74(10):3022–3029
4. So CM, Young L (1999) Isolation and characterization of a sulfate-reducing bacterium that anaerobically degrades alkanes. Appl Environ Microbiol 65(7):2969–2976
5. Davidova IA, Duncan KE, Choi OK, Suflita JM (2006) *Desulfoglaeba alkanexedens* gen. nov., sp. nov., an n-alkane-degrading, sulfate-reducing bacterium. Int J Syst Evol Microbiol 56(12):2737–2742
6. Caldwell ME, Garrett RM, Prince RC, Suflita JM (1998) Anaerobic biodegradation of long-chain n-alkanes under sulfate-reducing conditions. Environ Sci Technol 32(14):2191–2195
7. Townsend GT, Prince RC, Suflita JM (2003) Anaerobic oxidation of crude oil hydrocarbons by the resident microorganisms of a contaminated anoxic aquifer. Environ Sci Technol 37 (22):5213–5218
8. Lyles CN, Aktas DF, Duncan KE, Callaghan AV, Stevenson BS, Suflita JM (2013) Impact of organosulfur content on diesel fuel stability and implications for carbon steel corrosion. Environ Sci Technol 47(11):6052–6062
9. Aktas DF, Lee JS, Little BJ, Ray RI, Davidova IA, Lyles CN, Suflita JM (2010) Anaerobic metabolism of biodiesel and its impact on metal corrosion. Energ Fuel 24(5):2924–2928
10. Lee JS, Ray RI, Little BJ, Duncan KE, Oldham AL, Davidova IA, Suflita JM (2012) Sulphide

production and corrosion in seawaters during exposure to FAME diesel. Biofouling 28 (5):465–478

11. Aktas DF, Lee JS, Little BJ, Duncan KE, Perez-Ibarra BM, Suflita JM (2013) Effects of oxygen on biodegradation of fuels in a corroding environment. Int Biodeter Biodegr 81:114–126
12. Lee JS, Ray RI, Little BJ (2012) An investigation of anaerobic processes in fuel/natural seawater environments. Document, DTIC
13. Knothe G (2008) "Designer" biodiesel: optimizing fatty ester composition to improve fuel properties. Energ Fuels 22(2):1358–1364
14. Liu G, Larson ED, Williams RH, Kreutz TG, Guo X (2010) Making Fischer–Tropsch fuels and electricity from coal and biomass: performance and cost analysis. Energ Fuels 25 (1):415–437
15. Albuquerque M, Machado Y, Torres A, Azevedo D, Cavalcante C, Firmiano L, Parente E (2009) Properties of biodiesel oils formulated using different biomass sources and their blends. Renew Energ 34(3):857–859
16. Altıparmak D, Keskin A, Koca A, Gürü M (2007) Alternative fuel properties of tall oil fatty acid methyl ester–diesel fuel blends. Bioresour Technol 98(2):241–246
17. Conkle H, Marcum G, Griesenbrock E, Edwards E, Chauhan S (2012) Development of Surrogates of Alternative Liquid Fuels Generated from Biomass. ASC Document Number 88ABW-2012-2132
18. Hamilton LJ, Williams SA, Kamin RA, Carr MA, Caton PA, Cowart JS (2011) Renewable fuel performance in a legacy military diesel engine. Document number AIAA-2008-6412, In ASME 2011 5th International Conference on Energy Sustainability, pp. 1095–1107
19. Rodriguez B, Bartsch TM (2008) The United States Air Force's process for alternative fuels certification. Document number AIAA-2008-6412, 26th AIAA Applied Aerodynamics Conference, Honolulu, HI, 18—21 August 2008.
20. Richard TL (2010) Challenges in scaling up biofuels infrastructure. Science(Washington) 329(5993):793–796
21. Sarisky-Reed V (2009) Advanced Biofuels: Infrastructure Compatible Biofuels. US Department of Energy, Ed, ed, presentation to Biomass R&D Technical Advisory Committee. (www.biomassboard.gov/pdfs/advanced_biofuels_doejg.pdf)
22. DeMello JA, Carmichael CA, Peacock EE, Nelson RK, Samuel Arey J, Reddy CM (2007) Biodegradation and environmental behavior of biodiesel mixtures in the sea: an initial study. Marine Poll Bull 54(7):894–904
23. Owsianiak M, Chrzanowski Ł, Szulc A, Staniewski J, Olszanowski A, Olejnik-Schmidt AK, Heipieper HJ (2009) Biodegradation of diesel/biodiesel blends by a consortium of hydrocarbon degraders: effect of the type of blend and the addition of biosurfactants. Bioresour Technol 100(3):1497–1500
24. Sharma Y, Singh B, Upadhyay S (2008) Advancements in development and characterization of biodiesel: a review. Fuel 87 (12):2355–2373
25. Lee JS, Ray RI, Little BJ (2010) An assessment of alternative diesel fuels: microbiological contamination and corrosion under storage conditions. Biofouling 26(6):623–635
26. Wang W, Jenkins PE, Ren Z (2012) Electrochemical corrosion of carbon steel exposed to biodiesel/simulated seawater mixture. Corro Sci 57:215–219
27. Wang W, Jenkins PE, Ren Z (2011) Heterogeneous corrosion behaviour of carbon steel in water contaminated biodiesel. Corro Sci 53 (2):845–849
28. ASTM, G 1–03 (2003), Standard Practice for Preparing, Cleaning, and Evaluating corrosion test specimens.ASTM International, pp. 1–9.
29. Stookey LL (1970) Ferrozine–a new spectrophotometric reagent for iron. Anal Chem 42 (7):779–781
30. Lovley DR, Phillips EJ (1986) Availability of ferric iron for microbial reduction in bottom sediments of the freshwater tidal Potomac River. Appl Environ Microbiol 52(4):751–757
31. Duncan KE, Perez-Ibarra BM, Jenneman G, Harris JB, Webb R, Sublette K (2014) The effect of corrosion inhibitors on microbial communities associated with corrosion in a model flow cell system. Appl Microbiol Biotechnol 98(2):907–918
32. Widdel F, Bak F (1992) Gram-negative mesophilic sulfate-reducing bacteria. In: The prokaryotes. Springer New York, pp 3352–3378
33. Gieg LM, Suflita JM (2002) Detection of anaerobic metabolites of saturated and aromatic hydrocarbons in petroleum-contaminated aquifers. Environ Sci Technol 36(17):3755–3762

Protocols for Measuring Methanogenesis

Oleg Kotsyurbenko and Mikhail Glagolev

Abstract

Methanogenesis is one of the most important terminal processes in the microbial degradation of organic matter in many anoxic environments. Since ancient times, methane was known as a combustion gas, but its microbiological origin was proved only in the nineteenth century. The contribution of methane to the global warming and its beneficial importance in ecological biotechnology and bioenergetics dictate the need in proper estimations of its fluxes and measurements of its production rates in different microbiological processes.

Measuring methanogenesis is mostly conducted in laboratory experiments with different types of methanogenic samples, in fields or in ruminants. The samples used for such measurements are either liquid methanogenic cultures and slurries prepared by homogenization and dilution or intact soil cores. All types of methanogenic samples are incubated, and accumulated CH_4 is analyzed in order to calculate methanogenesis rate. The samples as slurries incubated under laboratory conditions are referred to as potential production rates, whereas rates measured in intact samples or in fields are referred to as actual (in situ) production rates.

To initiate methanogenesis, characteristic substrates of methanogens are used as additions to the samples. Radiotracers are also used to measure rates of certain methanogenesis pathways in samples.

Classification of methods of measuring methanogenesis is based on the mass balance equation relating the rate of change in concentration of methane with its source and flux. The two major methods are described in detail.

Keywords: Chamber method, Methanogenesis, Methanogens, Potential methane production, Radiotracers

1 Introduction

1.1 Role of Methanogenesis

Methanogenesis is the most important terminal process in the microbial degradation of organic matter in many anoxic environments. It is a type of anaerobic respiration using carbon as an electron acceptor with the production of methane.

Since ancient times, methane has been known as a combustible gas seeping from geological fissures. First scientific evidence for its originating from sediments and marshy places has been obtained by A. Volta in 1776 [1]. A century thence, its microbiological formation was proved in the experiments of Bechamp and Tappeiner [2]

T.J. McGenity et al. (eds.), *Hydrocarbon and Lipid Microbiology Protocols*, Springer Protocols Handbooks, (2017) 227–244,
DOI 10.1007/8623_2015_89, © Springer-Verlag Berlin Heidelberg 2015, Published online: 20 June 2015

and created widespread interest to study methanogenesis in different environments.

In the twentieth century, study of methanogenesis has led to remarkable discoveries in its biochemistry (coenzyme M, factors 420 and 430) and physiology (C1 compounds as substrates, alcohols as electron donors) of methanogens. New applied approaches such as Hungate technique have significantly facilitated their cultivation [1].

Methane is one of the important greenhouse gases that have been contributing to global warming due to its radiative effect which is 25 times greater than carbon dioxide. Increases in the atmospheric concentration of methane and its potential for global warming as a greenhouse gas have stimulated considerable research addressing CH_4 flux magnitudes from various ecosystems as well as studies focusing on the environmental and anthropogenic controls on flux intensities during the past few decades.

Nearly 90% of total methane emission originate from microbial processes [3]. Methane is produced from the decomposition of organic matter by strictly anaerobic archaeal methanogens, under highly reduced conditions. Methanogenesis occurs in moderate habitats such as rice paddies [4], soils [5], and lake sediments [6]; in extreme conditions such as hydrothermal vents [7] and permafrost soils [8, 9]; and also in the gastrointestinal tract of animals [10], termites [11], and ciliates [12].

Methanogens are considered to be one of the most ancient forms of life [13]. The detection of methane in the atmosphere of other planets can be an indication for extraterrestrial life presented by methane-producing organisms since methane should dissipate if there is nothing there to replenish it [14].

Methanogenesis can also be beneficially exploited. Human society generates enormous quantities of organic wastes from animal husbandry, food and beverage manufacture, pulp and paper processing, microalgae-based bioenergy, and municipal facilities. Anaerobic microbial digestion can be used to treat such organic wastes with production of different useful compounds including CH_4. Biogenic methane can be then collected and used as a sustainable alternative to fossil fuels [15].

The earliest methodology in measuring methanogenesis was based on cultivation of methanogenic microorganisms with further detection of methane by gas chromatography. Later, the method of use of radioactive substrates for short-term incubations with water and soil samples was developed [16, 17]. This radiotracer technique made possible quantitative estimations of methanogenesis rates in biogeochemical cycle of CH_4.

In 1987, a new layered mass balance method was developed for studying gas exchange processes [18–20]. It was in particular applied for measuring methanogenesis in intact soil cores named "mesocosm" [18] and in field in situ experiments as deep soil

chamber technique [21, 22]. In this method, the methanogenesis rate is calculated by mass balance equations for methane in soil profile.

1.2 Classification Concept of Methods of Measuring Methanogenesis

All methods of measuring methanogenesis can be classified by the criteria proposed below.

From the most general point of view, the evaluation of the magnitude of methanogenesis is the physics problem of determination of power of the mass source of methane. Rigorous quantitative basis for determining the power of the source is the fundamental law of conservation of mass.

The time rate of change or accumulation of the mass of methane within the control volume (*see* **Note 1**) is equal to the sum of the fluxes, or rate of transport per unit time, through all control surfaces. Also added or subtracted are any sources or sinks that occur, or

$$\underset{\text{Accumulation}}{\partial C/\partial t} = \underset{\text{Sources}}{w^{+}} - \underset{\text{Sinks}}{w^{-}} - \underset{\text{Transport}}{\operatorname{div}(j)},$$

where C is the concentration of methane ($M\ L^{-3}$), t is the time, w^{+} is the source intensity of CH_4 (the mass of methane generated per unit of volume and time), w^{-} is the sink intensity of CH_4 (the mass of methane consumed per unit of volume and time), and j is the net flux of methane ($M\ L^{-3}\ T^{-1}$) (*see* **Note 2**) [23].

The equation indicates two possible causes of physical conditions of methane in a limited space region: firstly, activity of sources and sinks of CH_4 in this region and, secondly, its flow through the surface limiting the region studied. Methane sources and sinks are those processes in which it is produced and consumed, respectively. The latter include oxidative photochemical reactions in the atmosphere, the biological consumption of methane by methanotrophic bacteria, and some others.

To classify the methods of measuring methanogenesis, it is important to properly identify two different regions (interior and exterior) limited by the surface boundary for the system where the chosen method is used (Fig. 1). To determine actual methanogenesis rates, the aforementioned equation should be solved correctly within the region studied. The region should be properly specified and differs in case of various methods. The interior region can be the content of a flask or soil where there are a methane source and transport processes. The exterior region can be all space over the soil where methane is emitted. In mathematical terms, we have internal or external boundary problems [24] to be addressed for making proper calculations in each chosen method of measuring methanogenesis. When solving the above equation for each method used, with all assumptions, the final simplified form of this equation can be derived. This equation form specific for each

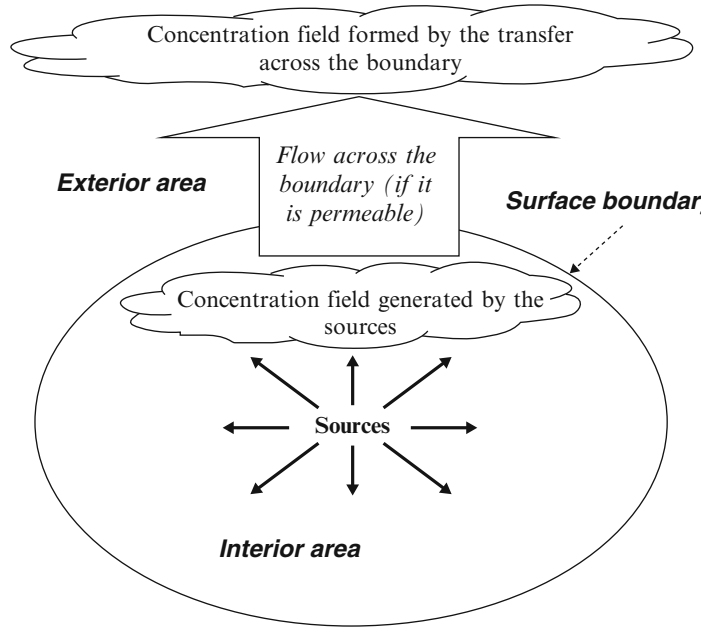

Fig. 1 Scheme of areas for identifying the boundary problem at the method classification

Table 1
Classification of methods of measuring methanogenesis

Method	System	Equation terms				Task
		w^+	w^-	$\partial C/\partial t$	div(j)	
Potential production (in vitro)	Cell cultures, water and soil samples (slurries), ruminants, termites, ciliates	≠0	0	≠0	0	Internal
Layered mass balance method (deep soil chamber technique)	Mesocosm in laboratory, mesocosm in situ partly isolated	≠0	0	≠0	≠0	Internal
Static (closed) chamber technique (dynamic (open) chamber technique)	Microcosm, mesocosm, fields, landfills, ruminants	≠0	≠0	≠0	0	External
Micrometeorological methods	A CH_4 source located at a square or in a volume starting from a few m^2 or m^3, respectively (wetland site, landfills, a ruminant, and others)	≠0	≠0	≠0	≠0	External

method as well as the type of the boundary problem mentioned above is in the basis of the classification concept (*see* **Note 3**). In Table 1, all main methods of measuring methanogenesis are presented and distinguished by the concept described above.

The same methods of measuring methanogenesis can be applied for different types of systems and vice versa.

In the incubation experiments in vitro on measuring methanogenesis in flasks or bottles, for example, samples from water bodies, soils, and ruminants as well as growing methanogenic cultures in a liquid medium can be studied. The soil slurries (suspensions) are usually prepared from different samples taken from various methane-generating ecosystems such as lake sediments, paddy soils, or peatlands. Such methanogenesis rates are referred to as potential production (turnover) rates [25–27] (*see* **Note 4**). Preparation of methanogenic samples is different and depends on the texture of the material used for the incubation experiment.

In the chamber technique, methanogenesis rates in microcosms or mesocosms as well as in fields obtained from mass balances are referred to as actual (in situ) production rates [25–27]. Soil microcosm (planted or unplanted) is the aggregate structure intact sample that is undisturbed or minimally disturbed. Mesocosm is a bigger volume soil core similar to microcosm in structure [28] for the experiments of a bigger scale (*see* **Note 5**).

1.3 Comparative Description of the Methods

Laboratory method of measuring potential methane production in different vessels during incubation experiments is well known and widely used. Methane is analyzed by a gas chromatograph equipped with flame ionization or thermal conductivity detectors. The former detects ions produced during combustion of methane molecules in a hydrogen flame, whereas the latter senses changes in the thermal conductivity of methane and compares it to a reference flow of carrier gas (helium or hydrogen for the highest sensitivity) with a signal production. Molecular sieves, Porapak Q, and SOV-POL can be used as sorbents.

Sampling should be made with tight hermetical syringes. The total gas volume sampled from the system (flask, bottle, chamber) during the experiment should not exceed 0.5–1% of its volume. Otherwise, some corrections for final calculations of methane concentration have to be made.

The rate of CH_4 production is finally calculated after chromatographic measurements taken periodically during methanogenesis experiments. In some cases, radiotracers are used in order to study the predominant methanogenesis pathway in the ecosystem. The radiotracers as typical methanogenic substrates added to the studied samples in a small amount are further converted to methane and can be then detected by a radioactive counter [29–31]. In order to estimate the rate of methanogenesis from a certain precursor and make carbon balance calculations, specific inhibitors are used to block either total methanogenesis or its particular pathway [32].

The static (closed) chamber method is the most commonly used technique for measuring gas exchange between soil or water surface and the atmosphere, probably because of its low cost and

ease of use. It is generally used worldwide in natural forests, wetlands, and natural lakes or artificial reservoirs particularly where a power supply is unavailable [33–36], but necessary for most other methods. Particularly, dynamic (open) chamber method and micrometeorological techniques need power supply for air flushing procedure and ultrasonic anemometer and gas analyzer, respectively. The dynamic chamber method is developed to avoid incorrect results due to possible influence of accumulated methane on its production. It is realized by flushing the chamber with air during measurements [37, 38].

The chamber technique is mostly designed to measure methane emission rates as the vector sum of the rates of production and consumption. In field experiments, the true methanogenesis can be determined by introduction of acetylene into the chamber gas phase (10% of the total volume at the incubation time of 1–2 h) by the inhibition of microbial methane consumption [39, 40]. In laboratory, the chamber containing mesocosm can be flushed with inert gas that prevents development of oxygen-dependent methanotrophs. Flux estimates are based on changes with time in chamber headspace gas (particularly CH_4) concentrations, measured after the chamber is placed on the soil surface [35]. Fluxes are further calculated from the slope of the concentration change over time, corrected to the surface area covered by the chamber and the "effective volume" of the chamber [41].

Nevertheless, the chamber technique can alter the local environment making it unrepresentative. Due to logistical problems, it is often difficult to employ chambers for long-term, continuous measurements or to deploy enough chamber replicates to obtain statistically reliable results. In opposite, micrometeorological techniques provide possibility for continuous measurements not disturbing the environment and an area-integrated, ensemble average of the exchange rates between the surface and the atmosphere [42].

Micrometeorological methods are based on measurements of wind velocity and methane concentration, but the number of measuring points and the theories used to calculate emission rates differ between variations of the method. Moreover, these methods are influenced by instabilities like nonsteady-state wind or movement of point emission sources and should be further developed. Micrometeorological methods are defined as measuring fluxes of gas in the free atmosphere and relating these fluxes to animal emissions [43]. The micrometeorological mass difference technique as well as the external tracer ratio technique, where a tracer gas is released in the paddock or barn and the concentrations of tracer and methane are measured in the surroundings [44], can be used as a modification.

Layered mass balance method is designed to measure the rates of methanogenesis in the soil profile of a microcosm under controlled laboratory conditions. In this method, change of methane concentrations in time is defined in different soil layers using a

plastic box and a set of tubes inserted in the soil on different depths. Methane production and mass transport (diffusion, advection) determine this concentration change and can be then calculated.

The deep soil chamber technique is a modification of the layered mass balance method that was developed for in situ measurements. A metallic cylinder and metallic tubes are used to be installed in a soil layer. Both techniques measure true methane production under anoxic conditions since no contacts to atmospheric air are provided.

Ruminants produce methane as a by-product of their digestion process. Nevertheless, the methodologies for measuring CH_4 emissions from ruminants are based on the main approaches mentioned above and range from in vitro potential gas production technique and animal respiration chambers to micrometeorological methods. The principle of the in vitro gas production technique is to ferment feed under controlled laboratory conditions by natural rumen microbes. Feedstuffs are incubated at 39°C with a mixture of rumen fluid, buffer, and minerals for a certain time period. The amount of total gas produced during incubation is measured and its composition analyzed, to obtain data on the in vitro production of methane. The principle of the animal chamber is to collect exhaled CH_4 emissions from all sources of enteric fermentation (mouth, nostrils, and rectum) from the animal and to measure the concentration [43]. Other methods of measuring methanogenesis in ruminants are the technique based on sampling air released by eructation during milking [45]; the technique of mass balance in enclosed barns (*see* **Note 6**), where ventilation rate and concentrations in inlet and outlet are used to estimate the emission [46]; and the sulfur hexafluoride (SF6) tracer technique [47–50]. The latter involves placing a permeation tube charged with SF_6 pre-calibrated for its release rate into the rumen of an animal and the subsequent collection of time-integrated breath samples for analysis of CH_4 and SF_6 as a marker and calculation of actual CH_4 emission. Micrometeorological technique can be successfully applied for measuring methanogenesis in ruminants as a difference between methane fluxes from the pasture with feeding animals and those without them.

There are also some other simplified and lower accurate laboratory techniques for measuring methanogenesis such as manometric [51] and volumetric methods [52].

2 Materials

2.1 Materials for Measurements of Potential Production Rates In Vitro

In the incubation experiments, mineral anoxic medium is used to grow methanogenic cultures. Native liquid fraction in the samples taken and sterile distilled water or a buffered mineral solution for dilution are used to prepare slurries.

2.1.1 Mineral Medium for Growing Methanogens

Components to be added to 1 l of oxygen-free water:

1. $Na_2S \times 9H_2O$ as reducing agent (0.5 g/l).
2. $NaHCO_3$ as a buffer (1.5 g/l).
3. Resazurin (0.02 g/l) as an indicator of anoxic conditions.
4. Yeast extract (0.2 g/l) as a growth factor if necessary.
5. Vitamin solution (10 ml/l) [53].
6. Acidic microelement solution (2 ml/l) adjusted to pH 2.0 by HCl containing the following compounds (in g/l): $FeSO_4 \times 7H_2O$ (0.30), $CoCl_2 \times 6H_2O$ (0.18), $MnCl_2 \times 4H_2O$ (0.10), $ZnSO_4 \times 7H_2O$ (0.15), $KAl(SO_4)_2 \times 12H_2O$ (0.025), $NiCl_2 \times 6H_2O$ (0.18), H_3BO_3 (0.010), $CuCl_2 \times 2H_2O$ (0.025).
7. Alkaline microelement solution (2 ml/1) adjusted to pH 10 by KOH containing the following components (in g/l): Na_2SeO_4 (0.14), $Na_2MoO_4 \times 2H_2O$ (0.06), $Na_2WO_4 \times 2H_2O$ (0.17).
8. Acetate, methanol, or trimethylamine as methanogenic substrates (20 mmol/l is recommended for methanogenesis rate determination). H_2/CO_2 (4:1) gas mixture can be also used as a substrate and a headspace component.
9. N_2/CO_2 (4:1) gas mixture as a the headspace component.

2.1.2 Materials for Anaerobic Cultivation Technique

1. Culture vessels (bottles, flasks, or tubes) with rubber stoppers and screw caps
2. Crimpers and decrimpers
3. Anaerobic flushing system to flush the vessels with an inert gas or the required gas mixture
4. Dispensers to fill the vessels with anaerobic medium
5. Inert gases (N_2 or Ar)
6. Incubators with a set temperature for a longtime incubation
7. A gas chromatograph equipped with a flame ionization detector

2.1.3 Materials for Radiotracers Technique

Additional materials for anaerobic cultivation technique (Sect. 2.1.2) (*see* **Note 7**):

1. Solution of carrier-free radioactive Na-[2-^{14}C]-acetate, Na-[1-^{14}C]-acetate, $NaH^{14}CO_3$
2. 5 N H_2SO_4 solution
3. Gas proportional counter
4. A gas chromatograph equipped with a radioactivity detector

2.2 Materials for Static Chamber Method

1. Boardwalks
2. Stainless steel [54] or plastic collars [55]

3. Chamber: open-bottomed gas collection cover made from polyvinyl chloride (PVC) [56] or aluminum [55] fitted with a fan [57] (*see* **Note 8**)
4. Reflecting aluminum fabric
5. Plastic syringes (60 ml [54] or 20 ml [22] or 10 ml [55])
6. Evacuated gas-tight flasks (10 ml [54] or 9 ml [55])
7. Barometer
8. Chamber temperature detector
9. Gas chromatographic system (with flame ionization detector)

3 Methods

In this paragraph, two main methods of measuring potential methane production and actual in situ methanogenesis are described in detail. The layered mass balance technique is not yet widespread used. Micrometeorological methods are designed to measure rather methane emission rates and can be used for measuring methanogenesis conditionally.

3.1 Measuring Potential Methanogenesis Rates In Vitro

This method is based on measuring methanogenesis in methanogenic cultures or samples taken from different ecosystems and incubated for a certain period of time until methane production becomes stable. In methanogenic cultures, methane production can be measured at their growing. In natural samples producing CH_4, methanogenesis is normally measured once a steady state is established in the system in order to get a linear dependence of methane produced to the experiment time.

3.1.1 Preparation of Methanogenic Cultures in a Liquid Medium

Enrichment cultures or pure cultures of methanogenic archaea from the late exponential growth phase should be used for the inoculation.

1. Use serum bottles (60–120 ml) with butyl rubber stoppers and metallic caps to conduct the experiment on measuring methanogenesis.
2. Flush the bottles with an oxygen-free gas (N_2, Ar) or gas mixture (N_2/CO_2, H_2/CO_2) depending on the experimental purposes. If a gas mixture is used as substrate, then pressurize the bottles with the gas mixture to a total pressure of 150 kPa (*see* **Note 9**).
3. Prepare the defined bicarbonate-buffered and sulfide-reduced mineral medium described for freshwater or halophilic species of methanogenic archaea by anaerobic technique (*see* **Note 10**).
4. Fill the bottles anaerobically with the medium.

5. Add trace element solution and organic substrates from sterile concentrated stock solutions. Sterilize the medium before inoculation.
6. Inoculate the methanogenic microorganisms in a ratio 1:10 into the bottles in replicates.
7. Start the incubation experiment by placing them to the incubator (thermostat) at a certain temperature (*see* **Note 11**).
8. Take samples of the gas phase containing methane accumulated in the bottles periodically for their analysis.

The methanogenesis rate can be calculated from the slope of the line determined from a semilogarithmic plot of methane concentrations versus the incubation time. Only data points located at this slope line should be taken into account.

3.1.2 Preparation of Methanogenic Soil Samples for Serial Incubations

The samples taken from soil of different types or water sediments should be homogenized and suspended anaerobically. The soil should be mechanically crushed. The dry lumps should be broken. Some large pieces of plant material in the soil samples should be removed. The soil crushed should be passed through a stainless steel sieve with a mesh size of 0.5 mm and can be used immediately or stored at a 4–6°C temperature until use. The slurries are prepared by adding a certain amount of water fraction depending on the soil texture. The ratio between solid and liquid fractions of the prepared slurries should be equaled to that in native samples in order to estimate the true methanogenic potential of the native microbial community. The liquid fraction of the native samples should be taken to prepare slurries if not otherwise specified. In some cases, sterilized anoxic water can also be used. The experiments should be done in duplicate or triplicate (Fig. 2).

1. Flush serum bottles (20–120 ml) with an inert gas (N_2 or argon).
2. Transfer the anoxic slurry anaerobically into the serum bottles.

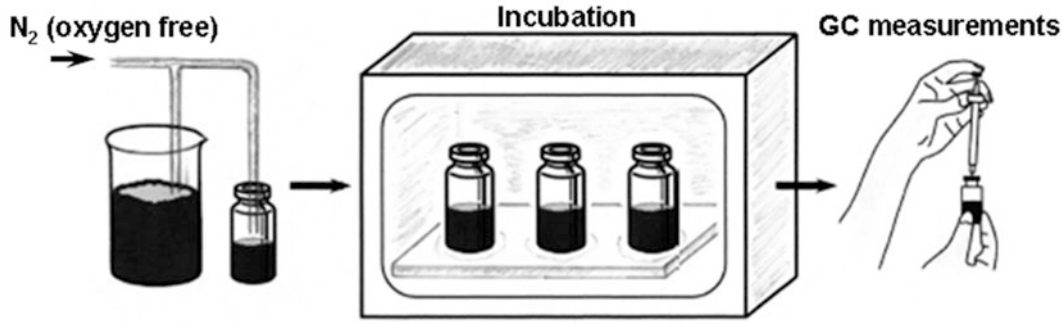

Fig. 2 Main steps of the method of potential methane production measuring

3. Close the bottles with butyl rubber stoppers.
4. Pre-incubate the bottles overnight at the required temperature.
5. Flush the bottles with an inert gas (N_2 or argon) until the headspace is free for CH_4.
6. Start the experiment by continuing the incubation at the required temperature.
7. Take the samples to analyze repeatedly the headspace for CH_4 at given time intervals. Shake the bottles vigorously for 30 s before sampling to ensure gas equilibration between liquid and gas phase.
8. Determine the production rates of CH_4 from their linear increase with time in the headspace.

3.1.3 Using Radioactive Tracers to Measure a Certain Methanogenesis Pathway in Samples

The introduction of radioactive substrates into methanogenic samples is used to study the rate of a particular methanogenesis pathway, usually hydrogen-dependent or acetoclastic ones. A trace amount of the substrate is converted into molecule of CH_4 and makes it radioactive. The radioactivity is further detected with a special counter, and the contribution of the particular methanogenic pathway to the total methanogenesis can be finally calculated.

1. Prepare soil slurries in tubes, flasks, or small bottles (10–50 ml) (*see* **Note 12**).
2. Pre-incubate the samples for a short period at a required temperature.
3. Exchange the gas phase with an inert gas to remove traces of methane.
4. Start the experiment by the addition of 0.1–1 ml solution of a radiotracer to have the final radioactivity 10–100 mCi $mmol^{-1}$.
5. Incubate the samples with radiotracers, take gas samples, and measure total and radioactive methane and CO_2 for a time period until the radioactive substrate is incorporated in CH_4.
6. Stop the experiment by 1 ml of 5 N H_2SO_4 injected. This also liberates total CO_2 that is important for final calculations.
7. Calculate the specific radioactivities SR_{CH4} and SR_{CO2} (dpm mol^{-1}) from the data on total and radioactive CH_4 and CO_2.
8. Determine the fraction of CH_4 produced from H_2/CO_2 (f_{H2}) from the conversion of $H^{14}CO_3^-$ to $^{14}CH_4$ using the specific radioactivities (dpm mol^{-1}) of CH_4 (SR_{CH4}) and CO_2 (SR_{CO2}): $fH_2 = SR_{CH4}/SR_{CO2}$.
9. Using f_{H2}, calculate rates of hydrogen-dependent and acetoclastic methanogenesis.

3.2 Static Chamber Method

This method is based on measuring gas samples taken periodically from the headspace of a chamber covering a segment of a research site generating methane.

3.2.1 Field Measurements of Methanogenesis

The study sites should be equipped with boardwalks to prevent disturbance of the soil and vegetation during sampling [55]. One day prior to making flux measurements [57] at the measurement sites, the collars have to be inserted into the ground to a depth about 10 cm (at the waterlogged sites, the collars have to be placed on the sediments in water) (*see* **Note 13**). The chambers (Fig. 3) fit into a water-filled notch in the collars and should be well sealed [54] (*see* **Note 14**). The chamber should be equipped with a fan to mix the gas space in the chamber and balance gas concentration in its volume (*see* **Note 15**).

The chamber exposition time in different experiments is in the interval from 0.25 till 24 h [33, 34, 41, 54–63].

1. Take duplicate air samples with syringes [62] after careful pumping to mix the air in the chamber and tubing (inner diameter 1 mm, length 0.75 m) between the chamber and syringe.
2. Transfer immediately the gas in the syringe to a pre-evacuated glass flask. The syringes themselves can be used to analyze the gas samples when analyzing within 24 h [55].
3. Deliver the flasks to the laboratory [62].
4. Determine the content of methane in the laboratory using gas chromatographic systems (flame ionization detector).
5. Calculate the emission rate of C–CH_4 (F, mgC m^{-2} h^{-1}) as the difference between its concentrations in the beginning (C_b, ppmv) and at the end (C_e, ppmv) of the experiment

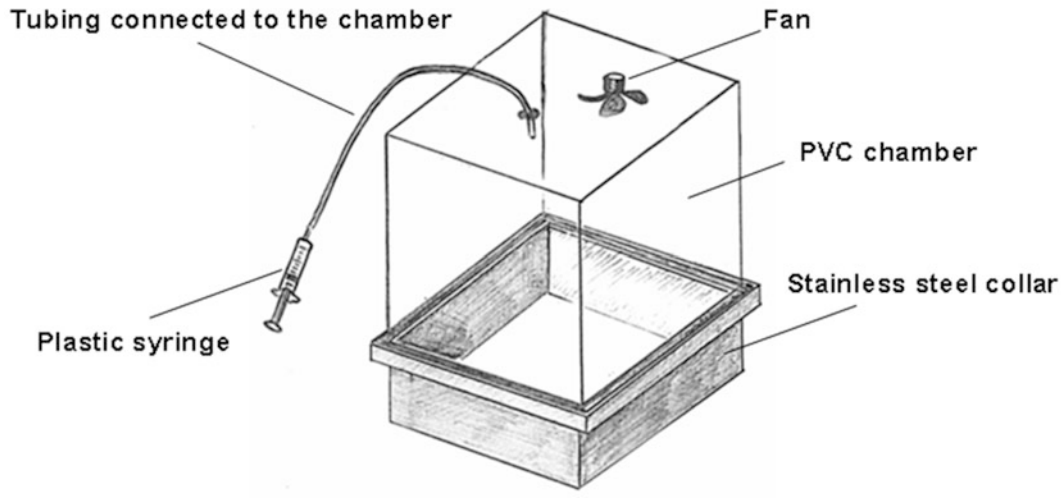

Fig. 3 Scheme of a chamber with a fan and a syringe for taking gas samples (kindly provided by Phillippov I.V.)

and referred to the area (S, m^2) and volume (V, m^2) of the chamber [56]:

$$F = \alpha P b V/(T \cdot S),$$

where $\alpha = 1.44 \cdot 10^{-3}$ mgC K J^{-1} $ppmv^{-1}$; P is the total pressure (almost equal to the atmospheric pressure Pa) of the gas mixture in the chamber during measuring (Pa); $b = (C_e - C_b)/t$; t is the chamber measurement time (h); and T is the temperature in the chamber during measuring (K).

Calculation example: Concentration of methane (C_b) was 2 ppm immediately after installing the cubical chamber (height $H = 0.37$ m). It increased to 4 ppm after 30 min (Ce). The atmospheric pressure (P) was $1.01 \cdot 10^5$ Pa. The average temperature (T) in the chamber was 293 K during measuring.

Then, $b = (4–2)/0.5 = 4$ ppm/h and

$$F = 1.44 \cdot 10^{-3} \cdot 1.01 \cdot 10^5 \cdot 4 \cdot 0.37/293 \approx 0.73 \text{ mgC } m^{-2}\ h^{-1}.$$

Since C_b and C_e may contain measurement errors, the more precise calculation is achieved by using additionally a few intermediate concentrations ($C_1 = C_b, C_2, \ldots, C_N = C_e$), measured at the times $t_1 = 0, t_2, \ldots, t_N = t$ ($N = 4 \div 6$) [55, 62].

Thus, methane flux can be calculated from the slope of the change in concentration over time [54, 62]. It is assumed that the uncertainty σ_i associated with each measurement C_i is known and that the t_i's (values if time) are known exactly; then [64]

$$b = (S_\sigma \cdot S_{X\Upsilon} - S_X \cdot S_\Upsilon)/S_\Delta,$$

where

$$S_\sigma = \sum_{i=1}^{N}\left(\frac{1}{\sigma_i^2}\right),\ S_X = \sum_{i=1}^{N}\left(\frac{t_i}{\sigma_i^2}\right),\ S_\Upsilon = \sum_{i=1}^{N}\left(\frac{C_i}{\sigma_i^2}\right),$$

$$S_{XX} = \sum_{i=1}^{N}\left(\frac{t_i}{\sigma_i}\right)^2,\ S_{X\Upsilon} = \sum_{i=1}^{N}\left(\frac{C_i \cdot t_i}{\sigma_i^2}\right), S_\Delta = S_\sigma \cdot S_{XX} - (S_X)^2.$$

The calculation was checked using the regression coefficient of the slope [54]: the data deviating significantly from linearity ($r^2 < 0.8$) were discarded [62] (*see* **Note 16**).

3.2.2 Preparation of Microcosm (Mesocosm)

The soil sample should be taken so that its native structure is kept undestroyed. It should be then quickly transported to the laboratory, anaerobically handled, and kept until use.

1. Transfer the sample into a bottle, flask (microcosm) or a box, or a container (mesocosm) flushed with an inert gas, hermetically sealed, and equipped with a stopper for taken gas samples.

2. Place the sample into an incubator or a room set for a required temperature for its incubation.
3. Perform the incubation of the sample without shaking to avoid damage of the methanogenic community.
4. Take gas samples from the headspace periodically not disturbing the structure of the microcosm and calculate methanogenesis rate after the experiment is finished as a linear increase with time.

4 Notes

1. The term "control volume" is commonly used for derivation of mass balance equations [23, 65]. It can be defined as a bounded space region where flows of matter, energy, and impulse can come in, come out, and change within its boundary and the external forces can act on it. Such definition is relevant for mathematical description of the mass balance equation used further for the concept of classification of methods.
2. In mathematical terms, div($\mathbf{j}$) is the divergence operator of vector [66]. For a certain physical process (here is for methanogenesis), it expresses a net mass flow (methane flow) by means of diffusion at existing concentration gradient [23]. It also indicates if there is a source or a sink of a substance (methane).
3. Generally, all terms of the equation should be measured to define the true methanogenesis rate. In some cases, one or two terms can be eliminated from the equation as equaled to zero. An example is an anaerobically prepared sample with active methanogens placed in a bottle and incubated at a certain temperature.

   In such system:

   $w^- = 0$ assuming strictly anaerobic conditions

   $\mathrm{div}(\mathbf{j}) \approx 0$ due to a small volume where all concentration gradients resulting in mass transport are rapidly balanced

   Hence, the final equation is

   $$\partial C/\partial t = w^+.$$
4. The term "potential methane production" rather than "true (actual) methane production" is used assuming that the conditions in a vessel with impenetrable boundaries containing a sample generating CH_4 can be significantly different from those in the sample source environment.
5. The term "microcosm" is used for undisturbed natural samples placed in different vessels and imitated the ecosystem in little.

The term "mesocosm" is mostly used for the system being a natural undisturbed sample enclosed in a big vessel or a box for the experiments of a bigger scale [67]. In case of opened systems, it can be also containers or artificial basins representing an intermediate between experimental microcosms and natural ecosystems (macrocosms).

6. Brouček [43] refers this technique to micrometeorological methods. However, it is rather a variety of the chamber method where the whole bam can be assigned to a chamber.
7. All materials used for working with radiotracers should be kept in a special room where the control of radioactivity is provided in order to avoid radioactive contamination. All working procedures should correspond to radiation safety standards.
8. The size of chambers usually varies in the following intervals [33, 34, 41, 54–63]: area of base (m^2) 0.03–1.0, volume (m^3) 0.08–0.8, and height (m) 0.13–0.8. The bigger the chamber, the more precise measurements of methanogenesis can be done assuming the decrease of soil heterogeneity and random errors.
9. In the anaerobic cultivation technique, it is the gas mixture N_2/CO_2 in a ratio 4:1 that is normally used to stabilize pH at growing cultures in a buffered mineral medium. If a low mineralized medium is used or the experiment on pH growth optimum is carried out, then a pure N_2 should be used in the headspace.
10. Additionally, the anaerobic technique is presented at DSMZ website: http://www.dsmz.de/fileadmin/Bereiche/Microbiology/Dateien/Kultivierungshinweise/englAnaerob.pdf.
11. The vessels should be shaken if H_2 is present in the headspace for fast-growing methanogens (normally for thermophiles).
12. The smaller is the headspace, the higher is the sensitivity for detecting radioactivity.
13. While installing the chamber to the ground, the vegetation should not be removed to keep the conditions maximally closed to natural ones.
14. To minimize the changes of chamber temperature, the PVC box should be covered with reflecting aluminum fabric.
15. Since methane is constantly emitted into the headspace of the chamber from soil, its concentration can be slightly different at different levels of the chamber. To make measurements more correct, it is necessary to balance CH_4 concentrations in the chamber volume prior to sampling by a fan.

16. Criteria for CH_4 flux measurements in the literature usually include two main points:
    1. Initial concentrations had to be very close to ambient CH_4 concentration.
    2. The correlation coefficient of the linear regression had to be significant to the 95% confidence level for $N = 4$ or 5 ($r^2 = 0.920$ or 0.841) [58].

The second criterion can be not so strong: the flux measurements of individual chambers were accepted if r^2 in a linear regression of the chamber concentration change with time is ≥ 0.8 [62, 68].

References

1. Wolfe RS (1993) A historical overview of methanogenesis. In: Ferry JG (ed) Methanogenesis, Chapman & Hall microbiology series. Chapman & Hall, New York
2. Barker HA (ed) (1956) Bacterial fermentation. Wiley, New York
3. Ehhalt DH, Schmidt U (1978) Sources and sinks of atmospheric methane. Pageoph 116:452–464
4. Großkopf R, Janssen PH, Liesack W (1998) Diversity and structure of the methanogenic community in anoxic rice paddy soil microcosms as examined by cultivation and direct 16S rRNA gene sequence retrieval. Appl Environ Microbiol 64:960–969
5. Garcia JL (1990) Taxonomy and ecology of methanogens. FEMS Microbiol Rev 87:297–308. doi:10.1111/j.1574-6968.1990.tb04928.x
6. Chan OC, Claus P, Casper P et al (2005) Vertical distribution of methanogenic archaeal community in Lake Dagow sediment. Environ Microbiol 7:1139–1149. doi:10.1111/j.1462-2920.2005.00790.x
7. Jeanthon C, L'Haridon S, Reysenbach AL et al (1999) *Methanococcus vulcanius* sp. nov., a novel hyperthermophilic methanogen isolated from East Pacific Rise, and identification of *Methanococcus* sp. DSM 4213T as *Methanococcus fervens* sp. nov. Int J Syst Evol Microbiol 49:583–589
8. Ganzert L, Jurgens G, Münster U et al (2007) Methanogenic communities in permafrost-affected soils of the Laptev Sea coast, Siberian Arctic, characterized by 16S rRNA gene fingerprints. FEMS Microbiol Ecol 59:476–488
9. Kobabe S, Wagner D, Pfeiffer EM (2004) Characterisation of microbial community composition of a Siberian tundra soil by fluorescence in situ hybridization. FEMS Microbiol Ecol 50:13–23. doi:10.1016/j.femsec.2004.05.003
10. Lin C, Raskin L, Stahl DA (1997) Microbial community structure in gastrointestinal tracts of domestic animals: comparative analyzes using rRNA-targeted oligonucleotide probes. FEMS Microbiol Ecol 22:281–294. doi:10.1111/j.1574-6941.1997.tb00380.x
11. Brune A (2010) Methanogenesis in the digestive tract of termites. In: Hackstein JHP (ed) (Endo)symbiotic methanogenic archaea, vol 19, Microbiology monographs. Springer, Berlin. doi:10.1007/978-3-642-13615-3_1
12. Hackstein JHP (2010) Anaerobic ciliates and their methanogenic endosymbionts. In: Hackstein JHP (ed) (Endo)symbiotic methanogenic archaea, vol 19, Microbiology monographs. Springer, Berlin. doi:10.1007/978-3-642-13615-3_1
13. Bapteste E, Brochier C, Boucher Y (2005) Higher-level classification of the Archaea: evolution of methanogenesis and methanogens. Archaea 1:353–363. doi:10.1155/2005/859728
14. Lefèvre F, Forget F (2009) Observed variations of methane on Mars unexplained by known atmospheric chemistry and physics. Nature 460 (7256):720–723. doi:10.1038/nature08228
15. Börjesson P, Mattiasson B (2008) Biogas as a resource-efficient vehicle fuel. Trends Biotechnol 26:7–13
16. Beliaev SS, Ivanov MV (1975) The rate of methane formation by bacteria determined by isotopic labeling technique. Microbiology 44:166–168 (in Russian)
17. Lein AY, Ivanov MV (eds) (2009) Biogeochemical cycle of methane in the ocean. Nauka, Moscow (in Russian)
18. Min'ko OI, Kasparov SV, Amosova YM (1987) Gaseous compounds metabolic products of

microbial coenoses of waterlogged soils. Biol Bull Rev 48:182–193

19. Orlov DS, Minko OI, Ammosova Ya M et al (1987) Research methods for soil gas function. In: Voroin AD, Orlov DS (eds) Modern physical and chemical methods of soil studies. MGU, Moscow (in Russian)
20. Alperin MJ, Reeburg WS, Whiticar MJ (1988) Carbon and hydrogen isotope fractionation resulting from anaerobic methane oxidation. Glob Biogeochem Cycles 2:279–288
21. Glagolev MV (1998) Modeling of production, oxidation and transportation processes of methane. In: Global Environment Research Fund: Eco-Frontier Fellowship (EFF) in 1997, Environment Agency. Global Environment Department. Research & Information Office, Tokyo
22. Panikov NS, Dedysh SN, Kolesnikov OM et al (2001) Metabolic and environmental control on methane emission from soils: mechanistic studies of mesotrophic fen in West Siberia. Water Air Soil Pollut Focus 1:415–428
23. Martin JL, McCutcheon SC (eds) (1999) Hydrodynamics and transport for water quality modeling. Lewis, Boca Raton
24. Arsenin VY (1984) Methods of mathematical physics and higher functions. Nauka, Moscow (in Russian)
25. Bridgham SD, Richardson CJ (1992) Mechanisms controlling soil respiration (CO_2 and CH_4) in southern peatlands. Soil Biol Biochem 24:1089–1099
26. Bodelier PLE, Hahn AP, Arth IR et al (2000) Effects of ammonium-based fertilisation on microbial processes involved in methane emission from soils planted with rice. Biogeochemistry 51:225–257
27. Blodau C, Basiliko N, Moore TR (2004) Carbon turnover in peatland mesocosms exposed to different water table levels. Biogeochemistry 67:331–351
28. Baldwin DS, Rees GN, Mitchell AM et al (2006) The short-term effects of salinization on anaerobic nutrient cycling and microbial community structure in sediment from a freshwater wetland. Wetlands 26:455–464
29. Conrad R, Klose M (1999) Anaerobic conversion of carbon dioxide to methane, acetate and propionate on washed rice roots. FEMS Microbiol Ecol 30:147–155
30. Schulz S, Conrad R (1996) Influence of temperature on pathways to methane production in the permanently cold profundal sediment of Lake Constance. FEMS Microbiol Ecol 20:1–14
31. Thebrath B, Mayer H-P, Conrad R (1992) Bicarbonate-dependent production and methanogenic consumption of acetate in anoxic paddy soil. FEMS Microbiol Ecol 86:295–302
32. Conrad R, Klose M (2000) Selective inhibition of reactions involved in methanogenesis and fatty acid production on rice roots. FEMS Microbiol Ecol 34:27–34
33. Bartlett KB, Harriss RC, Sebacher DI (1985) Methane flux from coastal salt marshes. J Geophys Res 90:5710–5720
34. Galy-Lacaux C, Delmas R, Jambert C et al (1997) Gaseous emissions and oxygen consumption in hydroelectric dams: a case study in French Guyana. Glob Biogeochem Cycles 11:471–483
35. Nakano T, Sawamoto T, Morishita T et al (2004) A comparison of regression methods for estimating soil-atmosphere diffusion gas fluxes by a closed-chamber technique. Soil Biol Biochem 36:107–113
36. Sabrekov AF, Runkle BRK, Glagolev MV et al (2014) Seasonal variability as a source of uncertainty in the West Siberian regional CH_4 flux upscaling. Environ Res Lett 9(4): 045008. doi:10.1088/1748-9326/9/4/045008
37. Pape L, Ammann C, Nyfeler-Brunner A et al (2009) An automated dynamic chamber system for surface exchange measurement of non-reactive and reactive trace gases of grassland ecosystems. Biogeosciences 6:405–429
38. Stefanik KC, Mitsch WJ (2013) Metabolism and methane flux of dominant macrophyte communities in created riverine wetlands using open system flow through chambers. Ecol Eng. doi:10.1016/j.ecoleng.2013.10.036
39. Bedard C, Knowles R (1989) Physiology, biochemistry, and specific inhibitors of CH_4, NH_4^+, and CO oxidation by methanotrophs and nitrifiers. Microbiol Rev 53:68–84
40. Novikov VV, Stepanov AL, Pozdnyakov AI et al (2004) Seasonal dynamics of CO_2, CH_4, N_2O, and NO emissions from peat soils of the Yakhroma river floodplain. Eurasian Soil Sci 37:755–761
41. Dise NB (1992) Winter fluxes of methane from Minnesota peatlands. Biogeochemistry 17:71–83
42. Baldocchi DD, Hicks BB, Meyers TP (1988) Measuring biosphere-atmosphere exchanges of biologically related gases with micrometeorological methods. Ecology 69:1331–1340
43. Brouček J (2014) Methods of methane measurement in ruminants. Slovak J Anim Sci 47:51–60

44. Harper LA, Denmead OT, Flesch TK (2011) Micrometeorological techniques for measurement of enteric greenhouse gas emissions. Anim Feed Sci Technol 166–167:227–239
45. Garnsworthy PC, Craigon J, Hernandez-Medrano JH et al (2012) On-farm methane measurements during milking correlate with total methane production by individual dairy cows. J Dairy Sci 95:3166–3180
46. Derno M, Elsner HG, Paetow EA et al (2009) Technical note: a new facility for continuous respiration measurements in lactating cows. J Dairy Sci 92:2804–2808
47. Lassey K, Walker C, McMillan A et al (2001) On the performance of SF_6 permeation tubes used in determining methane emission from grazing livestock. Chemosphere Global Change Sci 3:367–376
48. Martin C, Rouel J, Jouany JP et al (2008) Methane output and diet digestibility in response to feeding dairy cows crude linseed, extruded linseed, or linseed oil. J Anim Sci 86:2642–2650
49. Storm IMLD, Hellwing ALF, Nielsen NI et al (2012) Methods for measuring and estimating methane emission from ruminants. Animals 2:160–183
50. Hegarty RS (2013) Applicability of short-term emission measurements for on-farm quantification of enteric methane. Animal 7:401–408
51. Lü F, Ji J, Shao L et al (2013) Bacterial bioaugmentation for improving methane and hydrogen production from microalgae. Biotechnol Biofuels 6:92
52. Esposito G, Frunzo L, Liotta F et al (2012) Bio-methane potential tests to measure the biogas production from the digestion and co-digestion of complex organic substrates. TOENVIEJ 5:1–8
53. Wolin EA, Wolin MG, Wolfe RS (1963) Formation of methane by bacterial extracts. J Biol Chem 238:2882–2886
54. Nakano T, Kuniyoshi S, Fukuda M (2000) Temporal variation in methane emission from tundra wetlands in a permafrost area, northeastern Siberia. Atmos Environ 34:1205–1213
55. Silvola J, Saarnio S, Foot J et al (2003) Effects of elevated CO_2 and N deposition on CH_4 emissions from European mires. Glob Biogeochem Cycles 17(2):1068. doi:10.1029/2002GB001886
56. Augustin J, Merbach W, Rogasik J (1998) Factors influencing nitrous oxide and methane emissions from minerotrophic fens in northeast Germany. Biol Fertil Soils 28:1–4
57. Poth M, Anderson IC, Miranda HS et al (1995) The magnitude and persistence of soil NO, N_2O, CH_4, and CO_2 fluxes from burned tropical savanna in Brazil. Glob Biogeochem Cycles 9:503–513
58. Crill PM (1991) Seasonal patterns of methane uptake and carbon dioxide release by a temperate woodland soil. Glob Biogeochem Cycles 5:319–334
59. Frenzel P, Karofeld E (2000) CH_4 emission from a hollow-ridge complex in a raised bog: the role of CH_4 production and oxidation. Biogeochemistry 51:91–112
60. Glagolev MV, Sabrekov AF, Kleptsova IE et al (2012) Methane emission from bogs in the subtaiga of Western Siberia: the development of standard model. Eurasian Soil Sci 45:947–957. doi:10.1134/S106422931210002X
61. Granberg G, Mikkela C, Sundh I et al (1997) Sources of spatial variation in methane emission from mires in northern Sweden: a mechanistic approach in statistical modeling. Glob Biogeochem Cycles 11:135–150
62. Panikov NS, Dedysh SN (2000) Cold season CH_4 and CO_2 emission from boreal peat bogs (West Siberia): winter fluxes and thaw activation dynamics. Glob Biogeochem Cycles 14:1071–1080
63. Chanton JP, Whiting GJ, Showers WJ et al (1992) Methane flux from *Peltandra virginica*: stable isotope tracing and chamber effects. Glob Biogeochem Cycles 6:15–31
64. Press WH, Teukolsky SA, Vetterling WT et al (1995) Numerical recipes in FORTRAN. The art of scientific computing. Cambridge University Press, Cambridge
65. Kays WM (1966) Convective heat and mass transfer. McGraw-Hill, New York
66. Ertekin T, Abou-Kassem JH, King GR (2001) Basic applied reservoir simulation. Society of Petroleum Engineers, Richardson
67. Odum EP (1983) Basic ecology. Saunders College, Philadelphia
68. Christensen TR, Michelsen A, Jonasson S et al (1997) Carbon dioxide and methane exchange of a subarctic heath in response to climate change related environmental manipulations. OIKOS 79:34–44